JANUARY 27TH, 2026

The Muon's Wobble: Measuring Muon g−2 to Test the Standard Model

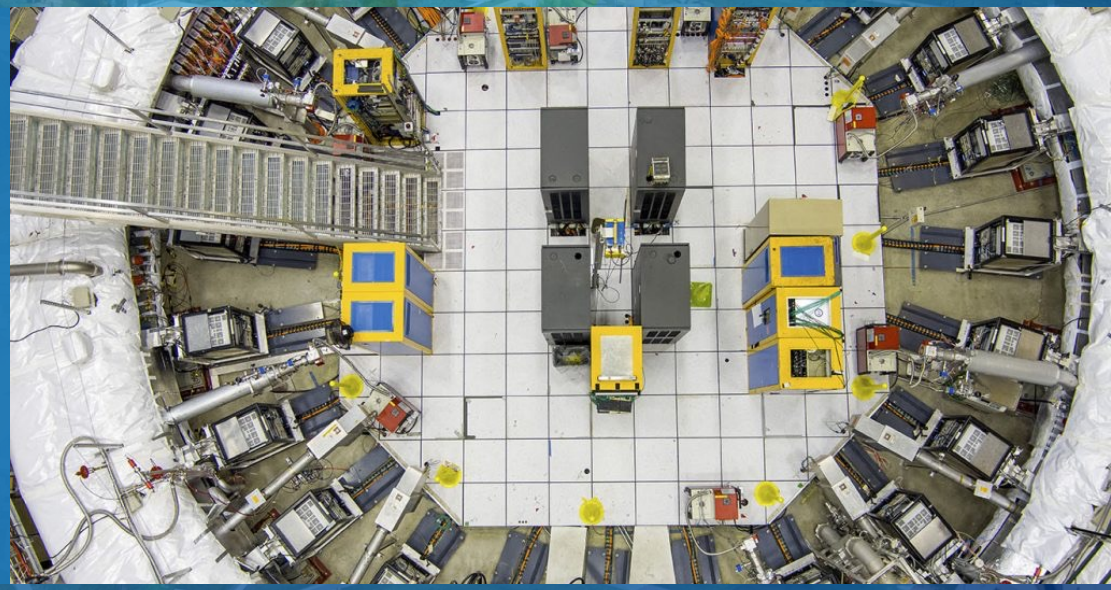

SIMON CORRODI
Argonne National Laboratory

Stony Brook University

Colloquium

U.S. DEPARTMENT of ENERGY

Argonne National Laboratory is a U.S. Department of Energy laboratory managed by UChicago Argonne, LLC.

Argonne NATIONAL LABORATORY

April 2021 – Muons made News

A Particle's Tiny Wobble Could Upend the Known Laws of Physics

By DENNIS OVERBYE

Evidence is mounting that a tiny subatomic particle seems to be disobeying the known laws of physics, scientists announced on Wednesday, a finding that would open a vast and tantalizing hole in our understanding of the universe.

The result, physicists say, suggests that there are forms of matter and energy vital to the nature and evolution of the cosmos that are not yet known to science.

"This is our Mars rover landing moment," said Chris Polly, a physicist at the Fermi National Accelerator Laboratory, or Fermilab, in Batavia, Ill., who has been working toward this finding for most of his career.

The particle under scrutiny is the muon, which is akin to an electron but far heavier, and is an integral element of the cosmos. Dr. Polly and his colleagues — an international team of 200 physicists from seven countries — found that muons did not behave as pre-

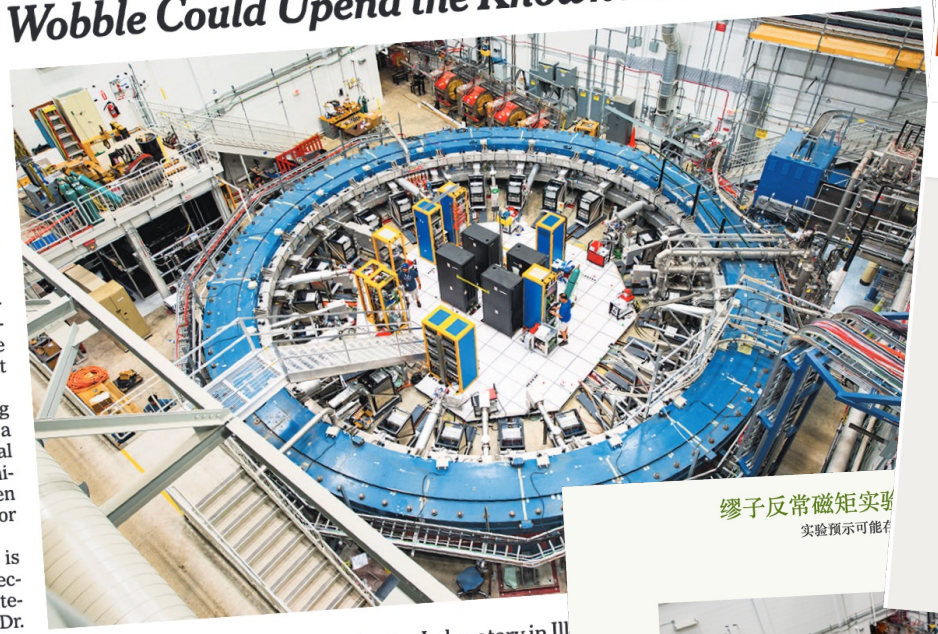

A ring at the Fermi National Accelerator Laboratory in Ill

particles in the universe (17 at last

The results, the first fr
d Muon g
xperimer
ational L
ve teased

seminar

缪子反常磁矩实验

实验预示可能存

缪子反常磁矩储存环

近日，在美国费米国家实验室进行的缪子反常磁
标准模型理论预言不相符，该结果与早期美国布鲁
的未知粒子或者作用力。

"这意味着原本经历了多次考验，堪称完美的
更完美的理论等待人类去发现。"缪子反常磁矩实验
《中国科学报》。

DER SPIEGEL

Menü Schlagzeilen SPIEGEL+ Magazine Coronavirus Kli

Französischer Philosoph: Intellektueller wirft Michel Foucault Kindesmissbrauch vor Vor 3 Min

Ausbruch von Süditalien: Das Er Europäer Vor 25 Mi

SPIEGEL+ Alle Artikel & digitales Magazin

Neue Erkenntnisse in der Teilchenphysik

Kundschafter ins Unbekannte

Seit 50 Jahren ersehnen Forscher Einblicke in die Welt jenseits der bekannten Naturgesetze. Mit den Erkenntnissen aus dem Myon-g-2-Experiment könnte sich das Tor zu einer neuen Physik öffnen. Von Johann Grolle

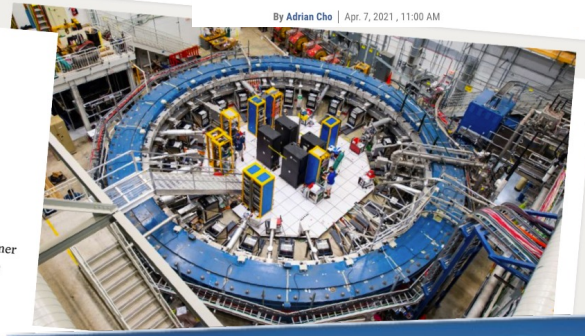

Le Monde

VENDREDI 9 AVRIL 2021

Une particul
élémentaire
polarise le m
de physique

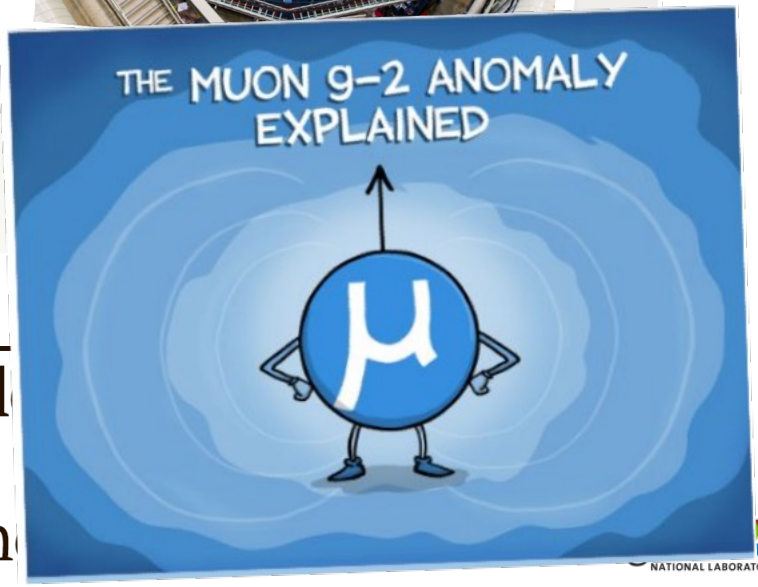

NATIONAL LABORATORY

Science Contents News Careers Journals

Read our COVID-19 research and news.

SHARE

Muons twirl as they circulate in this ring-shaped accelerator at Fermilab, like race cars perpetually spinning out. REIDAR HAHN/FERMILAB

Particle mystery deepens, as physicists confirm that the muon is more magnetic than predicted

By Adrian Cho | Apr. 7, 2021 , 11:00 AM

Why is this magnetic?

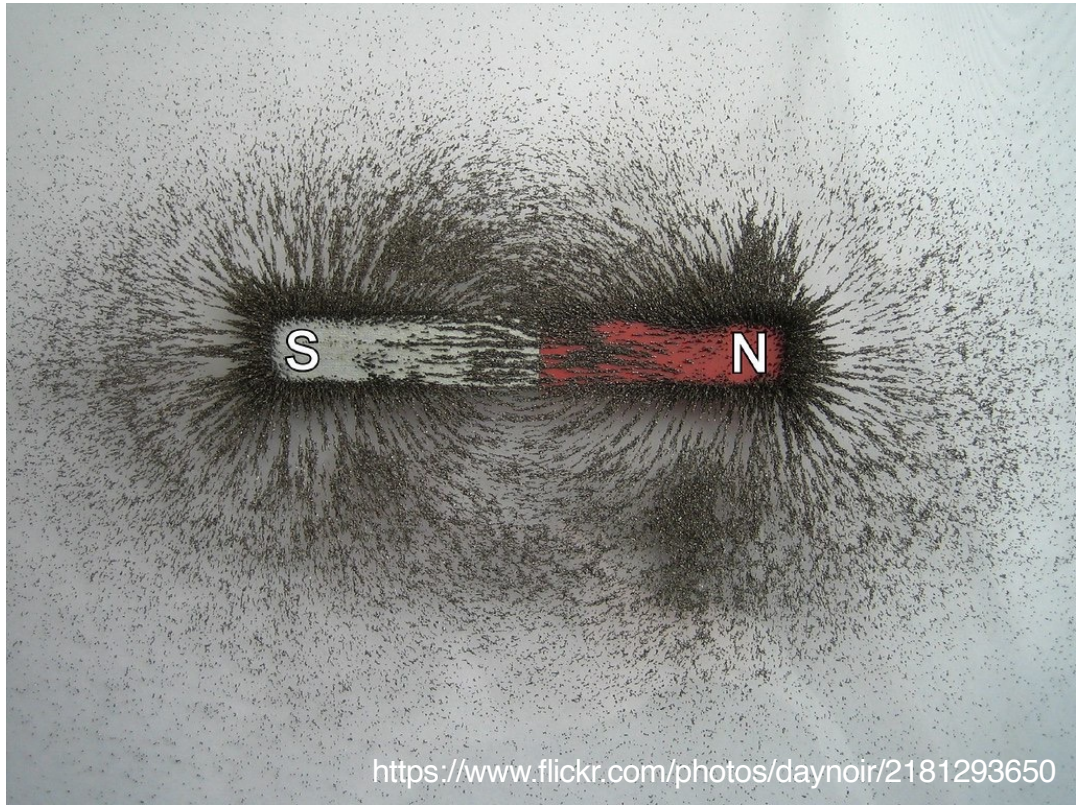

Classical

Is it full of tiny, circulating currents?
Ampère's molecular currents

Magnetic Moment: $\mu = I \cdot A = \frac{evr}{2}$

Angular Moment: $\mathrm{L} = mvr$

$$\frac{\mu}{L} = \frac{e}{2m} \qquad \mu = g\,\frac{e}{2m}\,L$$

Current loop: $g = 1$

Why is this magnetic?

Einstein measured g=1 at 10%-level!

> **Physics.** — "*Experimental proof of the existence of Ampère's molecular currents.*" By Prof. A. EINSTEIN and Dr. W. J. DE HAAS. (Communicated by Prof. H. A. LORENTZ),
>
> (Communicated in the meeting of April 23, 1915).

They "knew" that g=1, and measured it…

… but this turns out to be false!

Classical

Is it full of tiny, circulating currents?
Ampère's molecular currents

Magnetic Moment: $\mu = I \cdot A = \frac{evr}{2}$

Angular Moment: $\mathrm{L} = mvr$

$$\frac{\mu}{L} = \frac{e}{2m} \qquad \mu = g\,\frac{e}{2m}\,L$$

Current loop: $g = 1$

Why is this magnetic? Spin!

Later experimental work showed $g_e \approx 2$

Quantum Concept

Elementary particles are point-like: $r \to 0, A \to 0, L \to 0$, but there is magnetism

1928: Dirac's theory introduces an intrinsic spin for electrons

- Magnetism is an intrinsic property of elementary particle

The g-factor connects the spin ($\vec{s}$) of a particle to its intrinsic **magnetic moment** ($\vec{\mu}$)

$$\vec{\mu} = g \frac{e}{2m} \vec{s}$$

The g-factor

connects the spin ($\vec{s}$) of a particle to its intrinsic **magnetic moment** ($\vec{\mu}$)

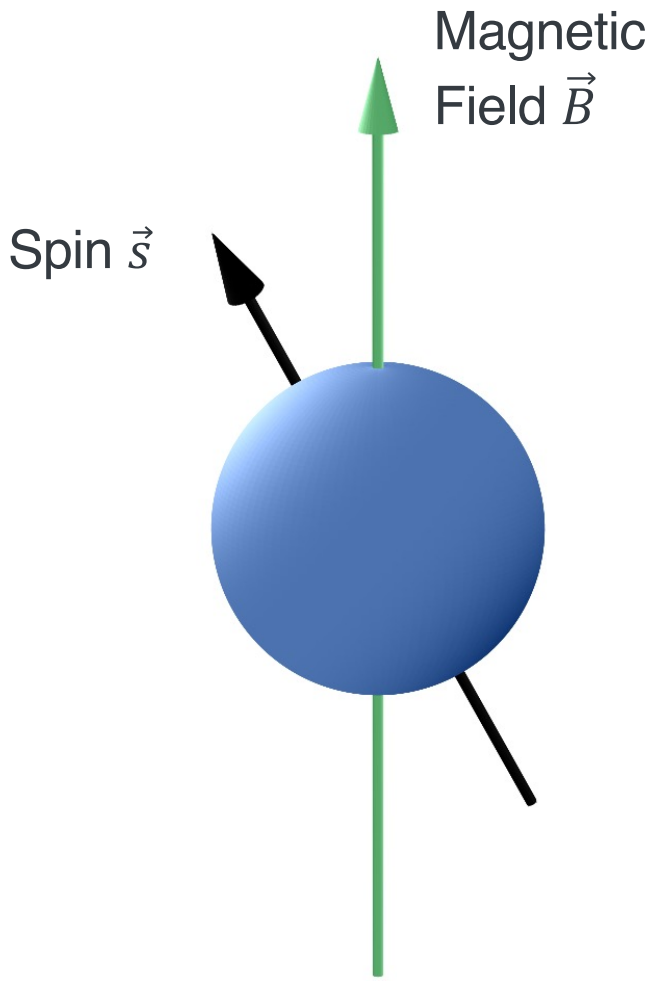

The g-factor

connects the spin ($\vec{s}$) of a particle to its intrinsic **magnetic moment** ($\vec{\mu}$)

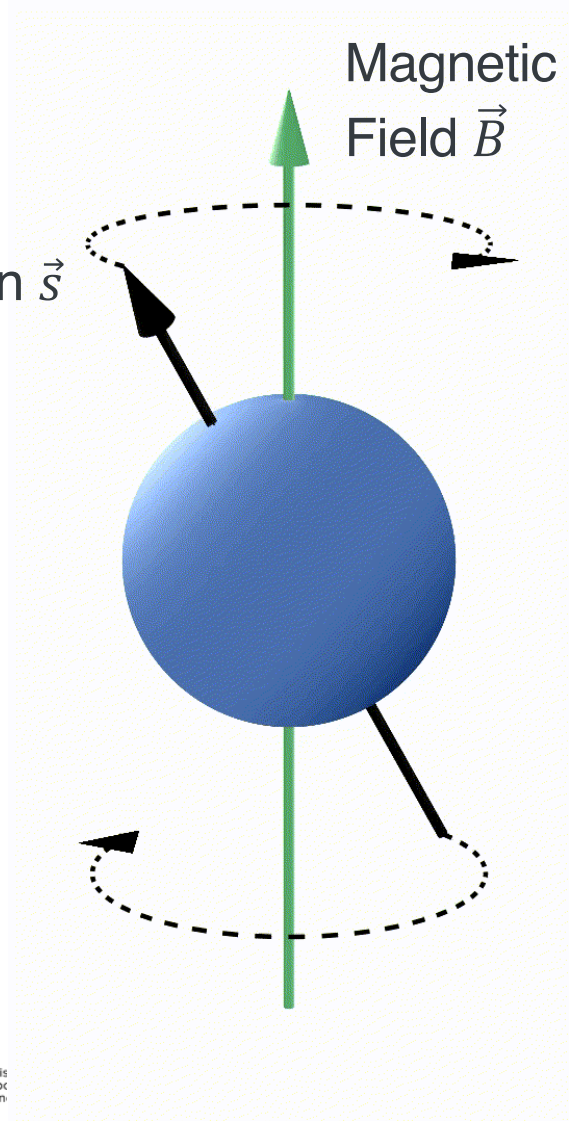

The **spin precession frequency** ω_s in a magnetic field $\vec{B}$ is proportional to the **g-factor**

$$\vec{\omega}_s = \frac{g}{2}\frac{q}{mc}\vec{B}$$

Magnetic Moments of Charged Leptons

A long history

Classical $g = 1$

From classical current loop $g = 1$.

Stern-Gerlach and atomic spectroscopy found $g_e \approx 2$

Dirac (1928) theory $g = 2$

For a pure Dirac spin-½ charged fermion, $g = 2$.

Schwinger (1948) and beyond $g > 2$

Interactions with **virtual particles** alter **g**

$g_e \approx 2 + \alpha/\pi$ *prediction, foundation for the Standard Model*

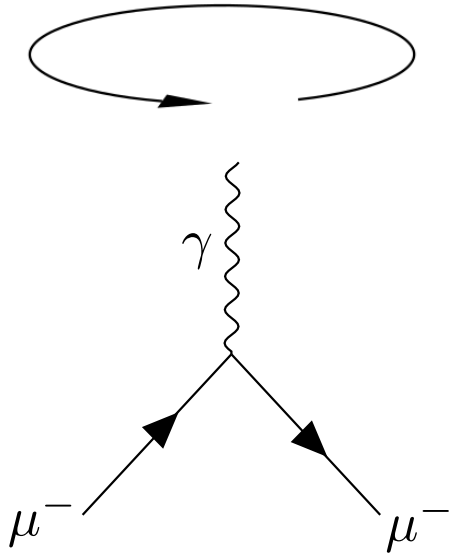

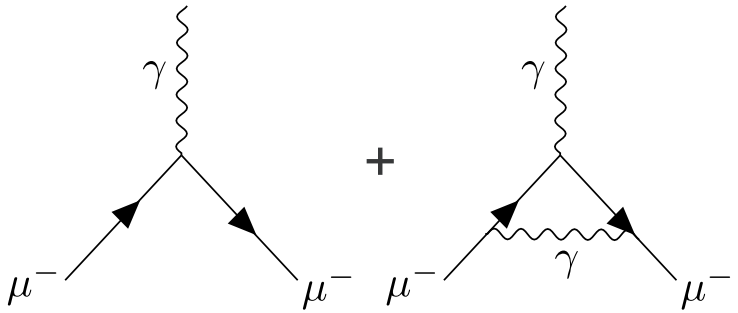

Feynman Diagrams

- ”Bookkeeping” and “visualization” of particle interactions
- Expansion in “number of loops”

The Standard Model

Encodes all known particles and interactions

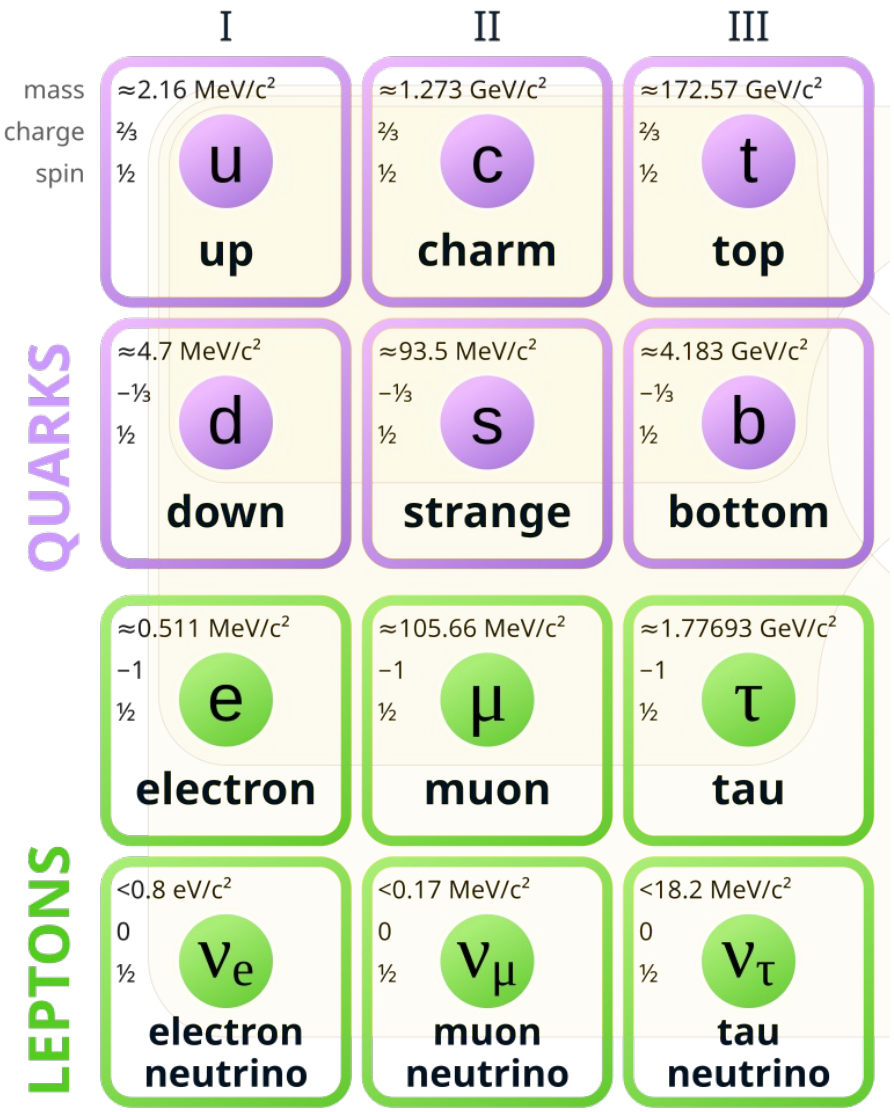

Interactions with **virtual particles** alter g

Dirac-Term (2)

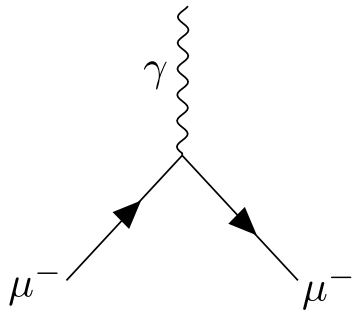

+

QED

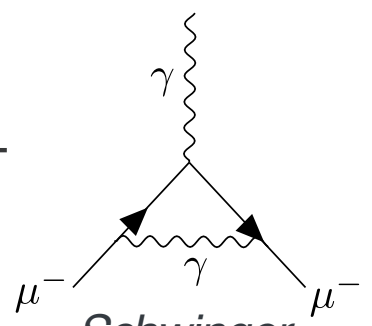

Schwinger

+

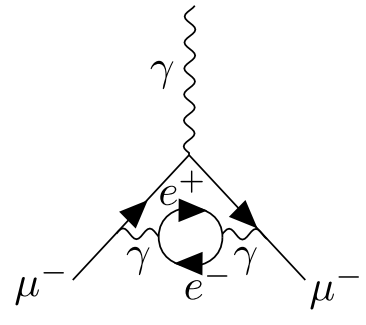

Hadronic Vacuum Polarization

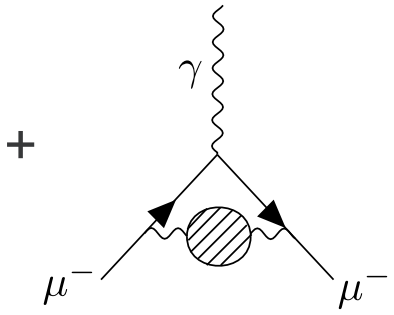

+

Hadronic Light-by-Light

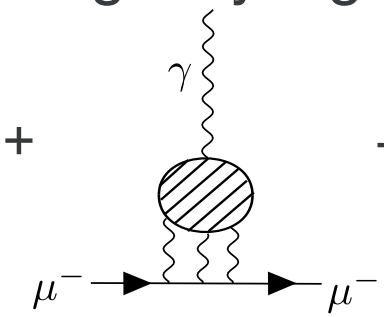

+

Electroweak

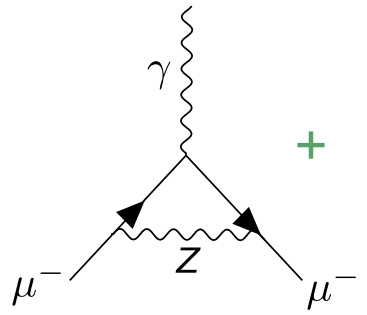

+

The Standard Model

Encodes all known particles and interactions

Quantum Electrodynamics QED

Over 12’000 QED diagrams (5 loops) calculated, extraordinary precision

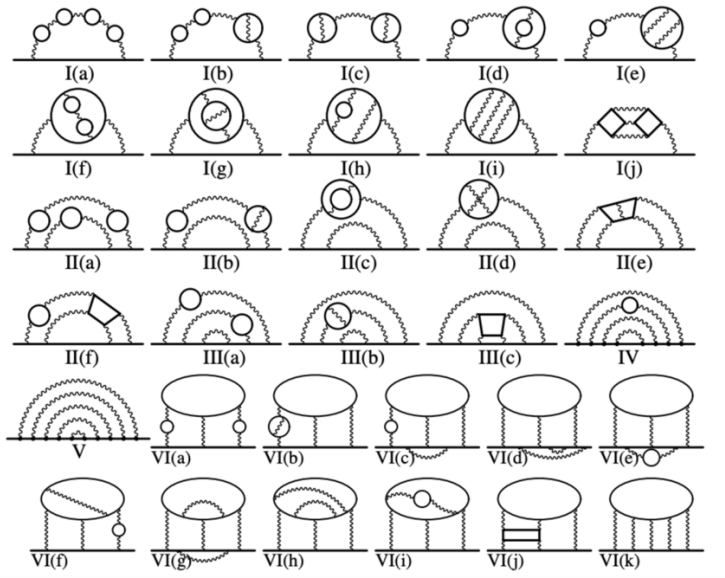

https://arxiv.org/abs/1205.5370

Interactions with **virtual particles** alter **g**

Dirac-Term (2)

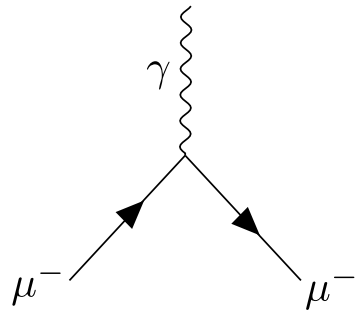

QED

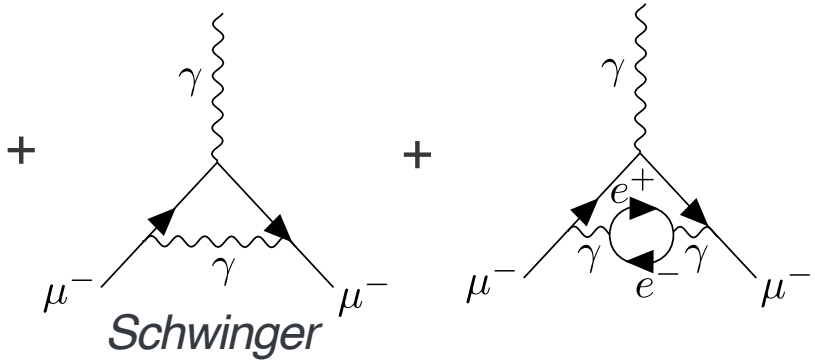

Hadronic Vacuum Polarization

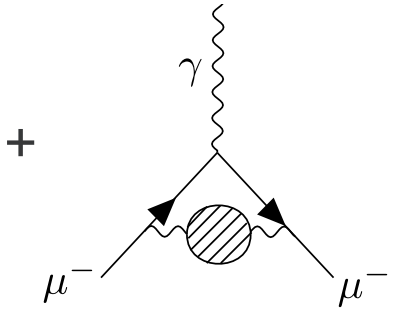

Hadronic Light-by-Light

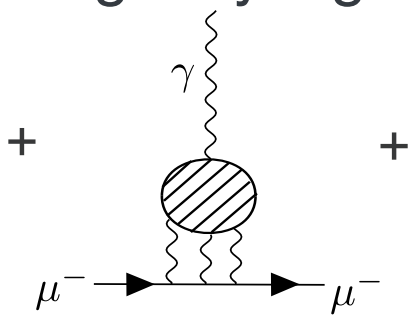

Electroweak

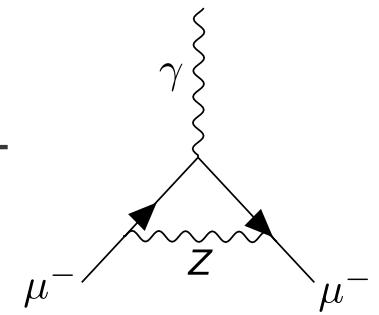

Hadronic Vacuum Polarization: HVP Data-driven Dispersive Approach

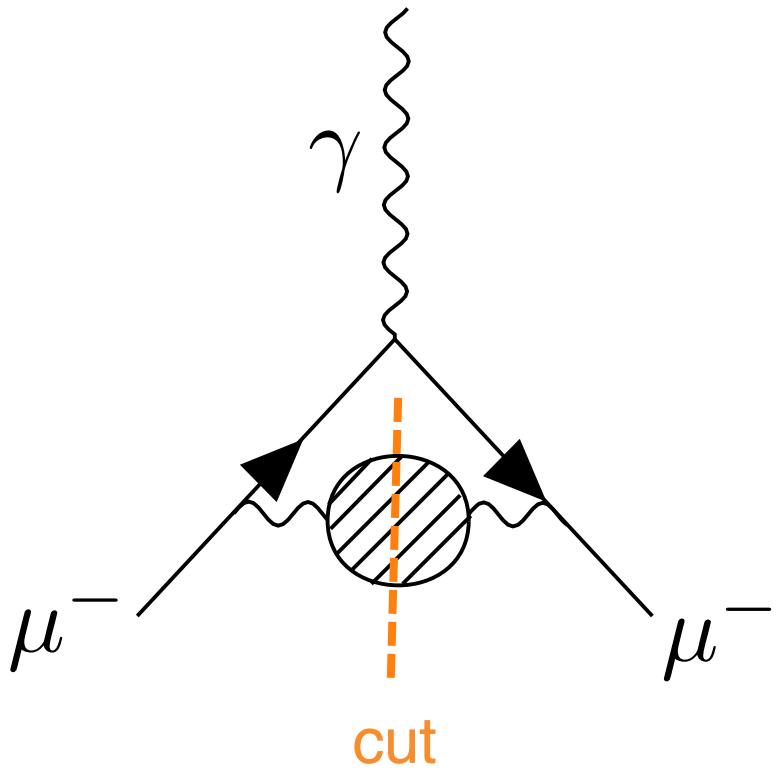

Hadronic Vacuum Polarization: HVP Data-driven Dispersive Approach

Dispersion relation connects $e^+e^- \to hadrons$ to leading order HVP contribution

$$a_\mu^{\mathrm{HVP,LO}} = \frac{\alpha^2}{3\pi^2}\int_{s_{th}}^{\infty}\frac{K(s)}{s}R(s)ds$$

$$R(s) = \frac{\sigma(e^+e^- \to hadrons)}{\sigma(e^+e^- \to muons)}$$

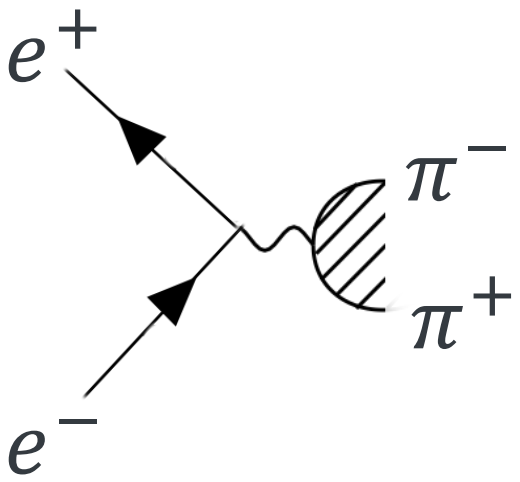

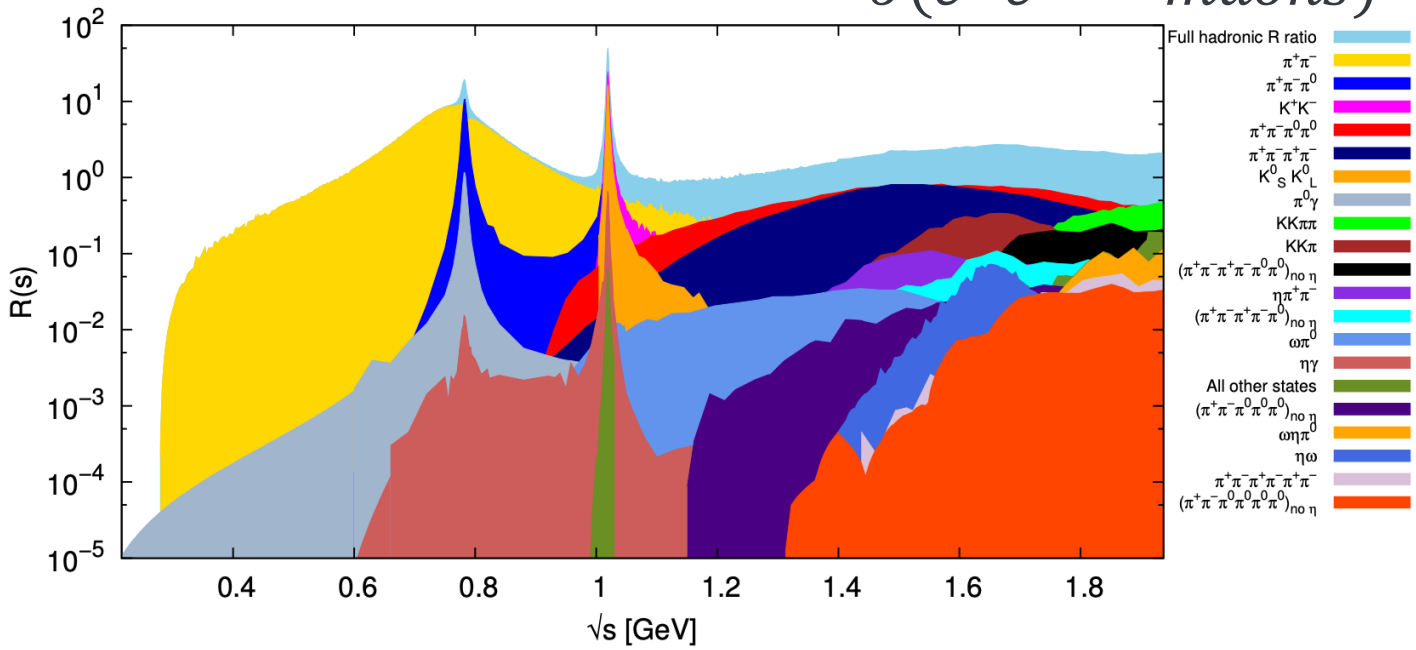

Figure 16: Contributions to the KNT data compilation of the total hadronic *R*-ratio from the different hadronic final states below 1.937 GeV [30, 265]. The full *R*-ratio is shown in light blue. Each final state is included as a new layer on top in decreasing order of the size of its contribution to $a_\mu^{\mathrm{HVP,\,LO}}$.

https://arxiv.org/pdf/2505.21476

Hadronic Vacuum Polarization: HVP Lattice QCD

Ab-initio calculation with massive computing power

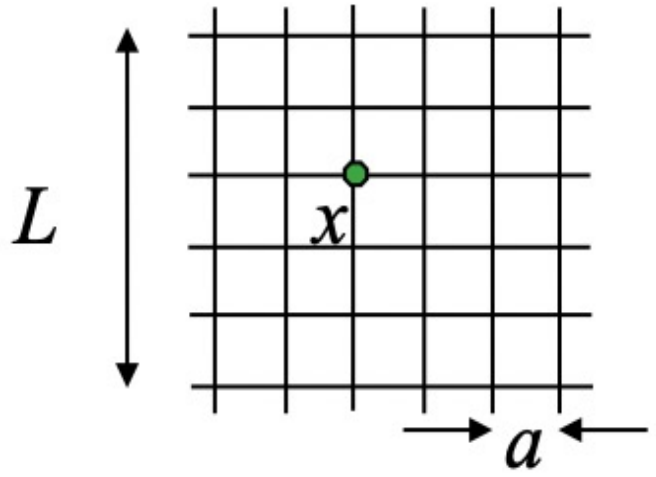

4D grid!

Calculated at supercomputers like Aurora at Argonne

Hadronic Vacuum Polarization: HVP
The pre-2021 view

data-driven dispersive

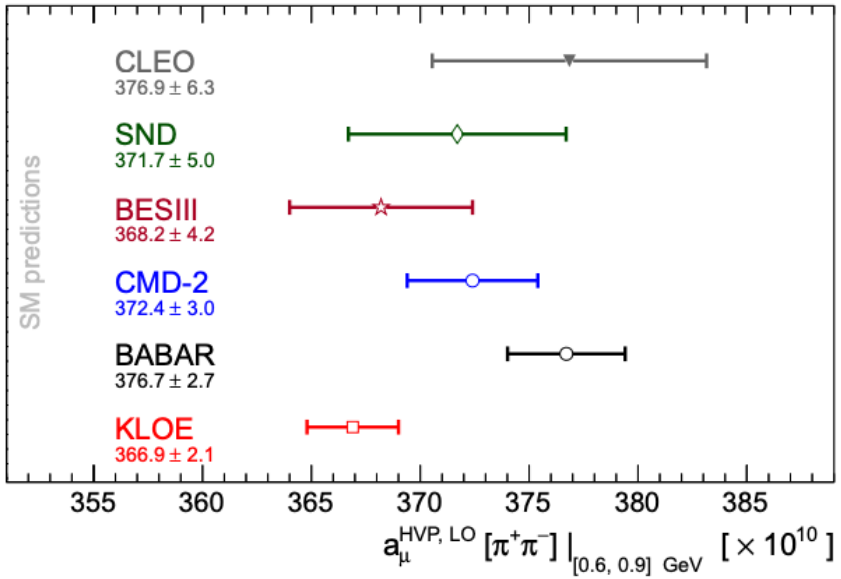

a flurry of experiments, different technique, some inconsistencies

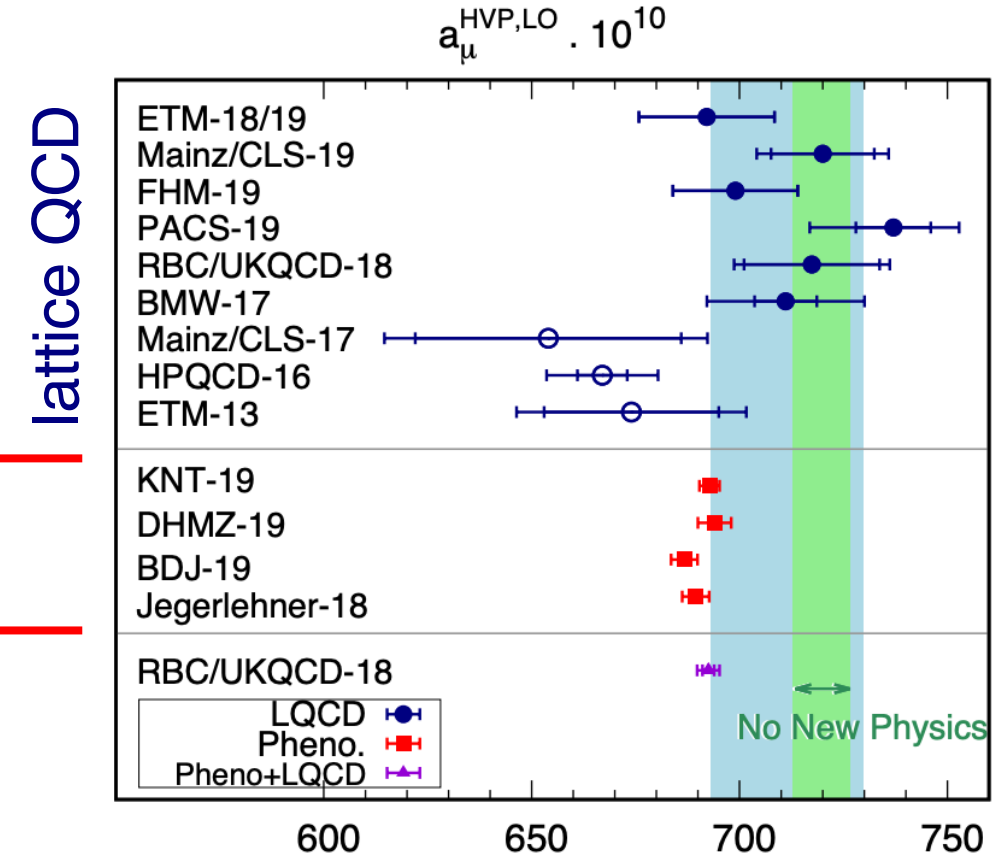

Figure 44: Compilation of recent results for $a_\mu^{HVP,\,LO}$ in units of 10^{-10}. The filled dark blue circles are lattice results that are included in the "lattice world average". The average, which is obtained from a conservative averaging procedure in Sec. 3.5.1, is indicated by a light blue band, while the light-green band indicates the "no new physics" scenario, where $a_\mu^{HVP,\,LO}$ results are large enough to bring the SM prediction of a_μ into agreement with experiment. The unfilled dark blue circles are lattice results that are older or superseded by more recent calculations. The red squares indicate results obtained from the data-driven methods reviewed in Sec. 2. See Table 8 for more information on the results included in the plot. Adapted from Ref. [443].

https://arxiv.org/pdf/2006.04822

https://arxiv.org/pdf/2505.21476

Hadronic Vacuum Polarization: HVP The

data-driv

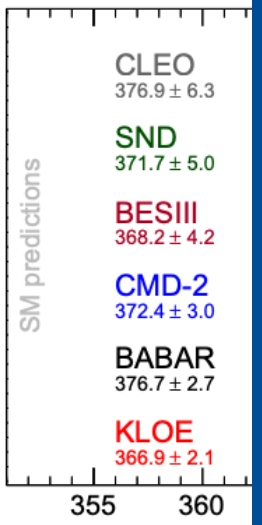

a flurry o
different
inconsist

~100 ppb (parts-per-billion)

- 8 significant digits or

weighting a Bison

has someone added a sunflower seed?

are included in the "lattice
light blue band, while the
ction of a_μ into agreement
. The red squares indicate
uded in the plot. Adapted

from Ref. [443].

https://arxiv.org/pdf/2006.04822

https://arxiv.org/pdf/2505.21476

Testing the Standard Model

Interactions with **virtual particles** alter **g**

QED

Dirac-Term (2)

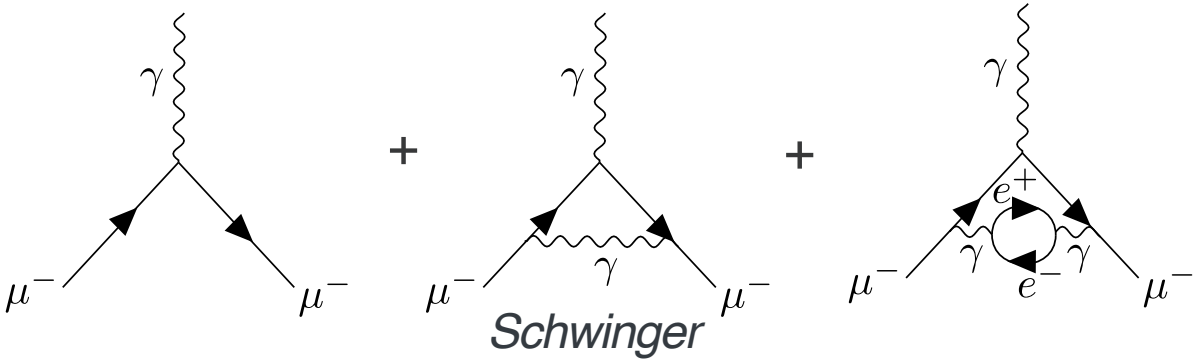

Hadronic Vacuum Polarization

Hadronic Light-by-Light

Electroweak

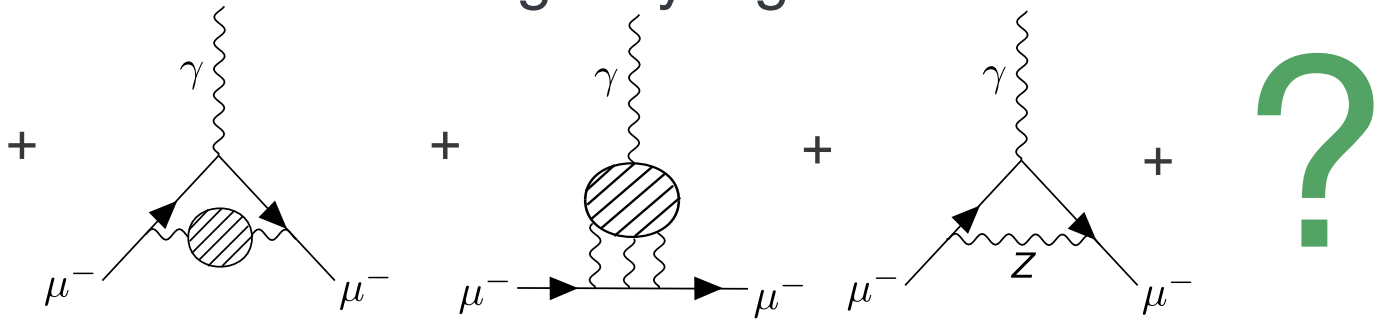

?

≠

?

Experiments measure the sum of all contributions

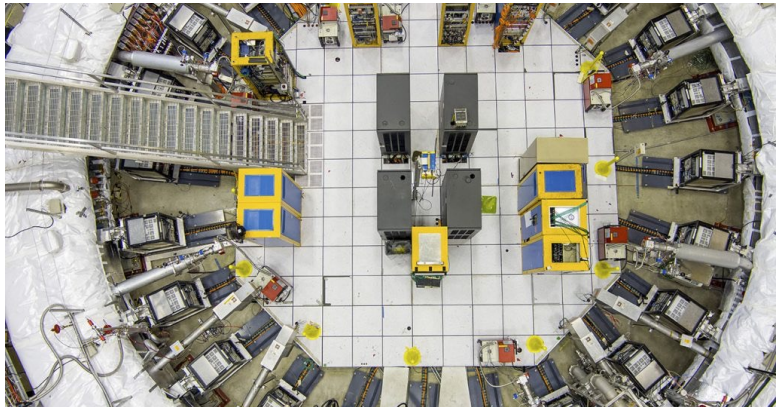

Muons, Why?

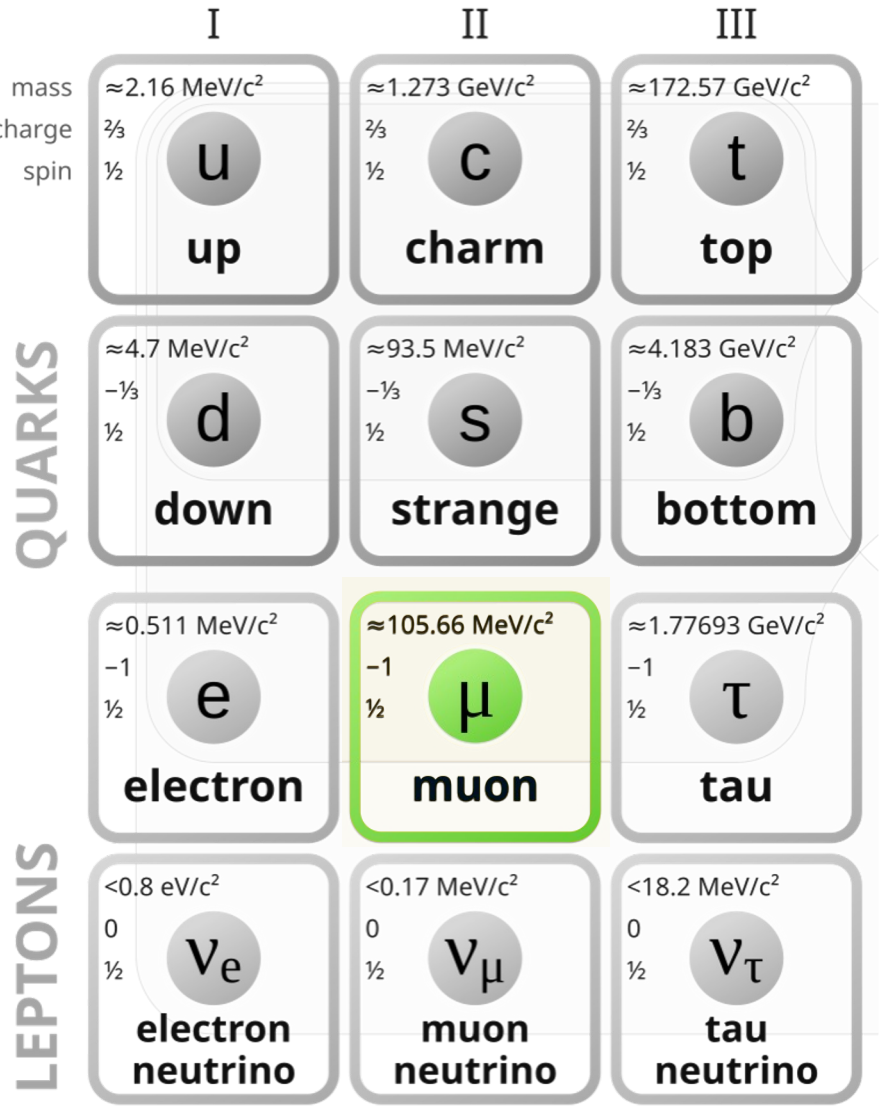

207 times more massive

Sensitivity of g-2 to heaver particles (M)

scales with $\left(\frac{m_l}{M}\right)^2$

$$\left(\frac{m_\mu}{m_e}\right)^2 \cong 43{,}000$$

Today: g_e has been measured to 0.13 ppt (!)

g_μ 3 orders of magnitude less precise

$\rightarrow$ g_μ still ~38 times more sensitive to heavy New Physics

Muons, Why?

Self-analyzing (parity-violating)
Positrons are preferentially emitted in the direction of the muon's spin

Muon decay: $\mu \rightarrow e\,\overline{\nu}_e\,\nu_\mu$

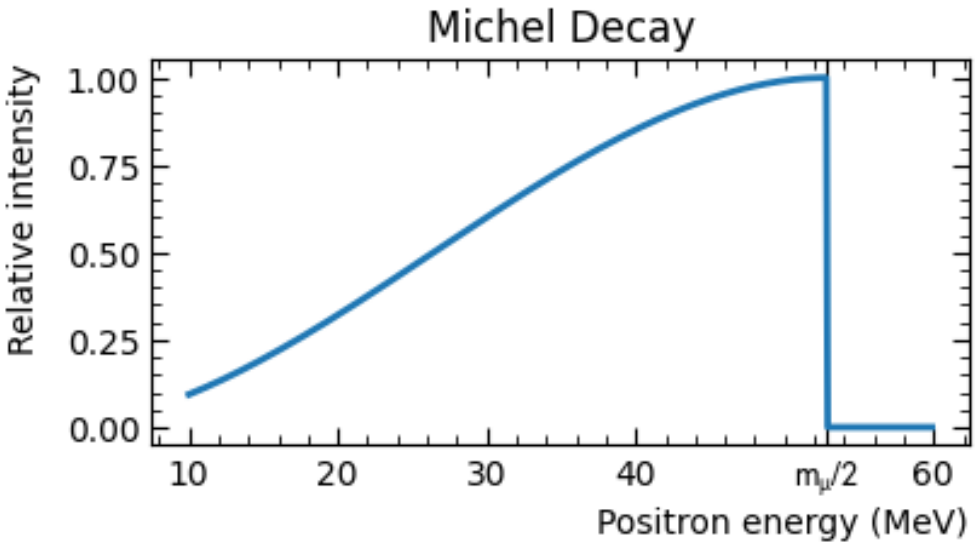

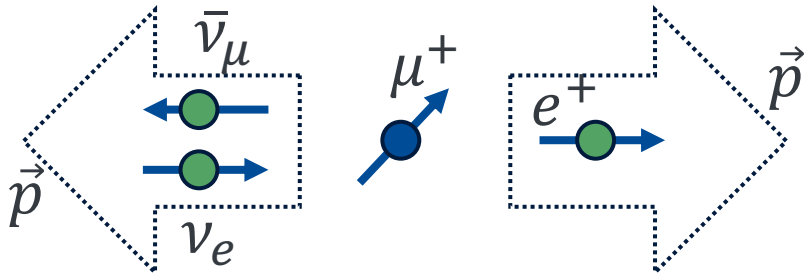

Weak force: parity violating

- Produces "right-handed" anti-particles, spin aligned with momentum
- Produces "left-handed" particles, spin anti-aligned with momentum

Muons, Why?

Self-analyzing (parity-violating)
Positrons are preferentially emitted in the direction of the muon's spin

Muon decay: $\mu \rightarrow e\,\overline{\nu}_e\,\nu_\mu$

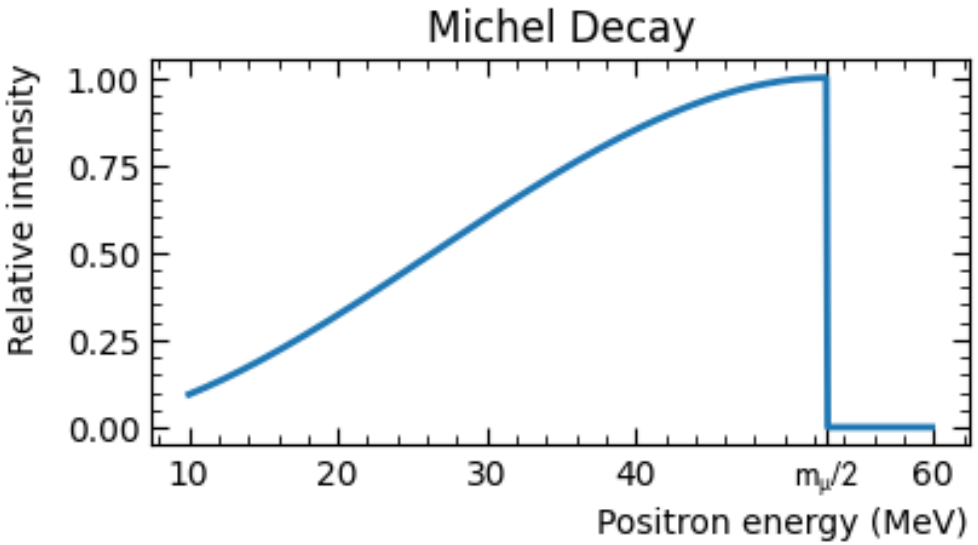

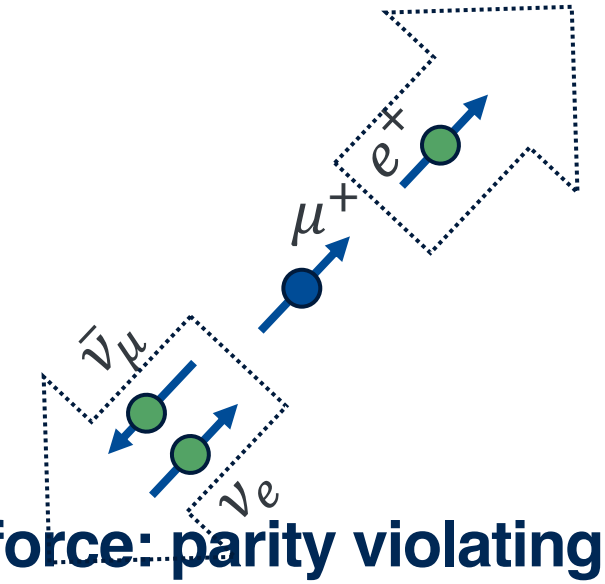

Weak force: parity violating

- Produces "right-handed" anti-particles, spin aligned with momentum
- Produces "left-handed" particles, spin anti-aligned with momentum

Muons, Why?

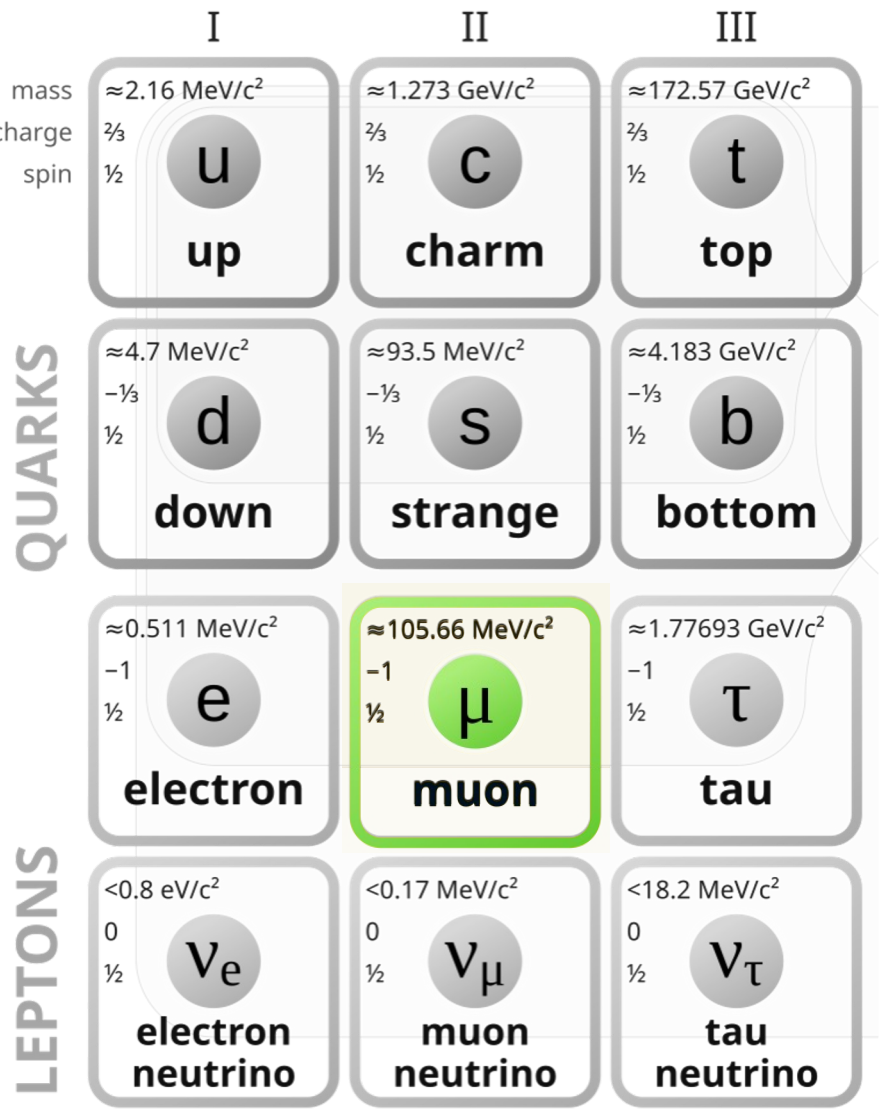

207 times more massive
than electrons, **more sensitive** to virtual particles

Self-analyzing (parity-violating)
Positrons are preferentially emitted in the direction of the muon's spin

High Statistics
Feasible to produce at particle accelerators, lifetime of 2.2 μs allows to measure spin precession

Muon g–2?

all corrections

$$g_\mu = 2.00233184143(290)$$

$$g_\mu - 2$$

Muon Anomaly:

$$a_\mu \equiv \frac{g_\mu - 2}{2}$$

Measure Muon g–2 to test the Standard Model

Standard Model
components to $g_\mu - 2$

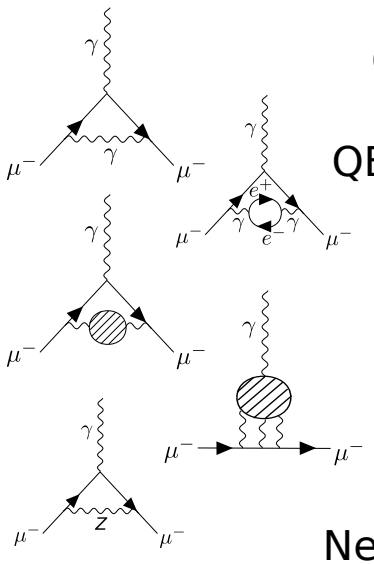

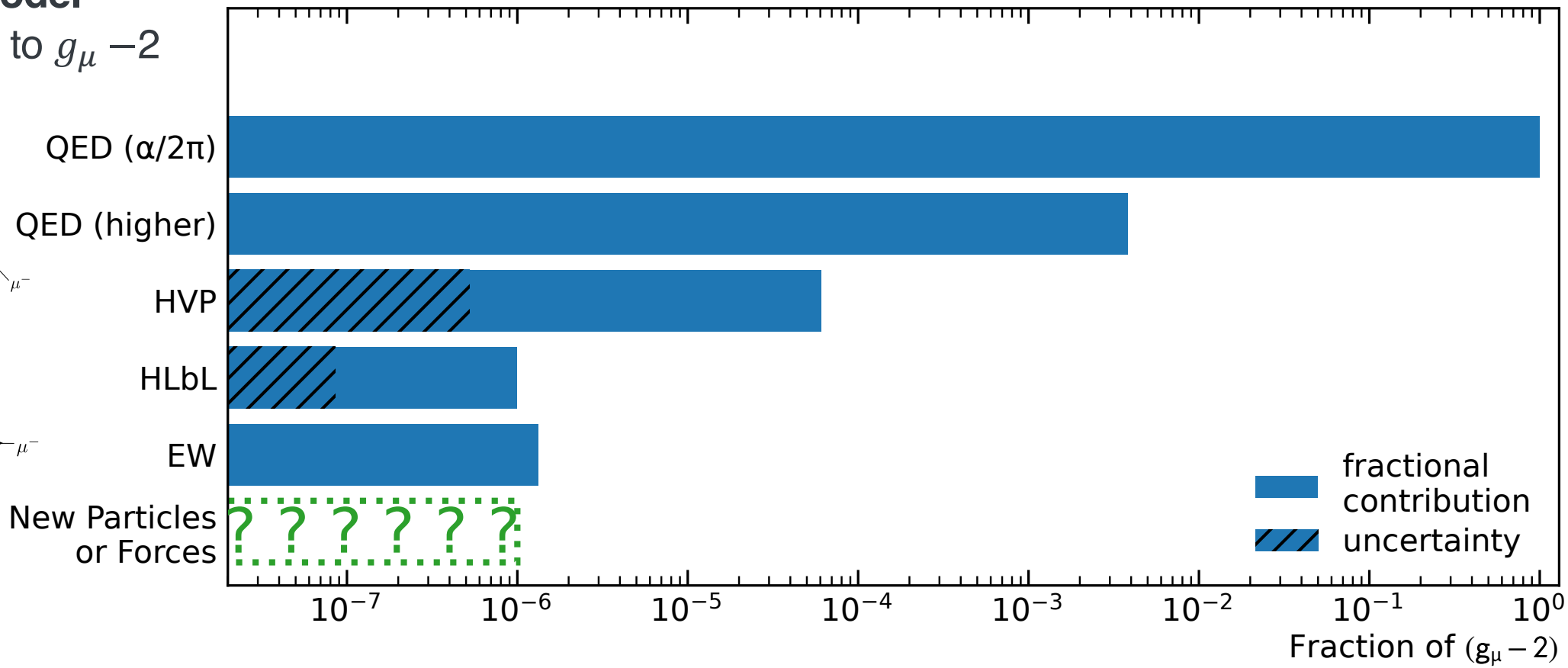

Measure Muon g–2 to test the Standard Model

Standard Model
components to $g_\mu - 2$

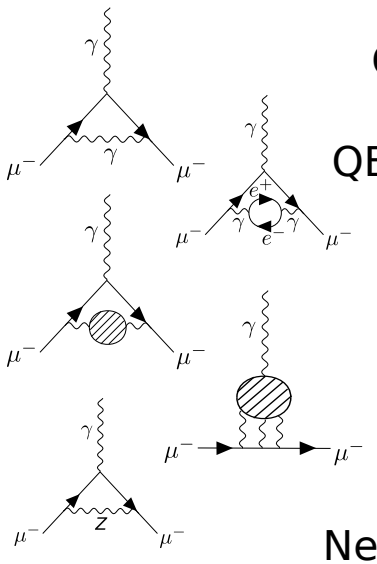

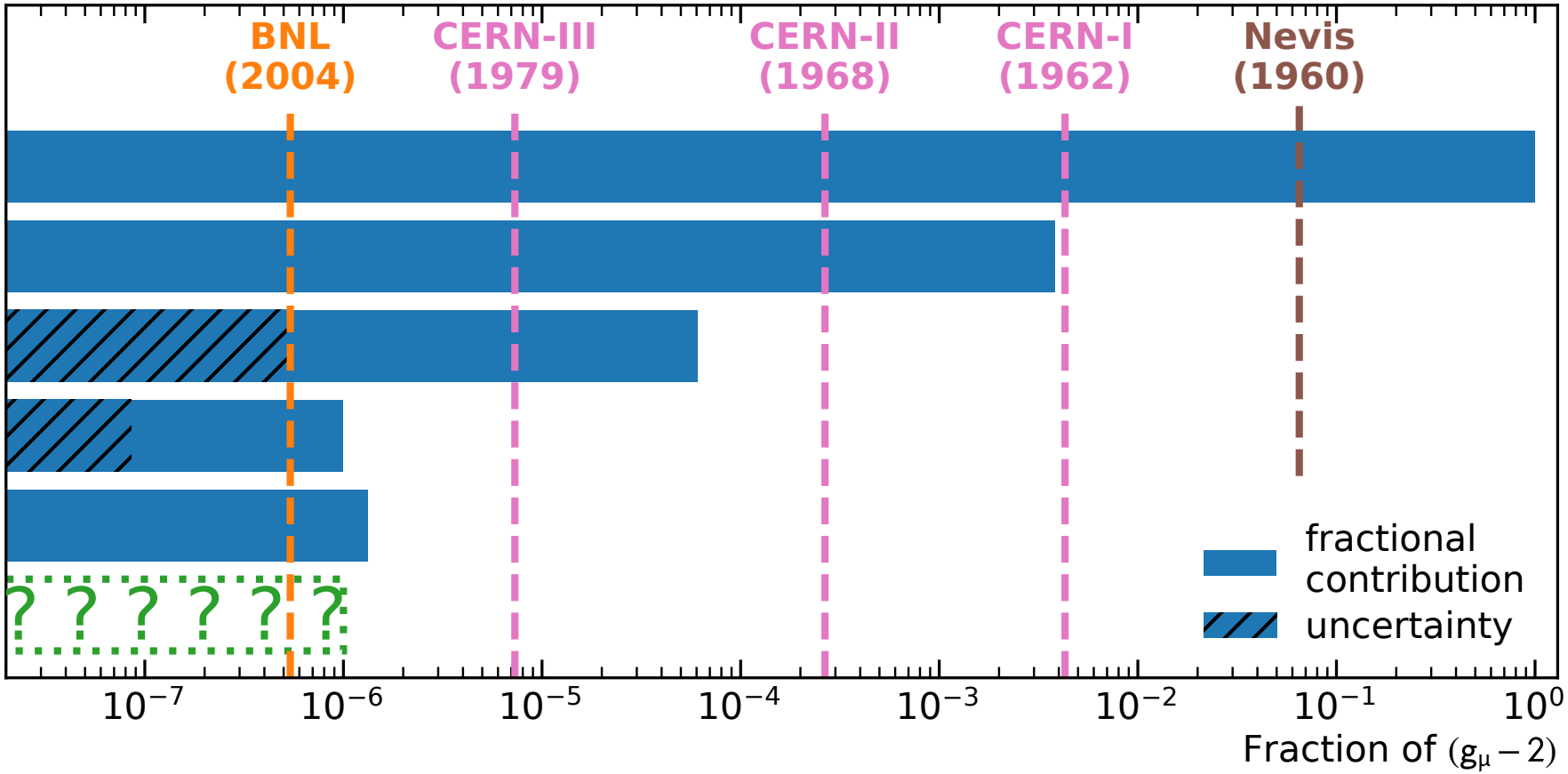

Measure Muon g–2 to test the Standard Model

Standard Model
components to $g_\mu - 2$

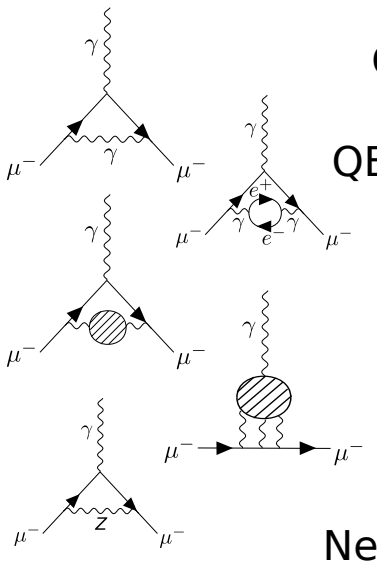

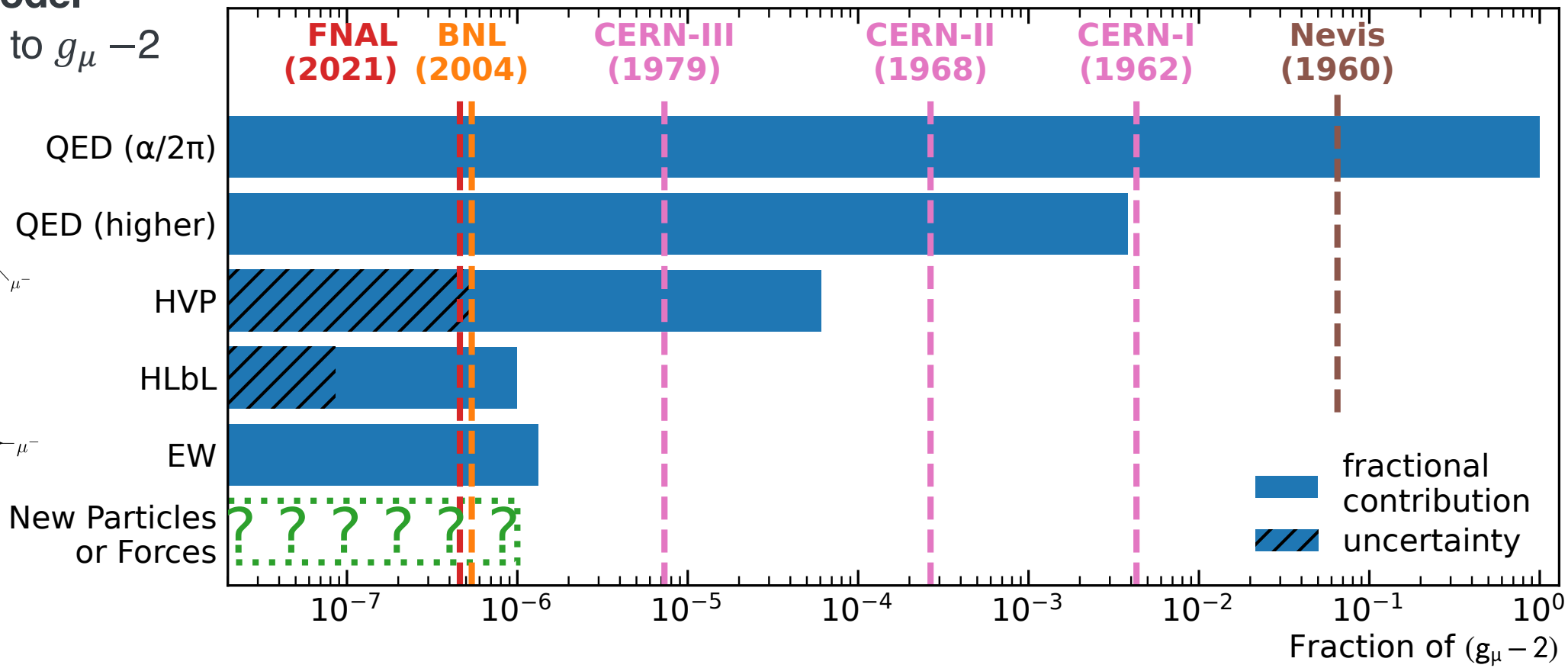

2021: Muons made News!

Measure Muon g–2 to test the Standard Model

Standard Model
components to $g_\mu - 2$

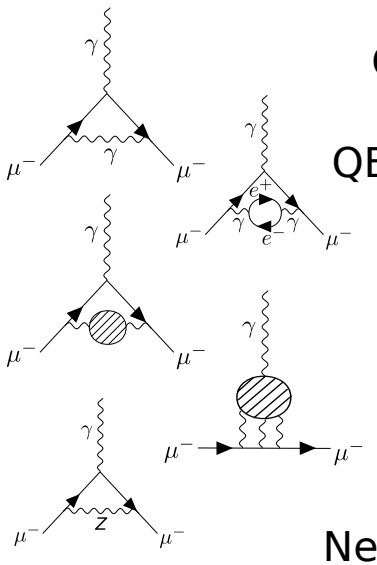

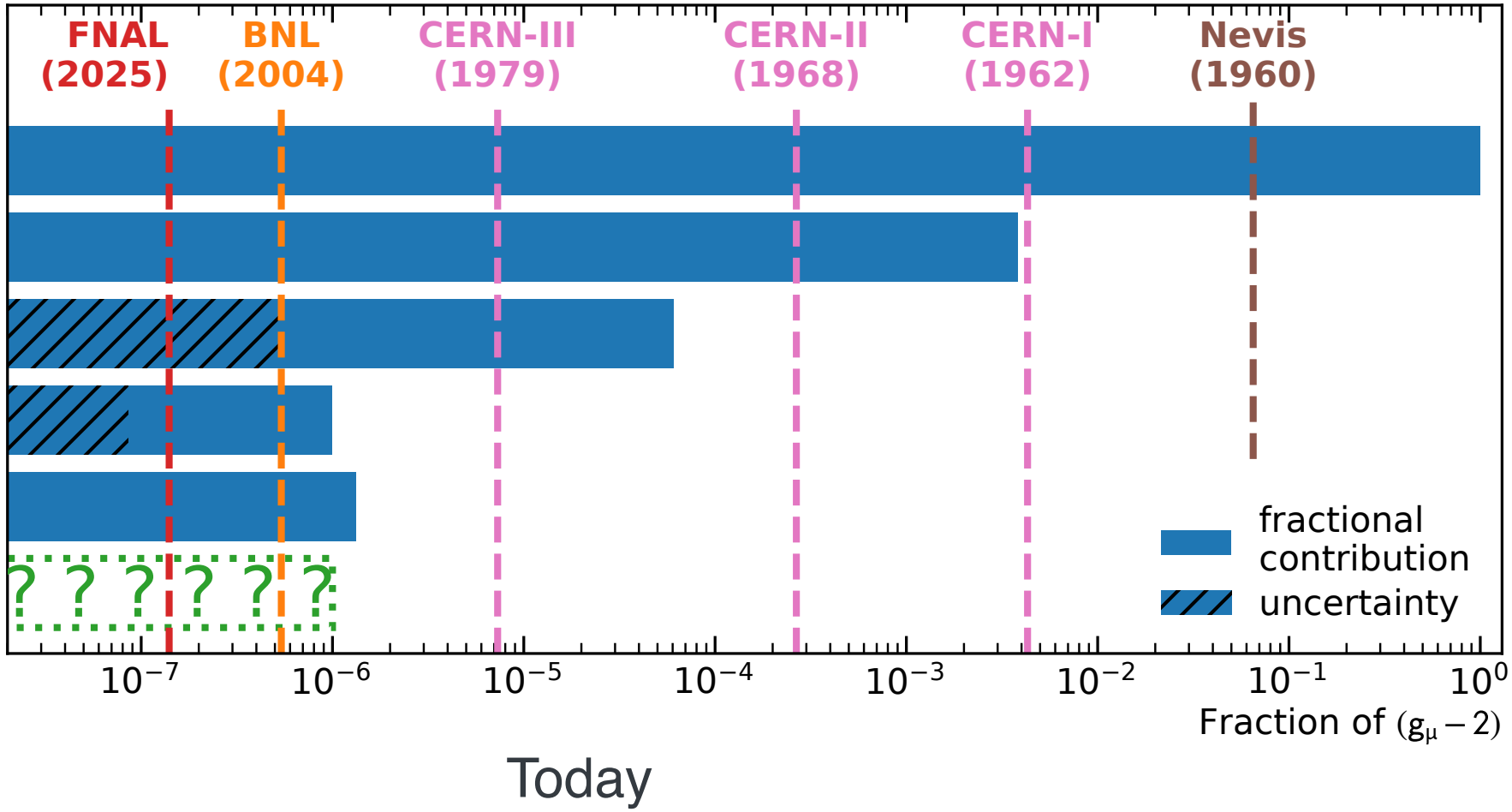

Measurement

Muon Spin precession in uniform magnetic field

Spin:

$$\vec{\omega}_s = \frac{g_\mu}{2}\frac{e}{mc}\vec{B}$$

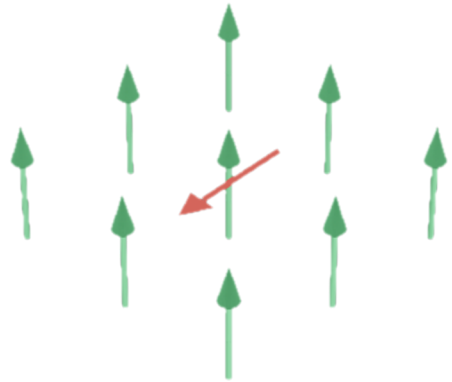

Measurement Principal

Store **Polarized Muons**

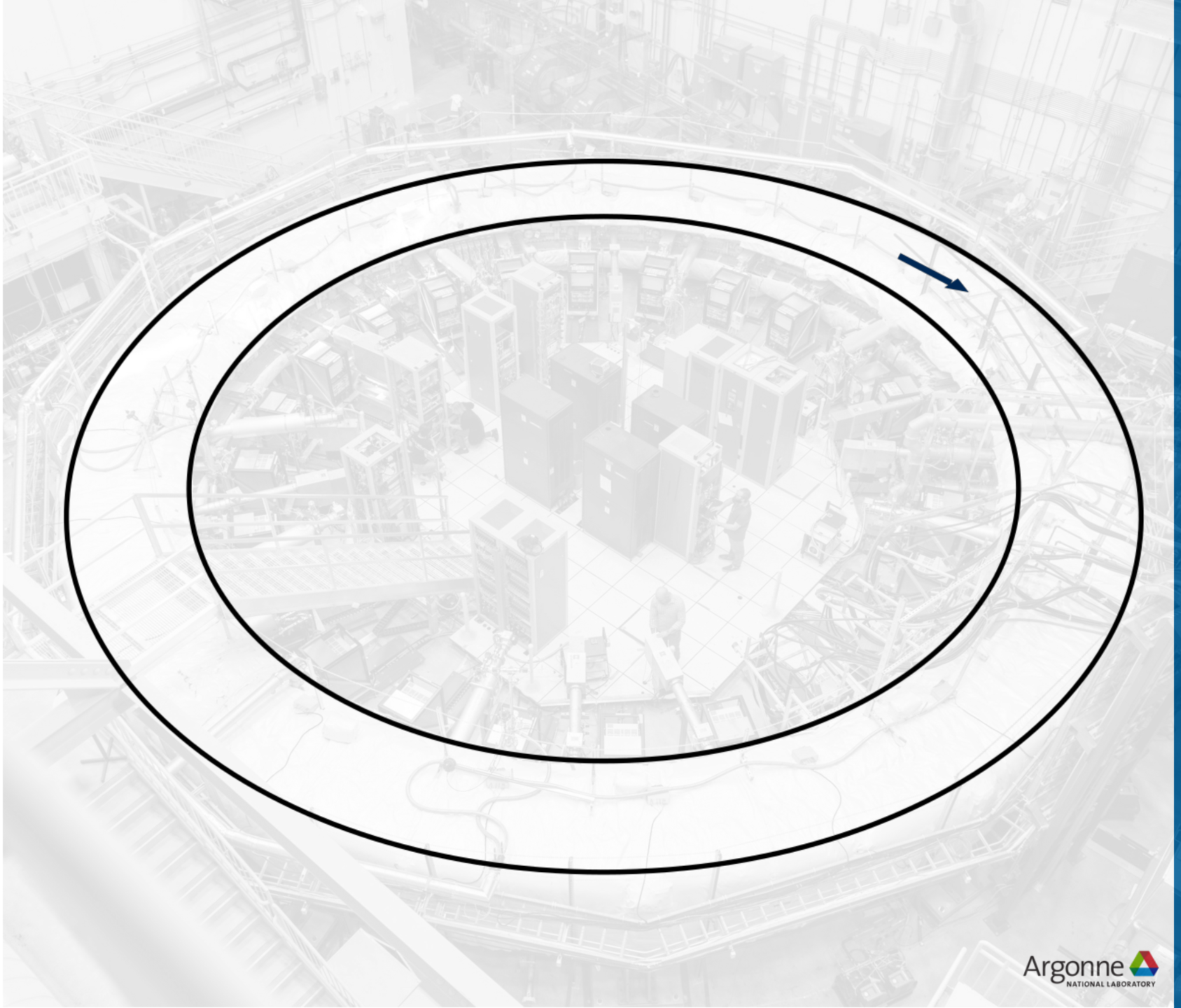

Measurement Principal

Store **Polarized Muons** in a **Dipole Magnetic Field**

Momentum: ⟶

$$\vec{\omega}_c = \frac{e}{mc}\vec{B}$$

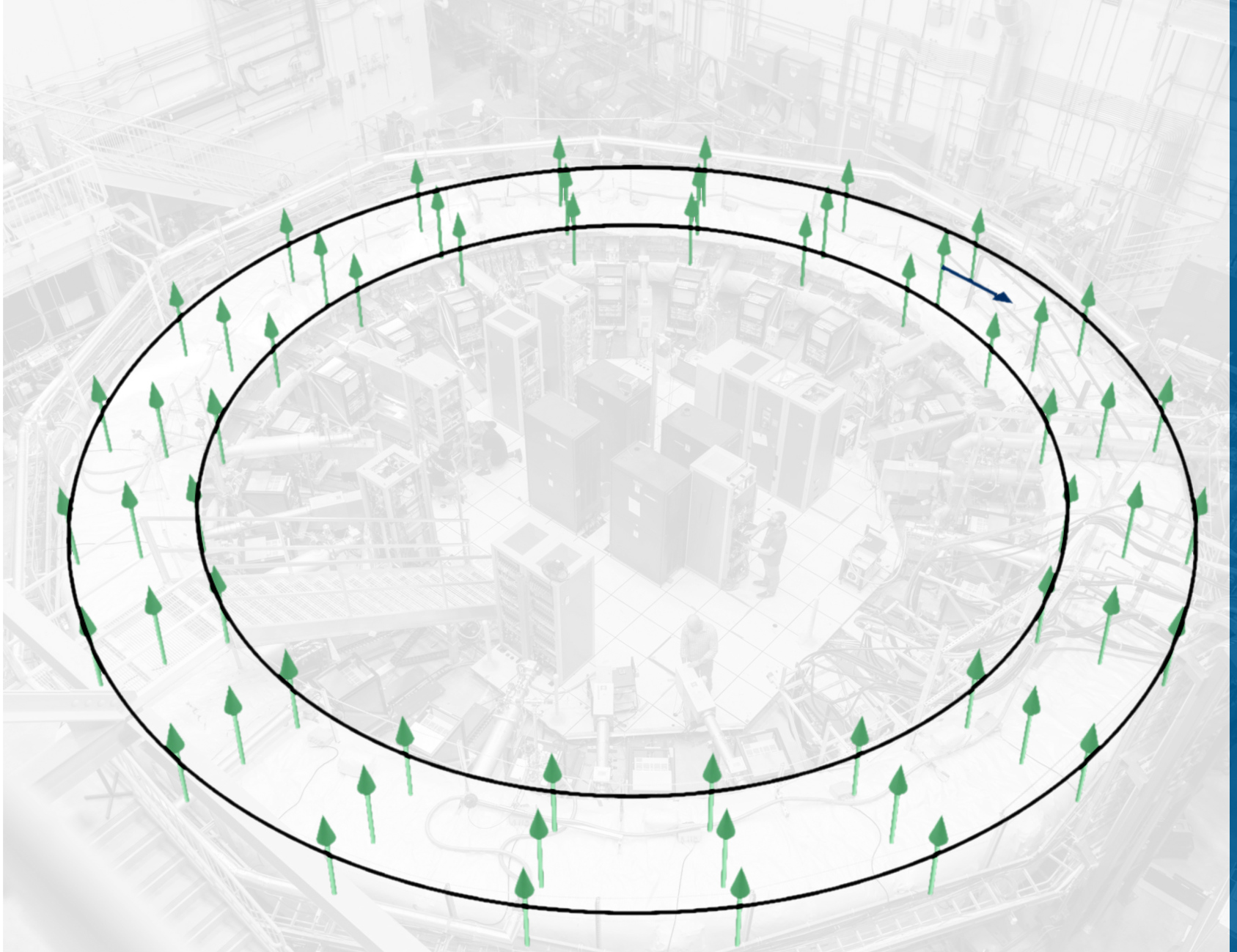

Measurement Principal

Store **Polarized Muons** in a **Dipole Magnetic Field**

Momentum: ⟶

$$\vec{\omega}_c = \frac{e}{mc}\vec{B}$$

Spin: ⇢

$$\vec{\omega}_s = \frac{g_\mu}{2}\frac{e}{mc}\vec{B}$$

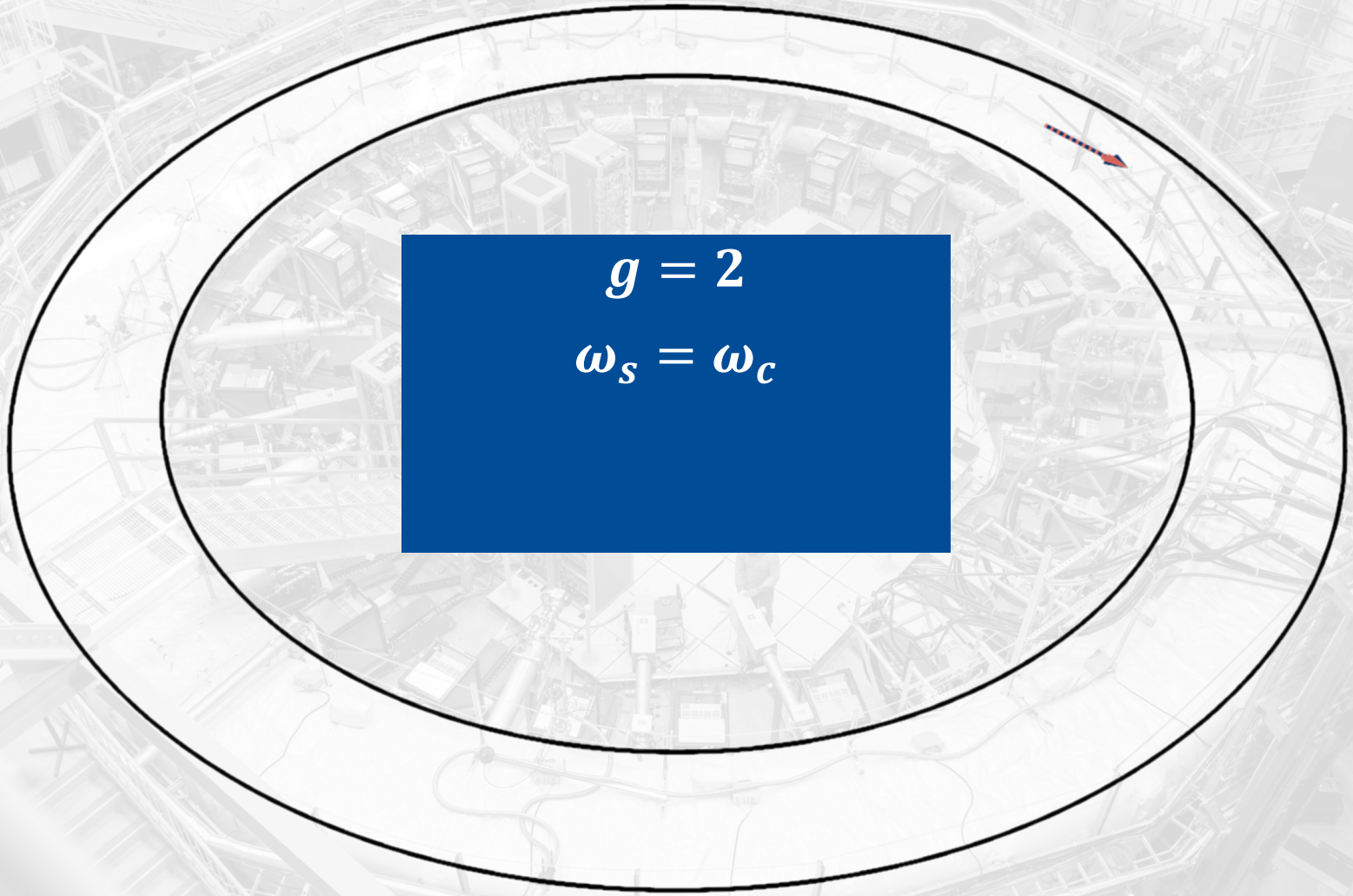

Measurement Principal

Store **Polarized Muons** in a **Dipole Magnetic Field**

Momentum: ⟶

$$\vec{\omega}_c = \frac{e}{mc}\vec{B}$$

Spin: ⇢

$$\vec{\omega}_s = \frac{g_\mu}{2}\frac{e}{mc}\vec{B}$$

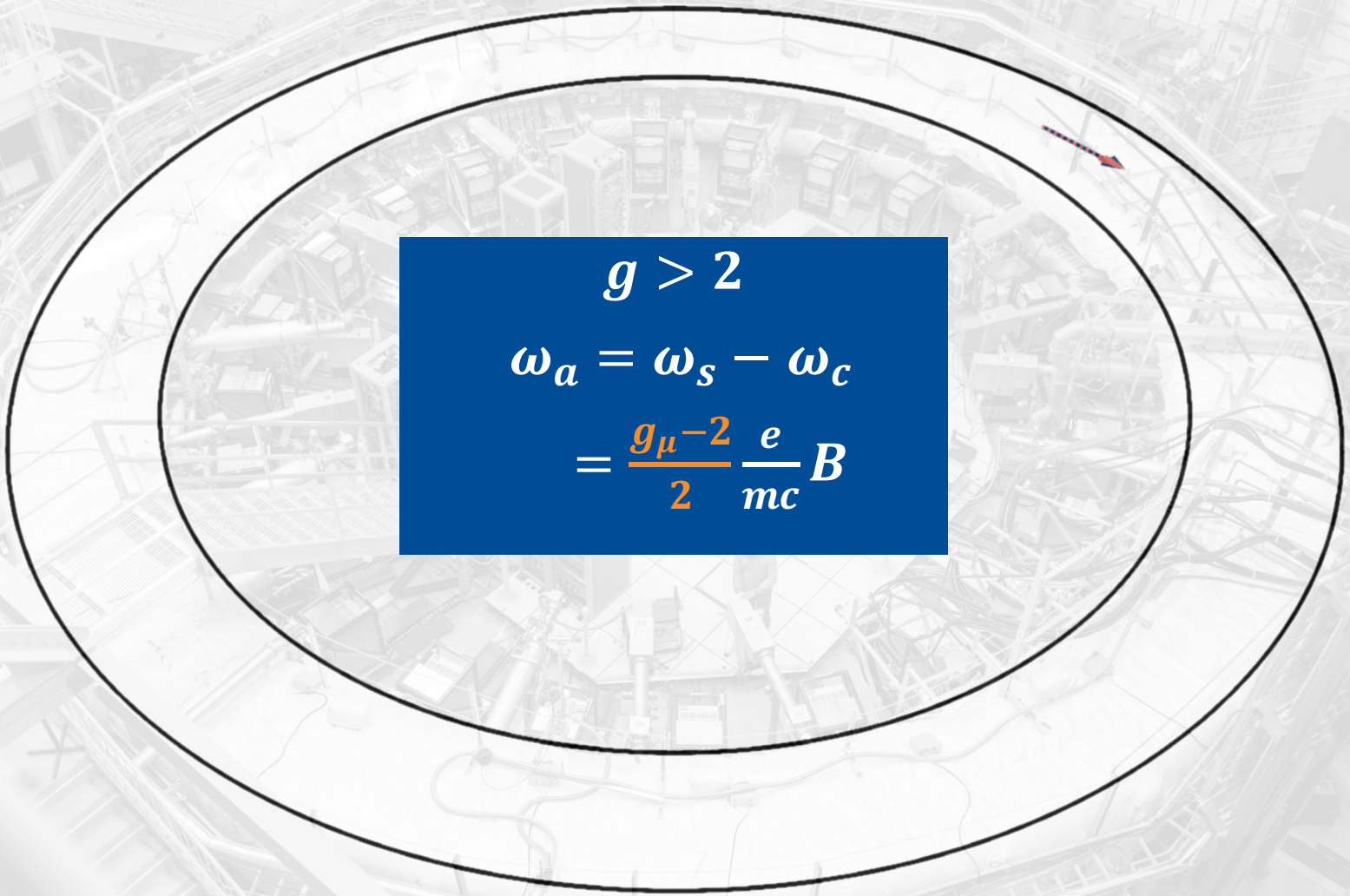

$$g > 2$$

$$\omega_a = \omega_s - \omega_c$$

$$= \frac{g_\mu - 2}{2}\frac{e}{mc}B$$

$$\boldsymbol{\omega_a = a_\mu \frac{e}{mc} B}$$

Measure: ω_a, B

Extract: a_μ

$$a_\mu \equiv \frac{g_\mu - 2}{2}$$

Magnetic Anomaly

$$\boldsymbol{\tilde{\omega}'_p = \gamma'_p B}$$

γ'_p: Gyromagnetic ratio of shielded **protons**

Measure the **magnetic field** in terms
the **precession frequency of protons**

Nuclear Magnetic Resonance (NMR)

Measuring the Spin Precession ω_a

Due to parity violation, “self-analyzing”,
the number of **high energy e⁺** oscillates as
the **μ⁺ spin** rotates

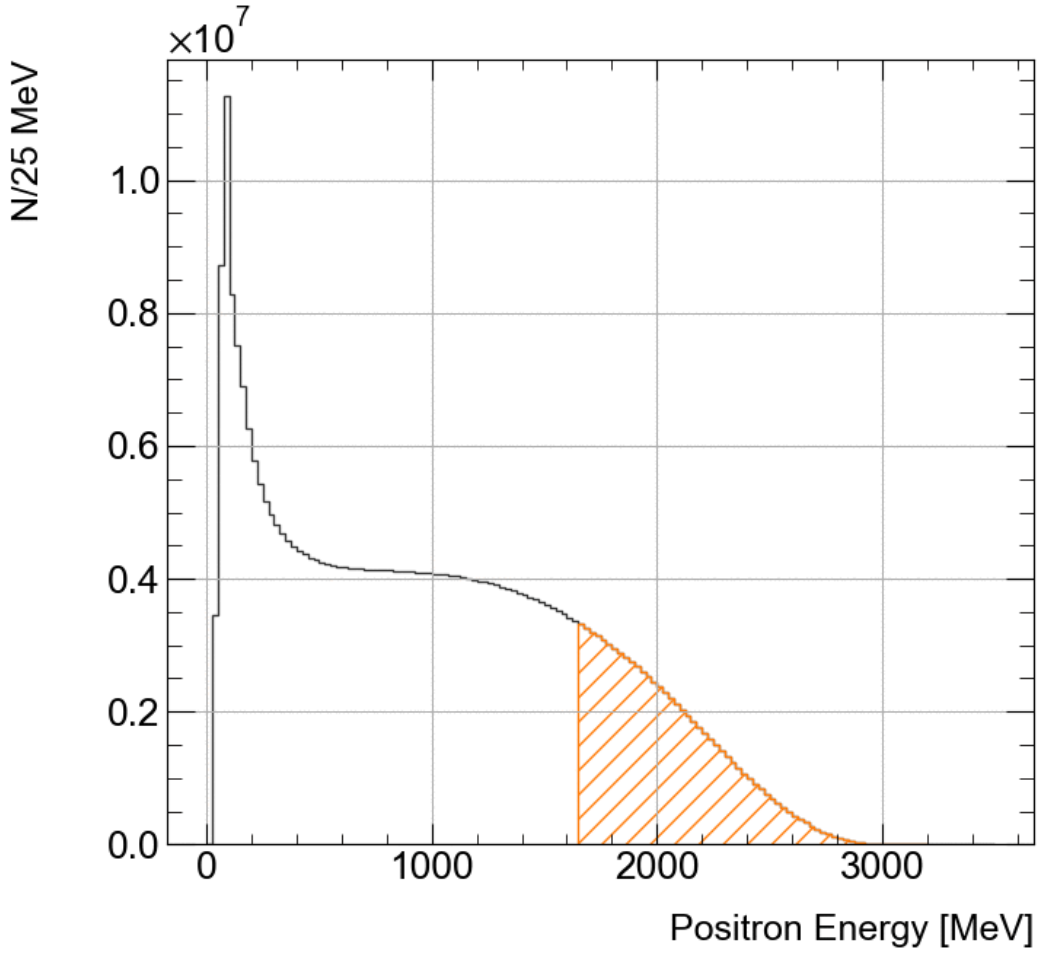

Measuring the Spin Precession ω_a

Simplest fit model captures **exponential decay** & **g-2 oscillation**

$$N(t) = N_0\, e^{-t/\tau}\,[1 + A\cos(\omega_a t - \phi_0)]$$

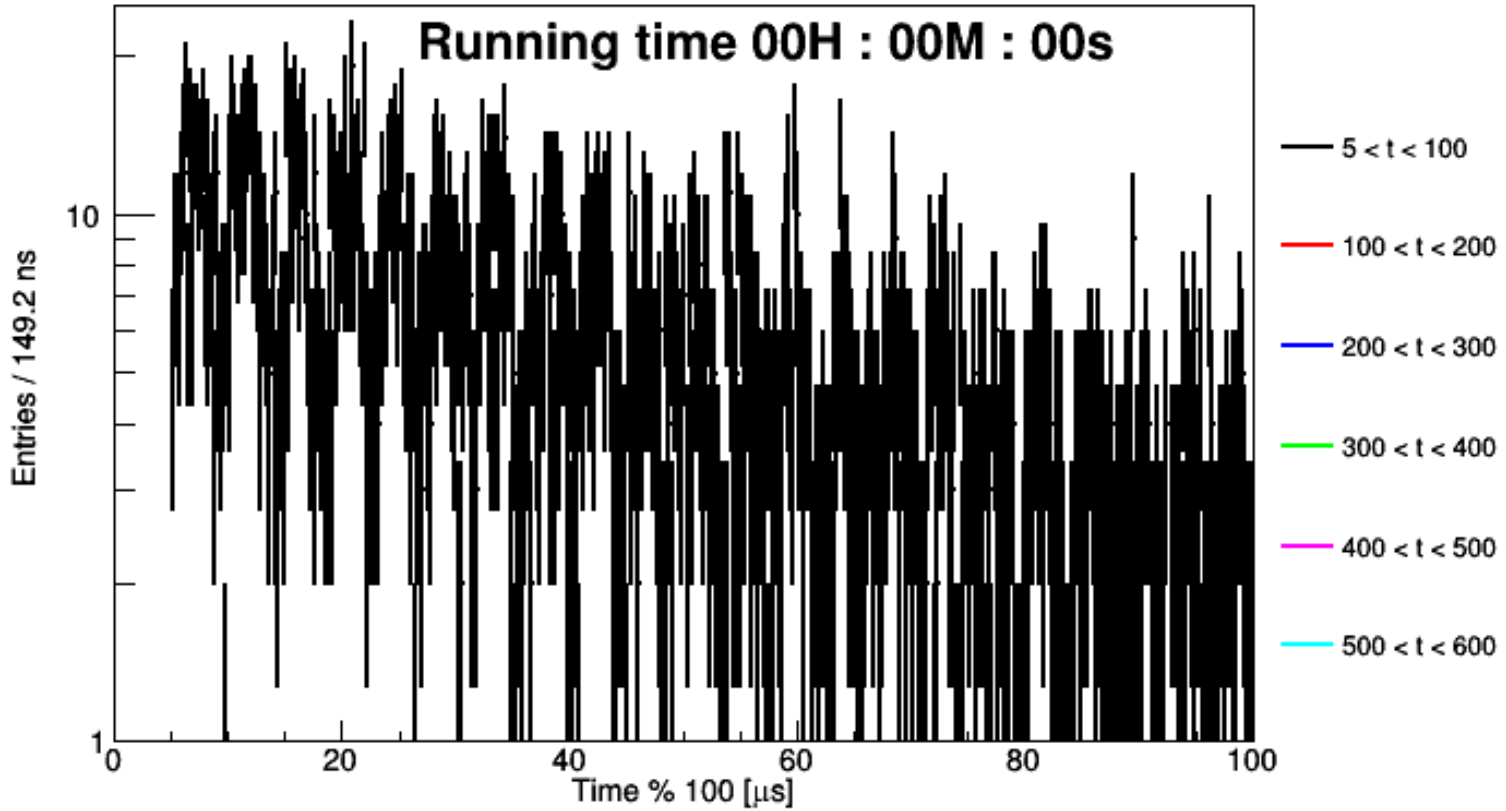

The Storage Ring Technique

CERN I (1962)

Direct measurement of

$a_\mu = \frac{g-2}{2}$

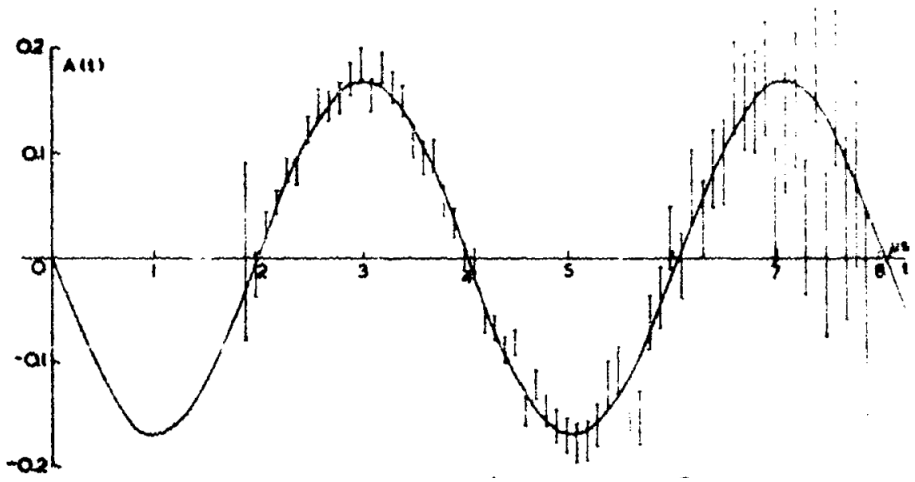

4’300’000 ppb

https://doi.org/10.1016/0031-9163(62)90263-9

CERN II (1968)

Pioneered Storage Ring technique, increased statistics!

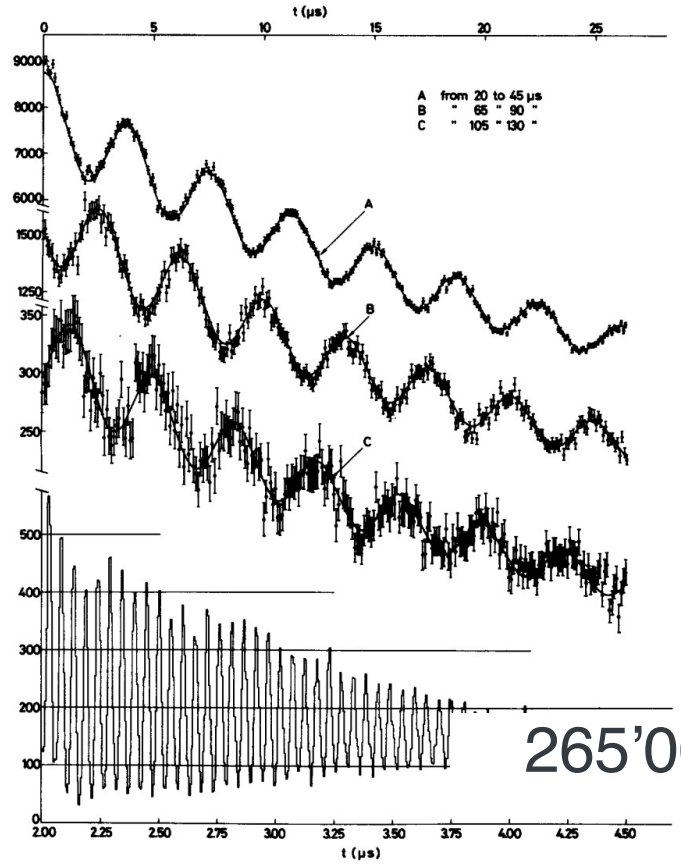

265’000 ppb

https://doi.org/10.1016/0370-2693(68)90261-X

The Magic Momentum

$$\overrightarrow{\omega_a} \approx \frac{e}{m}\left(a_\mu \vec{B} + \left(a_\mu - \frac{1}{\gamma^2 - 1} \right) \frac{\vec{\beta} \times \vec{E}}{c} \right)$$

~ 0

Measure: ω_a, B

Extract: a_μ

Magic Momentum: 3.1 GeV/c, $\gamma = 29.3$

Electric-Field term cancels

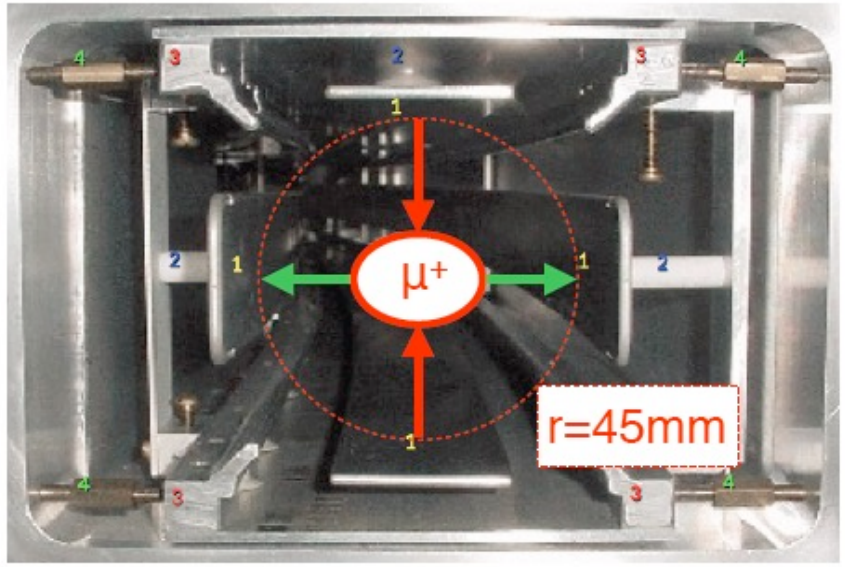

Focus muon beam with electric fields!

The Magic Momentum Era

CERN III (1979)

Pioneered Magic Momentum

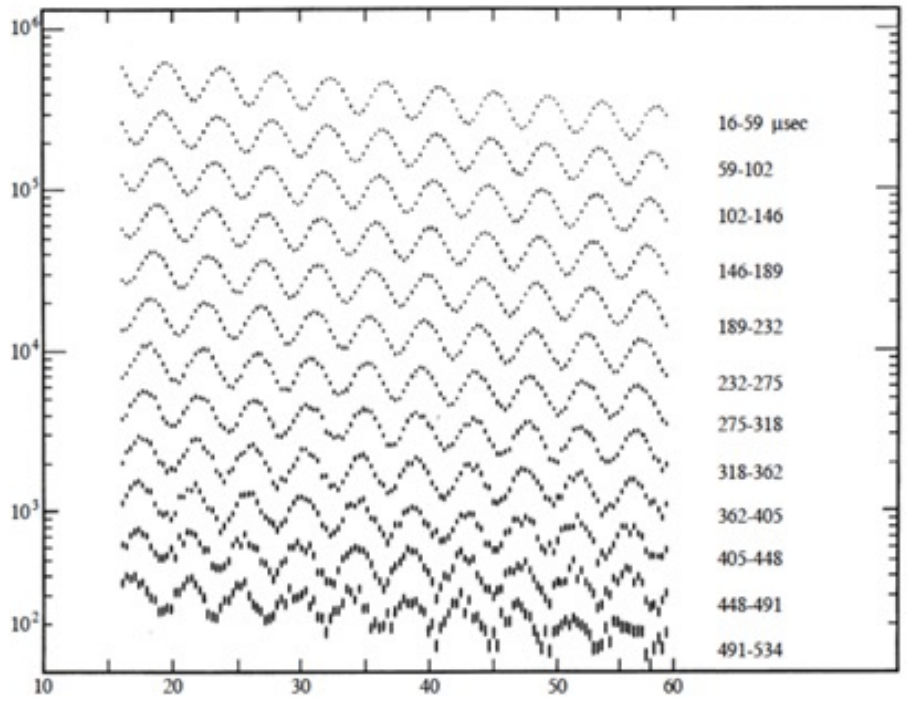

7’000 ppb

https://doi.org/10.1016/0550-3213(79)90292-X

BNL (2004)

Direct muon injection

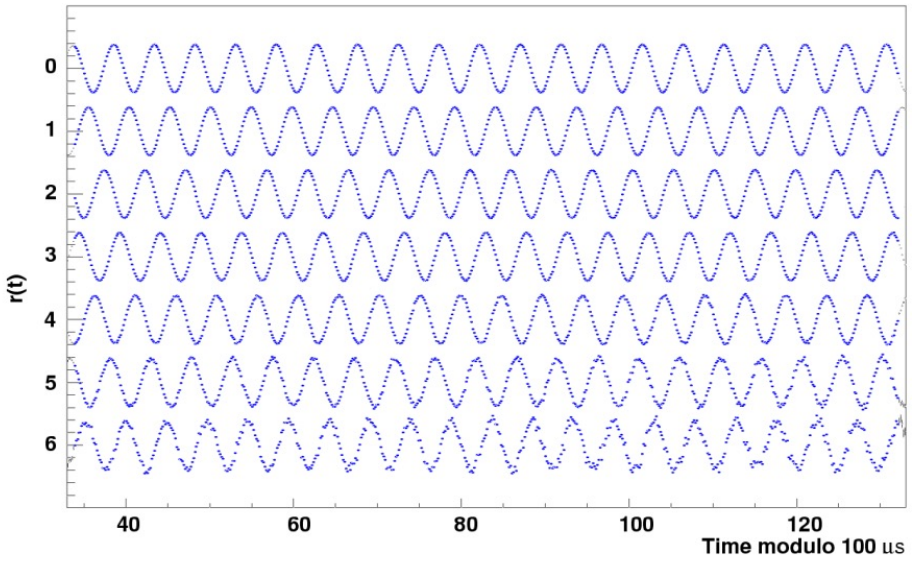

540 ppb

https://link.aps.org/doi/10.1103/PhysRevD.73.072003

2013: The Big Move

Credit: Fermi National Laboratory

Fermilab Muon Campus

Polarized 3.1 GeV/c
“magic momentum”
Muons to the **MC-1** building

from pions produced at the **target hall** (AP0) from 8 GeV/c protons from the Main Injector

2x8 bunches, every ~1.4s

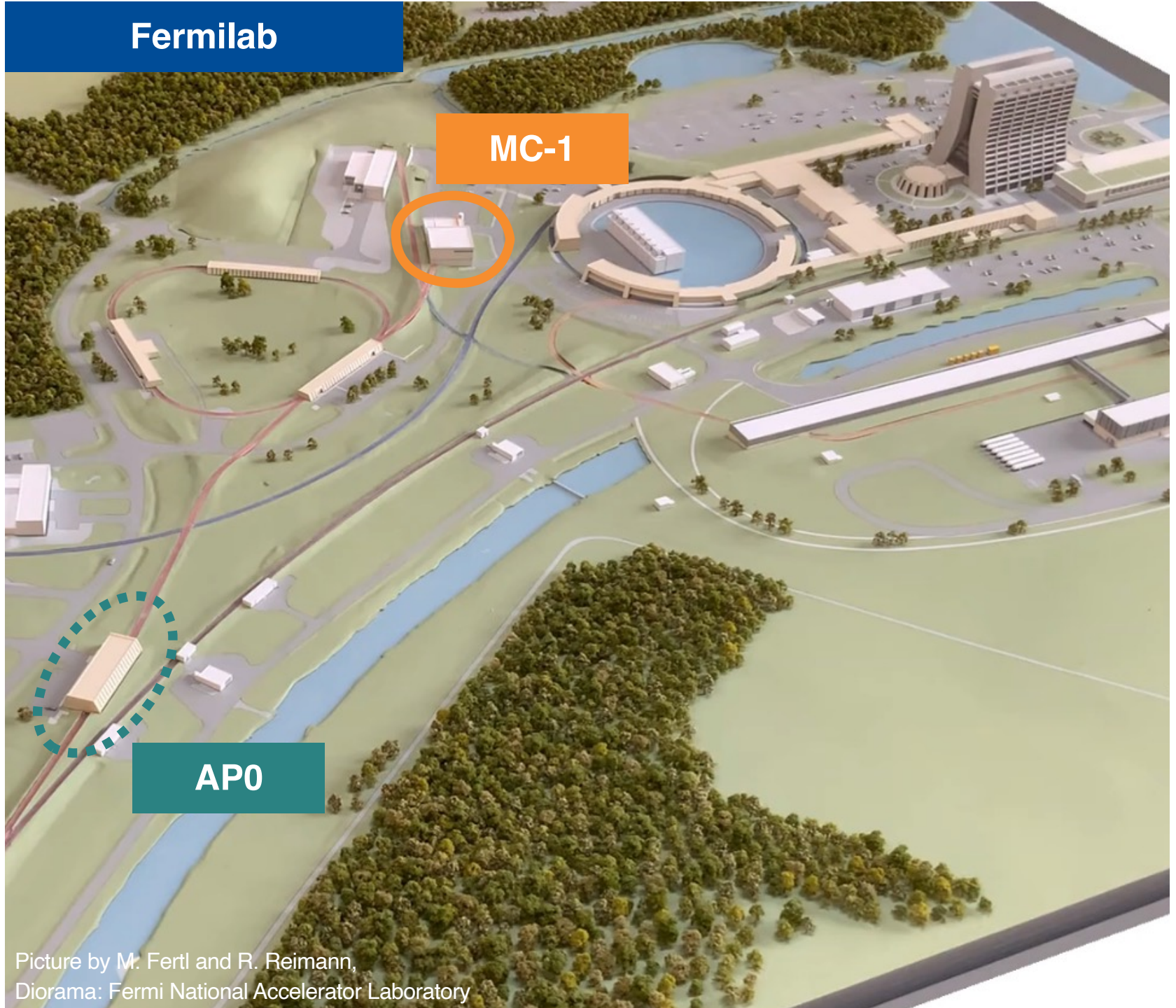

Picture by M. Fertl and R. Reimann,
Diorama: Fermi National Accelerator Laboratory

Measurement Principal

- Superconducting 1.45 T
- Designed and optimized for homogeneity

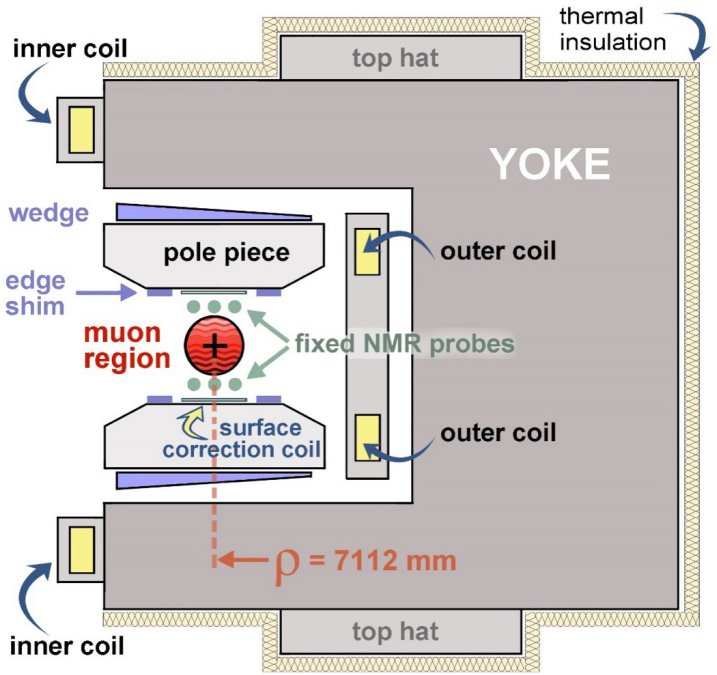

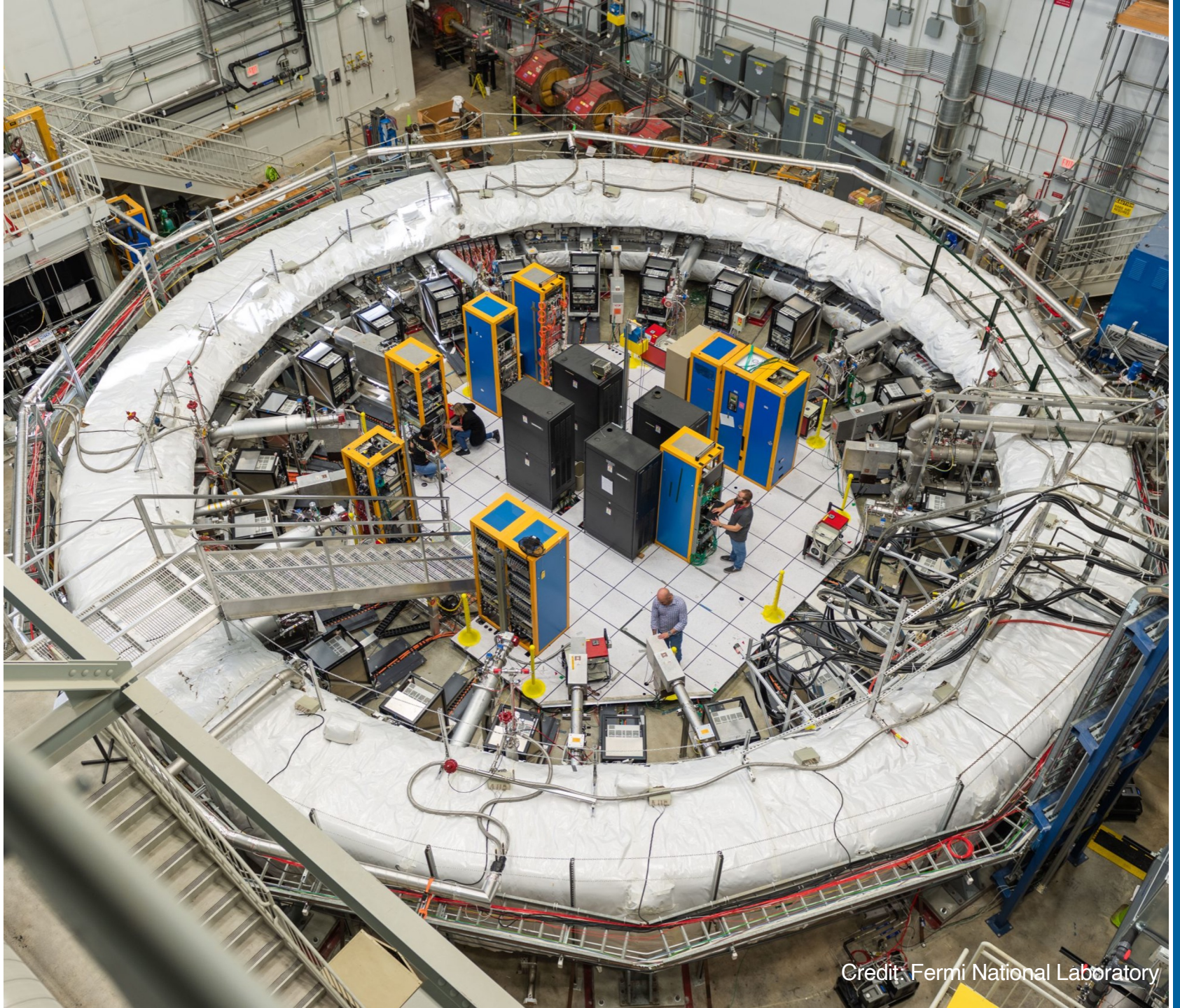

Credit: Fermi National Laboratory

Measurement Principal

- Superconducting 1.45 T
- Designed and optimized for homogeneity

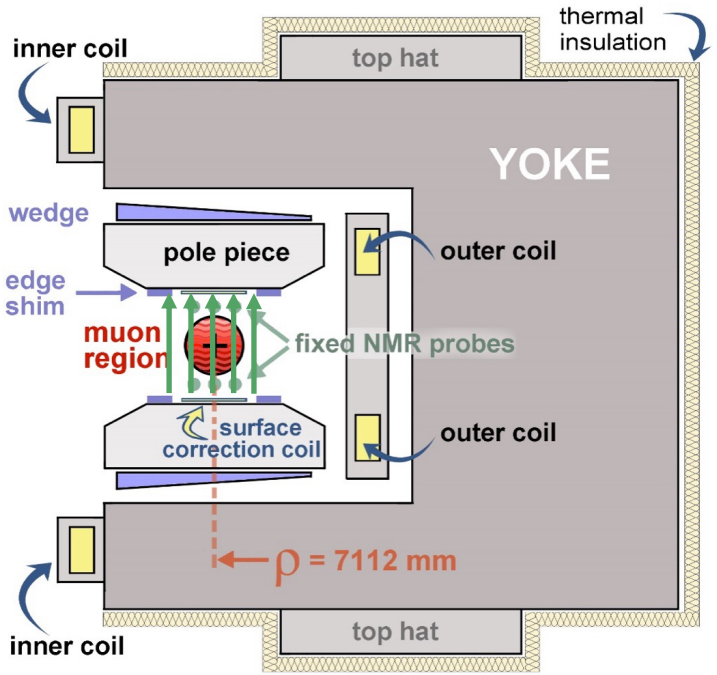

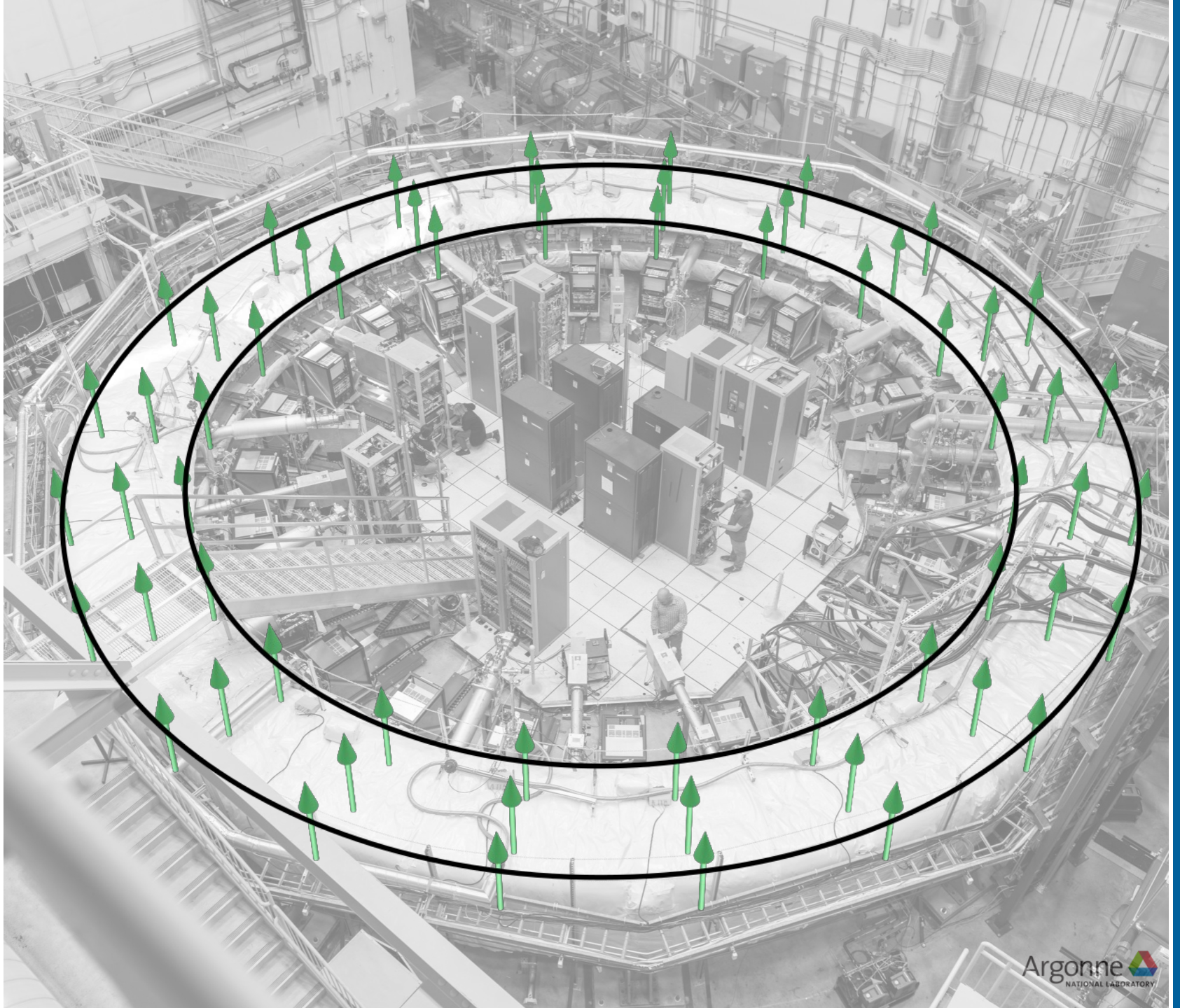

Magnetic Field Shimming

(Long) before any muons entered the ring

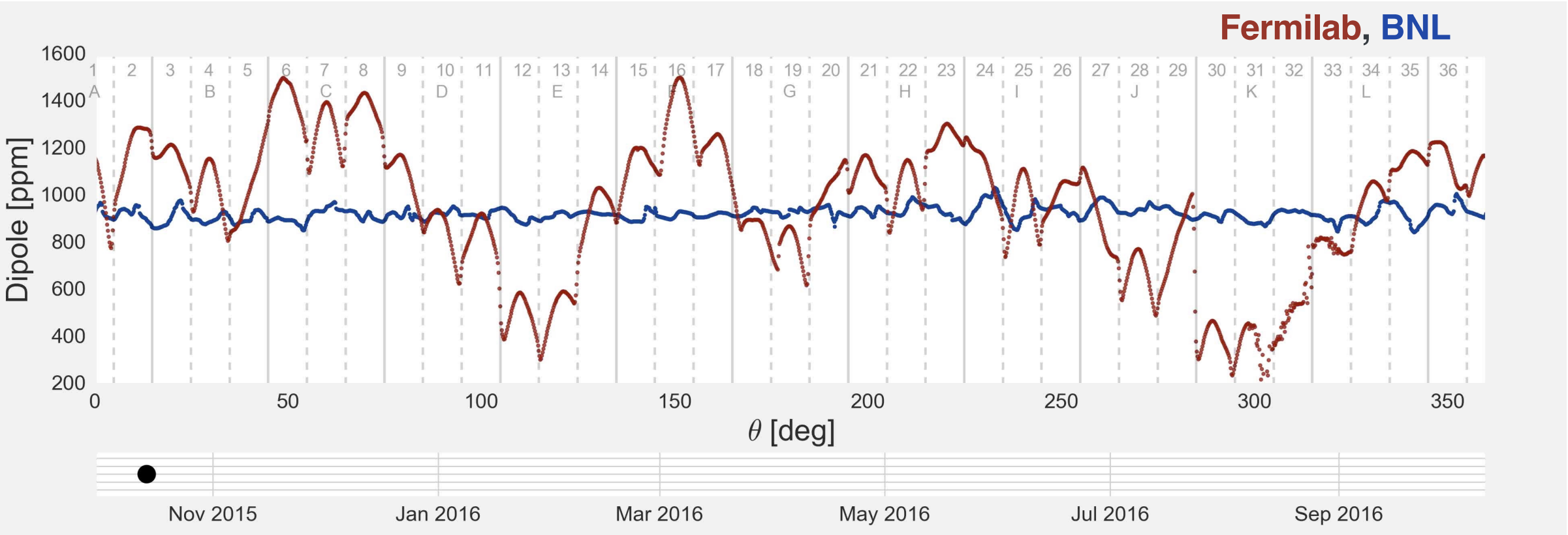

Magnetic Field Shimming

(Long) before any muons entered the ring

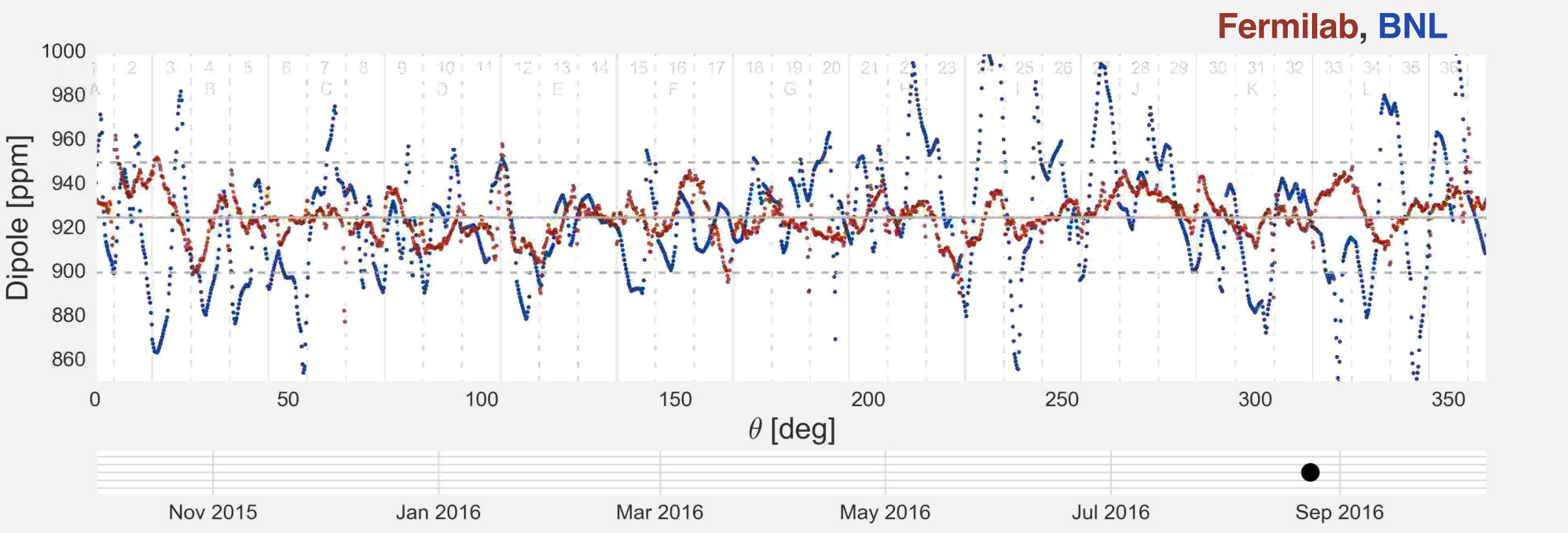

Injection

Field-free injection path through **inflector** magnet

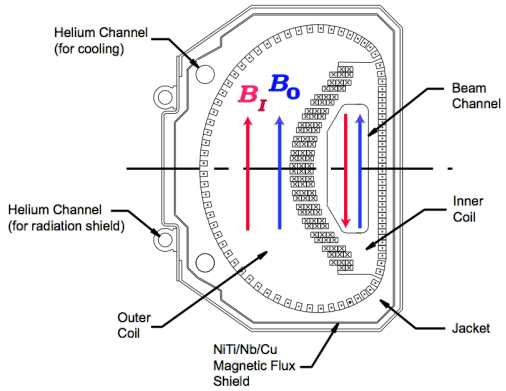

8 cm offset
from storage center

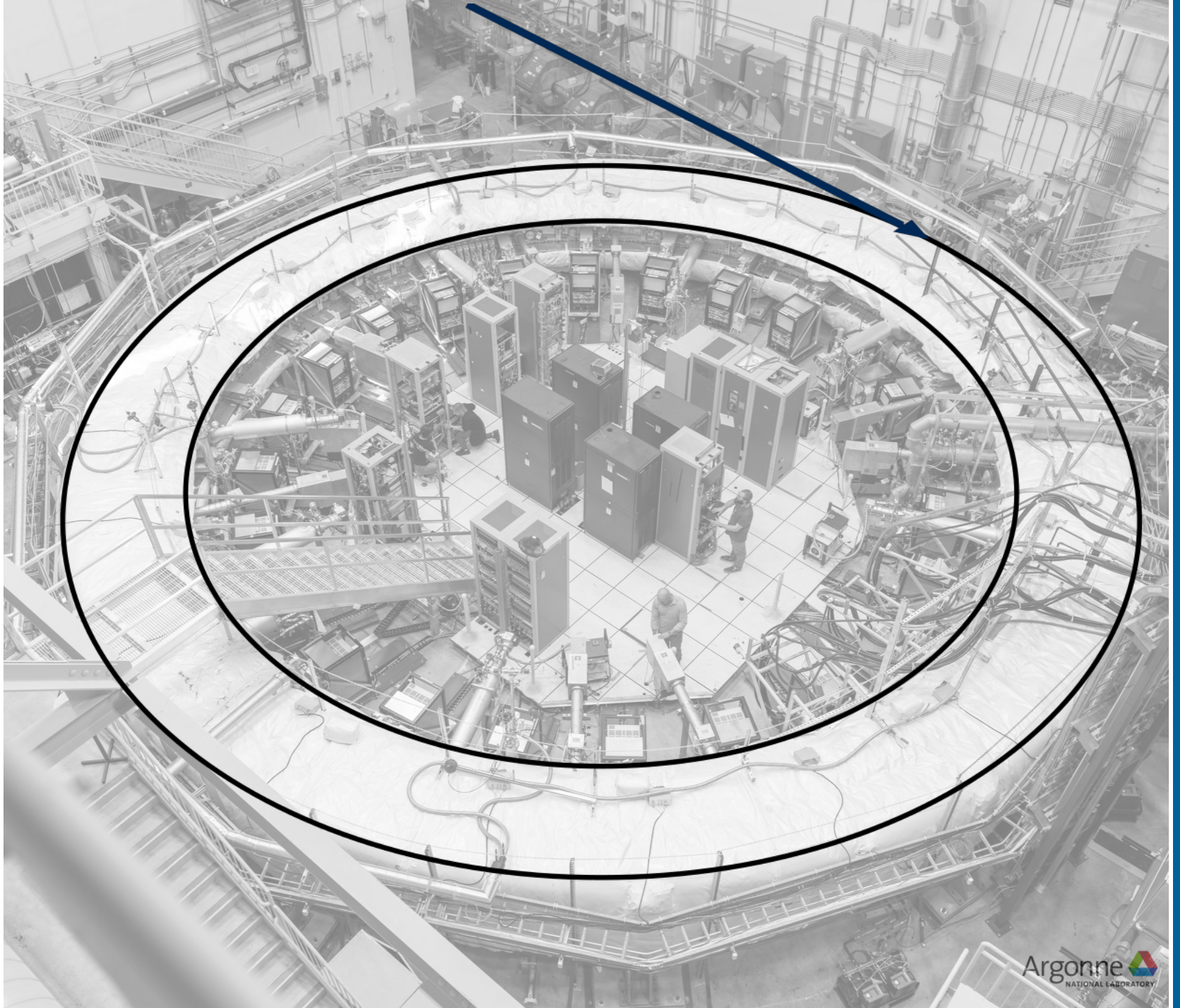

Injection

Field-free injection path through **inflector** magnet

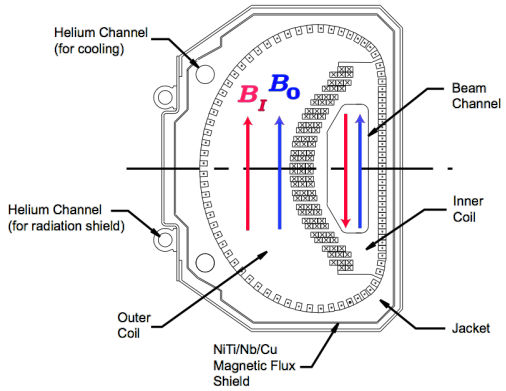

8 cm offset
from storage center

Kicker

steer muon onto orbit
in the first passing

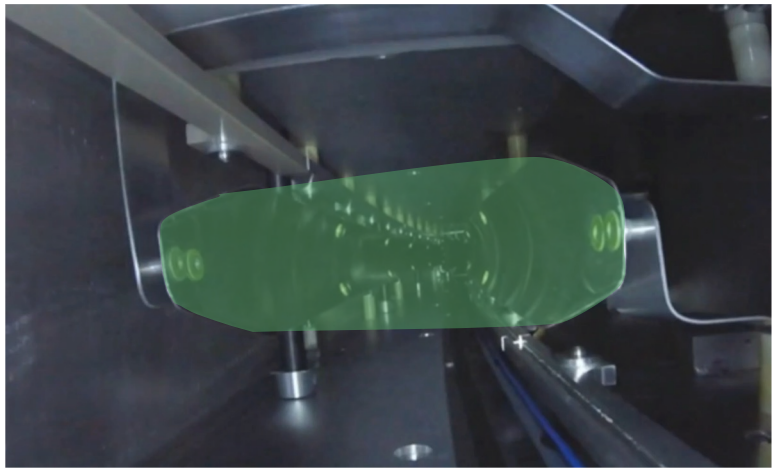

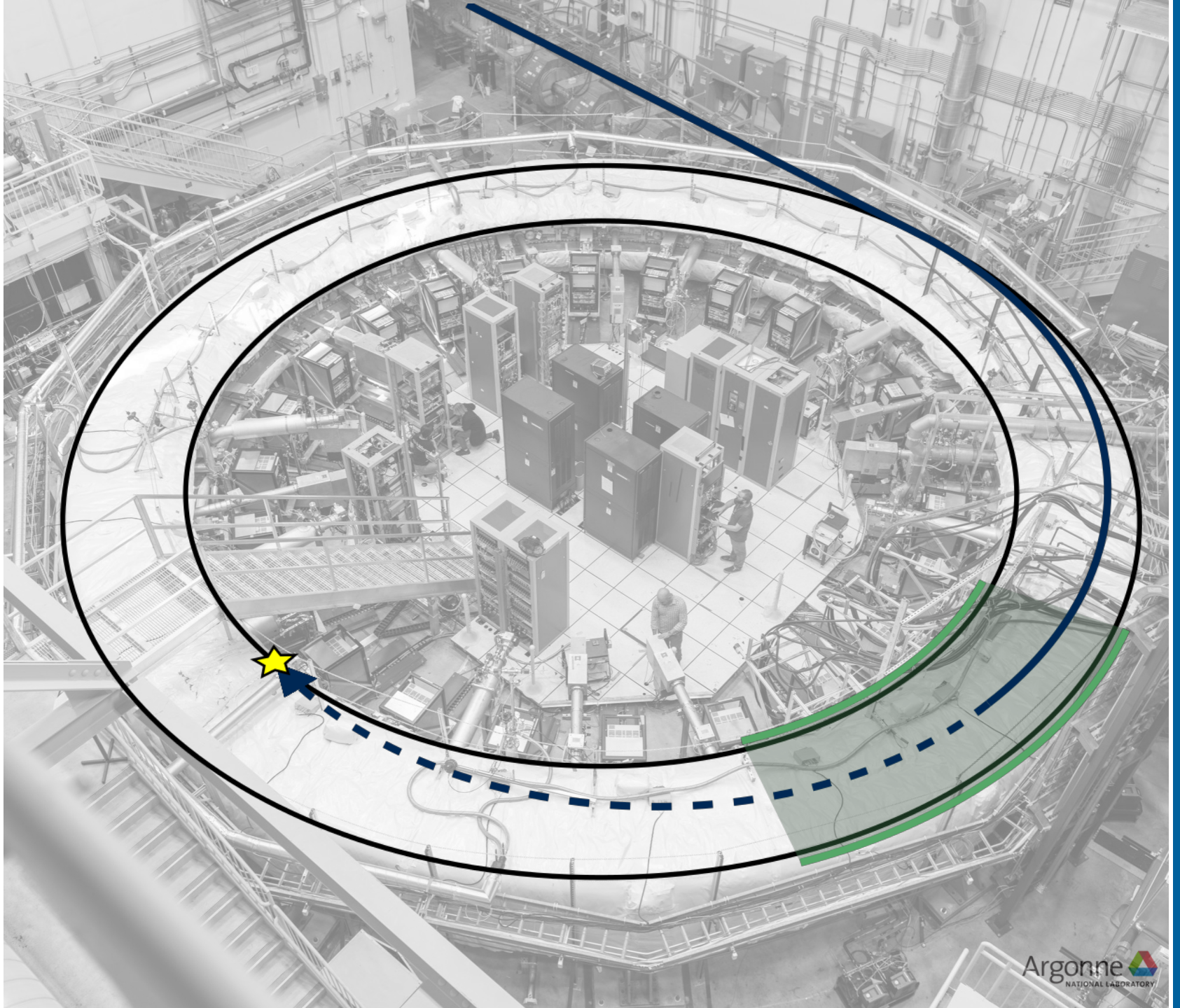

Kicker

steer muon onto orbit
in the first passing

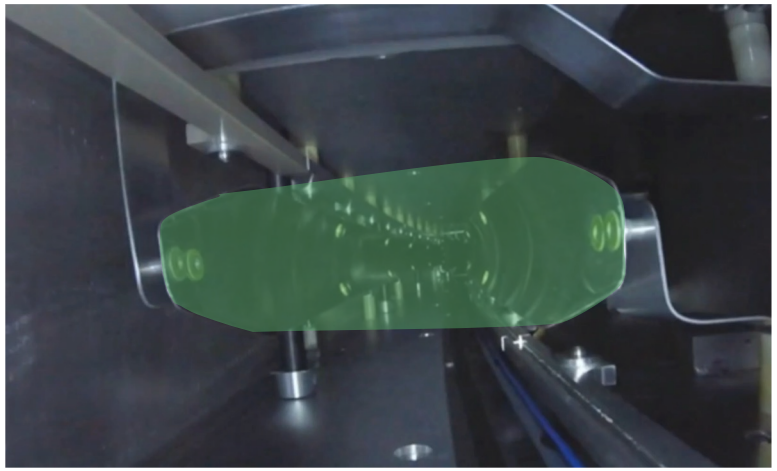

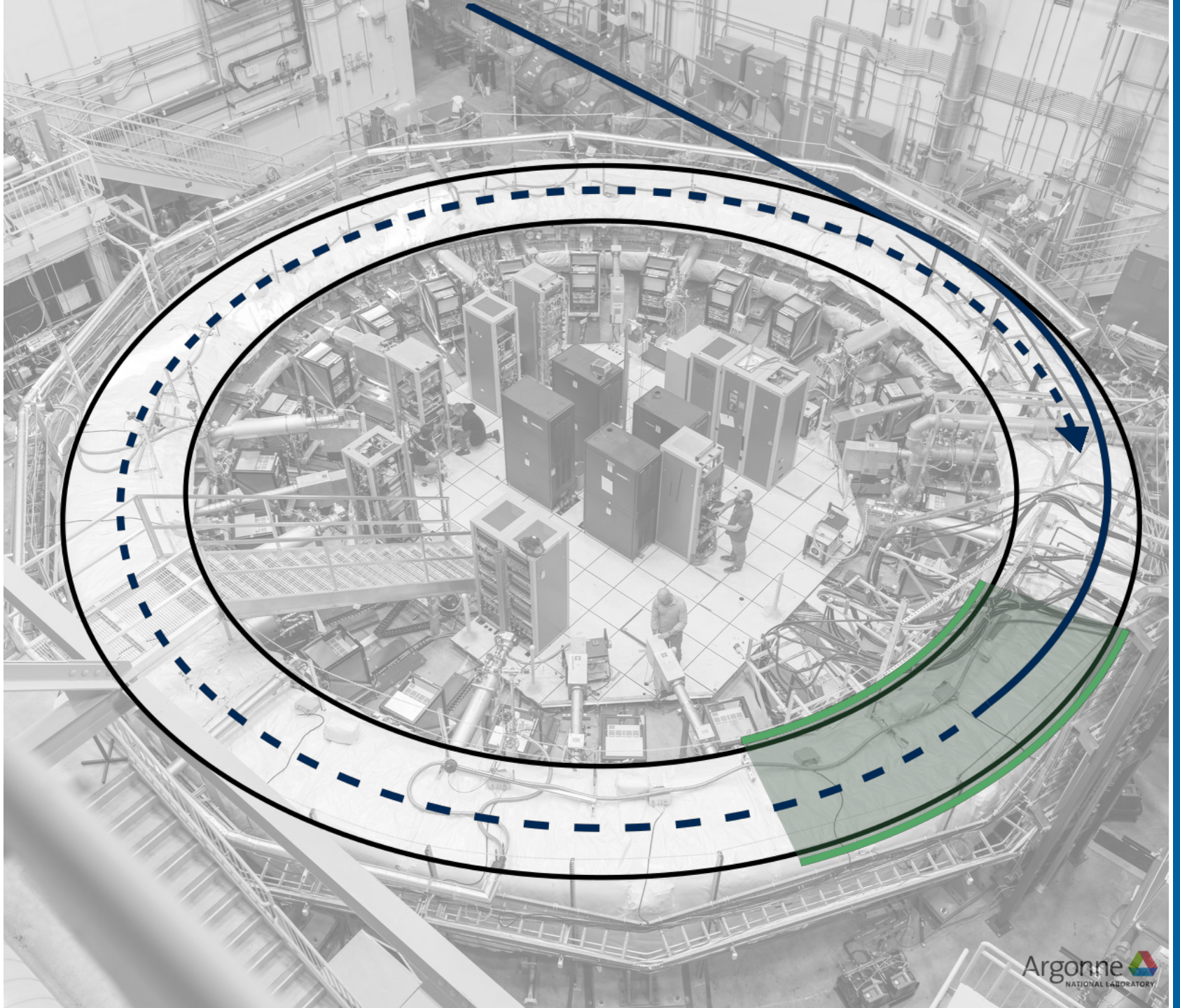

Kicker

steer muon onto orbit
in the first passing

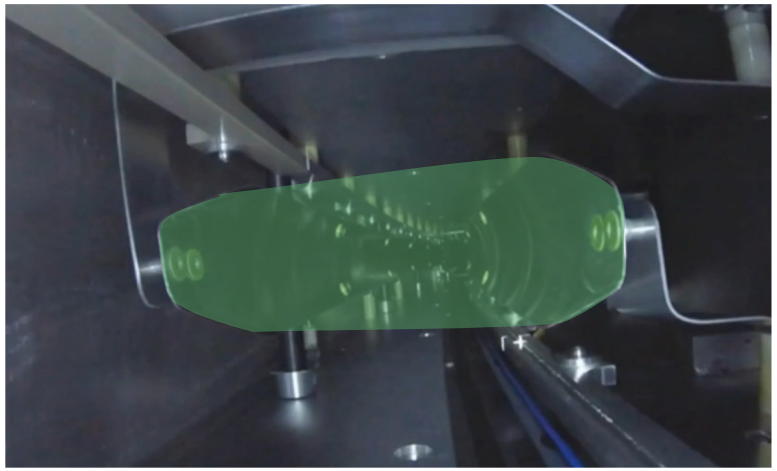

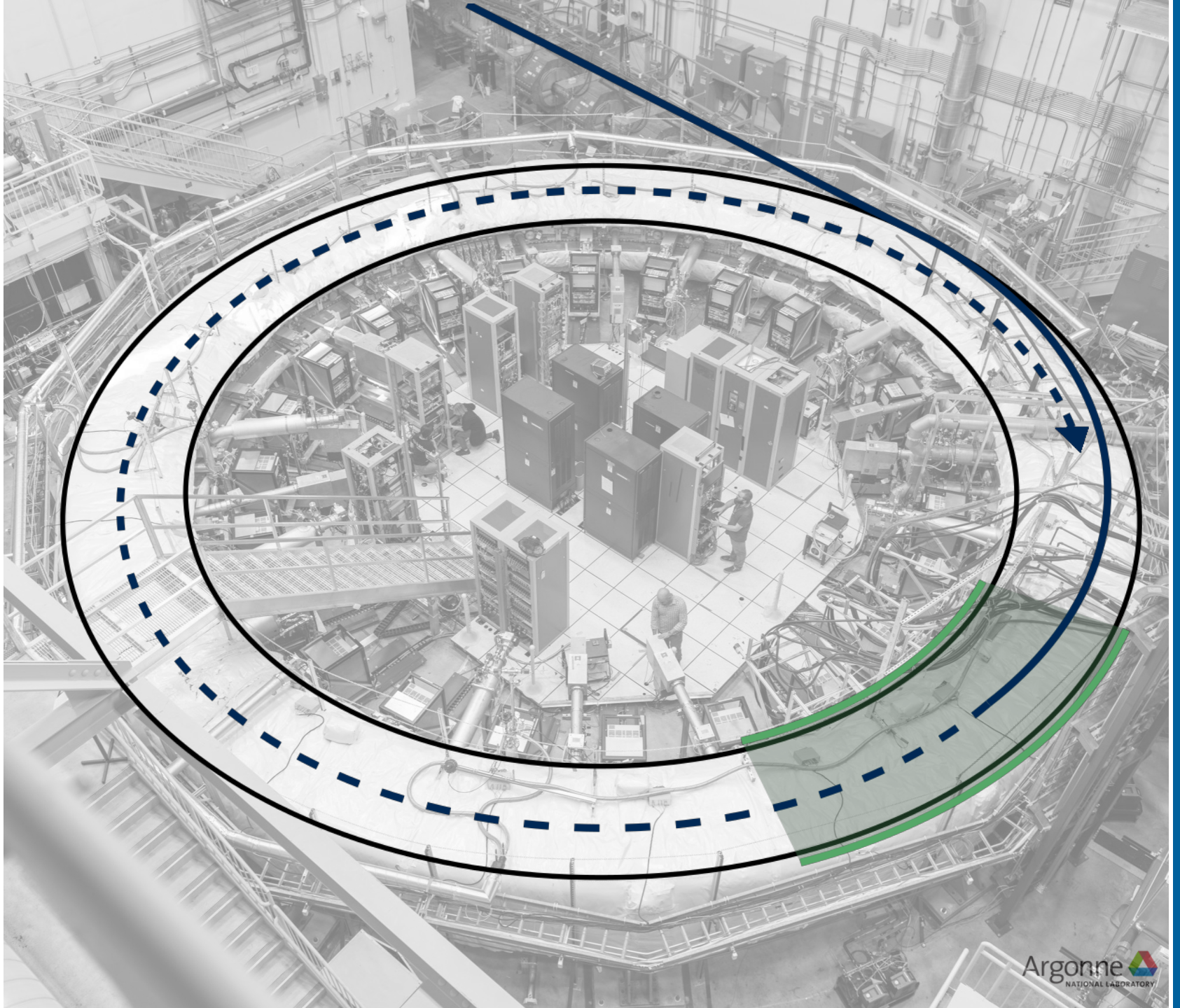

Kicker

steer muon onto orbit
in the first passing

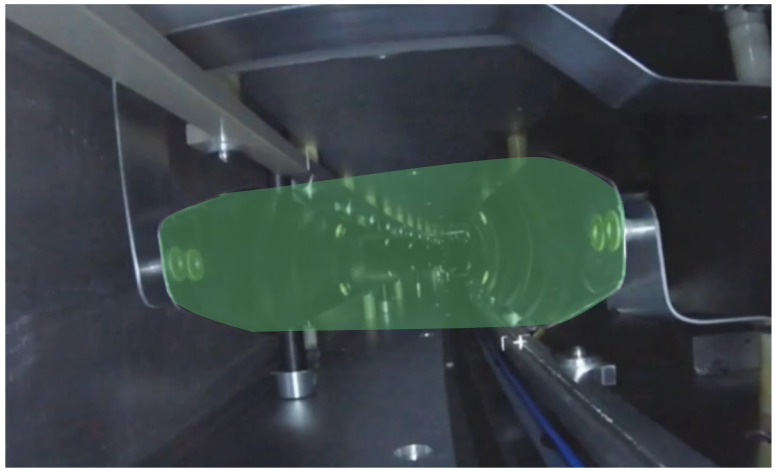

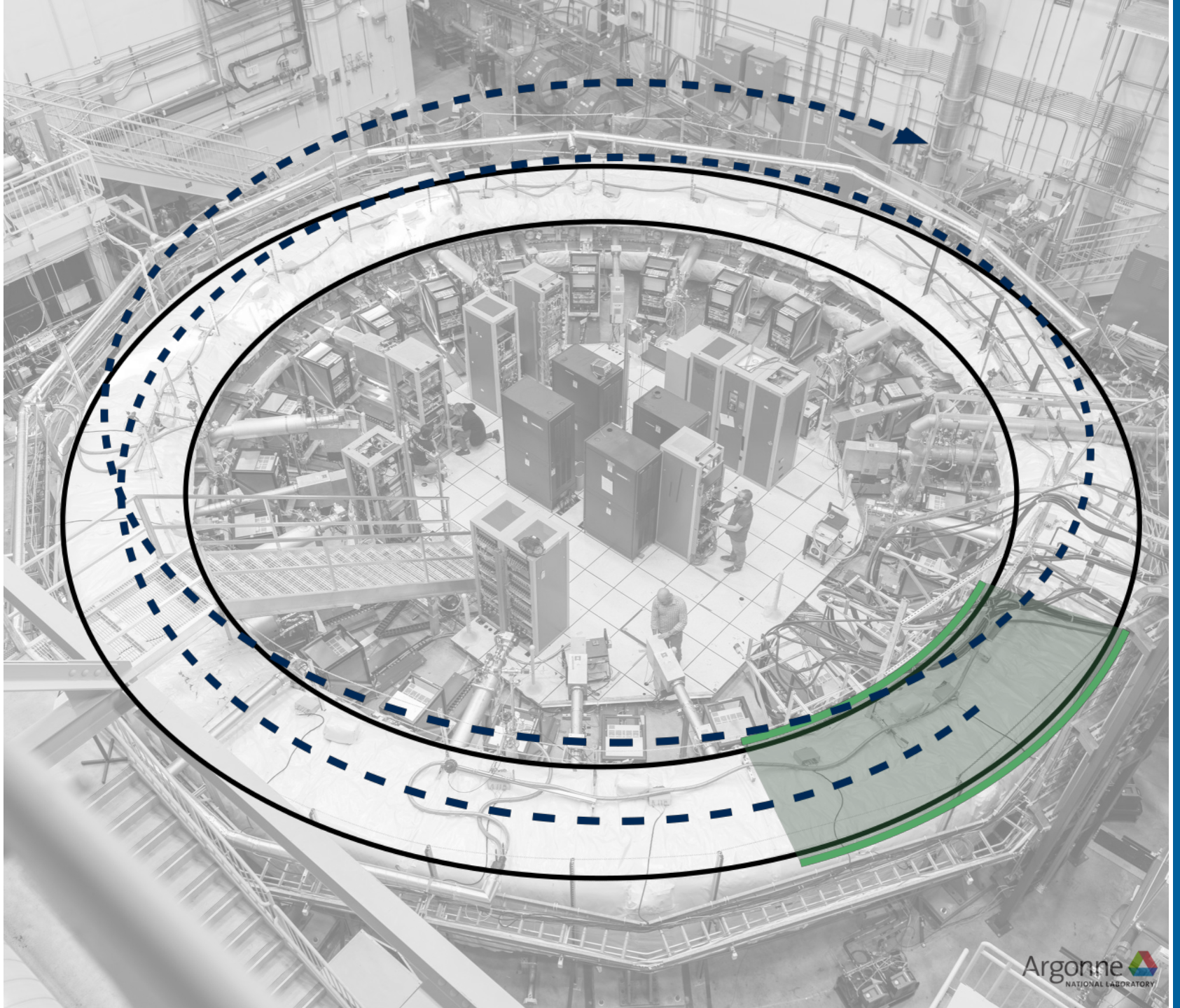

Electrostatic Quadrupoles

Electric fields for
vertical focusing

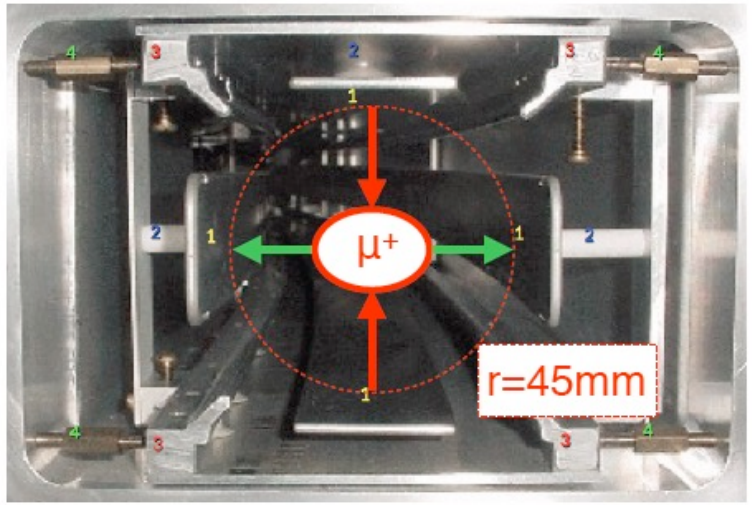

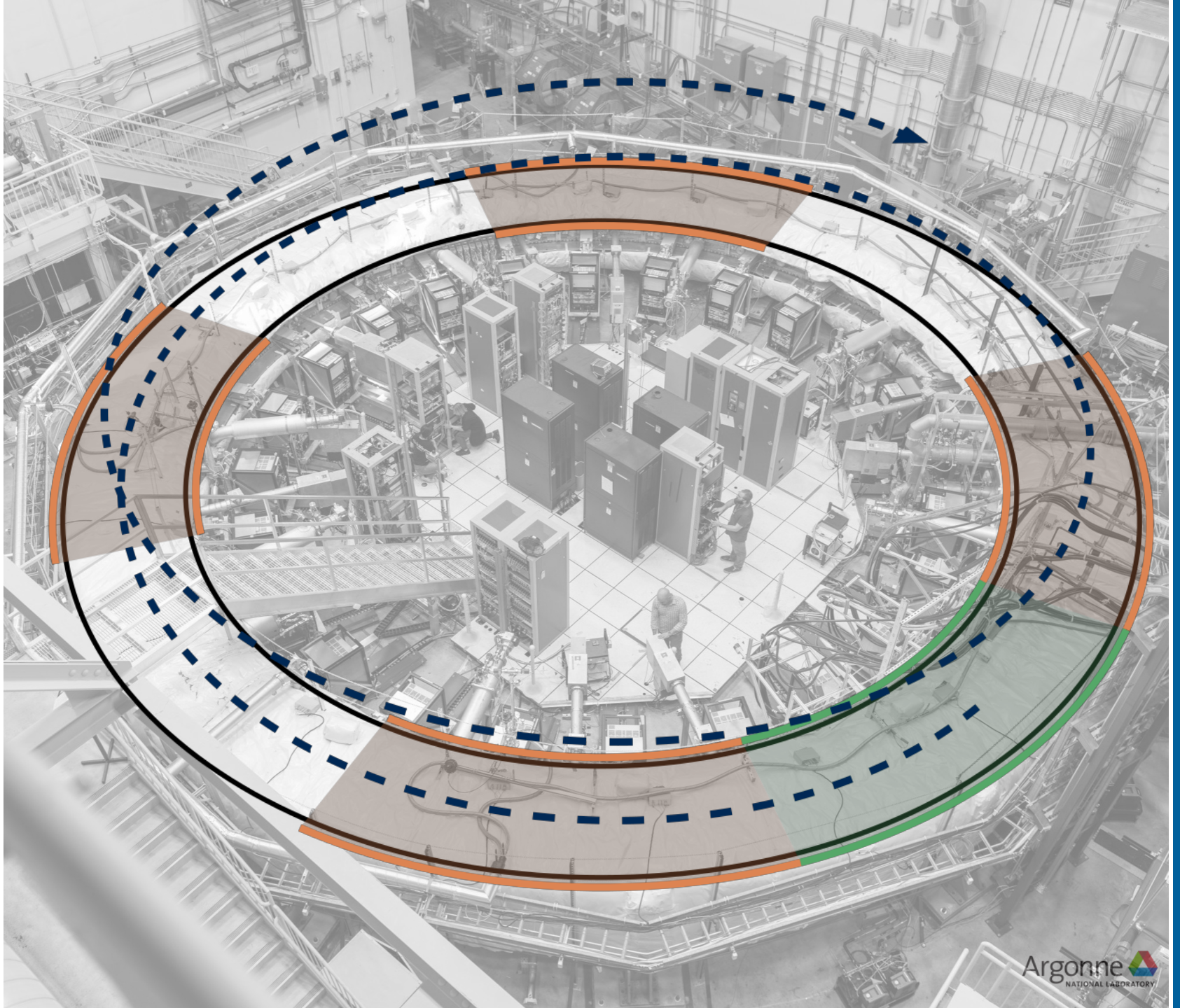

Electrostatic Quadrupoles

Electric fields for
vertical focusing

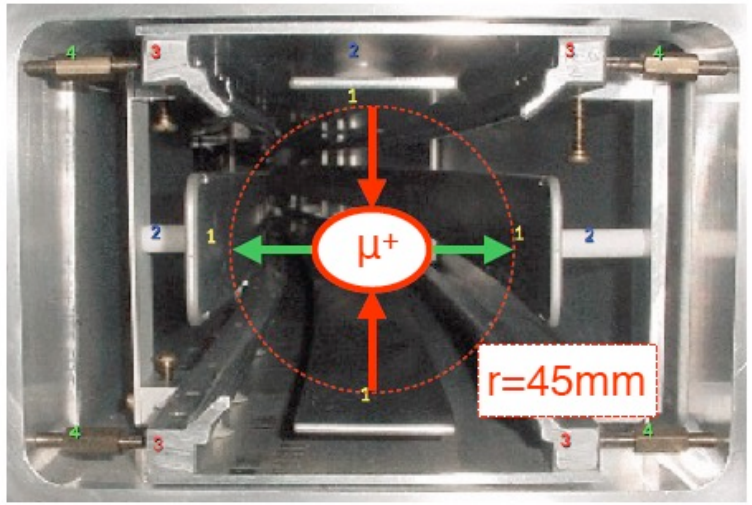

Muon Storage

Cyclotron period: 149.2ns

few 1000 muons at a time

Boosted lifetime: 64 μs

Storage up to 700 μs

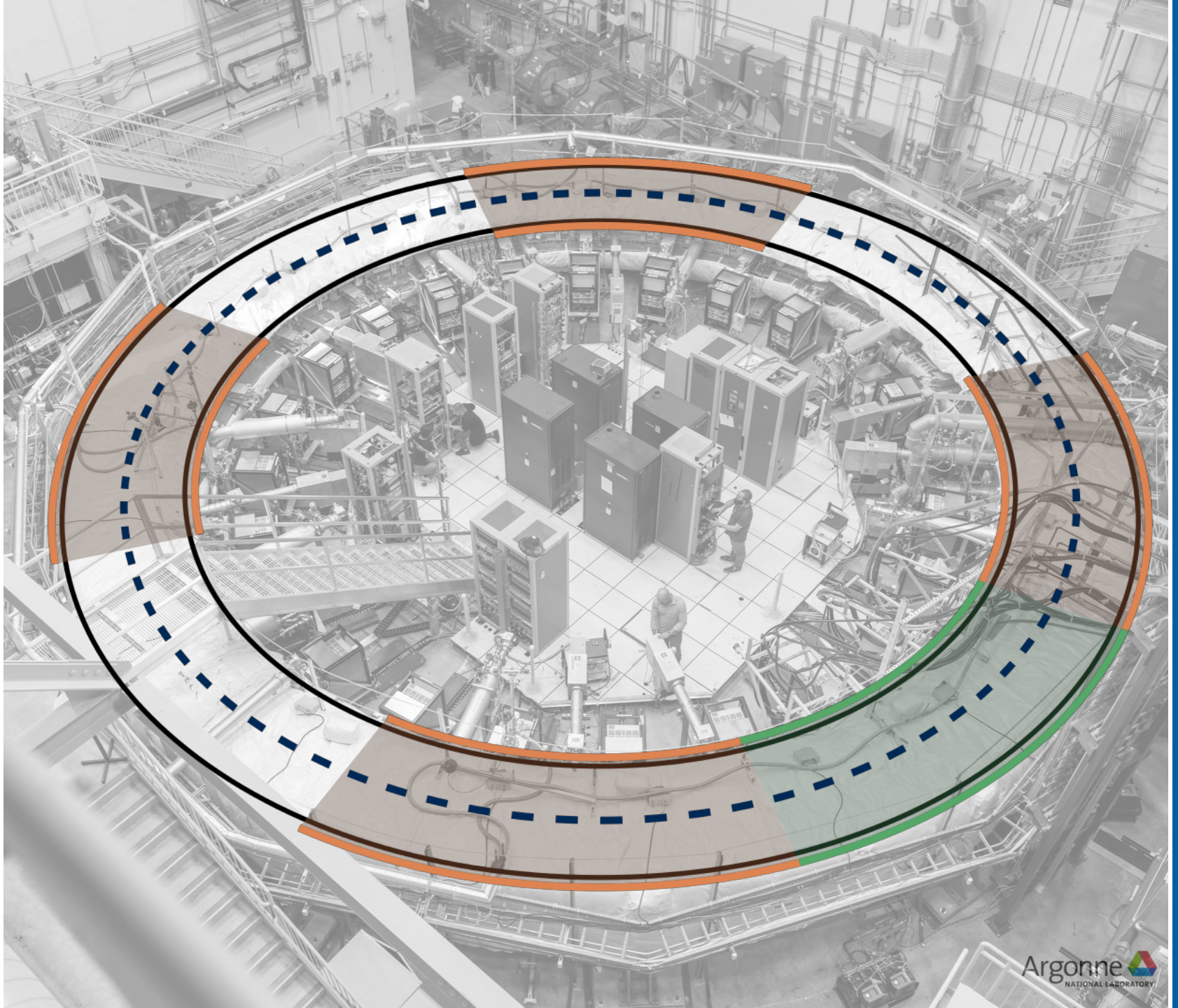

Muon Decay

Muon decay to positrons and invisible neutrinos

$$\mu^+ \rightarrow e^+ \nu_e \bar{\nu}_\mu$$

Parity Violation:

"self-analyzing"
μ^+ **spin** information encoded in e^+ **energy**

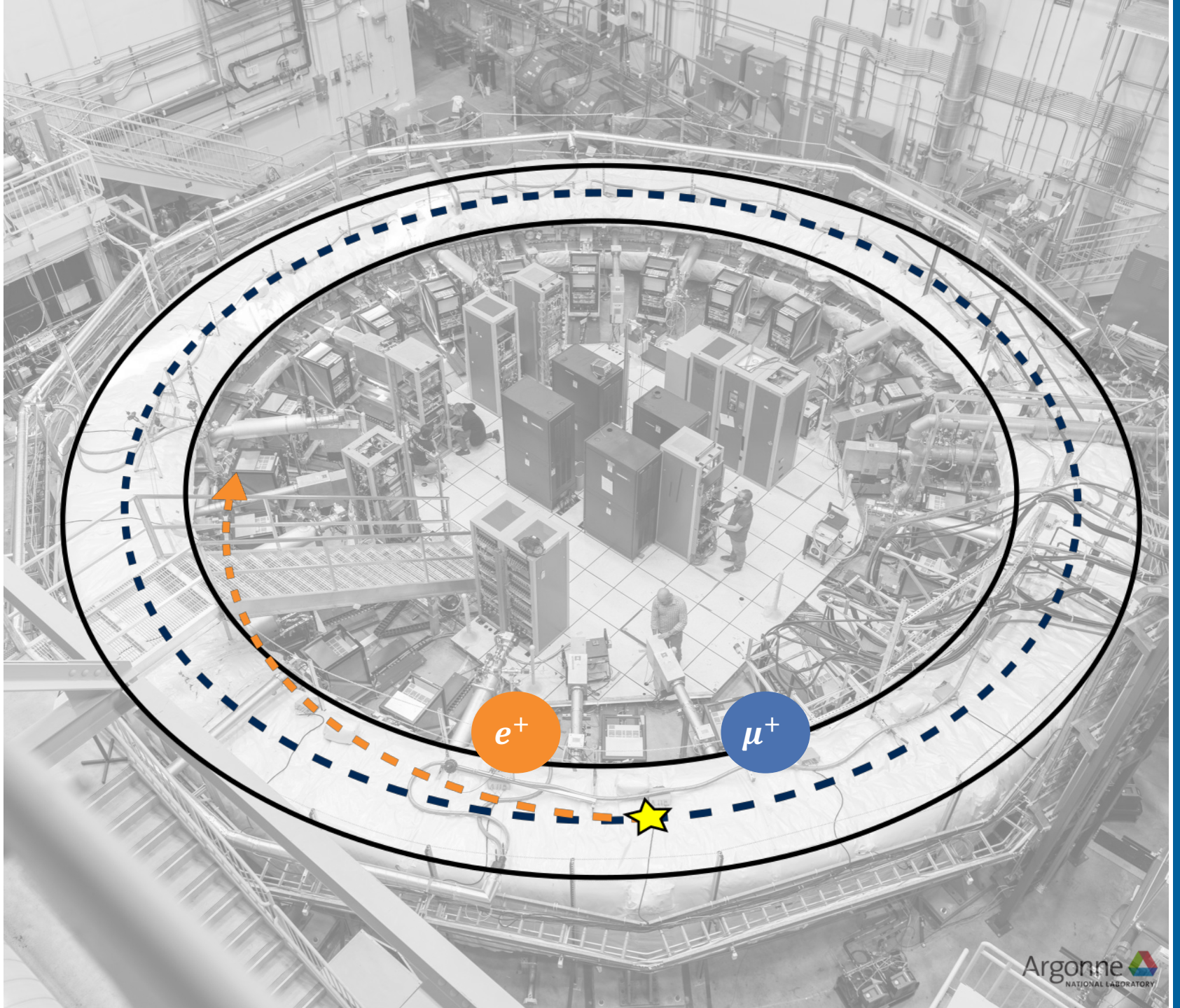

Calorimeters

24 Calorimeters

with 54 (9x6) Cherenkov PbF_2 crystals read out by SiPMs, arrival time (~100ps), energy of e^+ (~5% at 2GeV)

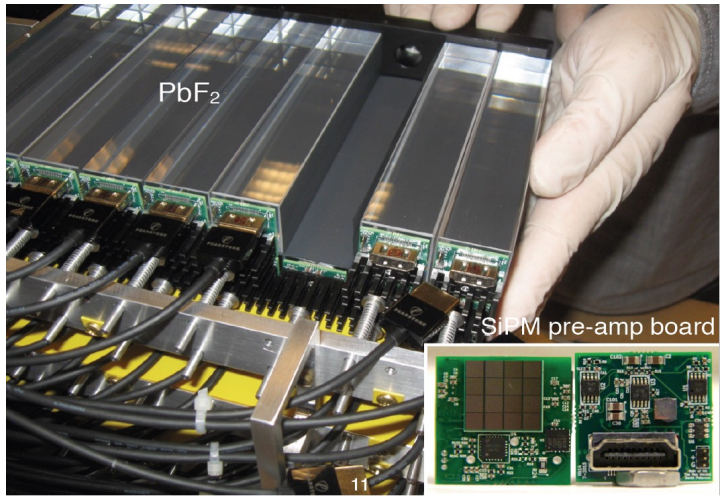

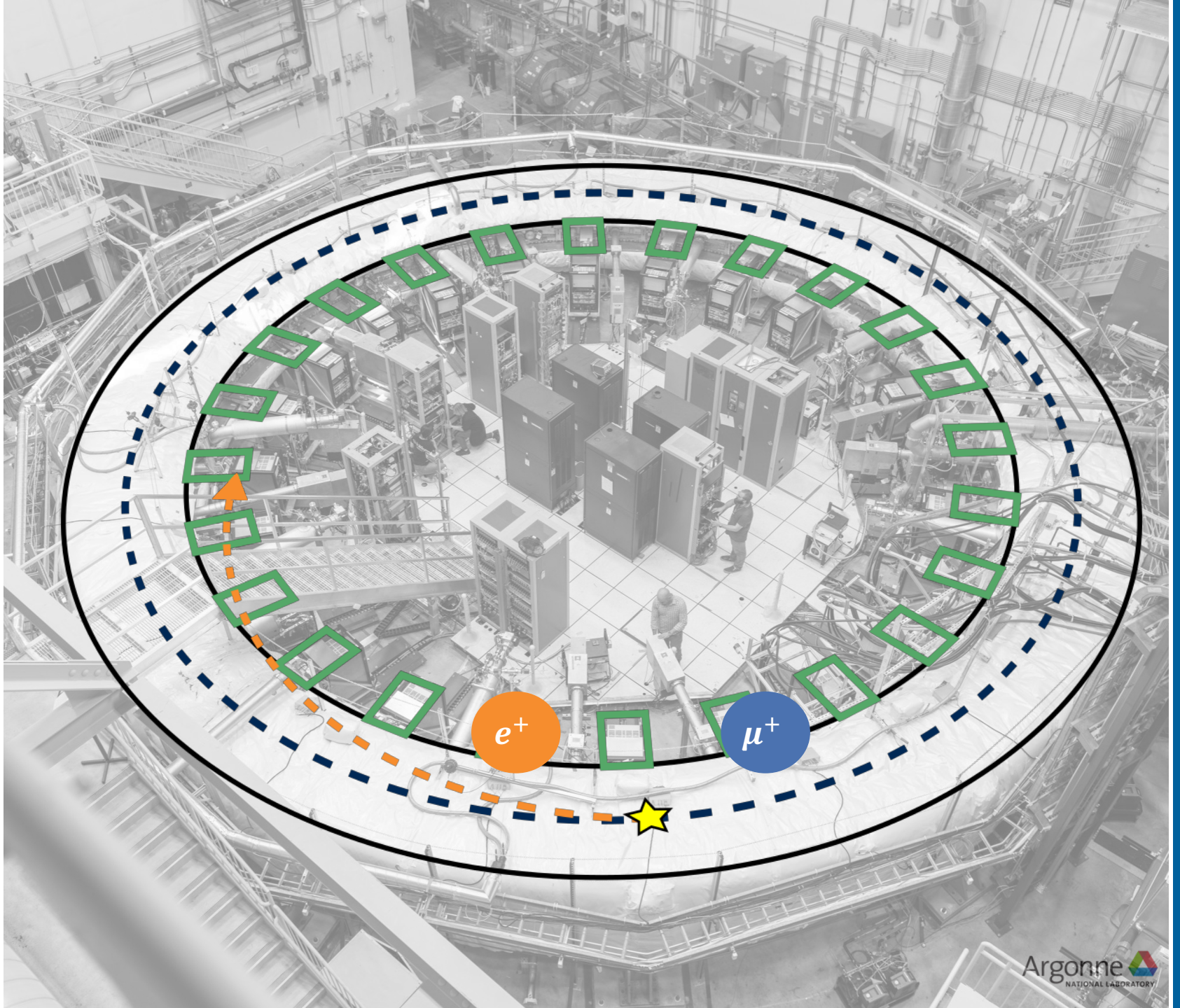

Calorimeters

24 Calorimeters
with 54 (9x6) Cherenkov PbF_2 crystals read out by SiPMs, arrival time (~100ps), energy of e^+ (~5% at 2GeV)

Laser system for gain calibration
stability 10^{-4} over a muon fill

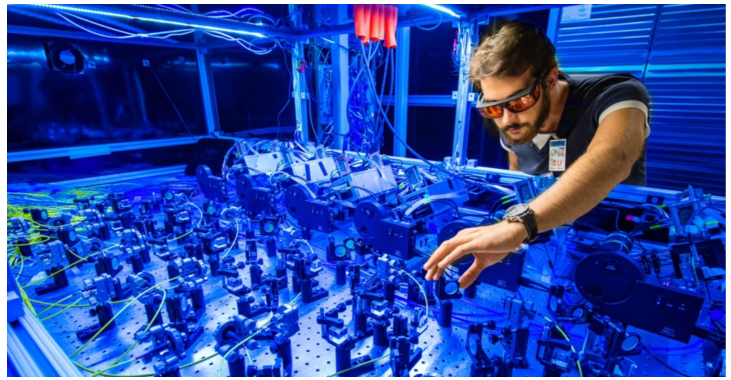

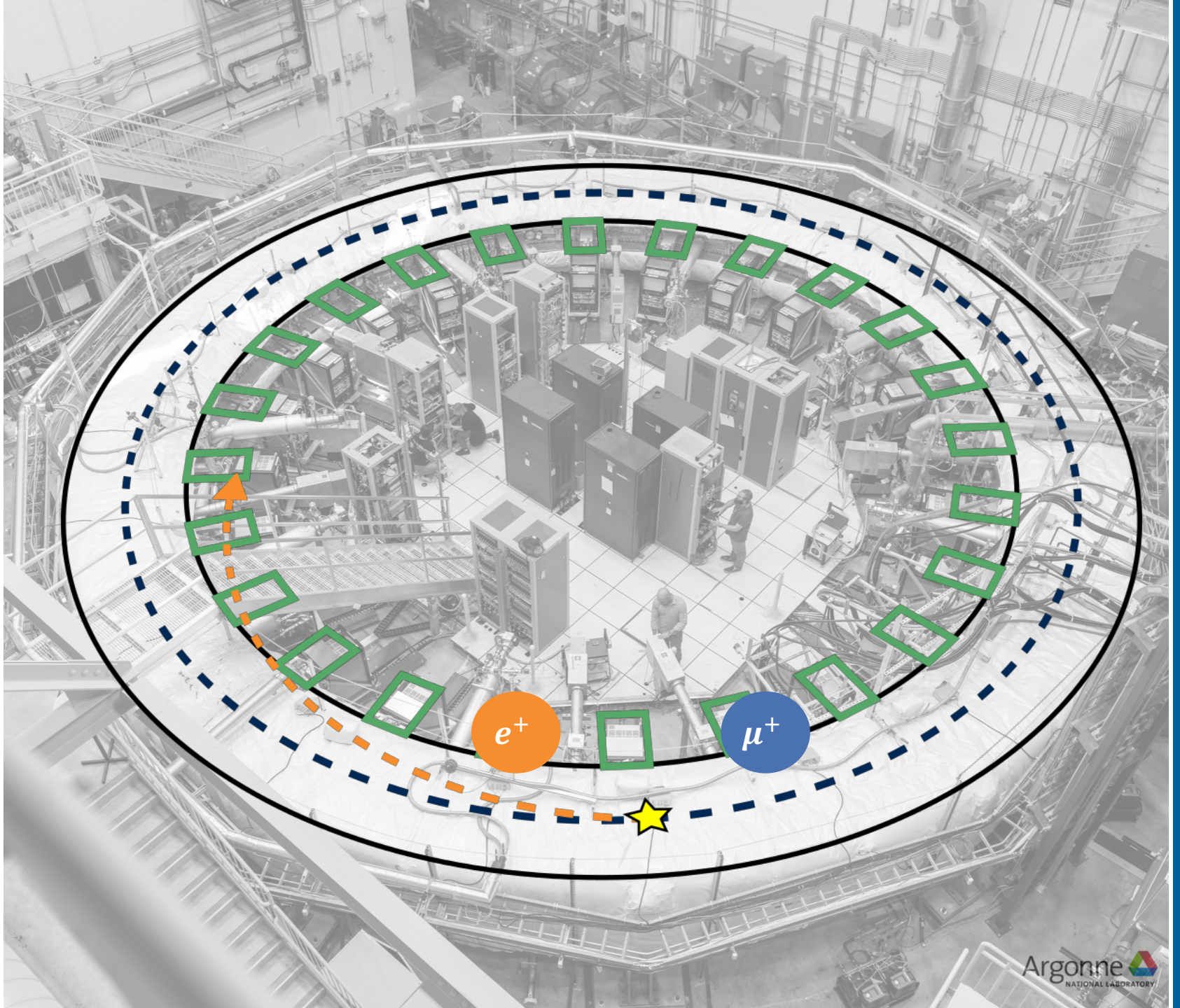

Measuring the Spin Precession

Simplest fit model captures **exponential decay** & **g-2 oscillation**

$$N(t) = N_0\, e^{-t/\tau}\,[1 + A\cos(\omega_a t - \phi_0)]$$

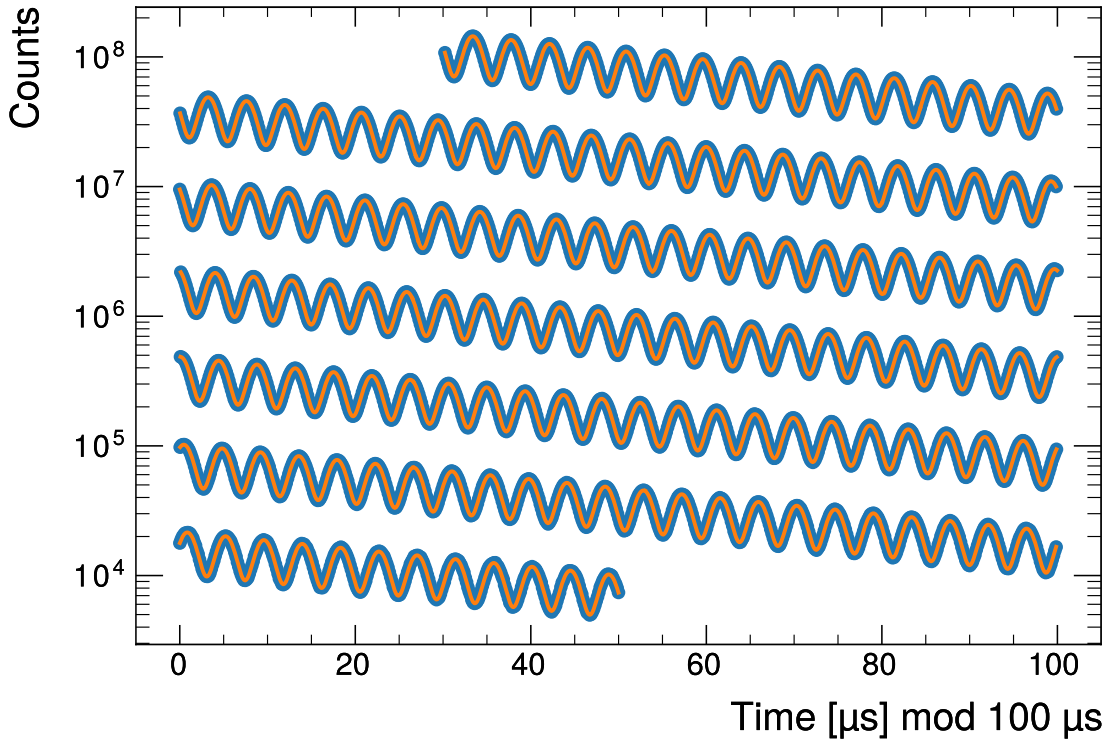

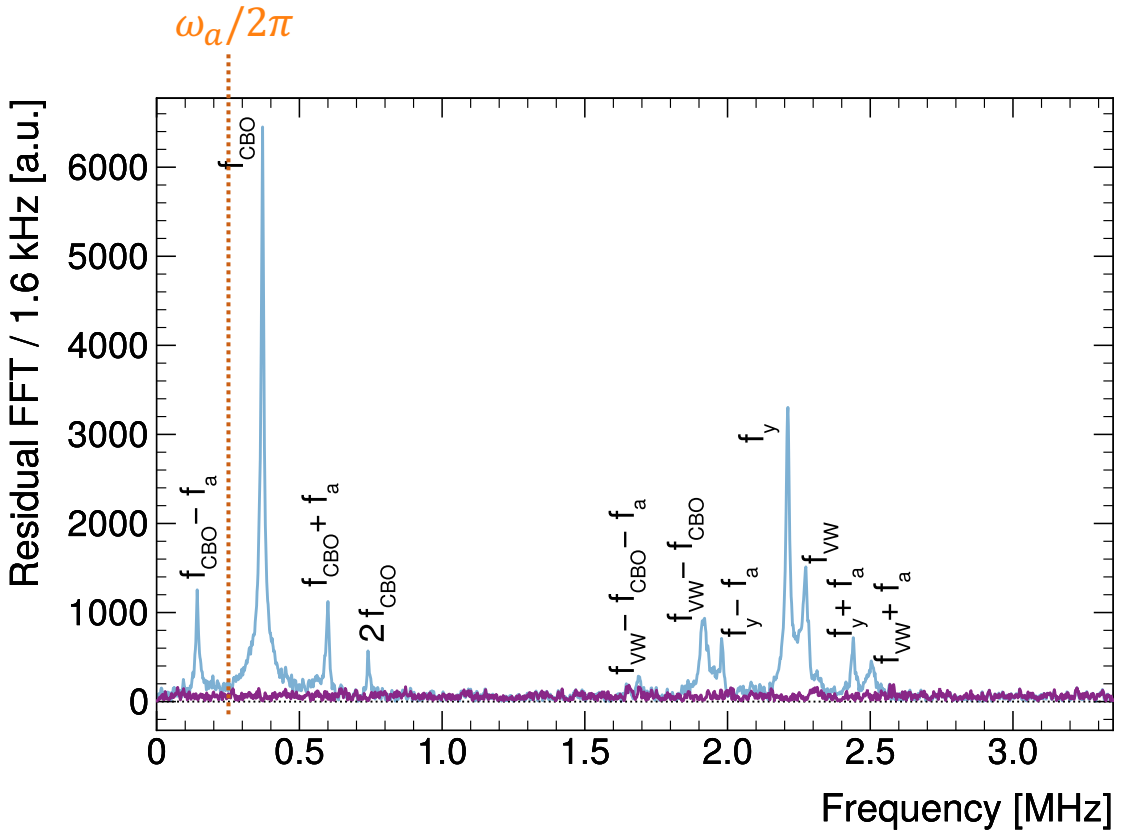

~350ppb ~170ppb ~30ppb

$$\omega_a = \omega_a^m\left(1 + C_e + C_p + C_{pa} + C_{dd} + C_{ml}\right)$$

Electric-field & Up/Down motion
Spin precesses slower than
in basic equation

Phase changes over each fill:
Phase-Acceptance, Differential
Decay, Muon Losses

Trackers

2 straw-tracker stations
each 8 modules, 4 layers of 32 straws, 50:50 Ar:Ethane

Reconstruct Muon Distribution

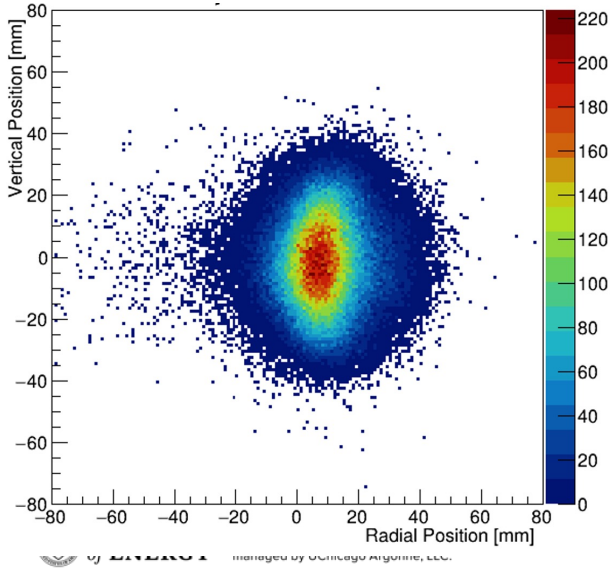

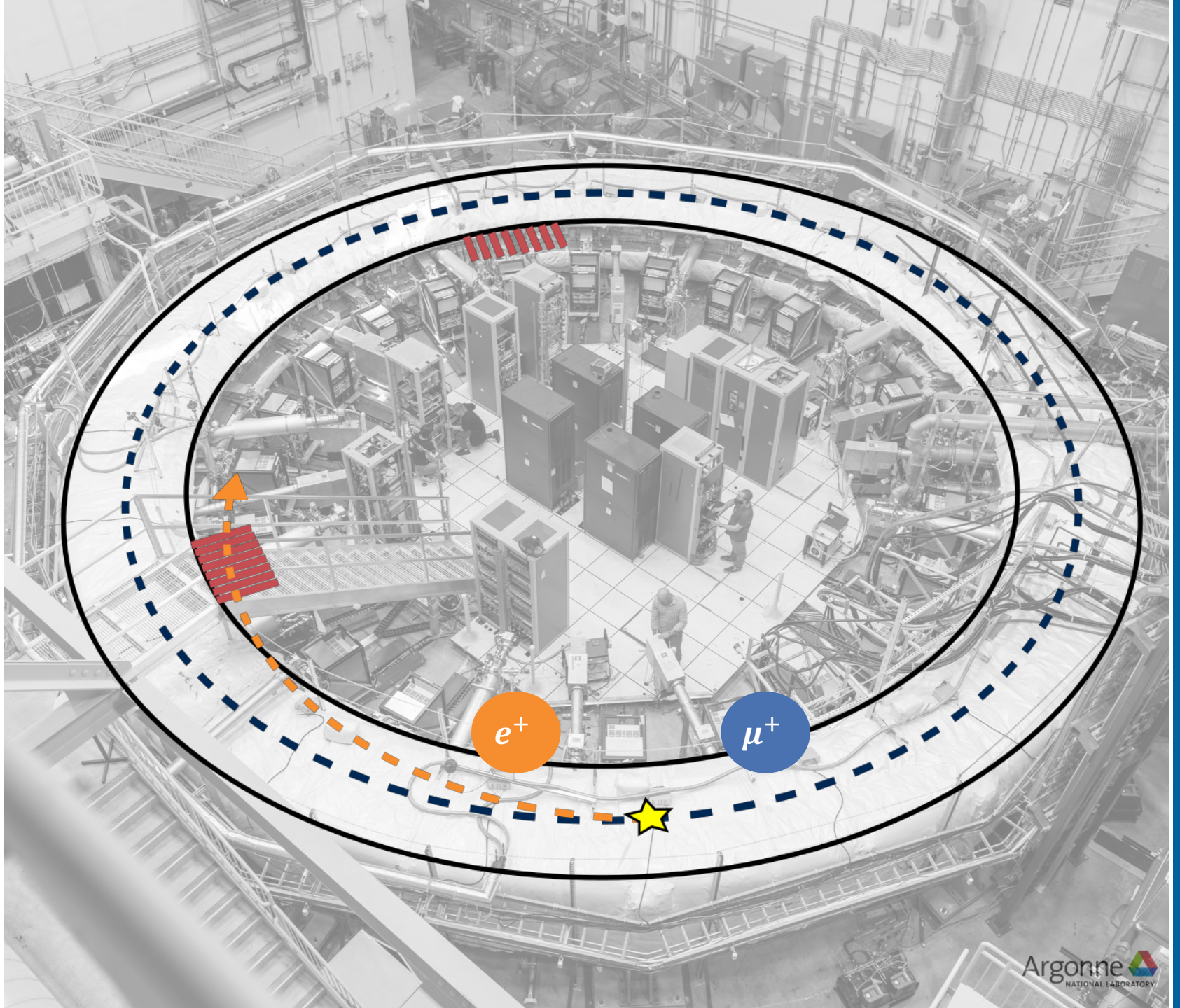

Muon Beam Motion

Example: Coherent Betatron Oscillation (CBO)

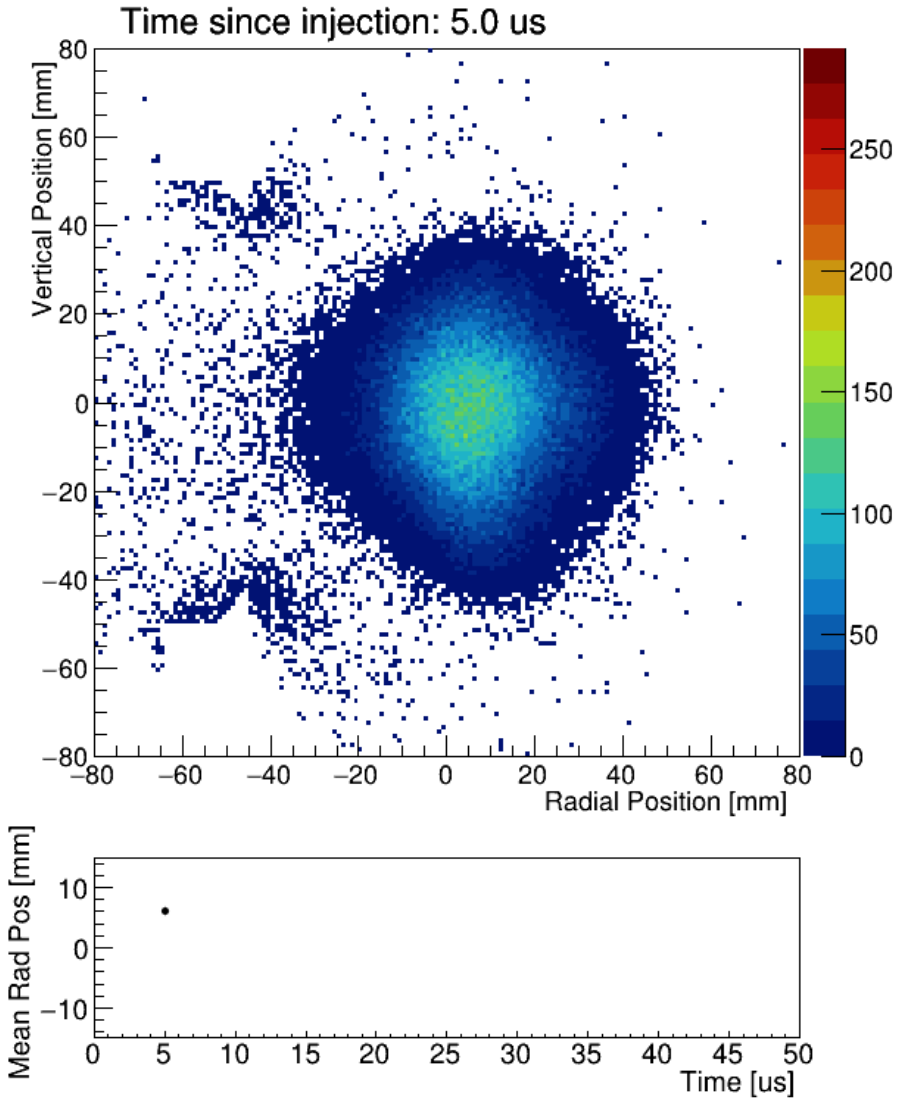

Magnetic Field Mapping & Tracking

Field Monitor: Fix installed NMR probes

at 72 azimuthal locations around the ring

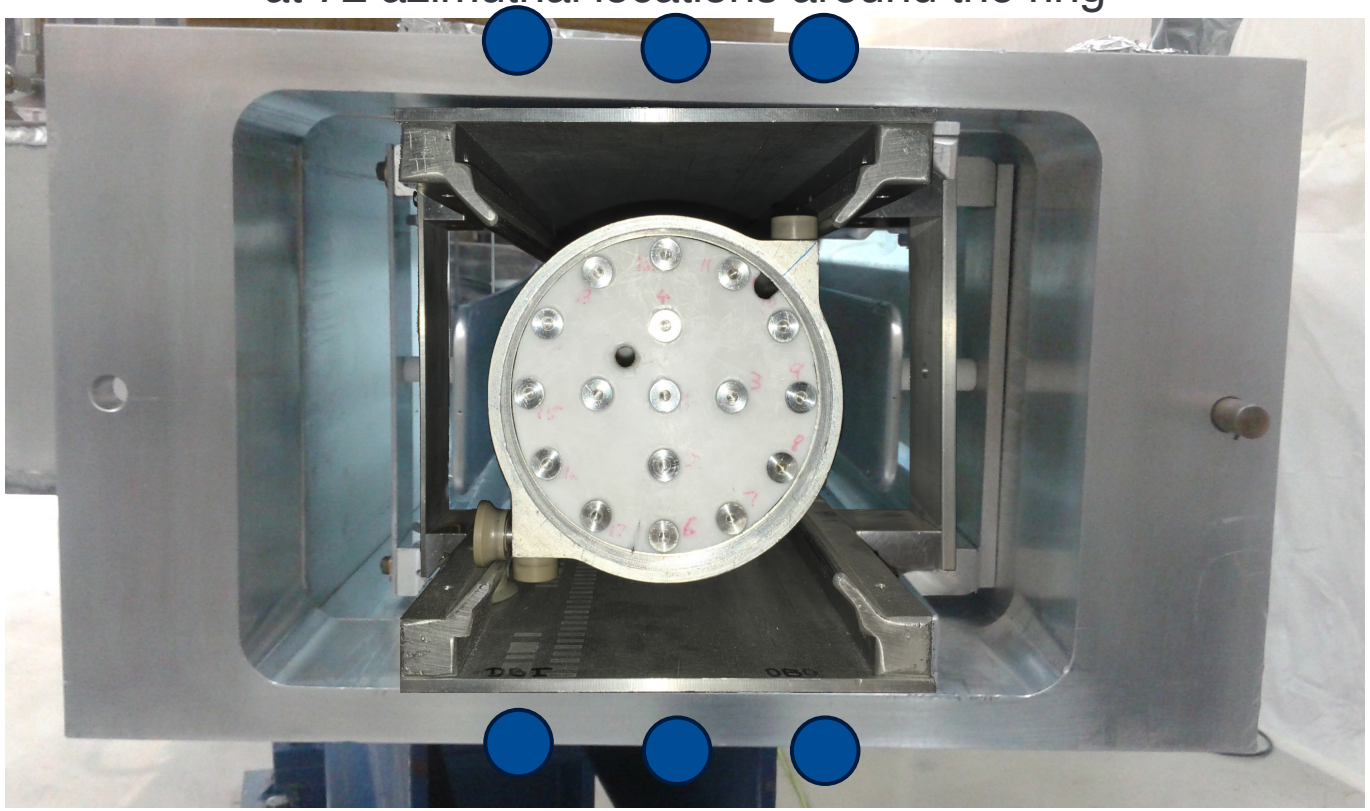

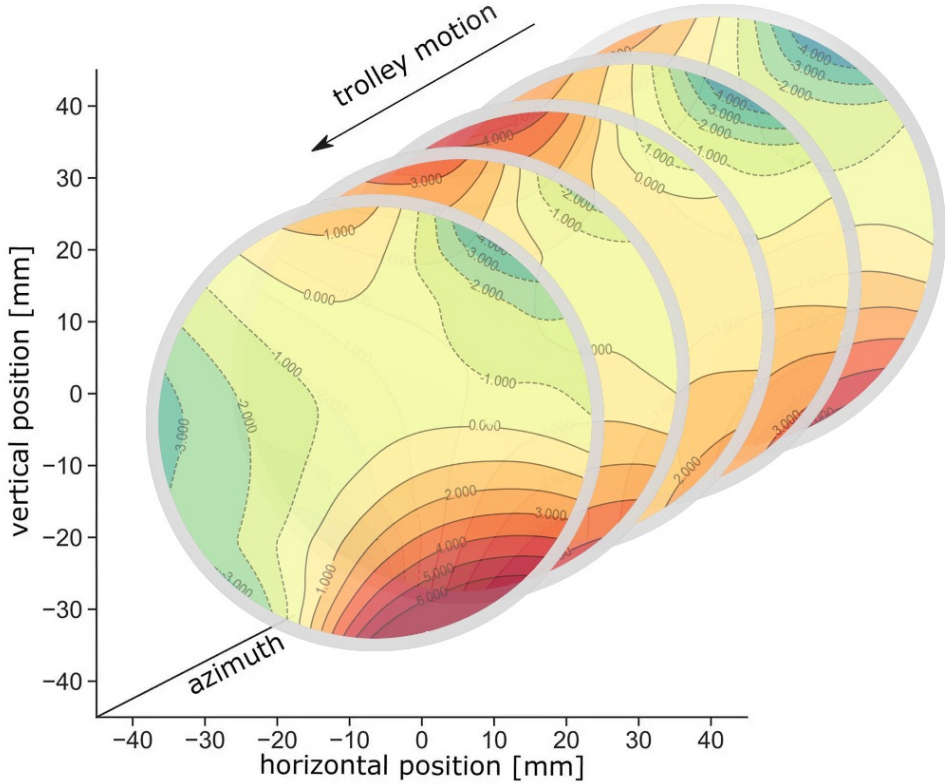

Trolley: Field Mapper

~9000 2D slices around the ring

The field between field maps (trolley runs) is tracked by the fixed NMR probes.

Magnetic Field Calibration

with respect to **shielded protons in a spherical sample**: ω_p'

NMR probes in the

”trolley’s magnetic environment”

in-situ

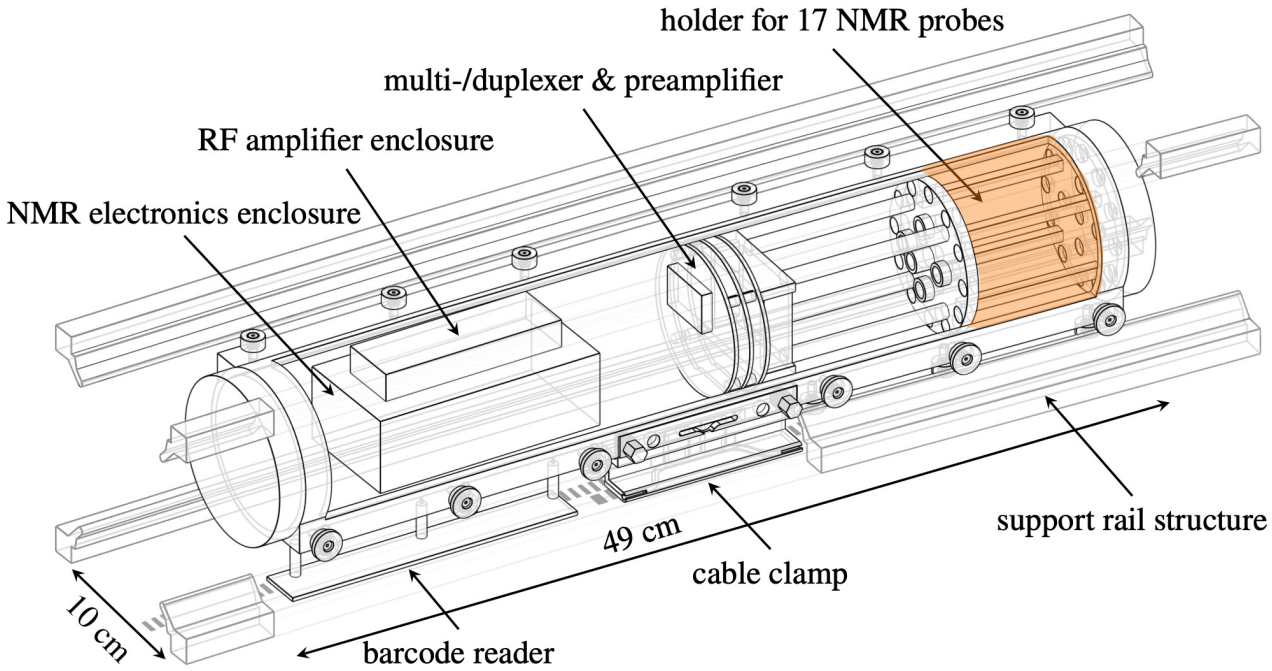

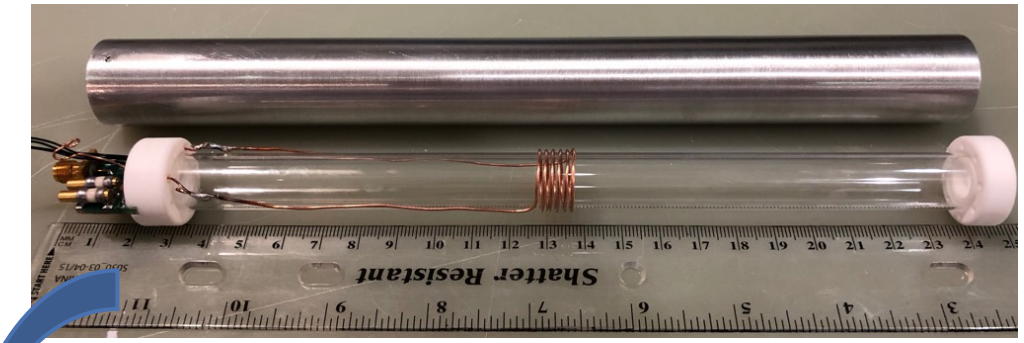

water-based cylindrical **Calibration Probe**

- Material effect
- sample shape

ω_p': shielded protons in a spherical sample

Argonne's 4T Test Solenoid

0 to 4T very homogenous magnetic field

Stony Brook led detector test

Magnetic Field Muon Weighting

$$\tilde{\omega}'_p = \langle \omega'_p \times M \rangle (1 + B_k + B_q)$$

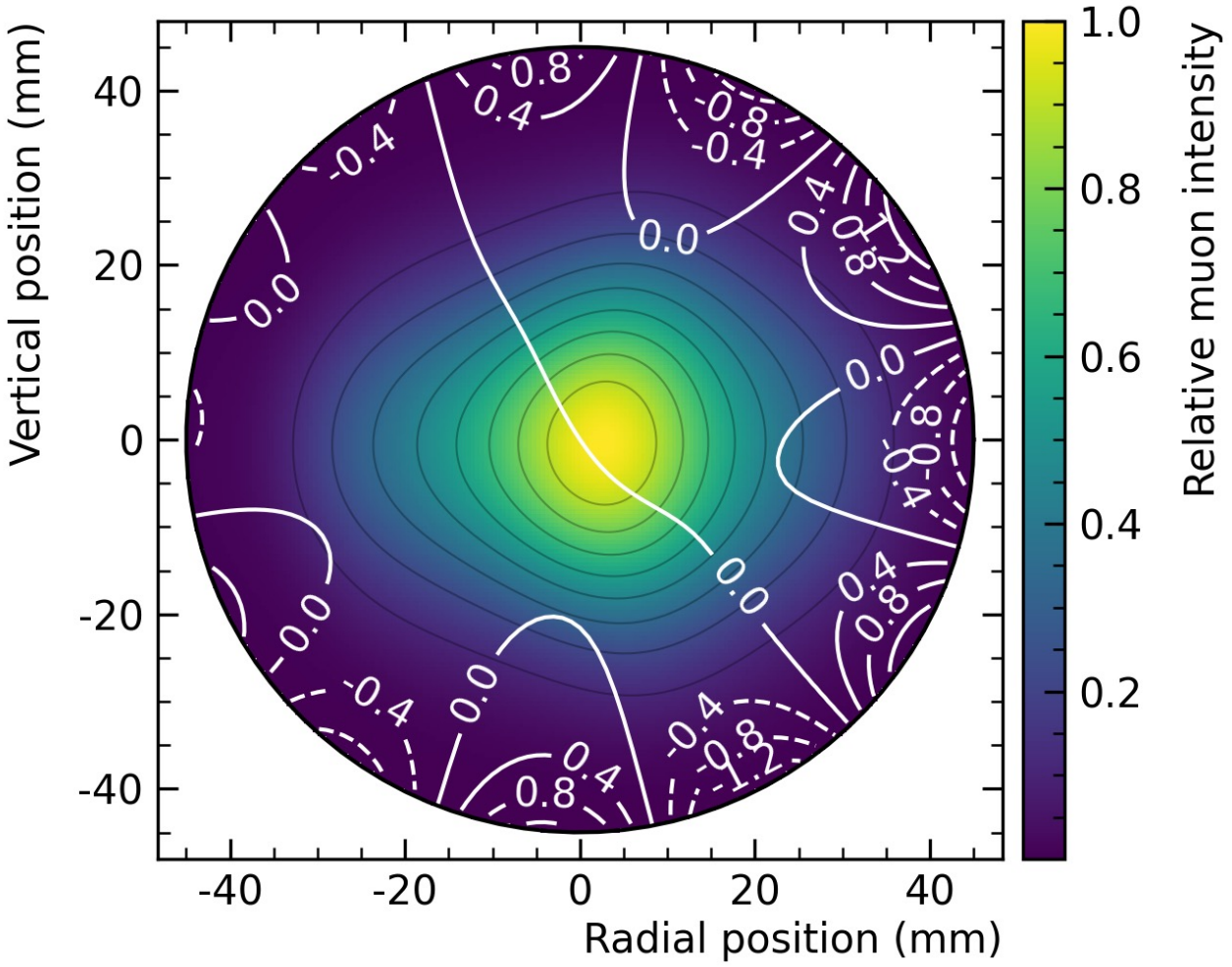

Magnetic field seen by the muons, weight by the Muon Distribution M

- Muon distribution from the **trackers**, propagated around the ring using our **simulation frameworks**

~30ppb ~20ppb

$$\tilde{\omega}'_p = \langle \omega'_p \times M \rangle \left(1 + B_k + B_q\right)$$

Transient magnetic fields
synchronous to the muon injection
not covered by the
asynchronous NMR measurements

Data Collection – 6 Runs over 6+ Years

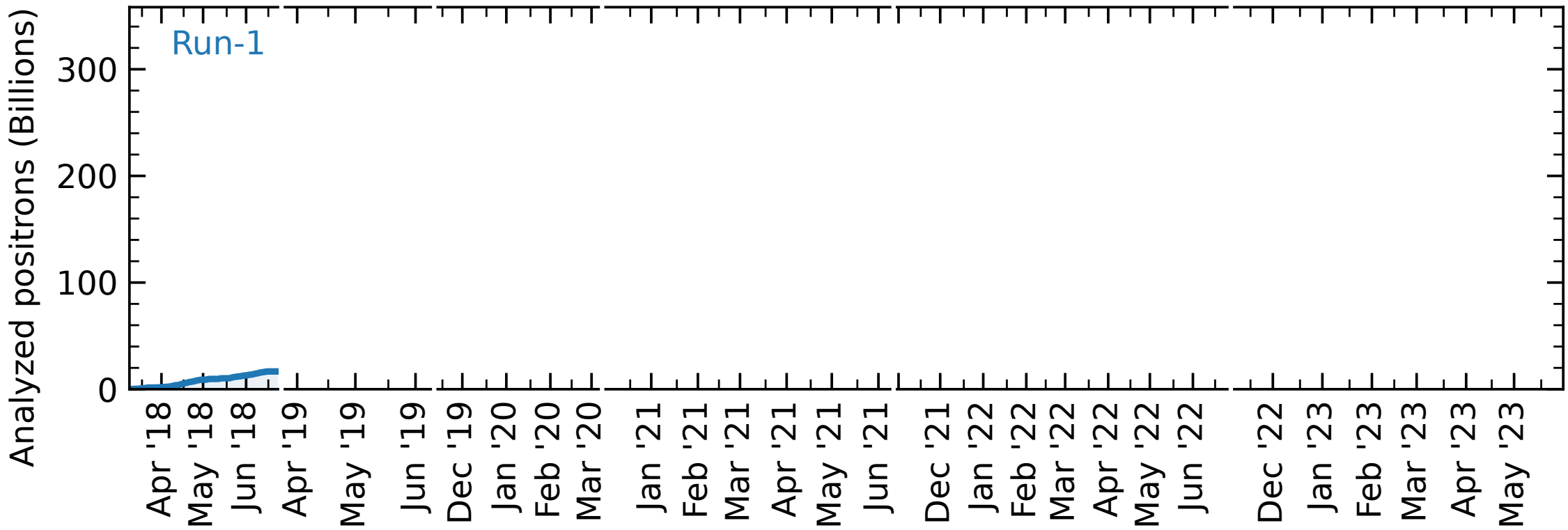

April 2021: **Run-1** results, roughly matching the BNL dataset

Data Collection – 6 Runs over 6+ Years

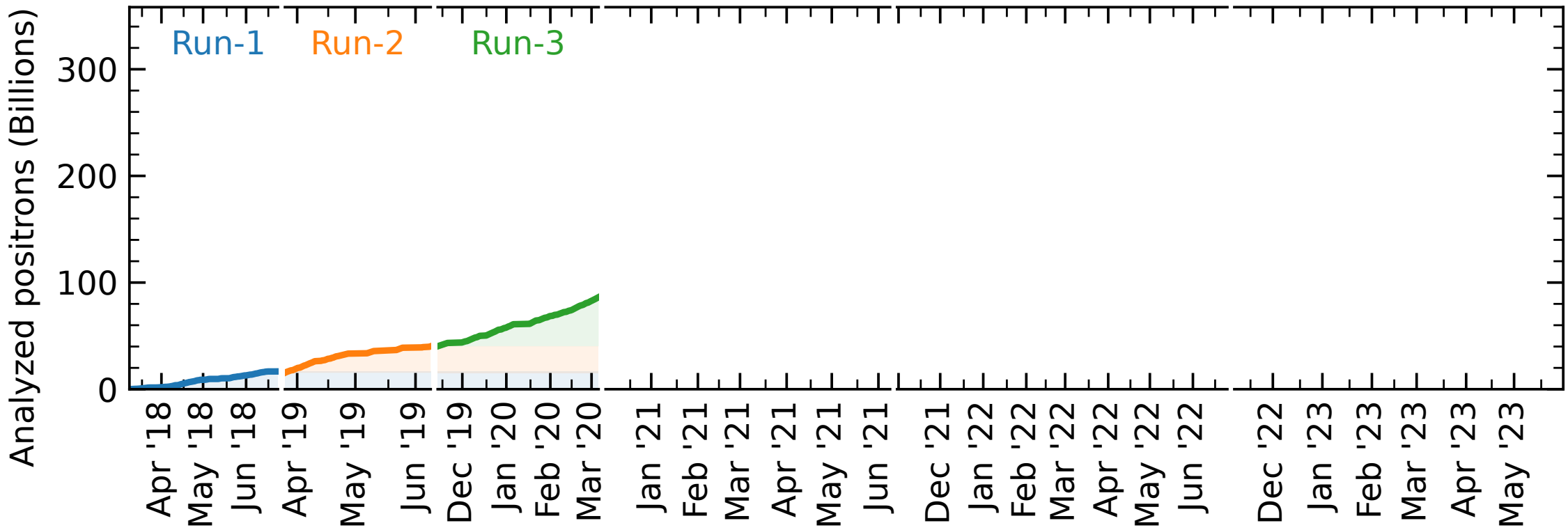

April 2021: **Run-1** results, roughly matching the BNL dataset

August 2023: **Run-2/3** results, 4.6 times more data than Run-1

Data Collection – 6 Runs over 6+ Years

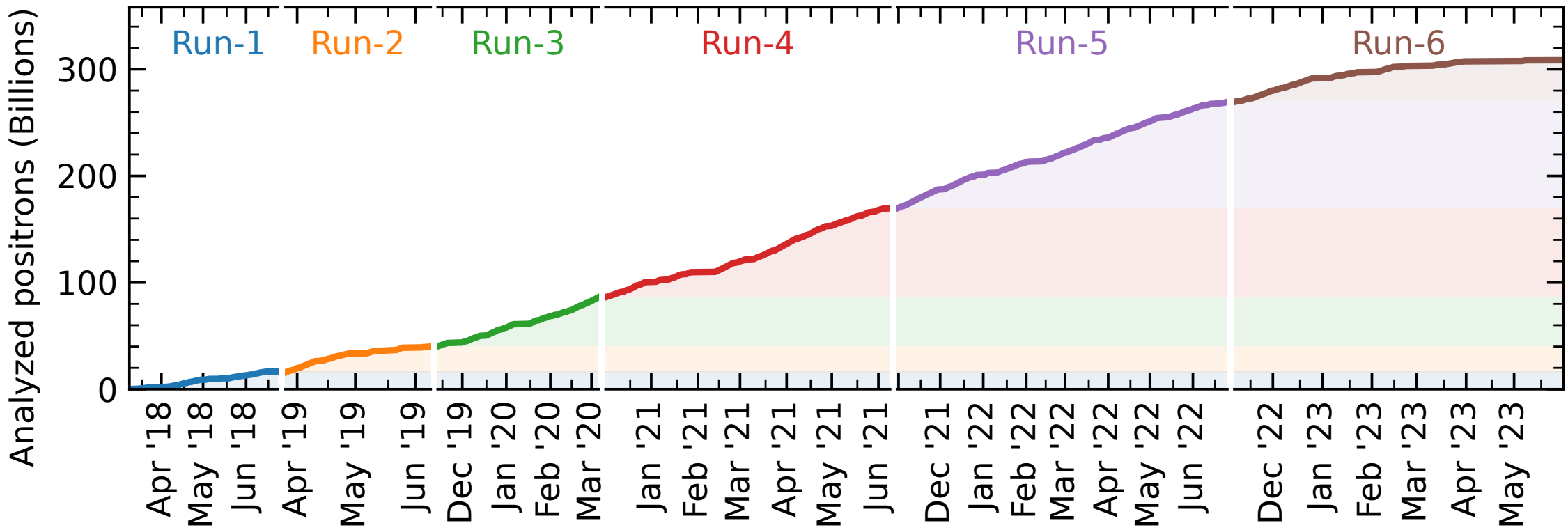

April 2021: **Run-1** results, roughly matching the BNL dataset

August 2023: **Run-2/3** results, 4.6 times more data than Run-1

June 2025: **Run-4/5/6** results, 2.6 times the Run-1/2/3 dataset

Muon g–2 Theory Initiative (TI)

100+ theorist compile the theoretical input and provide recommendations

muon-gm2-theory.illinois.edu

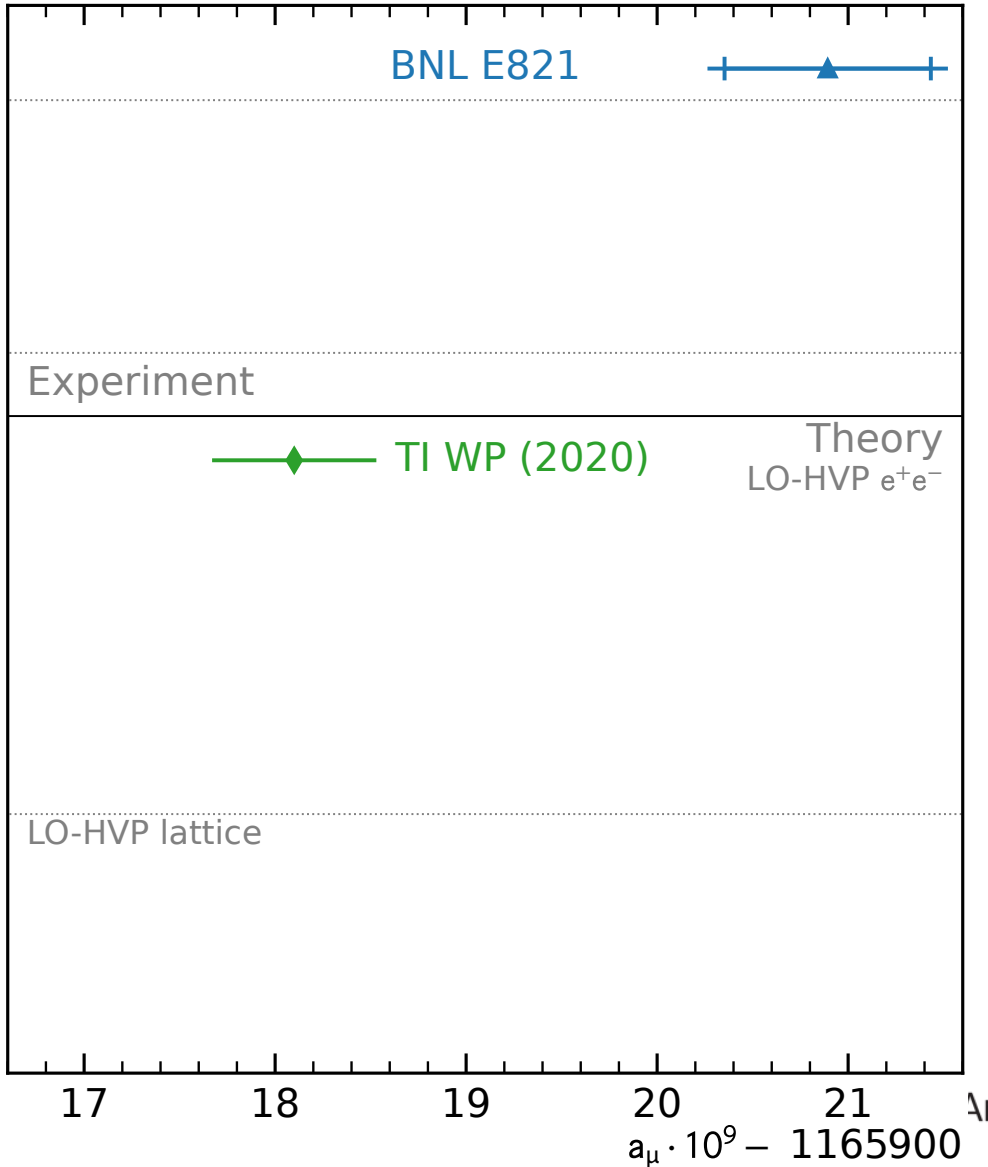

TI White Paper 2020
Physics Reports 887 (2020) 1-166

TI White Paper 2020

Hadronic Vacuum Polarization (HVP)

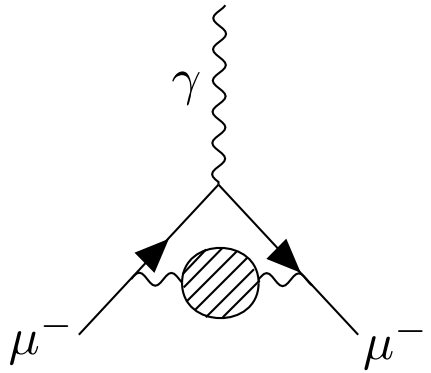

data-driven dispersive approach from $\sigma(e^+e^- \to hadrons)$ data from different experiments over 20+ years

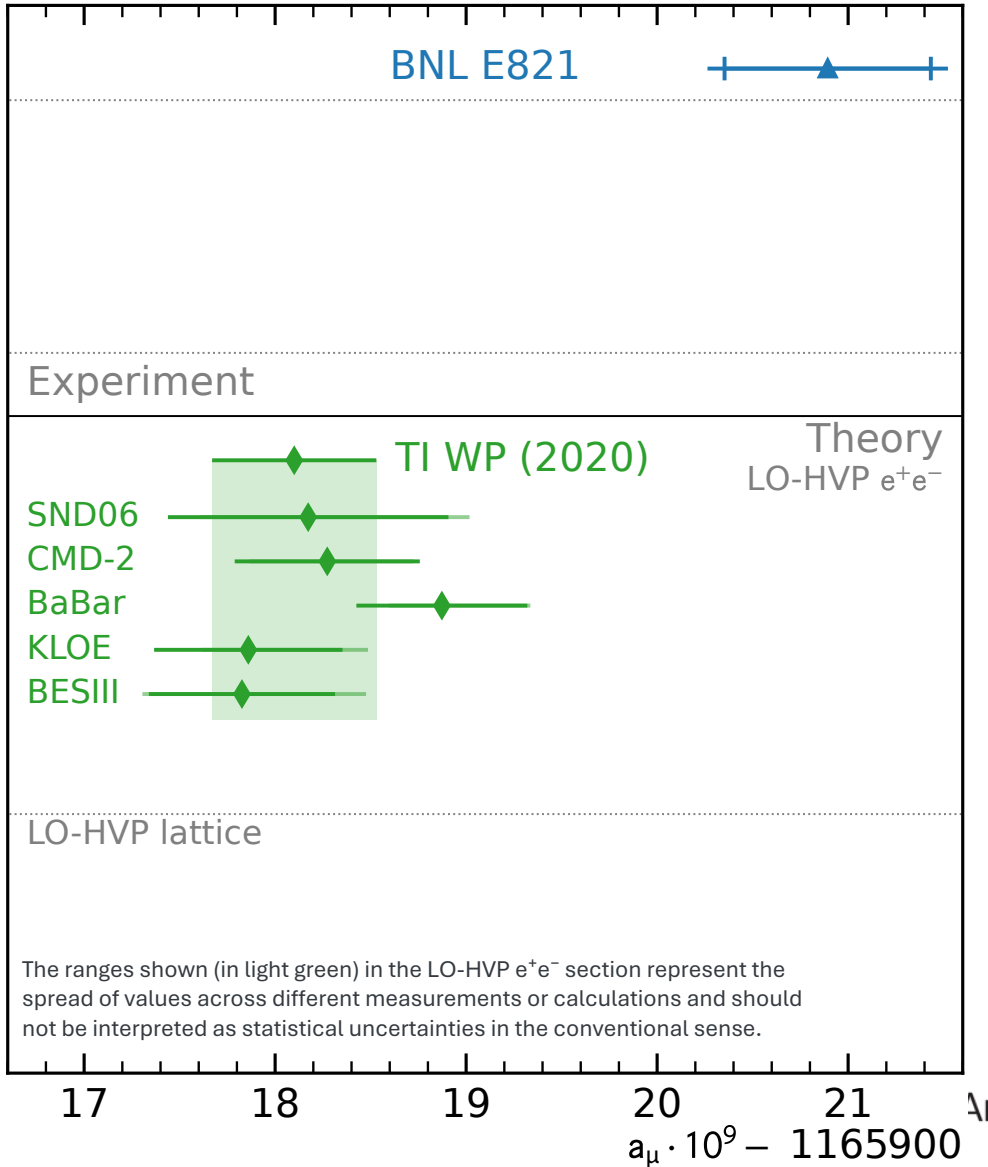

Blinded Analysis

Software & **Hardware blinded**

- Altered clock: 40 MHz - δ
  aka. value of ω_a is not knowable
- δ secret to the collaboration until the vote for hardware unblinding

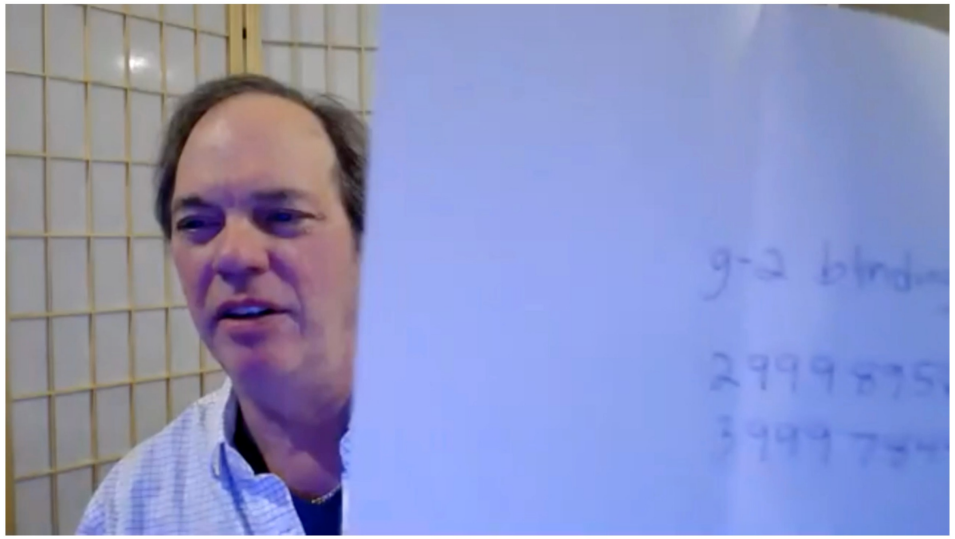

February 25th 2021, on Zoom

May 20th 2025, at Fermilab

April 2021: Run-1

- 5% of our full dataset
- In good agreement with previous results

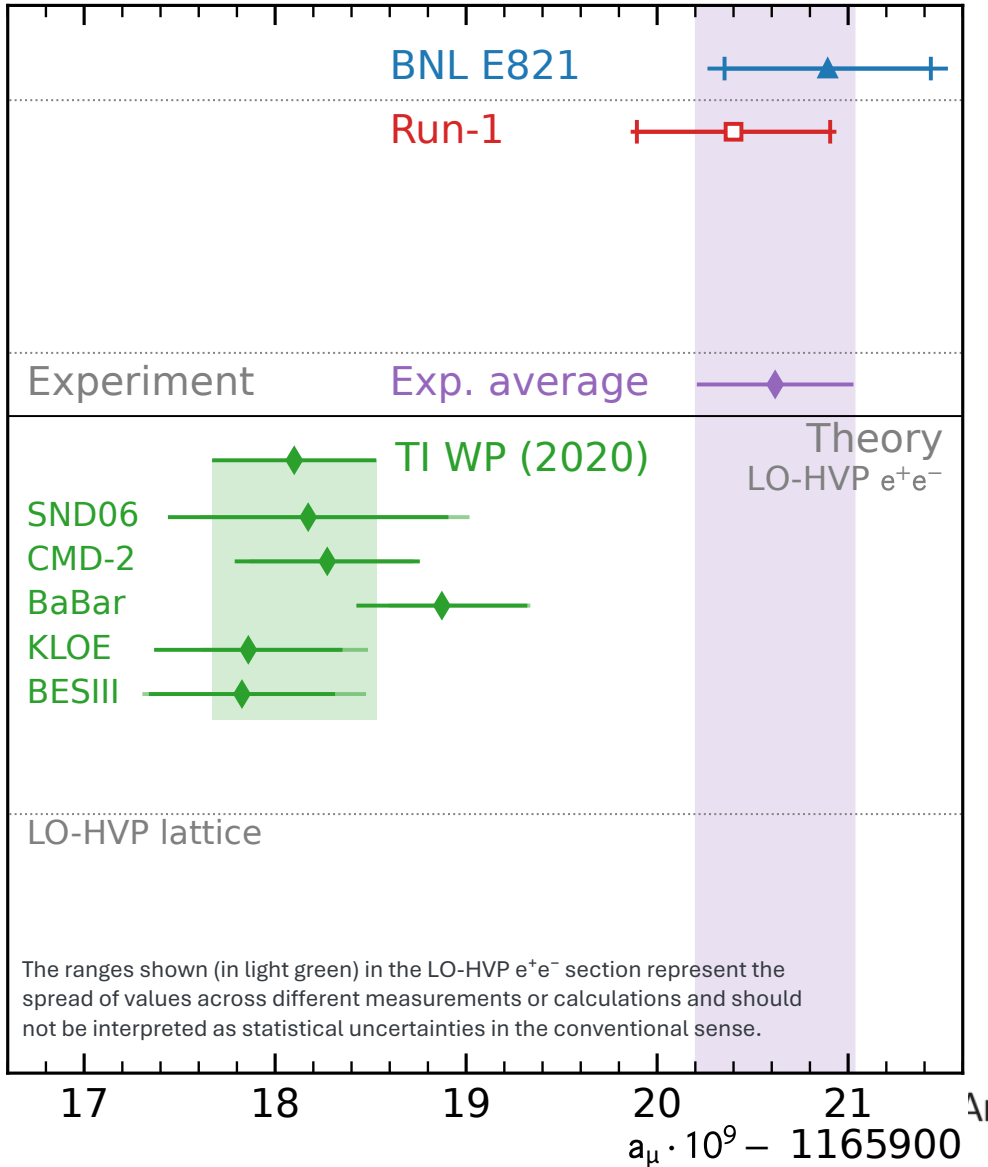

April 2021 – Muons made News

A Particle's Tiny Wobble Could Upend the Known Laws of Physics

By DENNIS OVERBYE

Evidence is mounting that a tiny subatomic particle seems to be disobeying the known laws of physics, scientists announced on Wednesday, a finding that would open a vast and tantalizing hole in our understanding of the universe.

The result, physicists say, suggests that there are forms of matter and energy vital to the nature and evolution of the cosmos that are not yet known to science.

"This is our Mars rover landing moment," said Chris Polly, a physicist at the Fermi National Accelerator Laboratory, or Fermilab, in Batavia, Ill., who has been working toward this finding for most of his career.

The particle under scrutiny is the muon, which is akin to an electron but far heavier, and is an integral element of the cosmos. Dr. Polly and his colleagues — an international team of 200 physicists from seven countries — found that muons did not behave as pre-

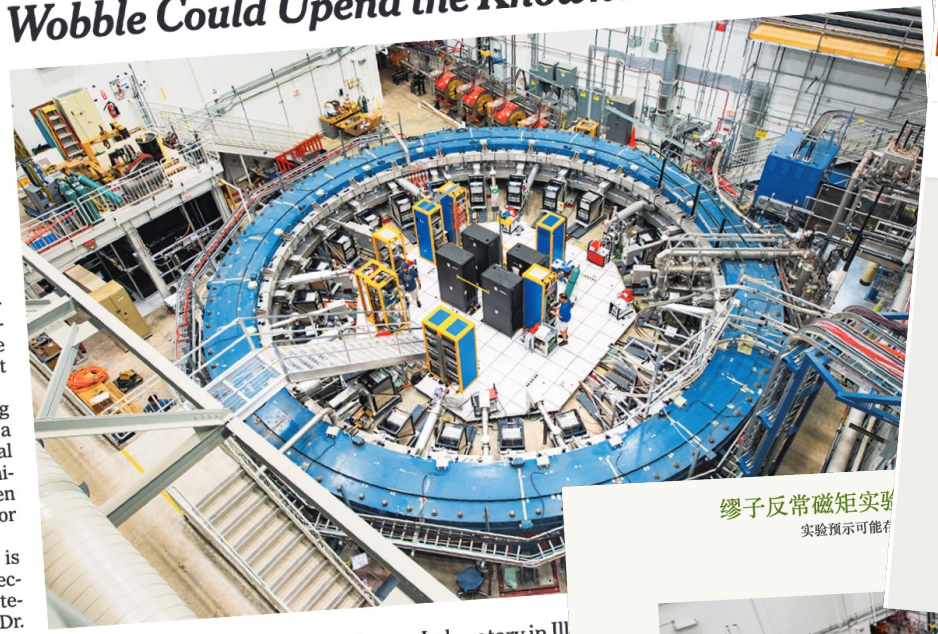

A ring at the Fermi National Accelerator Laboratory in Ill

particles in the universe (17 at last

The results, the first fr
d Muon g
xperimer
ational L
ve teased

seminar

缪子反常磁矩实验

实验预示可能存

缪子反常磁矩储存环

近日，在美国费米国家实验室进行的缪子反常磁
标准模型理论预言不相符，该结果与早期美国布鲁
的未知粒子或者作用力。

"这意味着原本经历了多次考验，堪称完美的
更完美的理论等待人类去发现。"缪子反常磁矩实验
《中国科学报》。

DER SPIEGEL

Menü Schlagzeilen SPIEGEL+ Magazine Coronavirus Kli

Französischer Philosoph: Intellektueller wirft Michel Foucault Kindesmissbrauch vor Vor 3 Min

Ausbruch von Süditalien: Das Er Europäer Vor 25 Mi

SPIEGEL+ Alle Artikel & digitales Magazin

Neue Erkenntnisse in der Teilchenphysik

Kundschafter ins Unbekannte

Seit 50 Jahren ersehnen Forscher Einblicke in die Welt jenseits der bekannten Naturgesetze. Mit den Erkenntnissen aus dem Myon-g-2-Experiment könnte sich das Tor zu einer neuen Physik öffnen. Von Johann Grolle

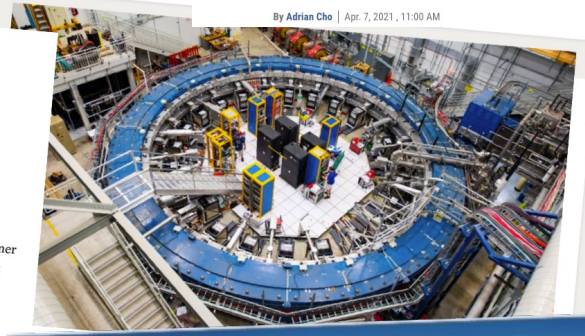

Le Monde

VENDREDI 9 AVRIL 2021

Une particul
élémentaire
polarise le m
de physique

Science Contents News Careers Journals

Read our COVID-19 research and news.

SHARE

Muons twirl as they circulate in this ring-shaped accelerator at Fermilab, like race cars perpetually spinning out. REIDAR HAHN/FERMILAB

Particle mystery deepens, as physicists confirm that the muon is more magnetic than predicted

By Adrian Cho | Apr. 7, 2021 , 11:00 AM

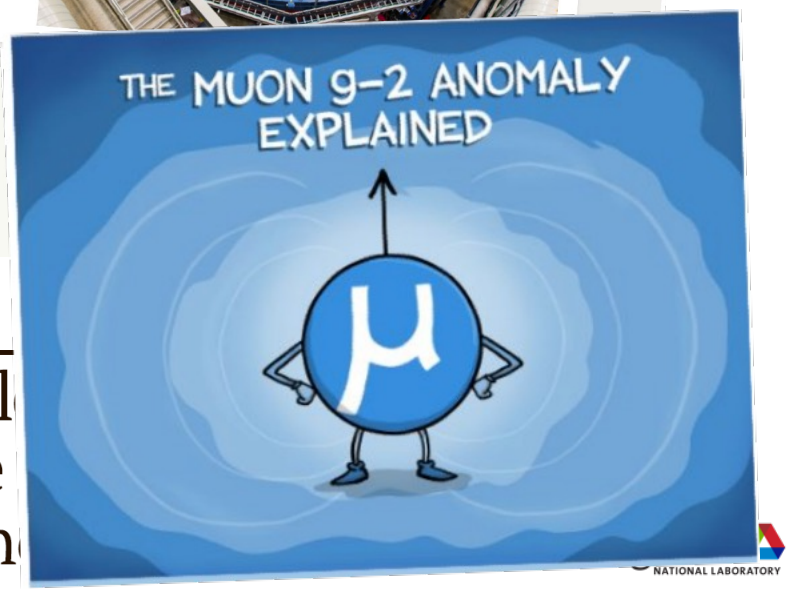

NATIONAL LABORATORY

HVP lattice calculation

First high-precision calculations of LO-HVP on lattice-QCD

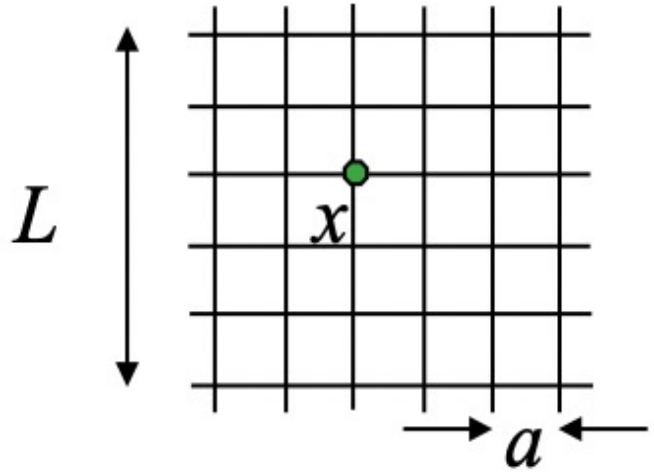

in tension with the data-driven e^+e^- approach

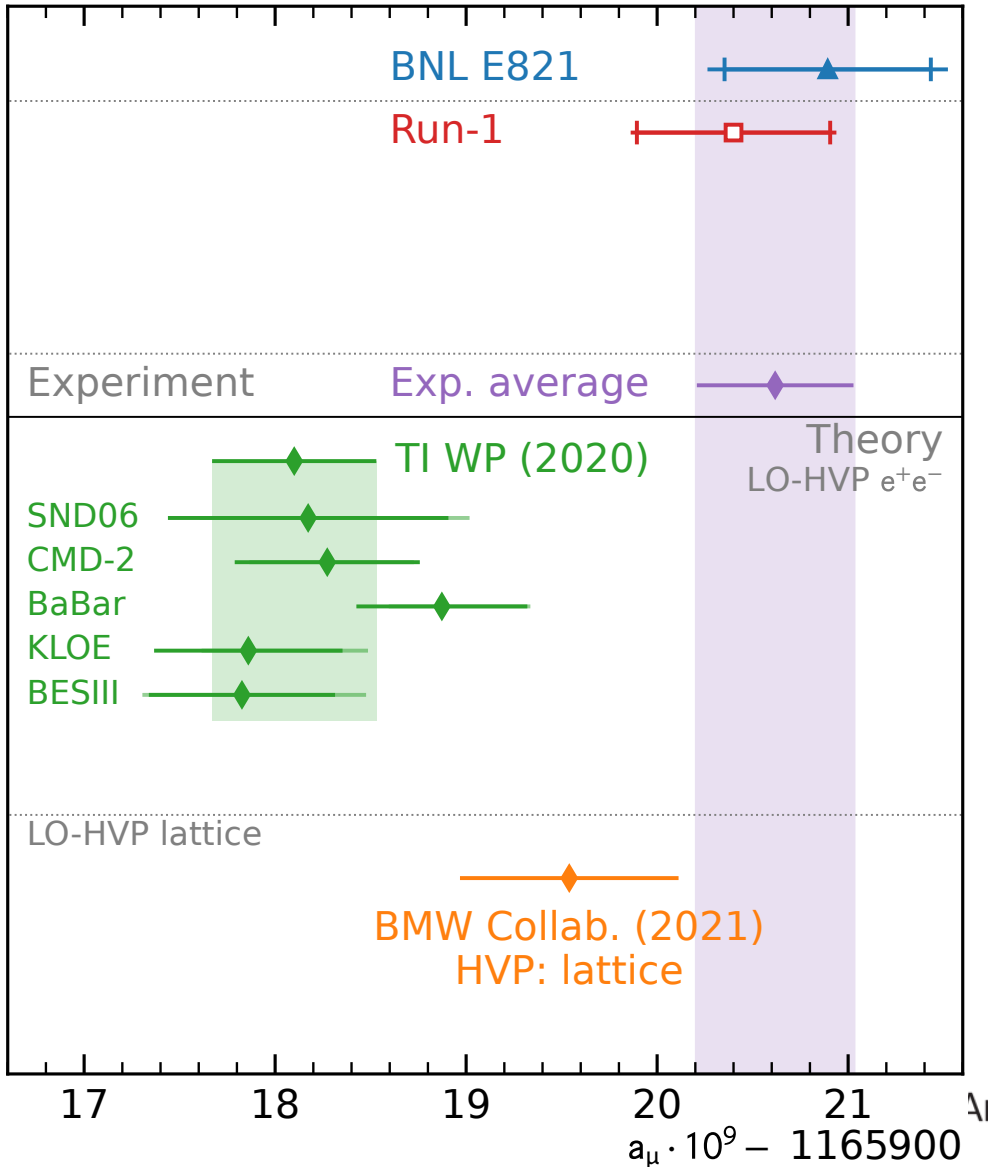

New e^+e^- Input Data

New $\sigma(e^+e^- \to hadrons)$ results from the **CMD-3 experiment** are in tension with WP (2020) input

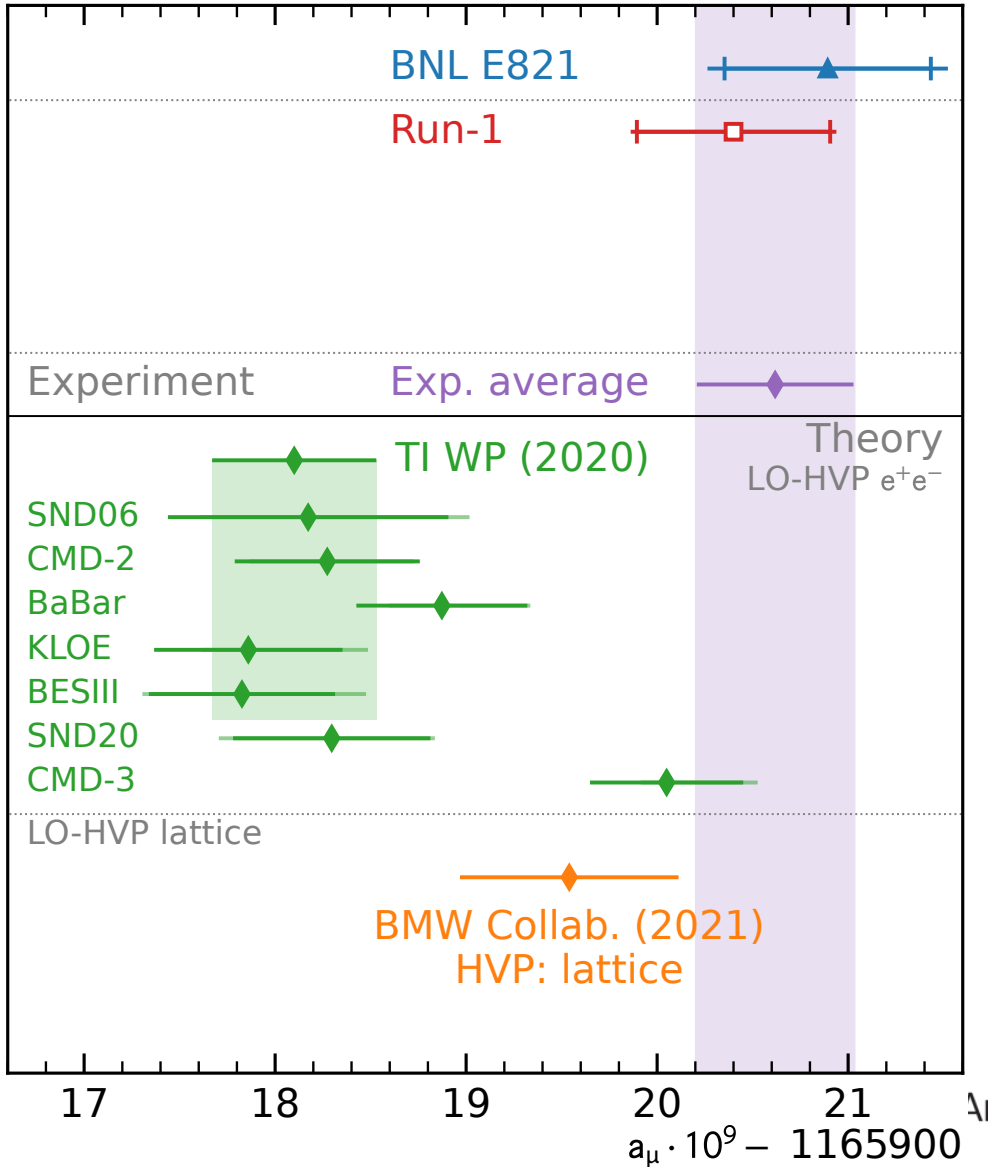

August 2023: Run-2/3

- 4.6 times more data
- More than a two-fold increase in precision

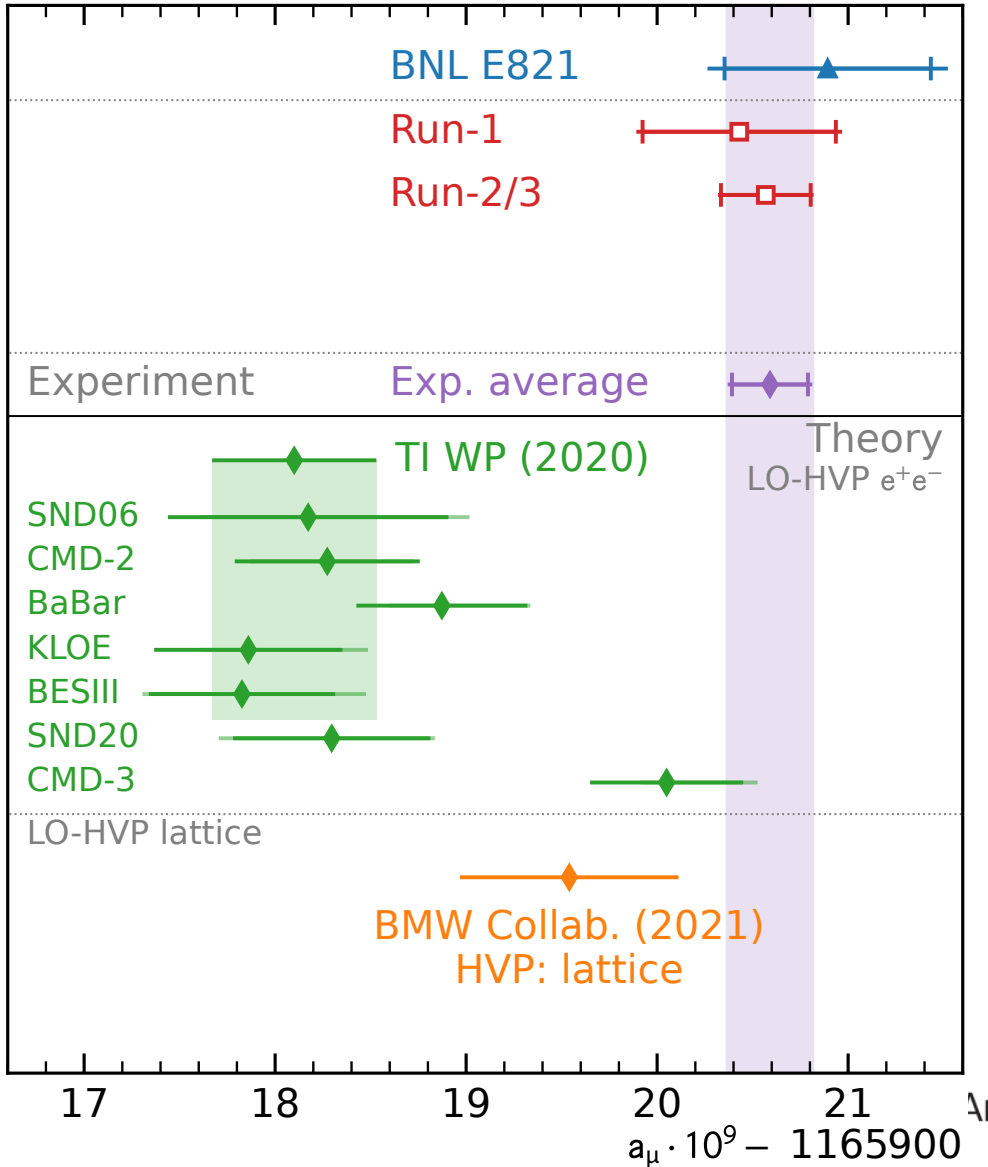

TI White Paper 2025

New **TI White Paper (2025)** using only lattice-QCD based LO-HVP determination

- Uses input from several published lattice-QCD calculations to compile the WP (2025) value

All the details in
TI White Paper 2025
arXiv:2505.21476

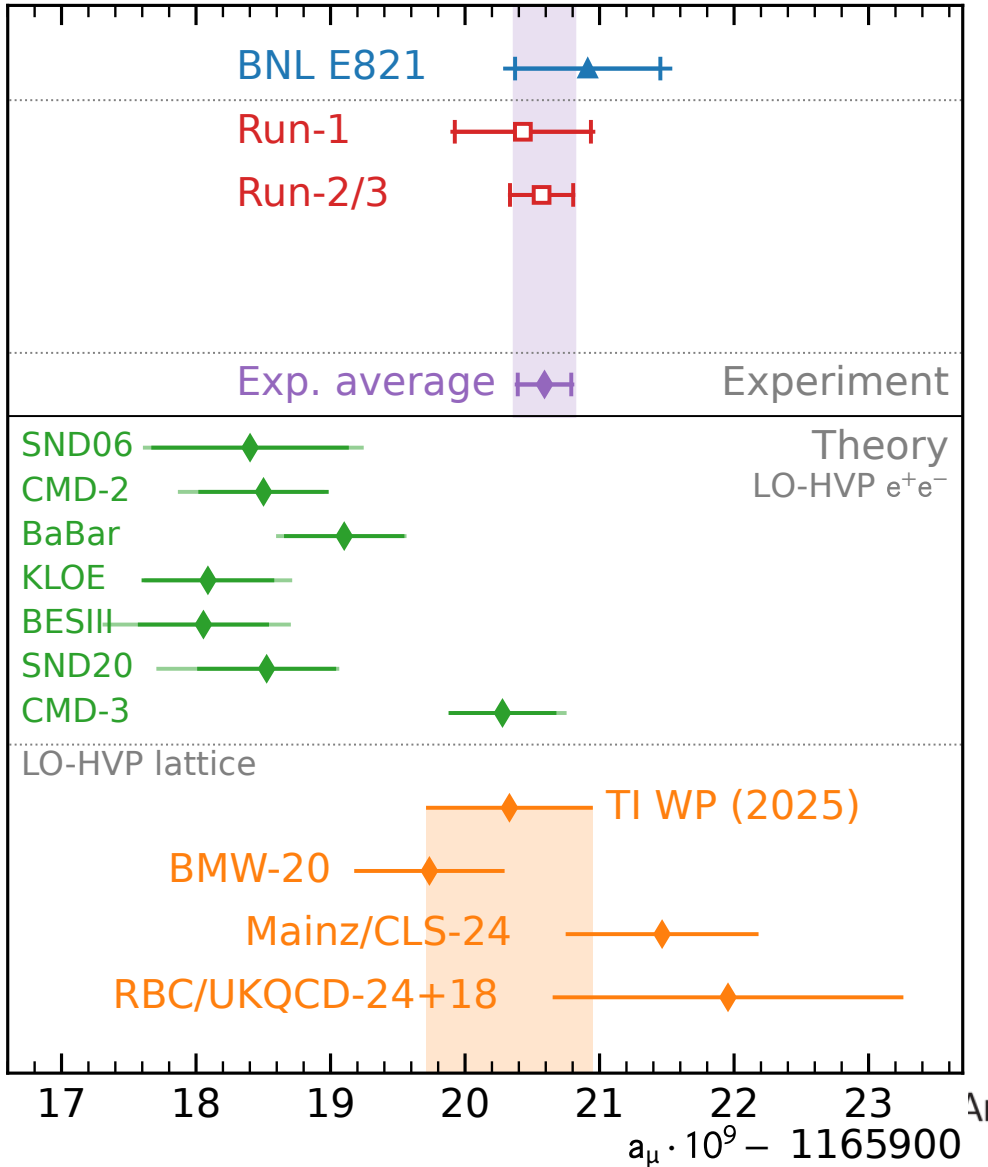

June 2025: Run-4/5/6

- 2.6 times more data

- Final precision of 127 ppb,
  more than a 4-fold improvement over
  the BNL result

Lepton-Photon 2025 (August)

2025 results are very consistent with 2009 for $\pi\pi$ contribution to a_μ

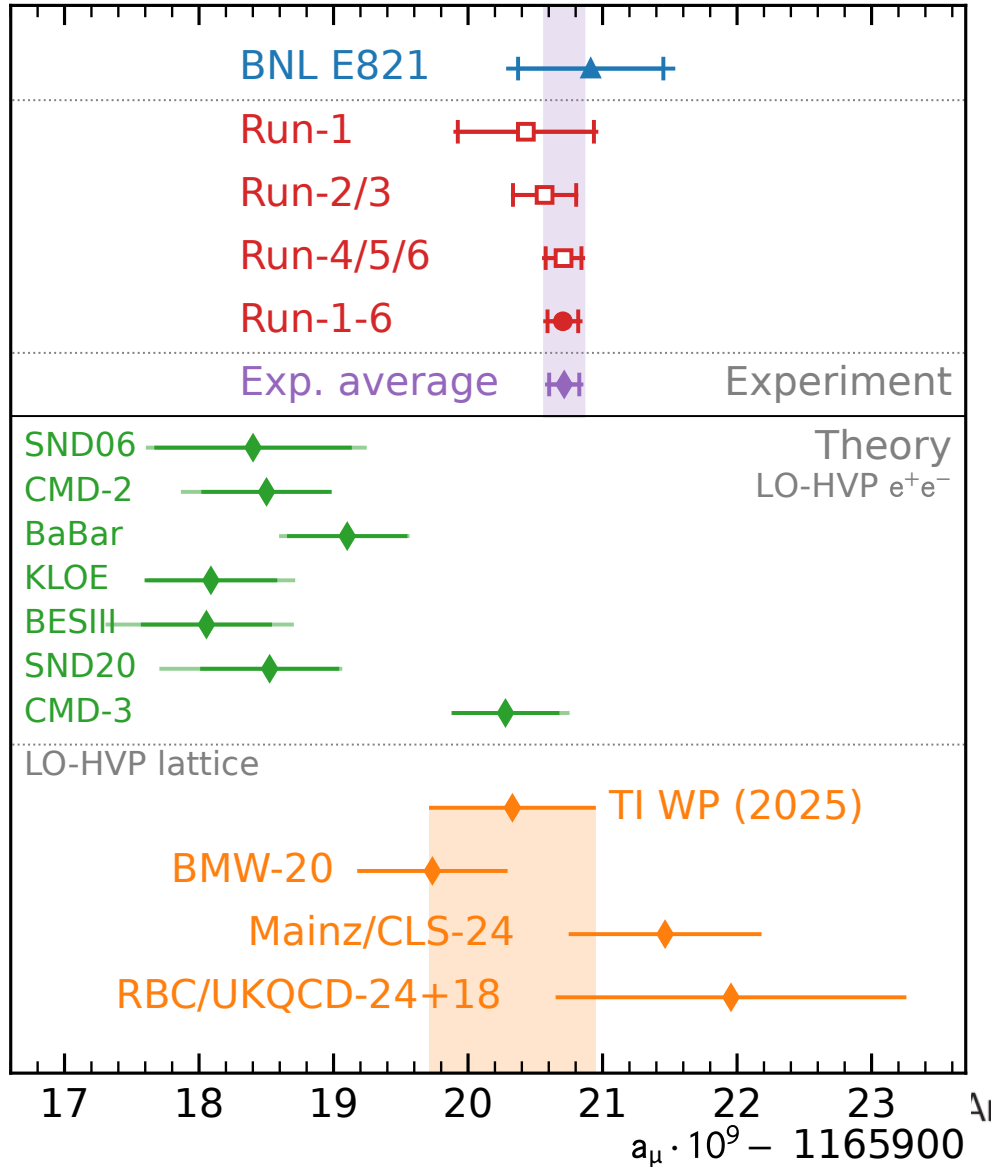

June 2025: Run-4/5/6

The MUonE

Alternative way of measuring HPV with muon-electron scattering

Under design/construction at CERN

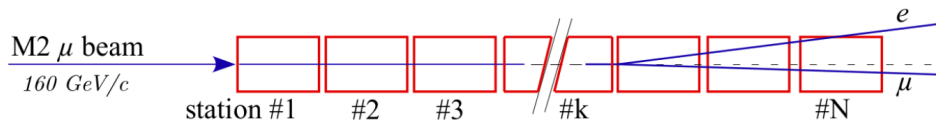

Figure 24: Schematic view of the MUonE experimental apparatus (not to

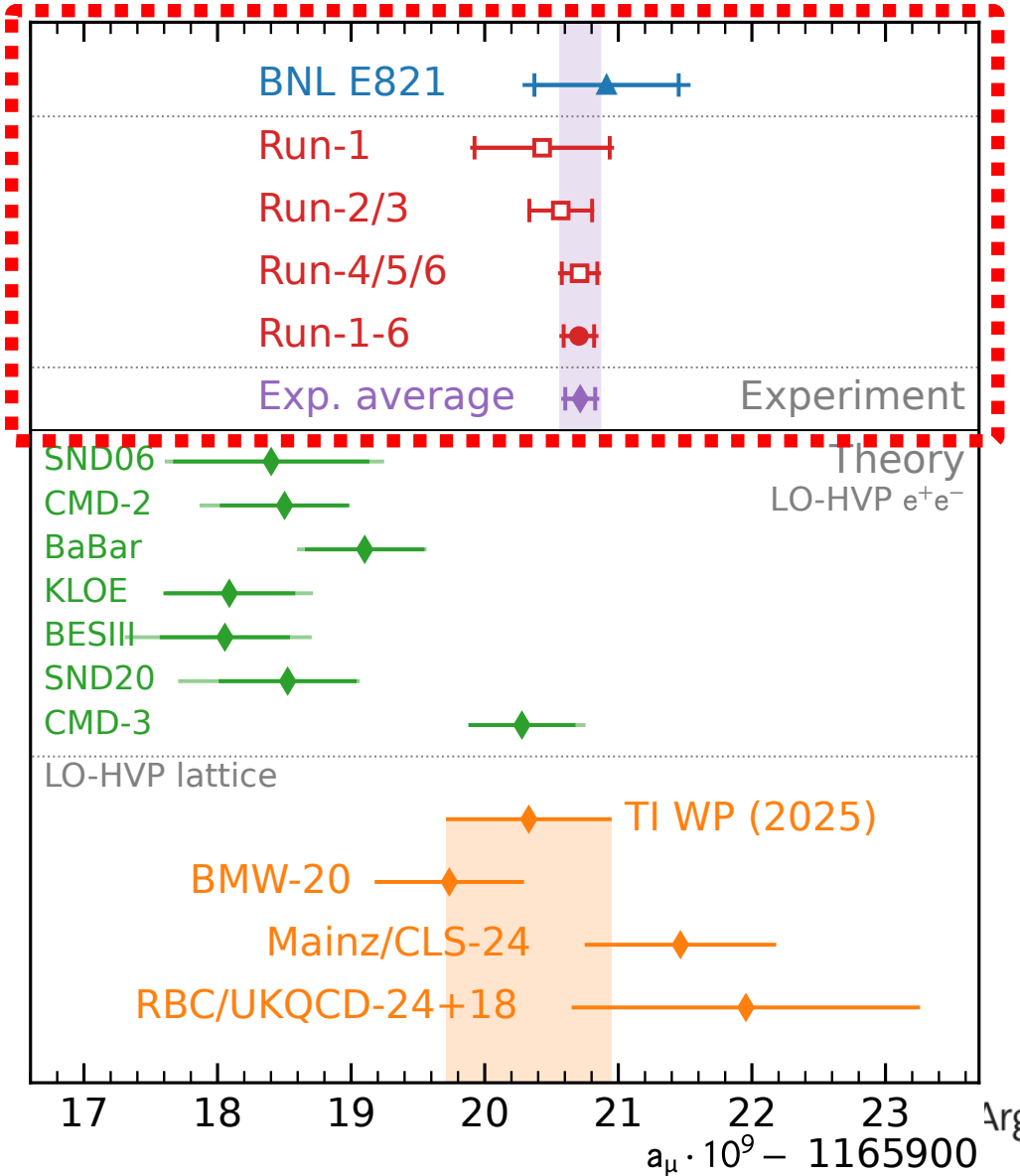

$$\frac{\omega_a}{\tilde{\omega}'_p} = \frac{\omega_a^m\left(1+C_e+C_p+C_{pa}+C_{dd}+C_{ml}\right)}{\langle\omega'_p\times M\rangle\left(1+B_k+B_q\right)}$$

Run-4/5/6

Quantity		Correction (ppb)	Uncertainty (ppb)
ω_a^m (statistical)		···	114
ω_a^m (systematic)		···	30
C_e	Electric Field	347	27
C_p	Pitch	175	9
C_{pa}	Phase Acceptance	-33	15
C_{dd}	Differential Decay	26	27
C_{ml}	Muon Loss	0	2
$\langle\omega'_p \times M\rangle$ (mapping, tracking)		···	34
$\langle\omega'_p \times M\rangle$ (calibration)		···	34
B_k	Transient Kicker	-37	22
B_q	Transient ESQ	-21	20
μ'_p/μ_B		···	4
m_μ/m_e		···	22
Total systematic for $\mathcal{R}'_\mu$		···	76
Total for a_μ		572	139

$$a_\mu = \frac{\omega_a}{\tilde{\omega}'_p}\,\frac{\mu'_p}{\mu_B}\,\frac{m_\mu}{m_e}$$

Ratio of shielded proton magnetic moment to Bohr magneton

μ'_p/μ_B: ± 4 ppb

Mass ratio m_μ/m_e: ± 22 ppb

both from CODATA

$$\frac{\omega_a}{\tilde{\omega}'_p} = \frac{\omega_a^m\left(1+C_e+C_p+C_{pa}+C_{dd}+C_{ml}\right)}{\langle\omega'_p\times M\rangle\left(1+B_k+B_q\right)}$$

Run-4/5/6

Quantity		Correction (ppb)	Uncertainty (ppb)
ω_a^m (statistical)		...	114
ω_a^m (systematic)		...	30
C_e	Electric Field	347	27
C_p	Pitch	175	9
C_{pa}	Phase Acceptance	-33	15
C_{dd}	Differential Decay	26	27
C_{ml}	Muon Loss	0	2
$\langle\omega'_p \times M\rangle$ (mapping, tracking)		...	34
$\langle\omega'_p \times M\rangle$ (calibration)		...	34
B_k	Transient Kicker	-37	22
B_q	Transient ESQ	-21	20
μ'_p/μ_B		...	4
m_μ/m_e		...	22
Total systematic for $\mathcal{R}'_\mu$		...	76
Total for a_μ		572	139

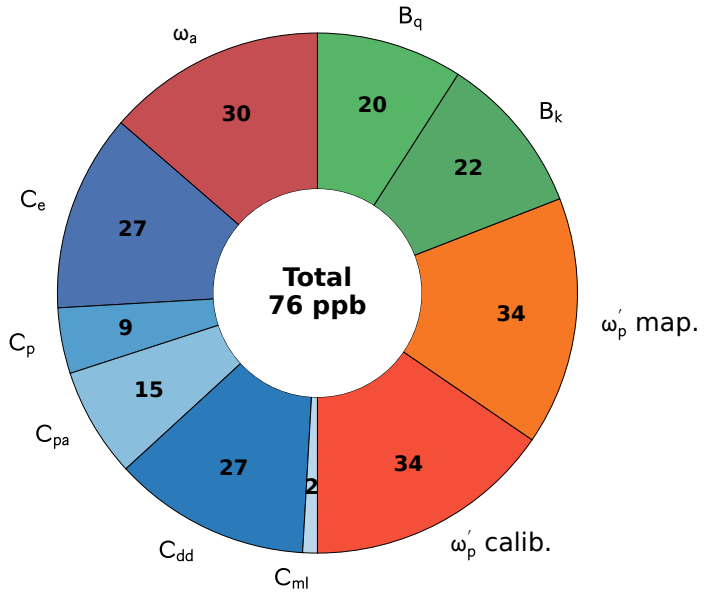

"evenly" distributed

- No dominant source
- Further improving would require to reduce in many categories

Uncertainties

$\frac{\omega_a}{\tilde{\omega}_p'}$	Stat. Uncertainty (ppb)	Syst. Uncertainty (ppb)	Total Uncertainty (ppb)
Run-1	434	159*	462
Run-2/3	201	78*	216
Run-4/5/6	114	76	137
Run-1-6	**98**	**78**	**125**
	TDR goal 100 ppb ✓	TDR goal: 100 ppb ✓	TDR goal: 140 ppb ✓

*corrected

Consistency Checks

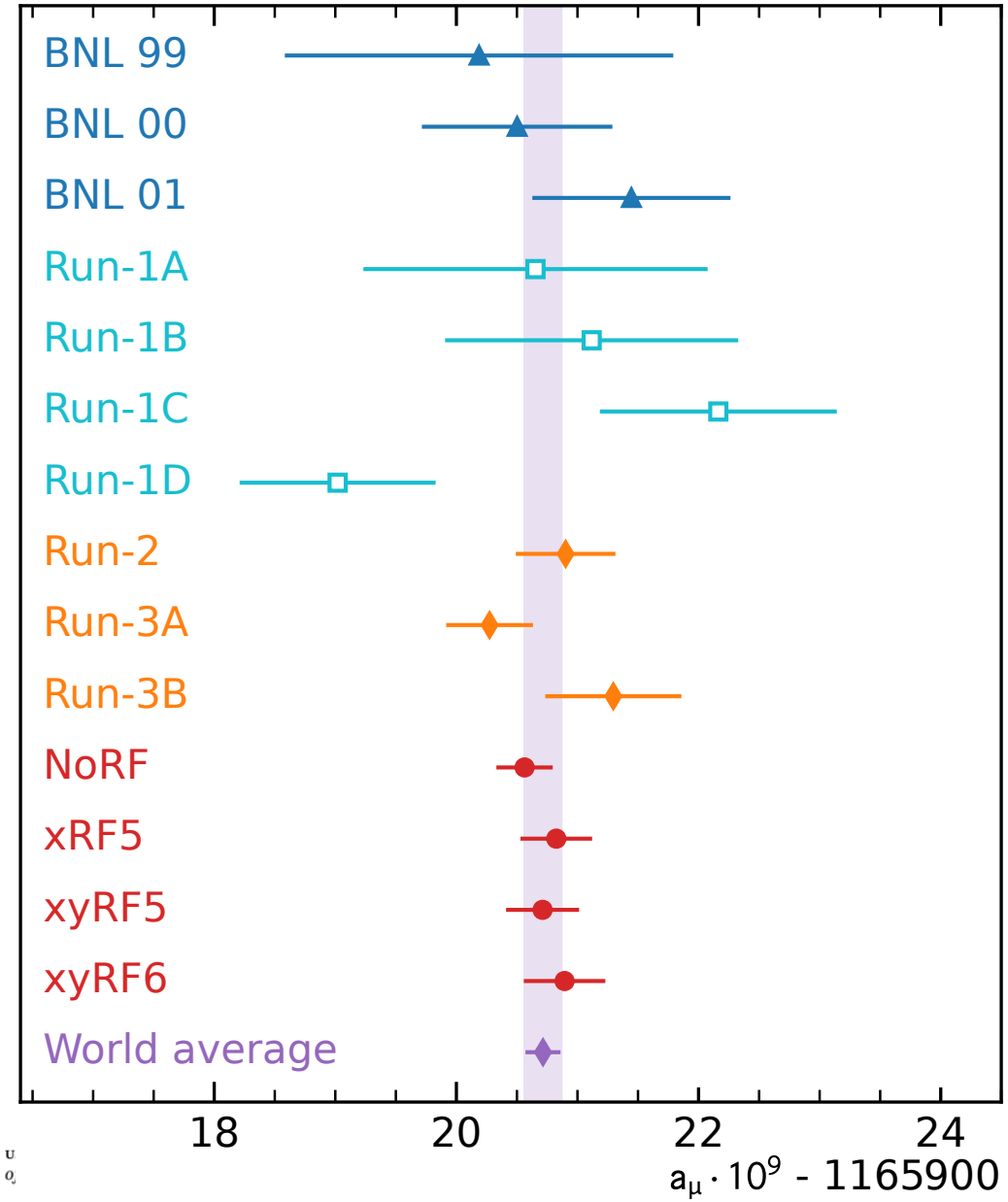

- Each dataset fitted separately
- Published data are averages of blue, orange, and red points

Consistency Checks

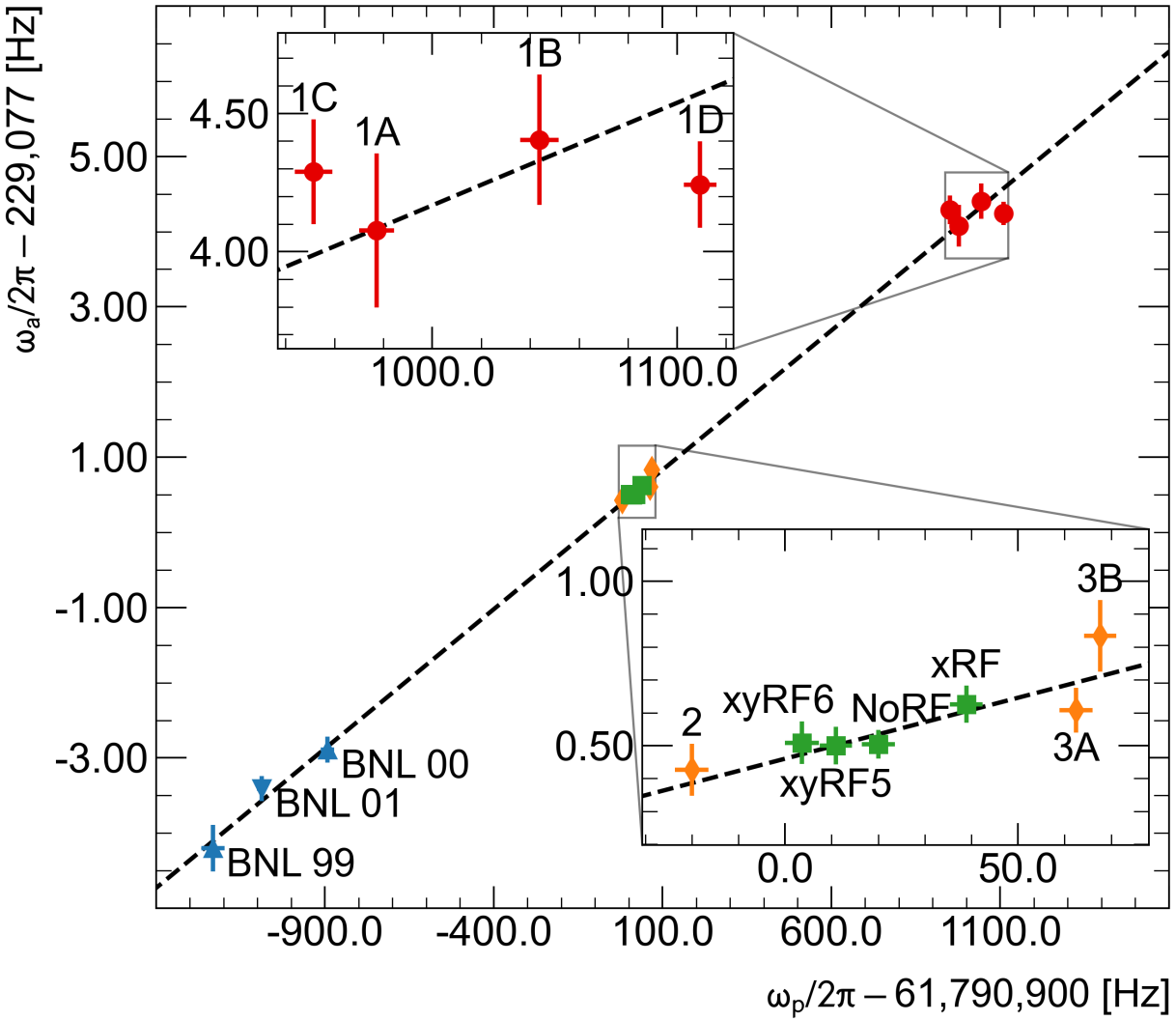

spanning ~30ppm

An incredible Team!

The Muon g-2 Collaboration:

176 collaborators, 34 institutes, 7 countries

Particle-, Nuclear-, Atomic-, Optical-, Accelerator-, and Theoretical-Physicists and Engineers

Is there more?

from **Muon g-2 at Fermilab**

- Muon EDM results
- More Beyond Standard Model Analysis:
  - CPT/Lorenz-violating
  - Ultra light Dark Matter

Muon EDM

non-zero EDM (η) modifies the spin equation

$$\vec{\omega}_{a\eta} = a_\mu \frac{e}{m}\vec{B} + \eta\frac{e}{2m}\left[\frac{\vec{E}}{c} + \vec{\beta}\times\vec{B}\right]$$

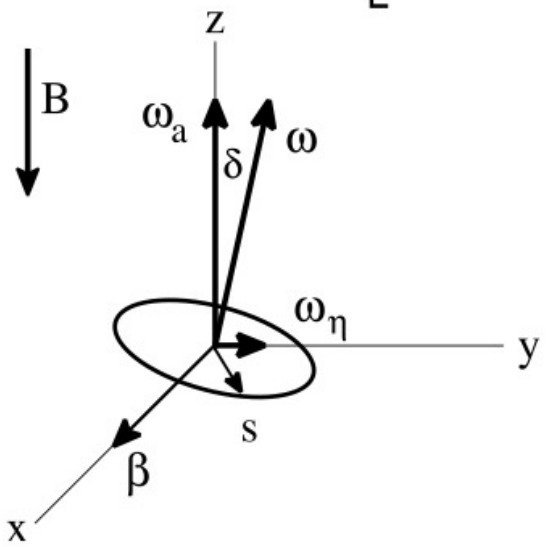

Search for an up/down asymmetry out of phase with ω_a

Is there more? J-PARC Muon g-2/EDM experiment

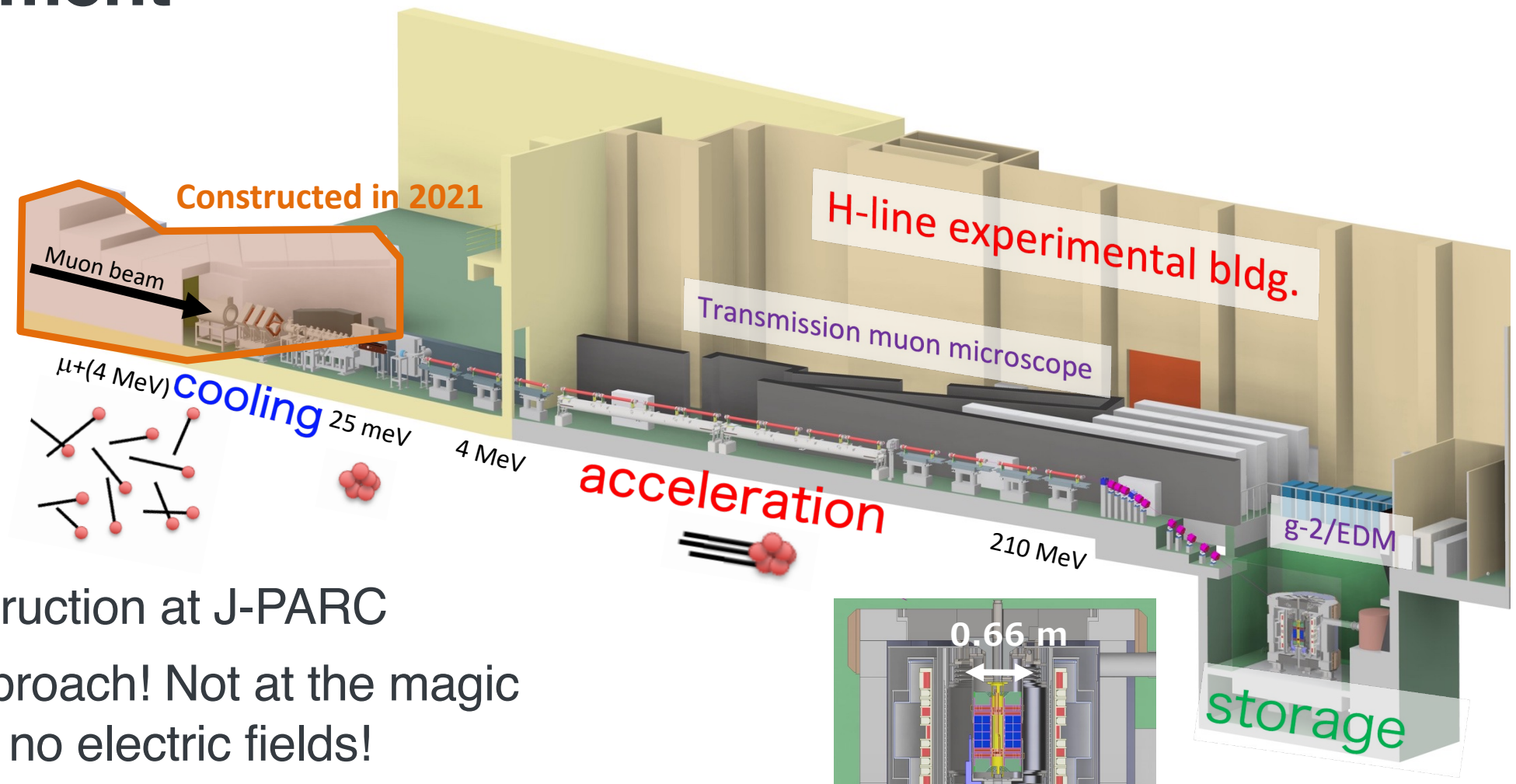

- Under construction at J-PARC
- Different approach! Not at the magic momentum/ no electric fields!
- Expected sensitivity of ~500ppb

Measuring Muon g−2 to Test the Standard Model

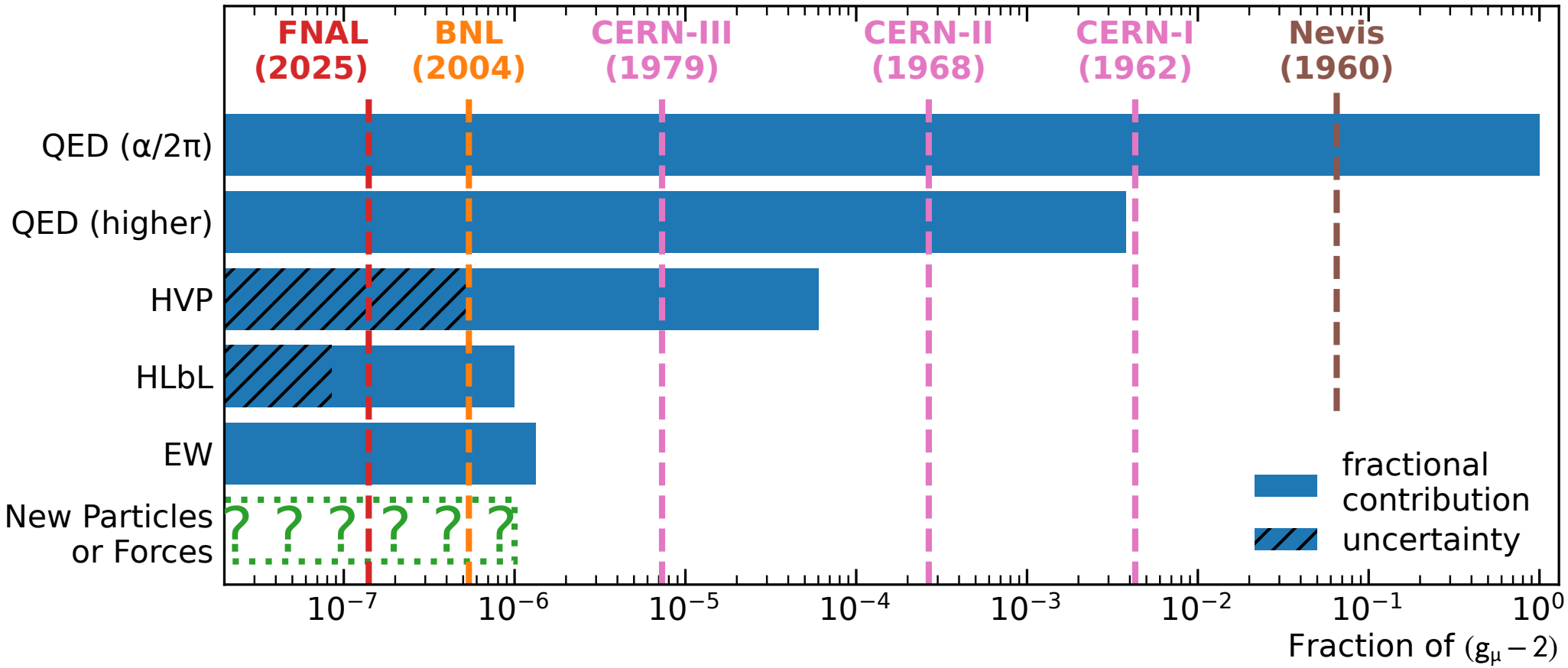

This document was prepared by the Muon g–2 Collaboration using the resources of the Fermi National Accelerator Laboratory (Fermilab), a U.S. Department of Energy, Office of Science, Office of High Energy Physics HEP User Facility. Fermilab is managed by FermiForward Discovery Group, LLC, acting under Contract No. 89243024CSC000002.

Muon g–2 Theory

TI White Paper 2025

Last week:

New **TI White Paper (2025)** using only lattice-QCD based LO-HVP determination

All the details in
TI White Paper 2025
arXiv:2505.21476

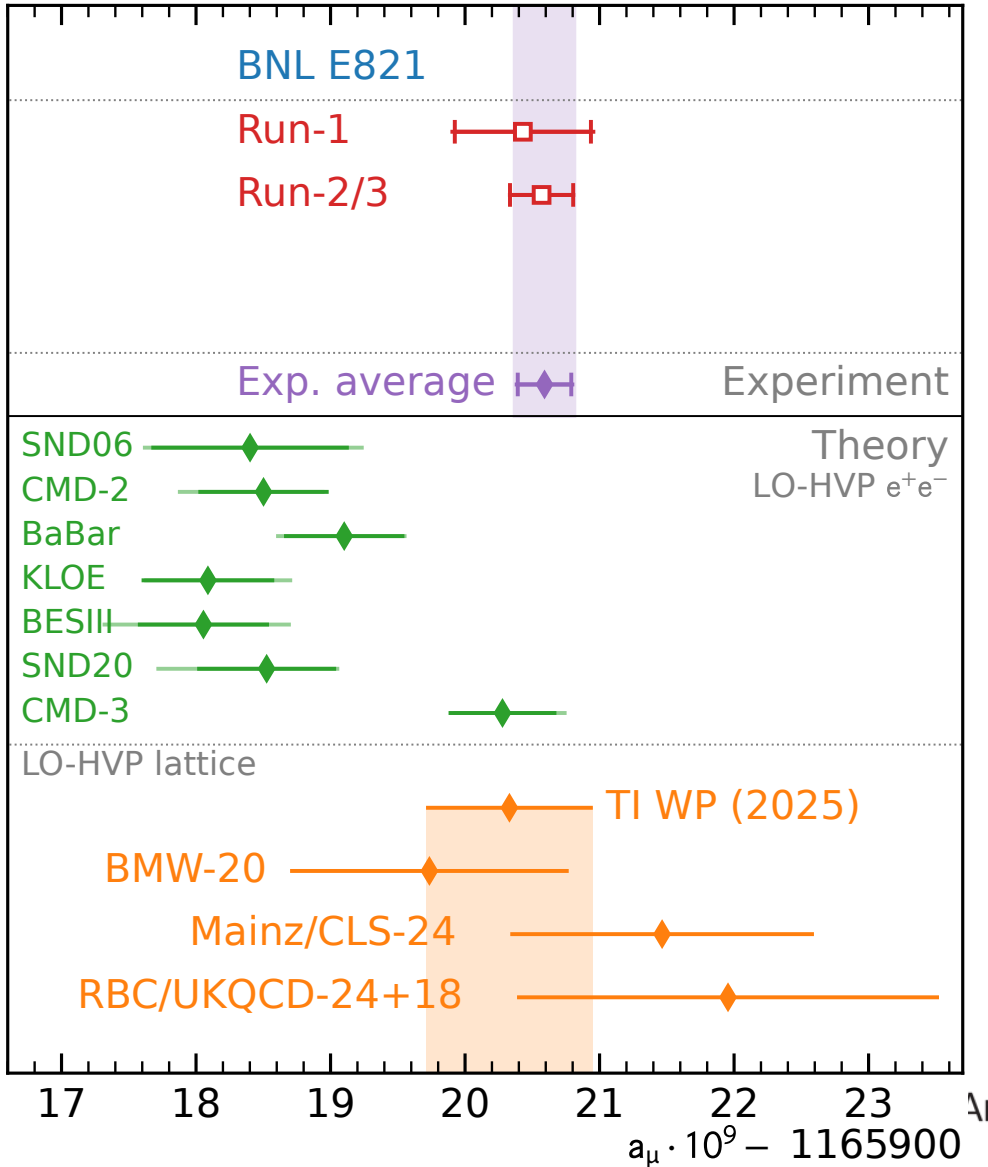

LO-HVP: dispersive e^+e^-

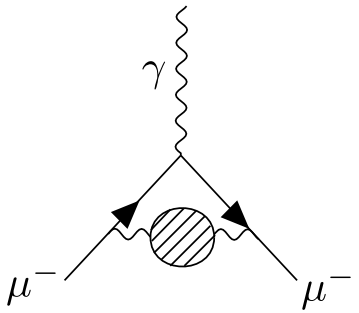

$$\text{Im}\left(\text{had.}\right) \sim \left|\;\right|^2 \longrightarrow a_\mu^{\text{HVP,LO}} = \frac{\alpha^2}{3\pi^2}\int_{s_{th}}^{\infty}\frac{K(s)}{s}R(s)ds$$

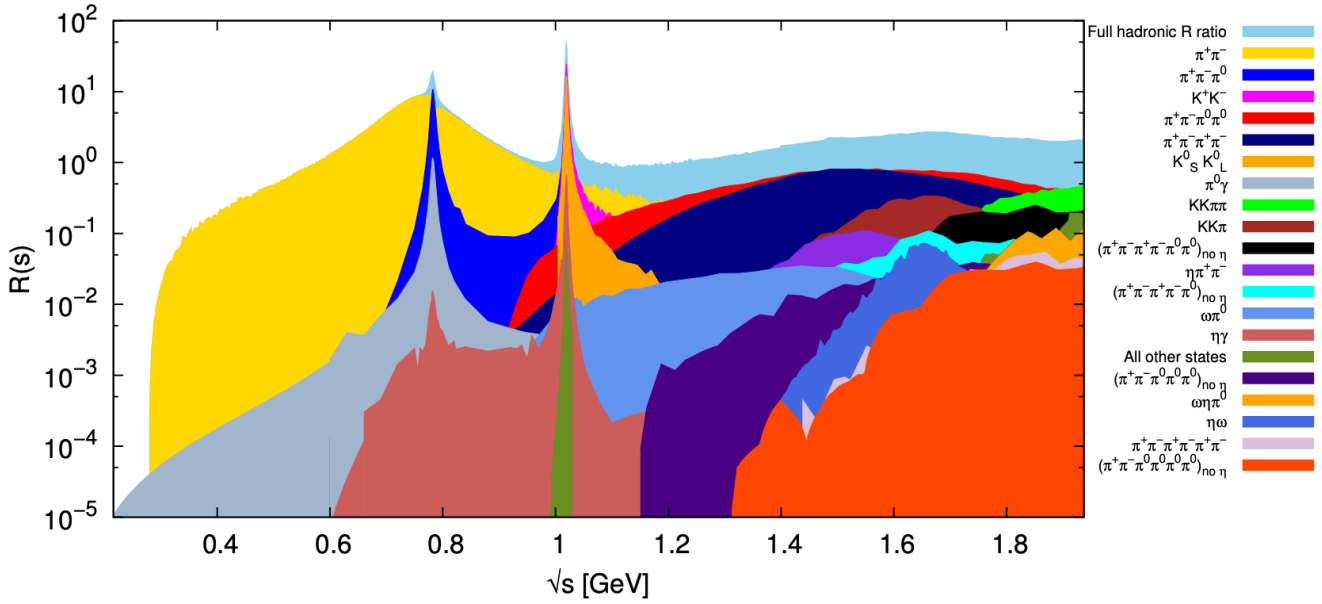

Figure 16: Contributions to the KNT data compilation of the total hadronic *R*-ratio from the different hadronic final states below 1.937 GeV [30, 265]. The full *R*-ratio is shown in light blue. Each final state is included as a new layer on top in decreasing order of the size of its contribution to $a_\mu^{\text{HVP, LO}}$.

https://arxiv.org/pdf/2505.21476

WP 2025 – Dispersive LO-HVP [pipi]

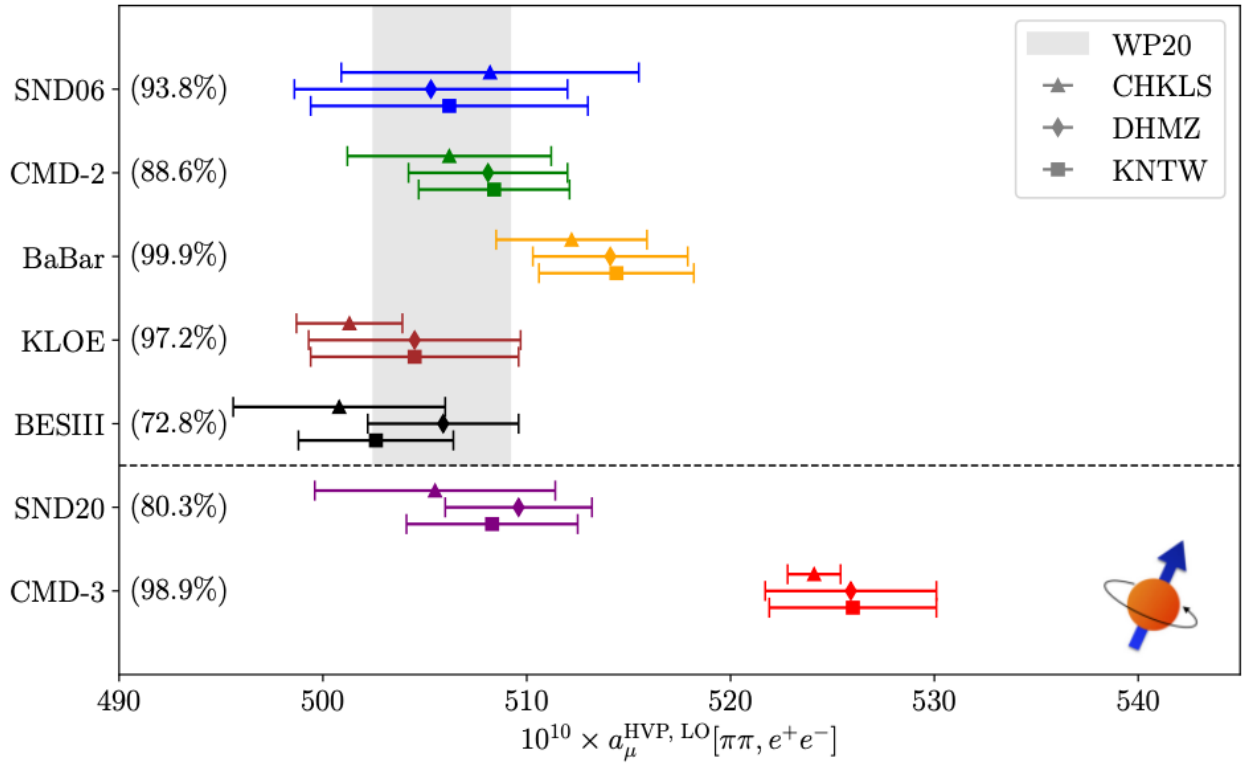

Figure 26: Dispersive theoretical predictions for $a_\mu^{\mathrm{HVP,\,LO}}[\pi\pi]$, based on various measurements of $e^+e^- \to \pi^+\pi^-$, fit/interpolated and complemented for the uncovered mass ranges (percentages of the integral covered by each measurement are shown), for the three approaches "CHKLS," "DHMZ," and "KNTW" as detailed in the main text. The gray band indicates the result from WP20, including the error inflation due to the BaBar–KLOE tension. The experiments above the dashed line entered the result for WP20, whilst those below are new measurements since then. The numerical values shown are reproduced in Table 5.

https://arxiv.org/pdf/2505.21476

WP 2025 – Dispersive a_μ

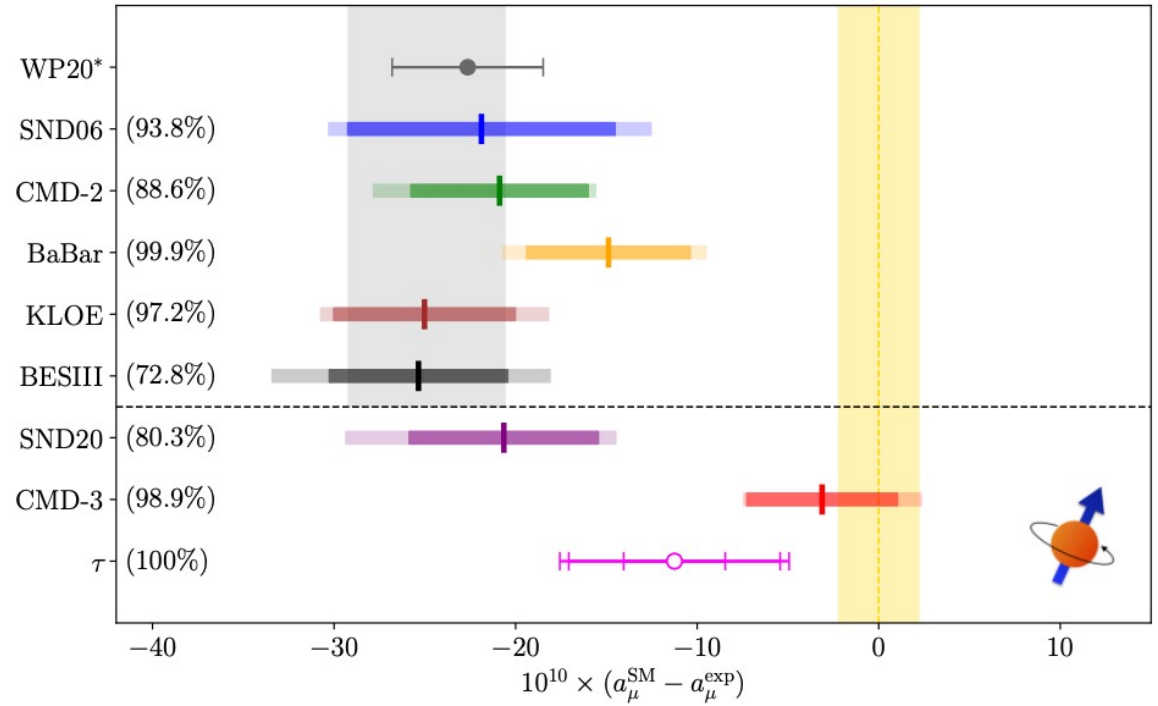

Figure 27: Summary of current data-driven evaluations of HVP, propagated to a_μ^{SM} (the yellow band indicates a_μ^{exp}, the gray band the WP20 SM prediction based on the e^+e^- data sets above the dashed line and the remainder from WP20, in particular, the WP20 HLbL value; the data point labeled WP20* indicates the shift upon using WP25 input for the other contributions besides LO HVP). The τ point corresponds to WP25 in Fig. 13, with the third, outmost error including the additional uncertainties beyond the 2π channel (the remainder of HVP is taken from WP20, the other contributions from WP25). The other points use input from the various $e^+e^- \to \pi^+\pi^-$ experiments according to Fig. 26 (again with HVP remainder from WP20 and the other contributions from WP25), where for each experiment the central values are obtained as simple average of the three combination methods, the inner ranges as simple average of the uncertainties obtained in each method, and the outer ranges reflect the maximal range covered by all methods (the percentages indicate how much of the 2π contribution to the HVP integral is covered by each measurement). We emphasize that these ranges are merely meant to illustrate the current spread, they cannot be interpreted as uncertainties with a proper statistical meaning. The numerical values follow from Tables 1 and 5.

https://arxiv.org/pdf/2505.21476

WP 2025 – a_μ

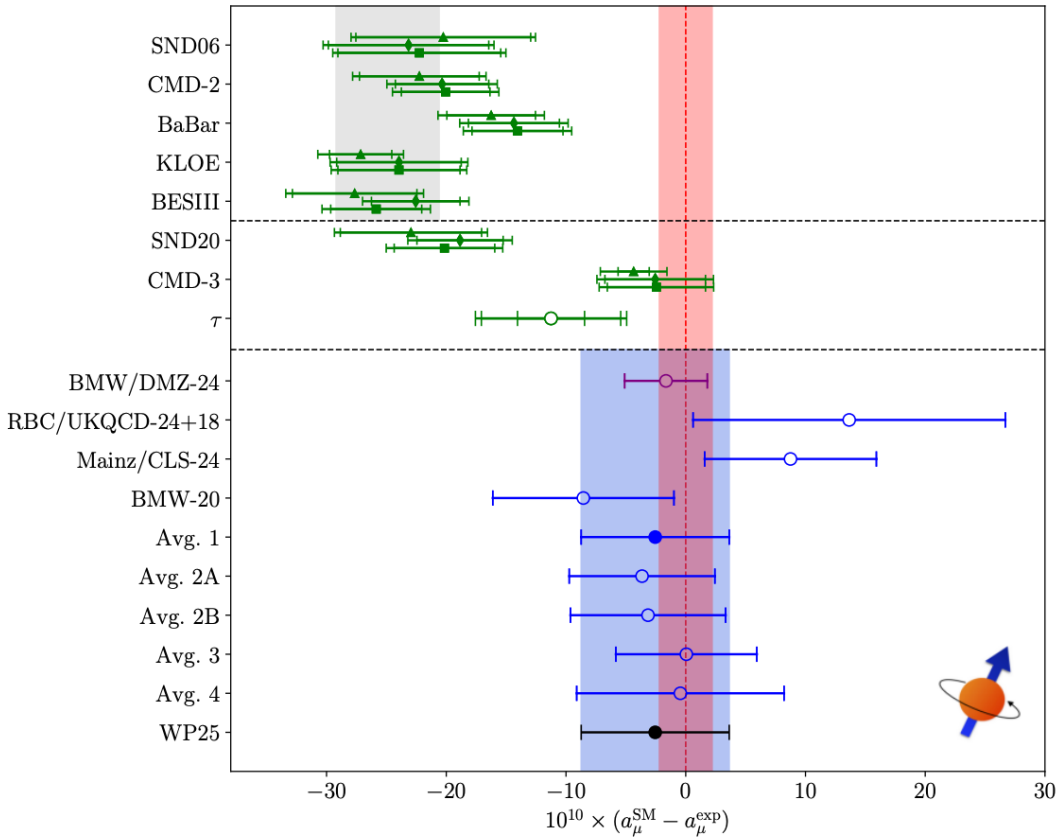

Figure 40: Final summary of various determinations of $a_\mu^{\mathrm{HVP,\,LO}}$ discussed in Secs. 2 and 3, propagated to a_μ^{SM}. The first two panels refer to data-driven determinations, where the three points for each e^+e^- experiment reflect the "CHKLS," "DHMZ," and "KNTW" methods, see Figs. 26 and 27 for more details. The gray band indicates the WP20 result, based on the e^+e^- experiments above the first dashed line. The τ point corresponds to Eq. (2.23). The last panel summarizes lattice-QCD determinations, including the hybrid evaluation [23], the three individual lattice-QCD calculations shown in Fig. 36, and the five lattice HVP averages from Fig. 37. The blue band refers to the final WP25 result, which coincides with "Avg. 1." In all cases, except for the gray WP20 band, the remaining contributions to a_μ^{SM} beyond $a_\mu^{\mathrm{HVP,\,LO}}$ are taken from WP25, as given in Table 1. The red band denotes the experimental world average.

https://arxiv.org/pdf/2505.21476

WP 2025 – a_μ

Contribution	Section	Equation	Value $\times 10^{11}$	References
Experiment (E989)		Eq. (9.5)	116 592 059(22)	Refs. [5–7, 9–12]
HVP LO (lattice)	Sec. 3.6.1	Eq. (3.37)	7132(61)	Refs. [13–29]
HVP LO (e^+e^-, τ)	Sec. 2	Table 5	Estimates not provided at this point	
HVP NLO (e^+e^-)	Sec. 2.9	Eq. (2.47)	−99.6(1.3)	Refs. [30, 31]
HVP NNLO (e^+e^-)	Sec. 2.9	Eq. (2.48)	12.4(1)	Ref. [32]
HLbL (phenomenology)	Sec. 5.10	Eq. (5.69)	103.3(8.8)	Refs. [33–56]
HLbL NLO (phenomenology)	Sec. 5.10	Eq. (5.70)	2.6(6)	Ref. [57]
HLbL (lattice)	Sec. 6.2.8	Eq. (6.34)	122.5(9.0)	Refs. [58–62]
HLbL (phenomenology + lattice)	Sec. 9	Eq. (9.2)	112.6(9.6)	Refs. [33–56, 58–62]
QED	Sec. 7.5	Eq. (7.27)	116 584 718.8(2)	Refs. [63–69]
EW	Sec. 8	Eq. (8.12)	154.4(4)	Refs. [50, 70–72]
HVP LO (lattice) + HVP N(N)LO (e^+e^-)	Sec. 9	Eq. (9.1)	7045(61)	Refs. [13–32]
HLbL (phenomenology + lattice + NLO)	Sec. 9	Eq. (9.3)	115.5(9.9)	Refs. [33–62]
Total SM Value	Sec. 9	Eq. (9.4)	116 592 033(62)	Refs. [13–72]
Difference: $\Delta a_\mu \equiv a_\mu^{\text{exp}} - a_\mu^{\text{SM}}$	Sec. 9	Eq. (9.6)	26(66)	

Table 1: Summary of the contributions to a_μ^{SM}. The experimental number refers to the world average completely dominated by E989. The subsequent block summarizes the pertinent hadronic contributions from Secs. 2, 3, 5, and 6 as well as the combination of data-driven and lattice-QCD evaluations of HLbL scattering from Sec. 9. The second block summarizes the quantities entering our recommended SM value, in particular, the total HVP contribution (using lattice QCD for LO and e^+e^- for higher-order iterations) and the total HLbL number. The construction of the total HLbL contribution takes into account correlations among the terms at different orders, and the final rounding includes subleading digits at intermediate stages.

https://arxiv.org/pdf/2505.21476

WP 2020 – Lattice

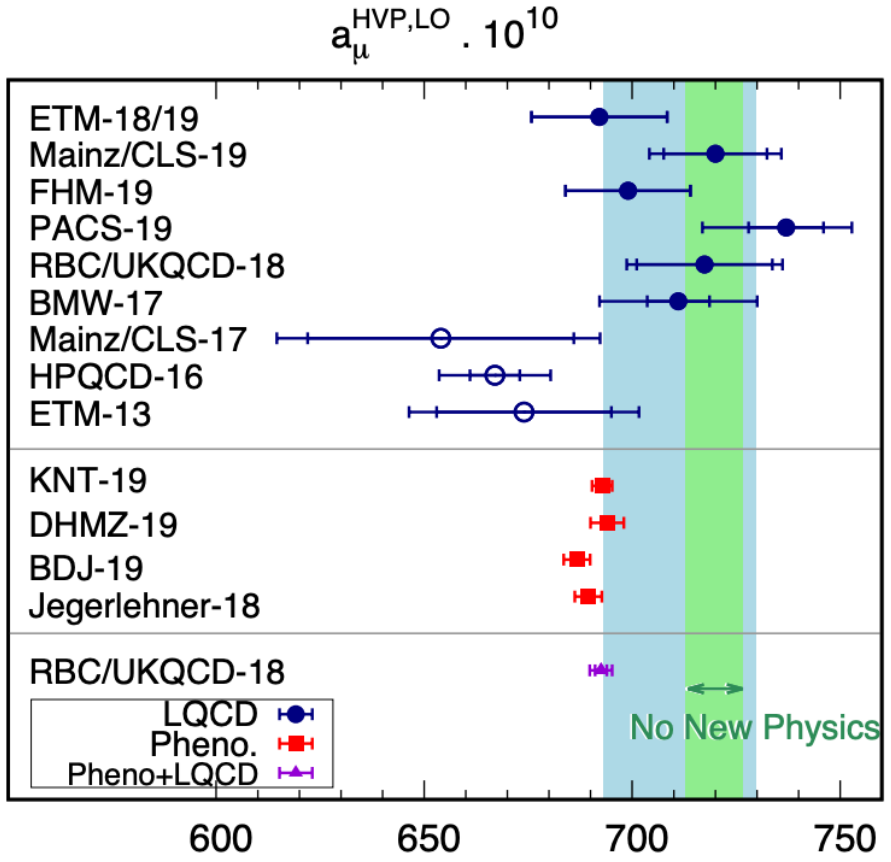

Figure 44: Compilation of recent results for $a_\mu^{\mathrm{HVP,\,LO}}$ in units of 10^{-10}. The filled dark blue circles are lattice results that are included in the "lattice world average". The average, which is obtained from a conservative averaging procedure in Sec. 3.5.1, is indicated by a light blue band, while the light-green band indicates the "no new physics" scenario, where $a_\mu^{\mathrm{HVP,\,LO}}$ results are large enough to bring the SM prediction of a_μ into agreement with experiment. The unfilled dark blue circles are lattice results that are older or superseded by more recent calculations. The red squares indicate results obtained from the data-driven methods reviewed in Sec. 2. See Table 8 for more information on the results included in the plot. Adapted from Ref. [443].

https://arxiv.org/pdf/2006.04822

Beam Dynamics

Momentum Distribution

Trackers

Parasitic: Dispersion & Beam Dynamics
(Improved uncertainties from MiniSciFi)

Calorimeters

Parasitic: Muon Dephasing
taking time-in-bunch into account
(improved robustness of method)

NEW! Minimally Intrusive Scintillating Fiber Detector (MiniSciFi)

Vertical and Horizontal versions

Dedicated studies: Cross-checks and uncertainty determination (tracker)

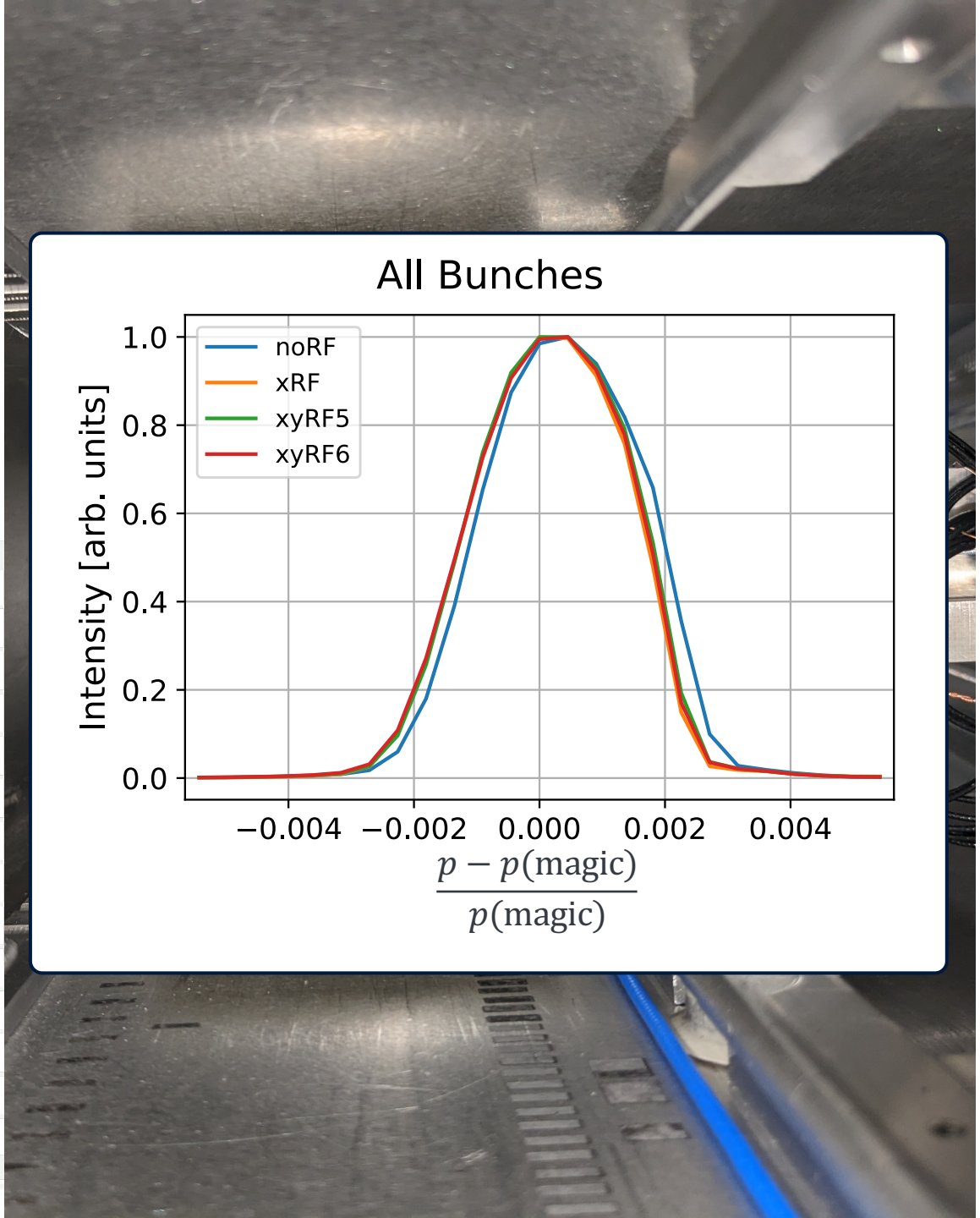

Electric-Field Correction: C_e

The **largest** correction

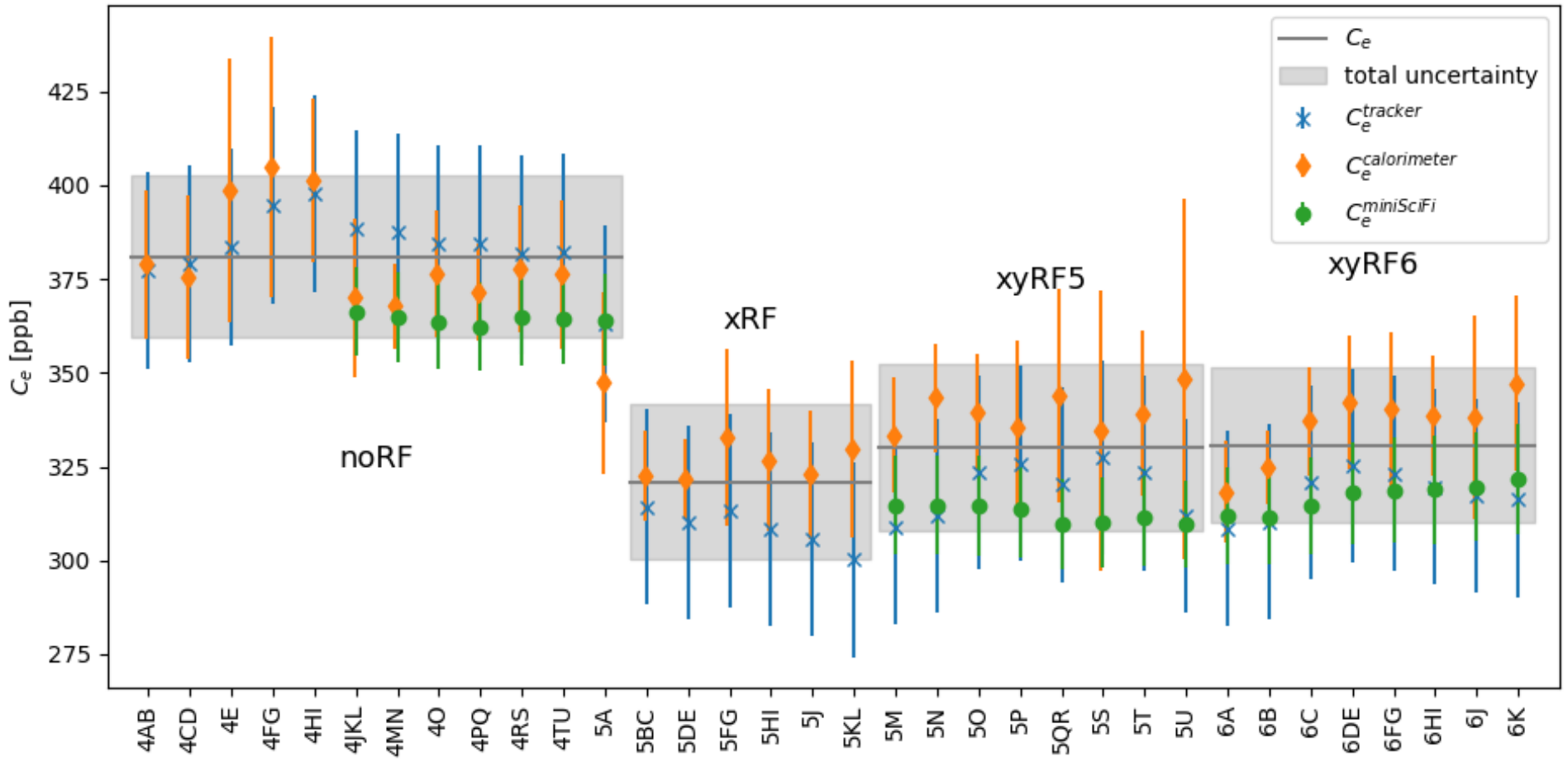

Increased confidence and small reduction of uncertainties to total of **27 ppb.**

Momentum Spectrum

Higher momentum muons:

- stored at **larger radii**
- take **longer** to go around

Lower momentum muons:

- stored at **smaller radii**
- take **shorter** to go around

Dephasing and **radial position** used to extract the stored momentum spectrum

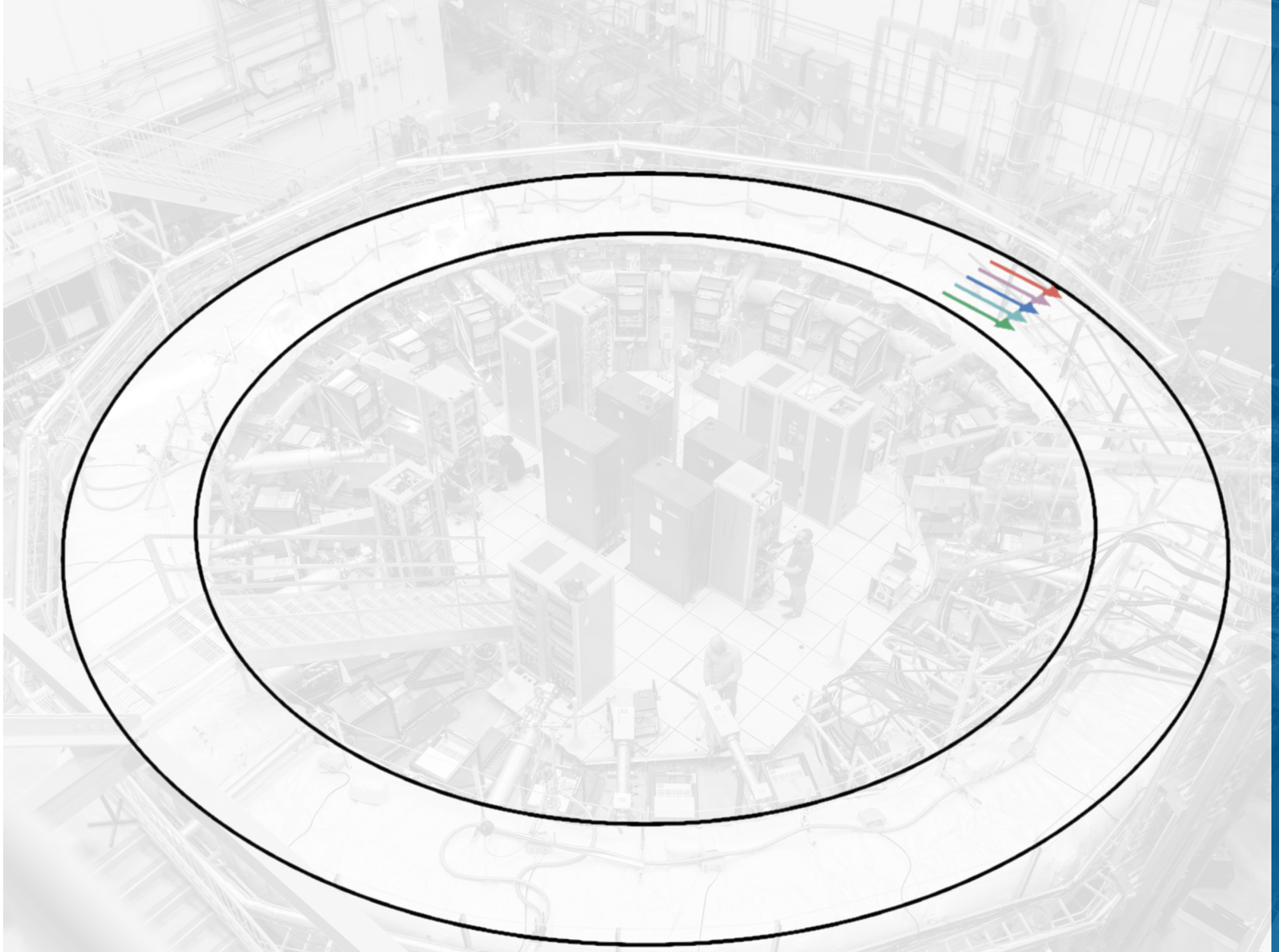

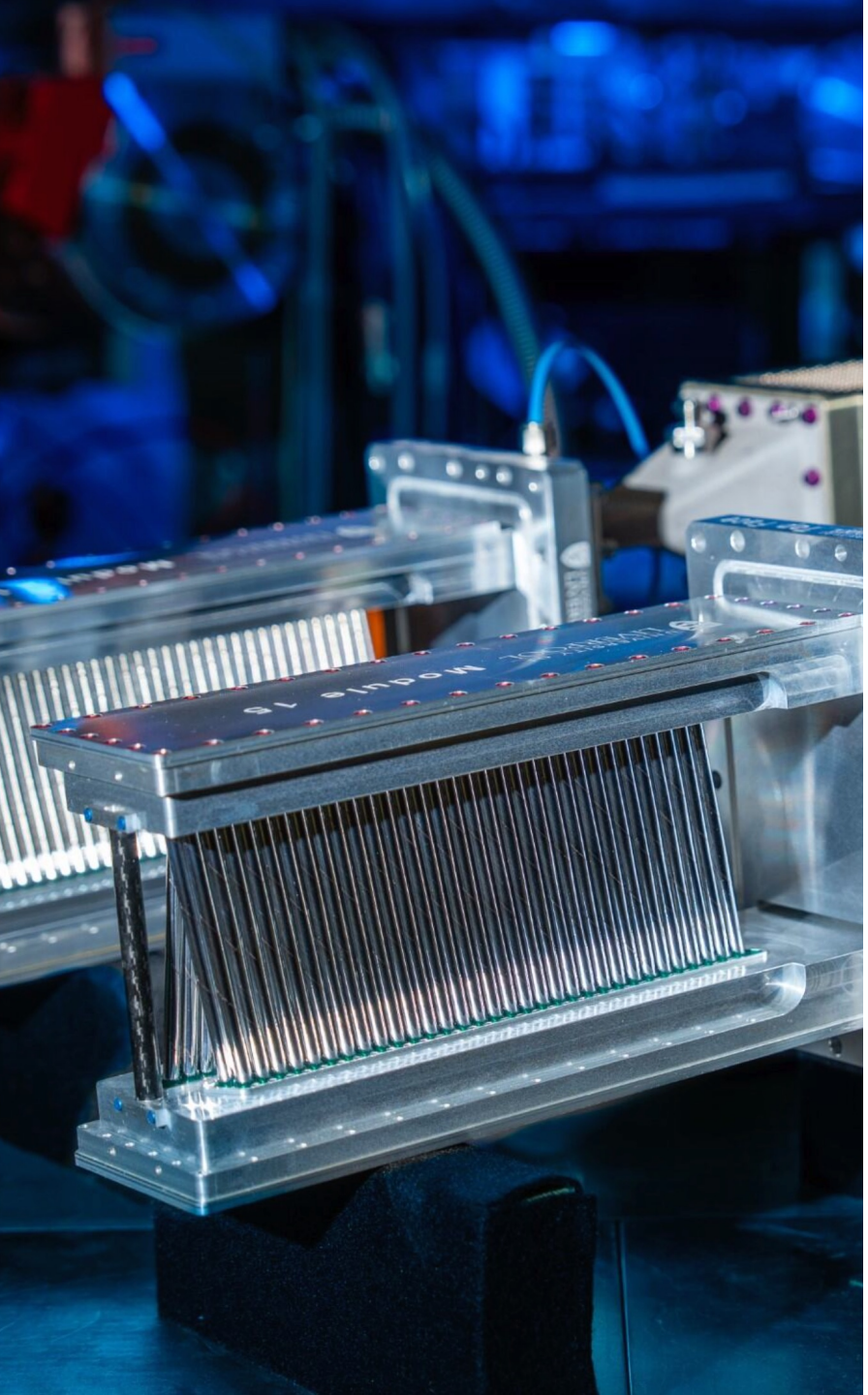

Pitch Correction C_p

A pitch reduces the measured spin precession

Trackers

Measure muon's vertical position,
derive **vertical oscillation amplitudes**

Simulation Frameworks

Extrapolate from trackers to around the ring

(also user for other analysis parts)

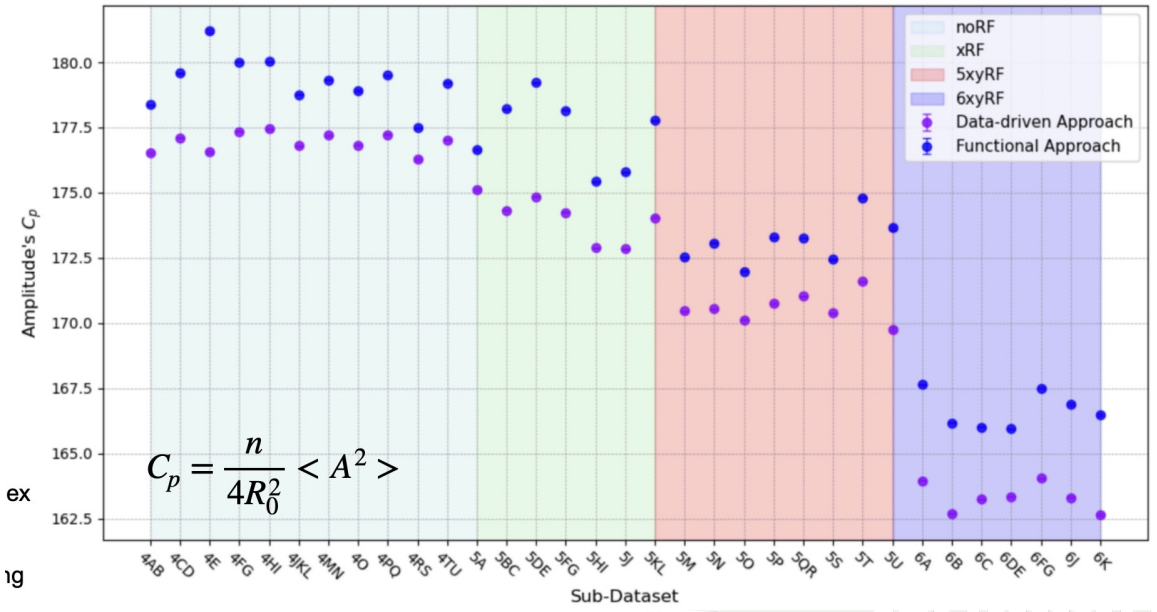

Corrections: Time-Dependent Mean Phase

Time-dependent phase changes of the muon ensemble bias ω_a^m

Phase Acceptance C_{pa}

Detector Acceptances x Beam Motion

Differential Decay C_{dd}

Momentum-dependent muon lifetime x phase-momentum correlations

Muon Loss C_{ml}

Mechanical muon losses

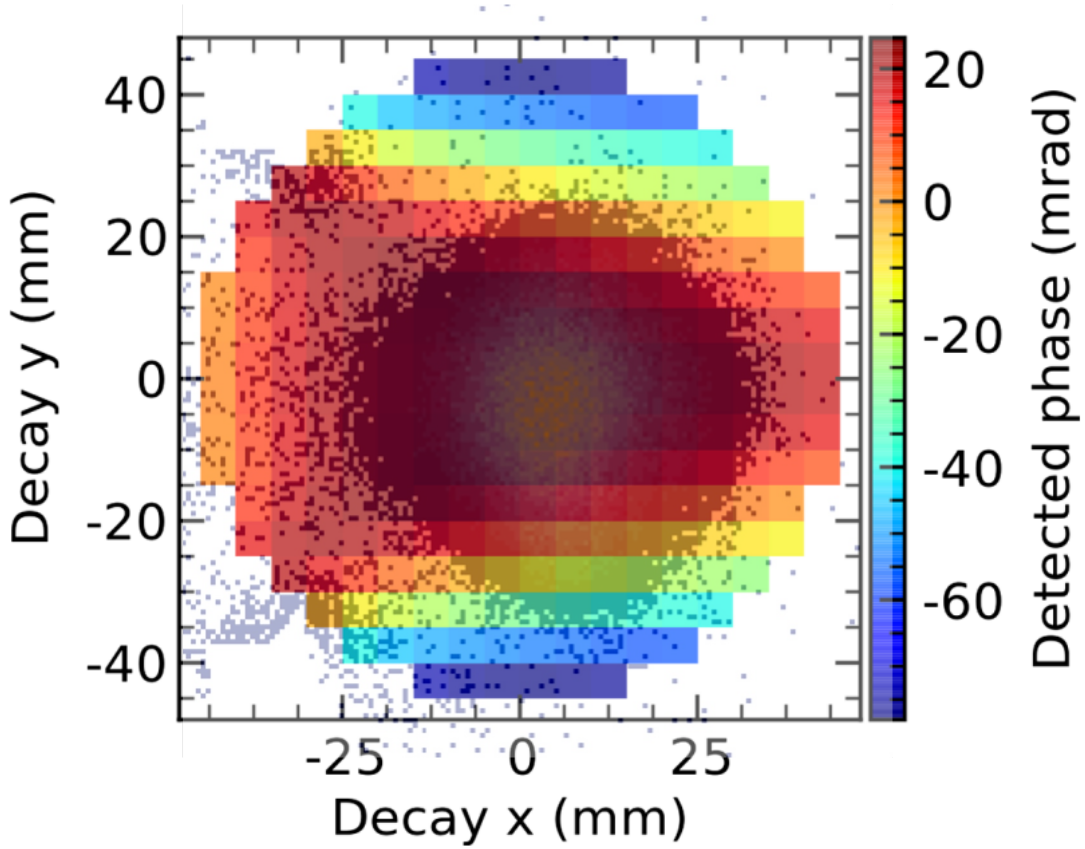

Corrections: Time-Dependent Mean Phase

Time-dependent phase changes of the muon ensemble bias ω_a^m

Phase Acceptance C_{pa}

Detector Acceptances x Beam Motion

Differential Decay C_{dd}

Momentum-dependent muon lifetime x phase-momentum correlations

Muon Loss C_{ml}

Mechanical muon losses

- 2 components: **Injection** and **longitudinal** components
- **New!** **Injection component** from simulation frameworks
  - Before: split into 2 components
  - Before: Sign mistake in one contribution $C_{dd}^{beamline}$
    +32 ppb shift in Run-2/3 results

How does the RF work?

Beam oscillation: average of all muons

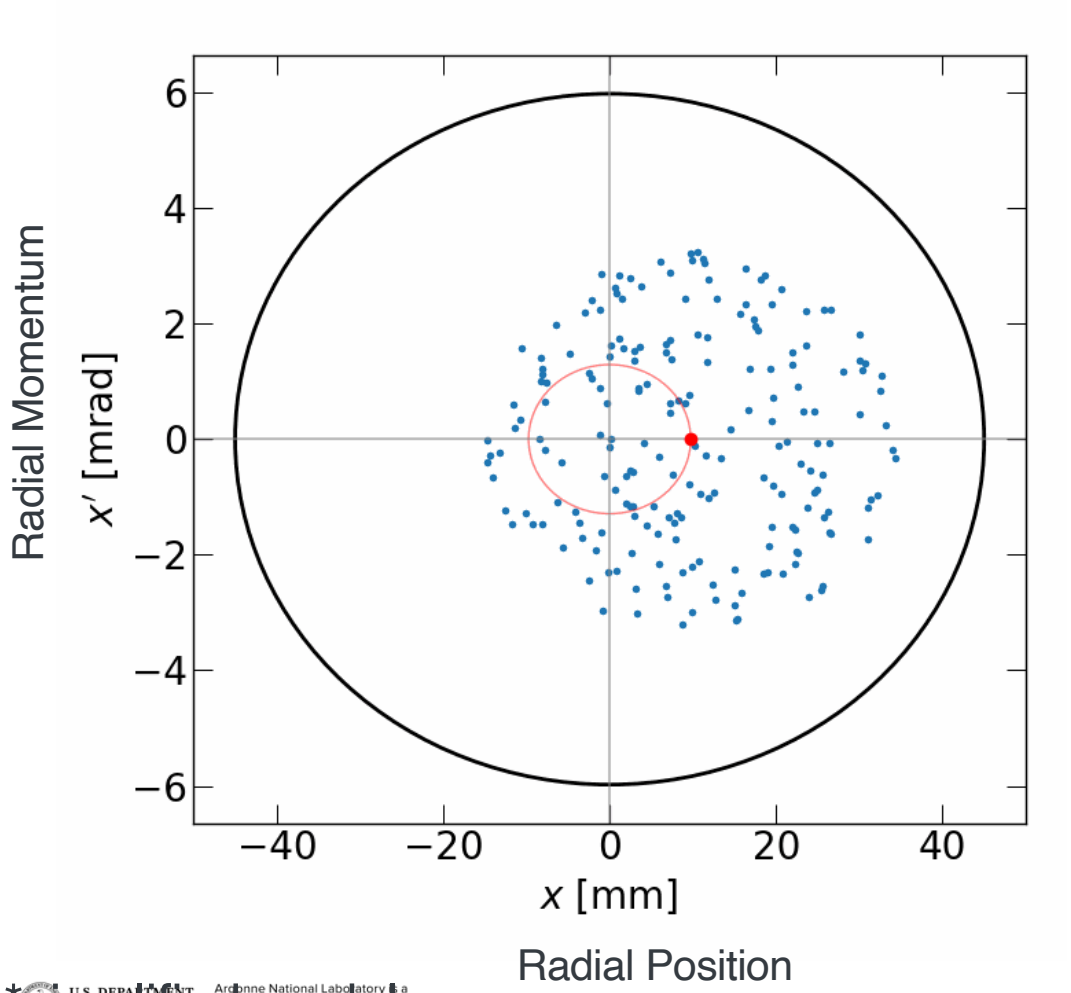

*Simplified model

How does the RF work?

Beam oscillation: average of all muons

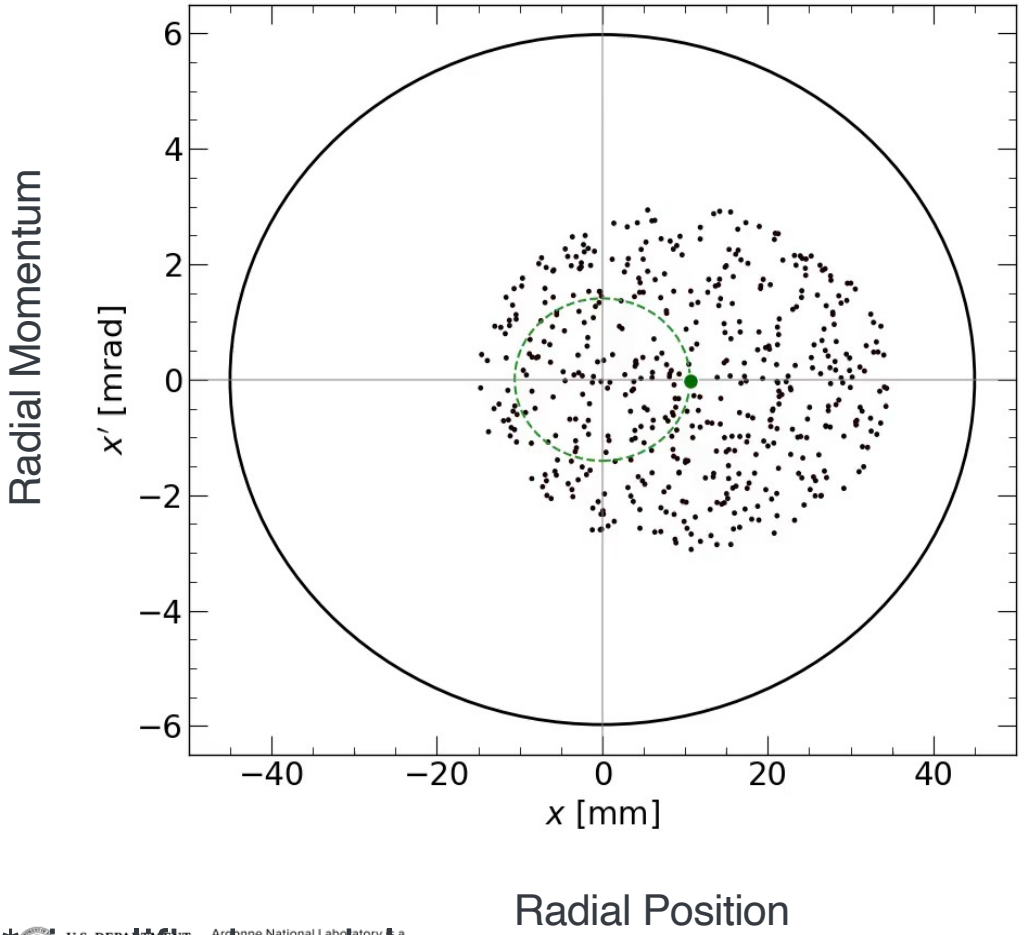

- RF acts like a forced harmonic oscillator (for 6 μs)
- If tuned correctly to the CBO frequency:
  - Phase-shifts different muon distributions
  - Reduces the oscillation of the **mean** of the particle ensemble (reduces the coherence)

*Simplified model

RF effect on CBO

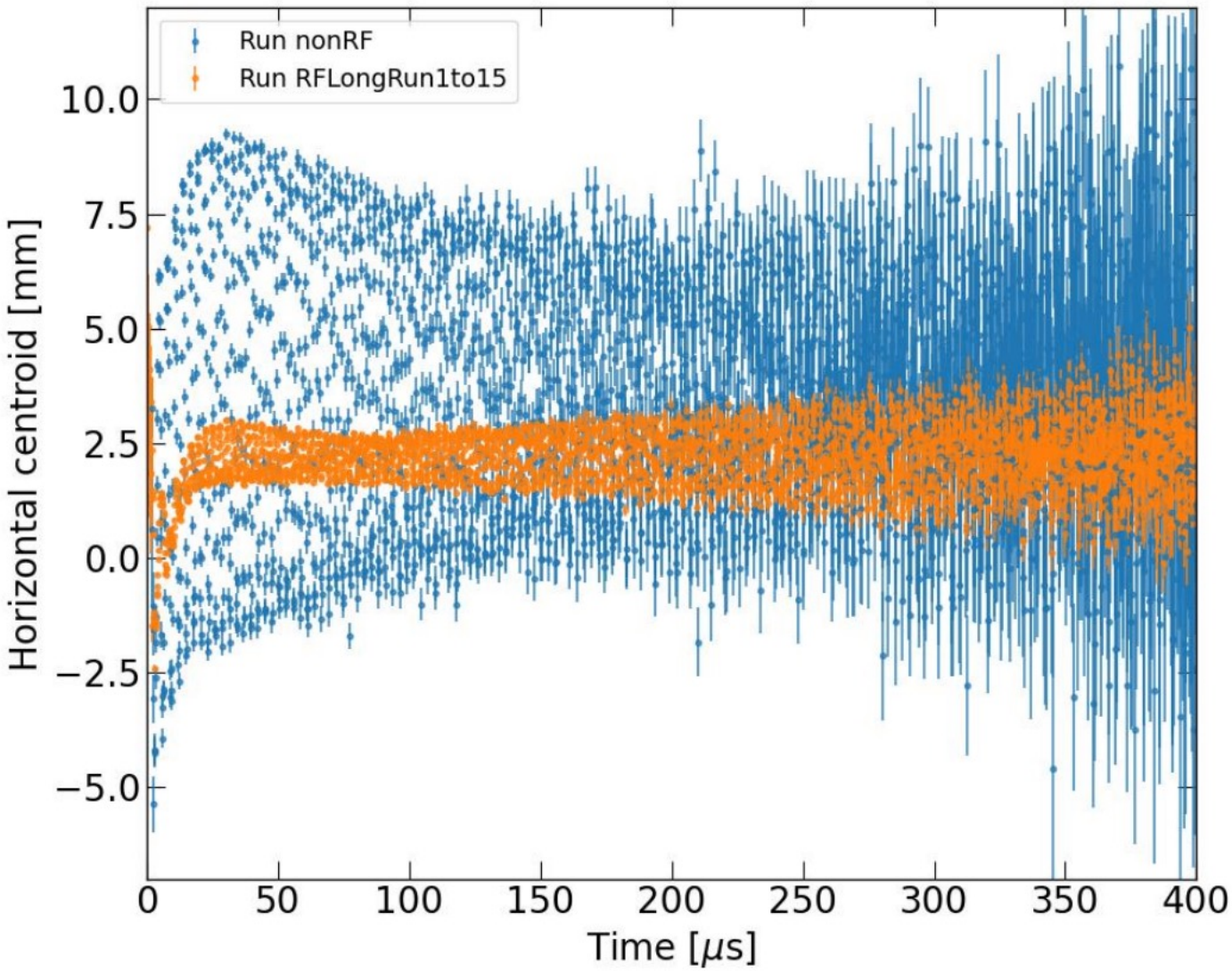

Electric-Field trackers

$$x_0 = D\delta + A\cos(\omega_{\mathrm{CBO}} t_0 + \phi) \qquad x_f = D\delta - A\cos(\omega_{\mathrm{CBO}} t_0 + \phi)$$

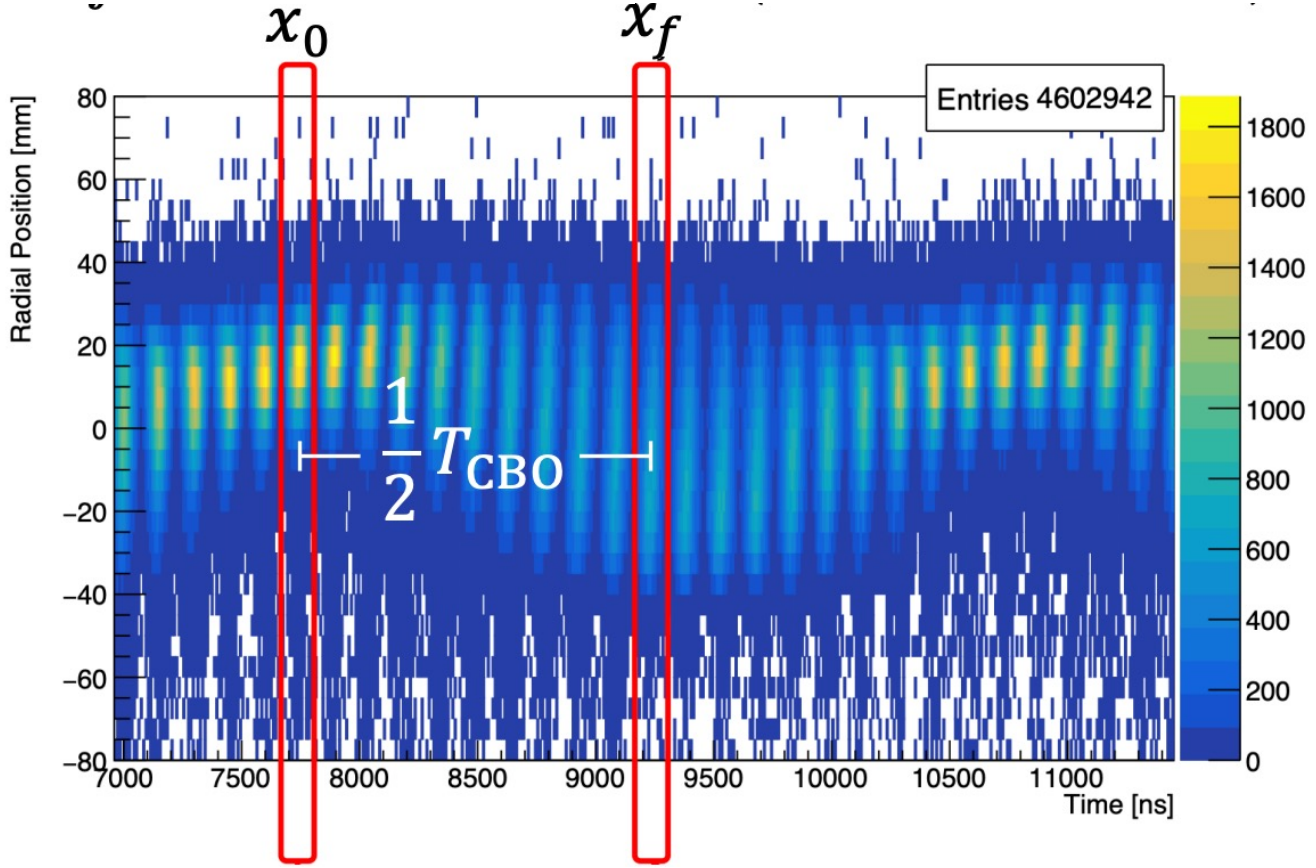

$$\langle \delta^2 \rangle = \frac{1}{2D_x^2} \left[\langle x_0^2 \rangle + \langle x_f^2 \rangle - \langle A^2 \cos(2\omega_{\mathrm{CBO}} t_0 + 2\phi) \rangle - \langle A^2 \rangle \right]$$

Electric-Field Calorimeters

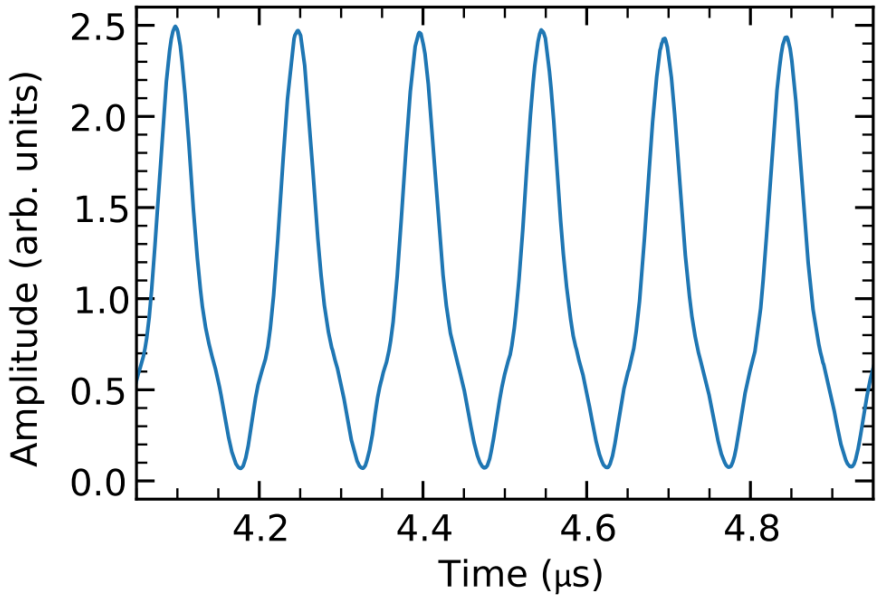

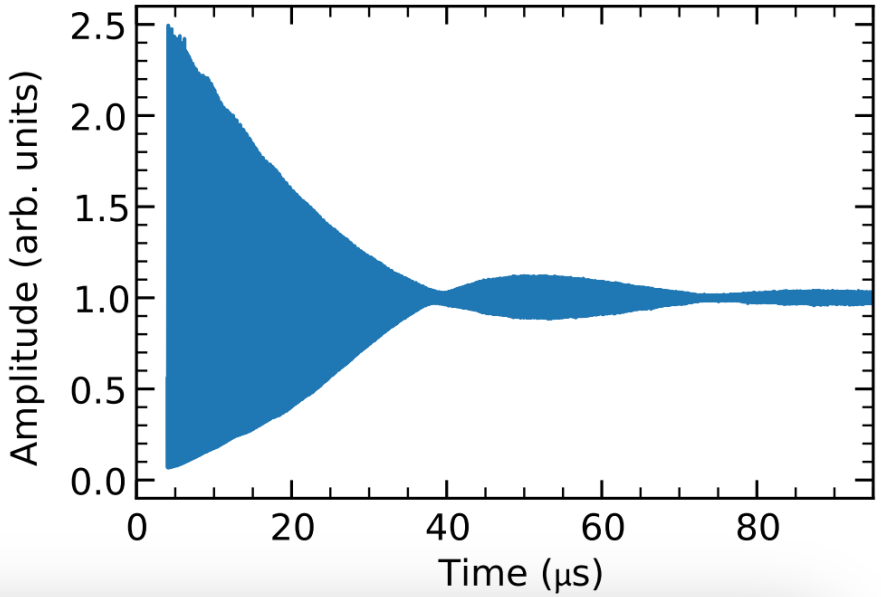

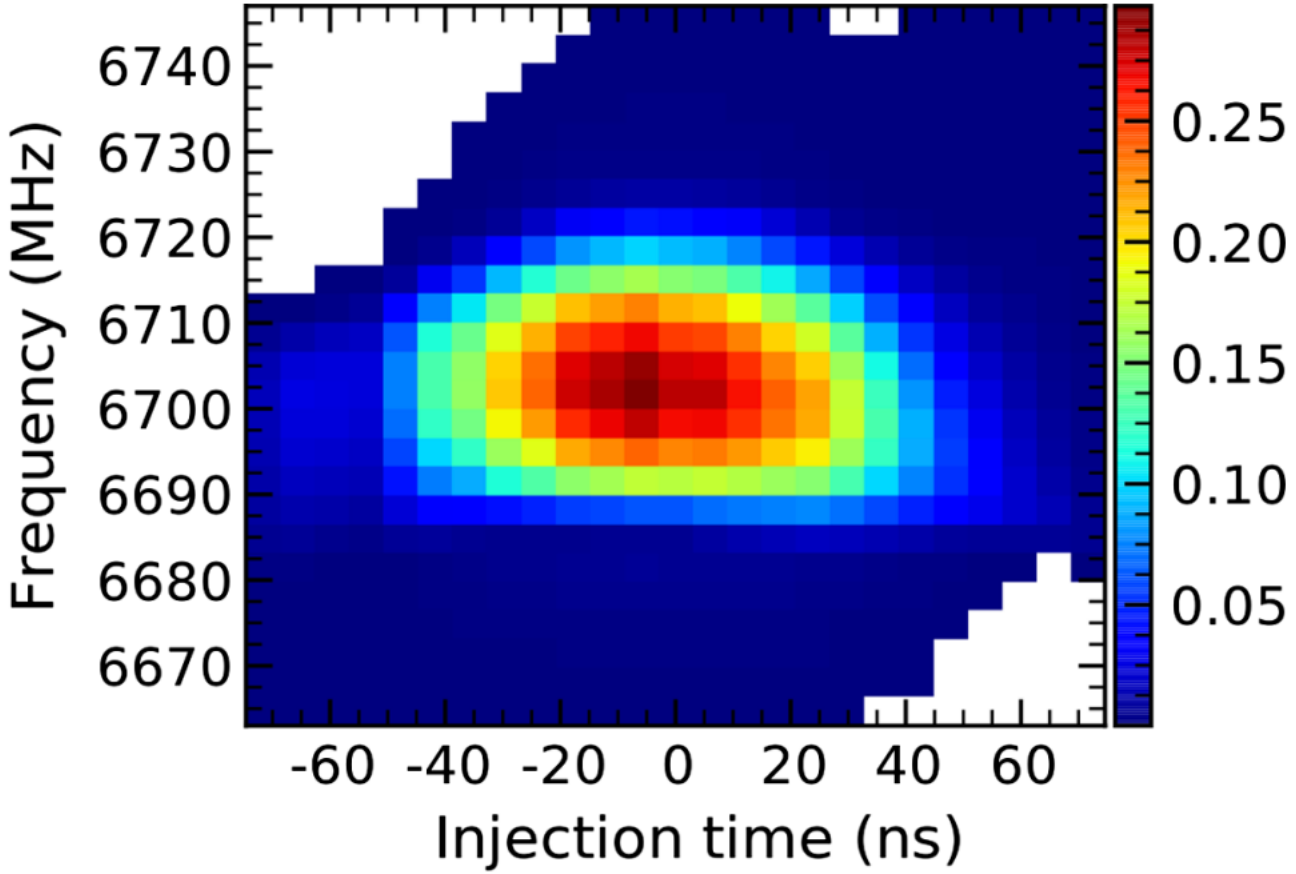

Magnetic Field

Magnetic Field Shimming

- Many “knobs” for shimming:
  - 72 Poles: Shaping & homogeneity
  - 864 Wedges: Quadrupole asymmetry
  - 48 Iron Top Hats: Change effective μ
  - 144 Edge Shims: Quad/sextapole asymmetry
  - 8000 Surface Iron Foils: Local changes of effective μ
  - 100 Active Surface Coils: Control current to add ring-wide average field moments

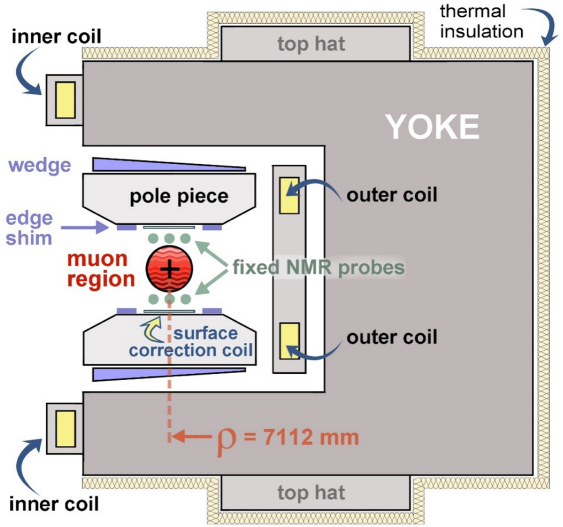

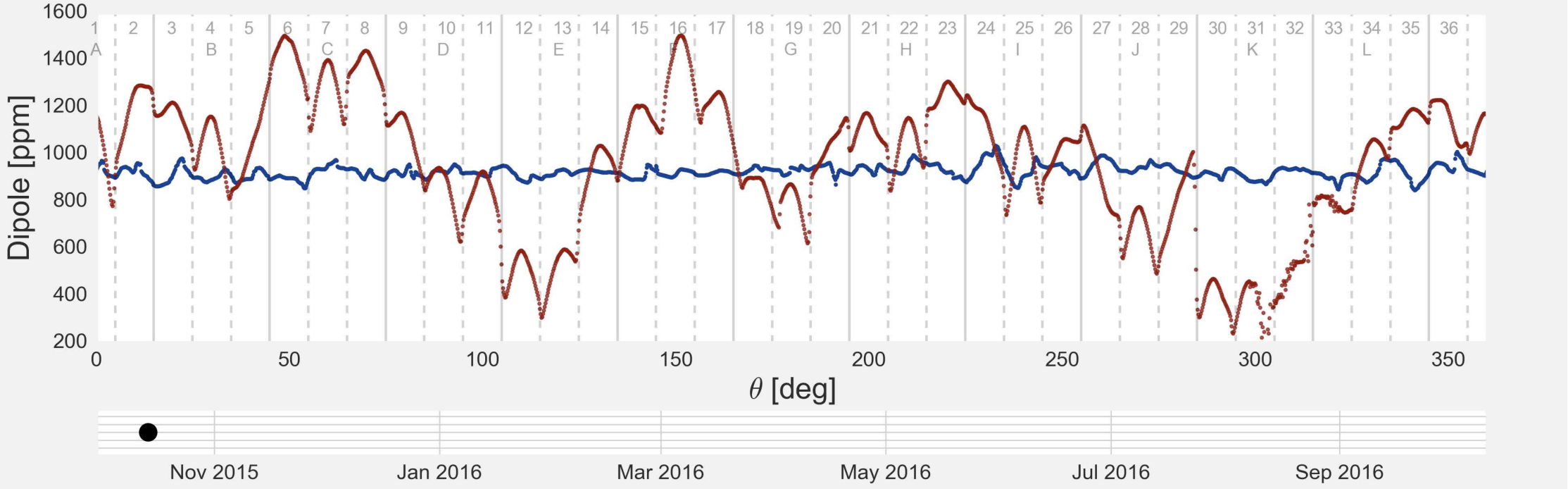

Magnetic Field Mapping & Tracking

The field between field maps (trolley runs) is tracked by the fixed NMR probes.

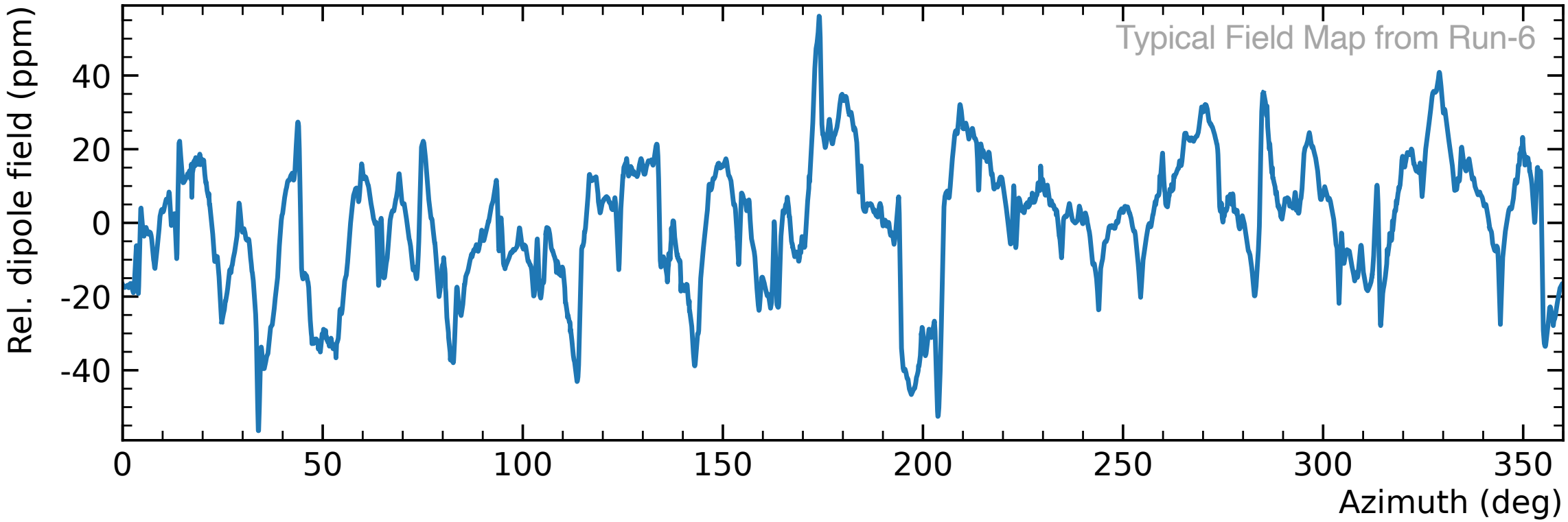

Take field maps every 3 to 7 days

For the Run-4/5/6 result we use 194 field (Run-1/6 total: 279)

Overall, the trolley traveled more than 100km!

Magnetic Field Calibration – Cross-Calibrations

J-PARC
Continuous Wave

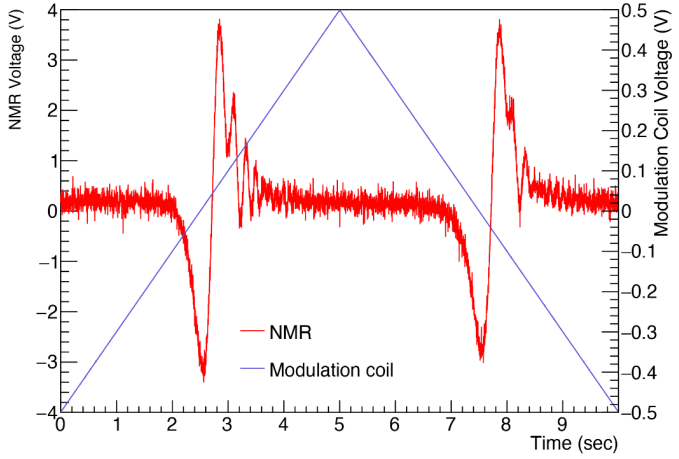

Water-Based Calibration Probe

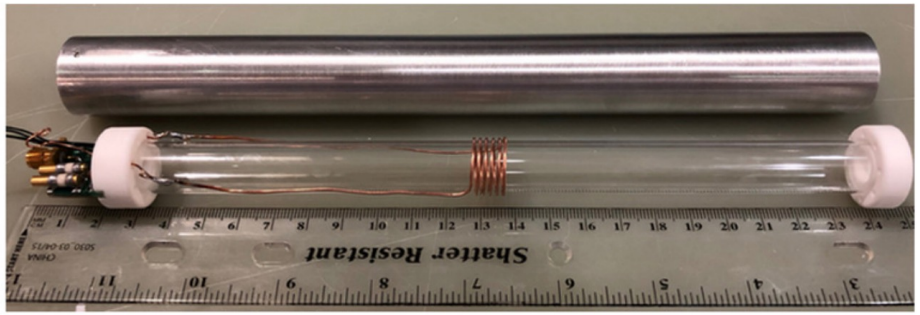

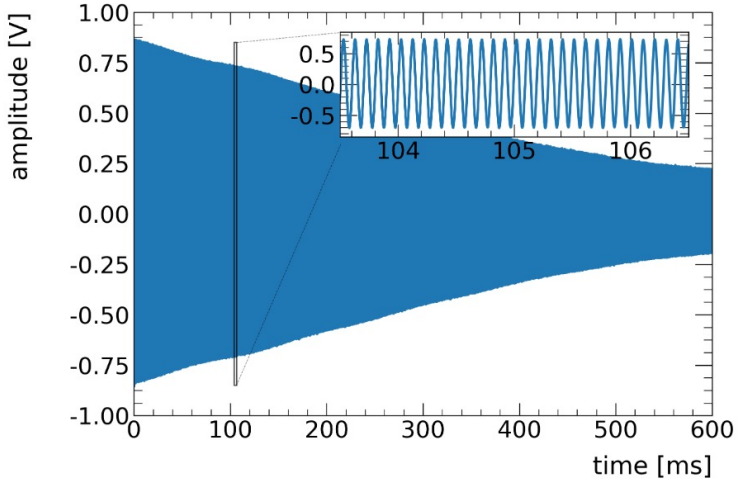

^{3}He-based
Calibration Probe

- 2019 (1.45T), 2019 (1.7T) campaigns: some inconsistencies
- 2022 (3T), 2023 (1.45T) campaigns, in good agreement

- Agreement on the 1.7 σ-level

Magnetic Transients: Kicker

Kick causes **eddy currents** → **transient** magnetic field

Measured **newly** with **two different magnetometers**
both based on Faraday effect in TGG crystals

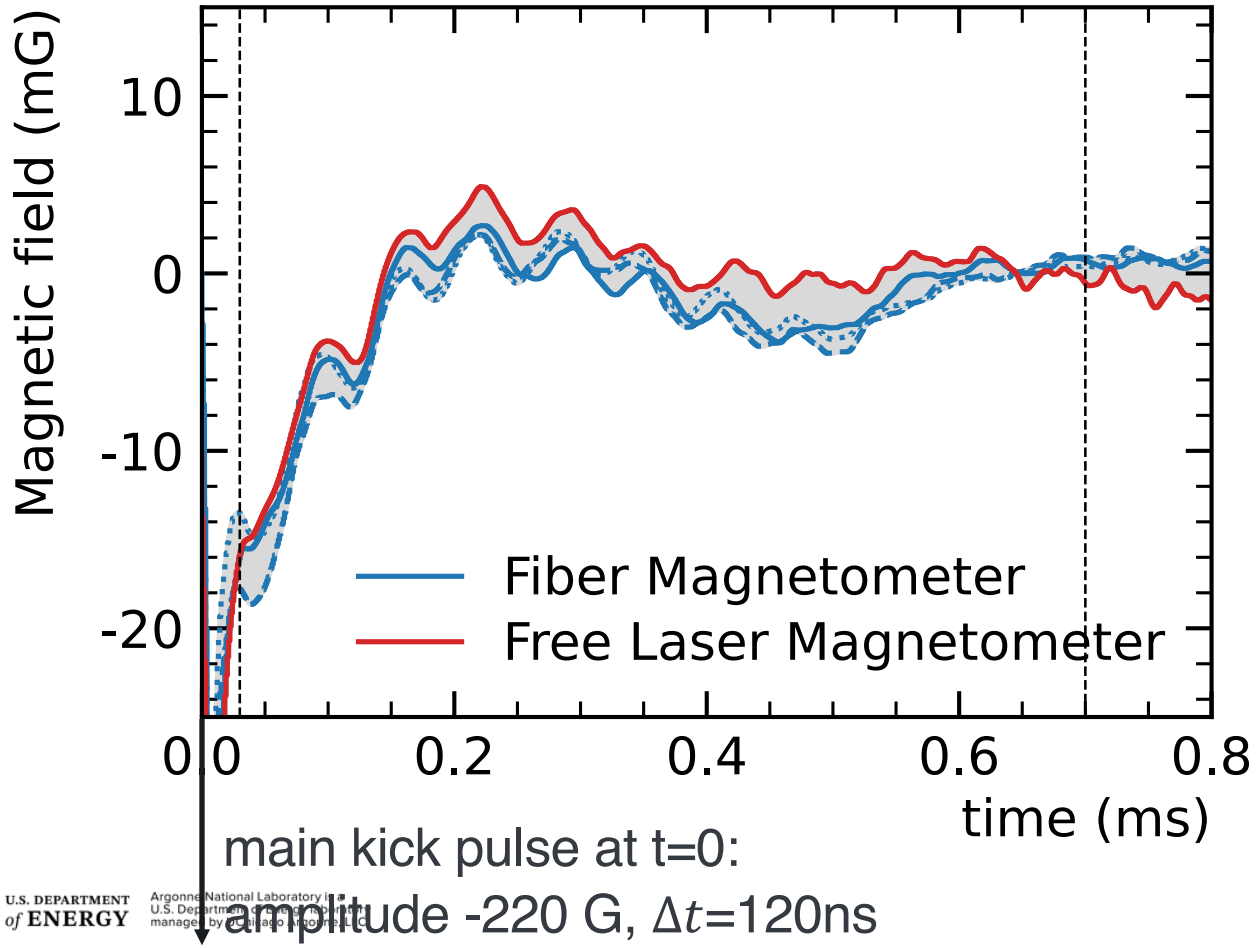

Fiber magnetometer

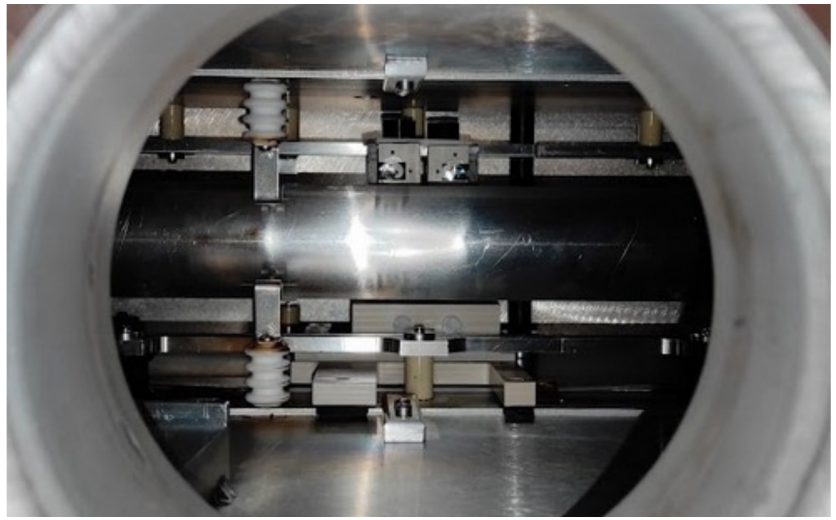

Free laser magnetometer

Magnetic Transients: Kicker

Kick causes **eddy currents** → **transient** magnetic field

Measured **newly** with **two different magnetometers** both based on Faraday effect in TGG crystals

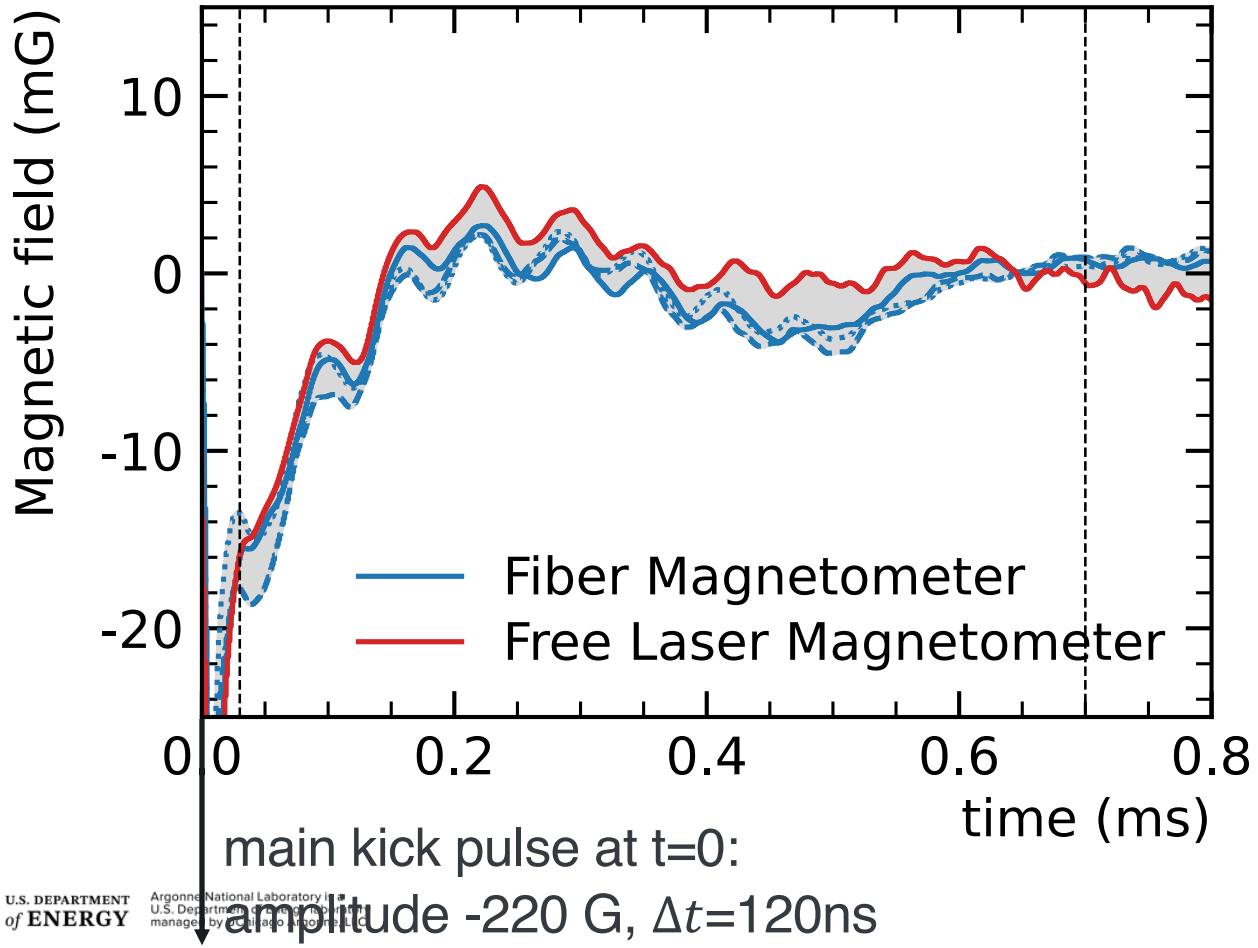

Measurement on a **Mock-Up** in the lab to refine modeling of transverse dependence

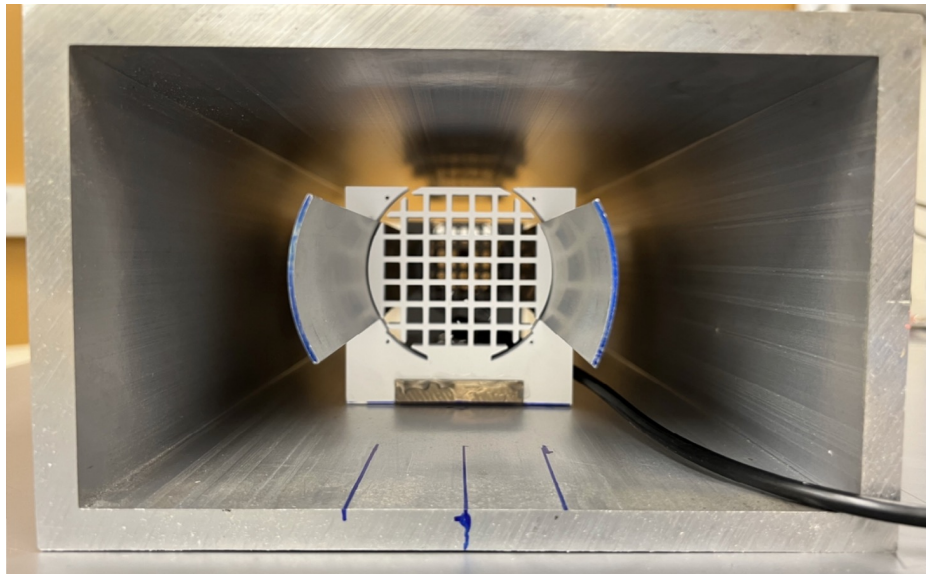

Kicker mock-up

Transient from ESQ B_q

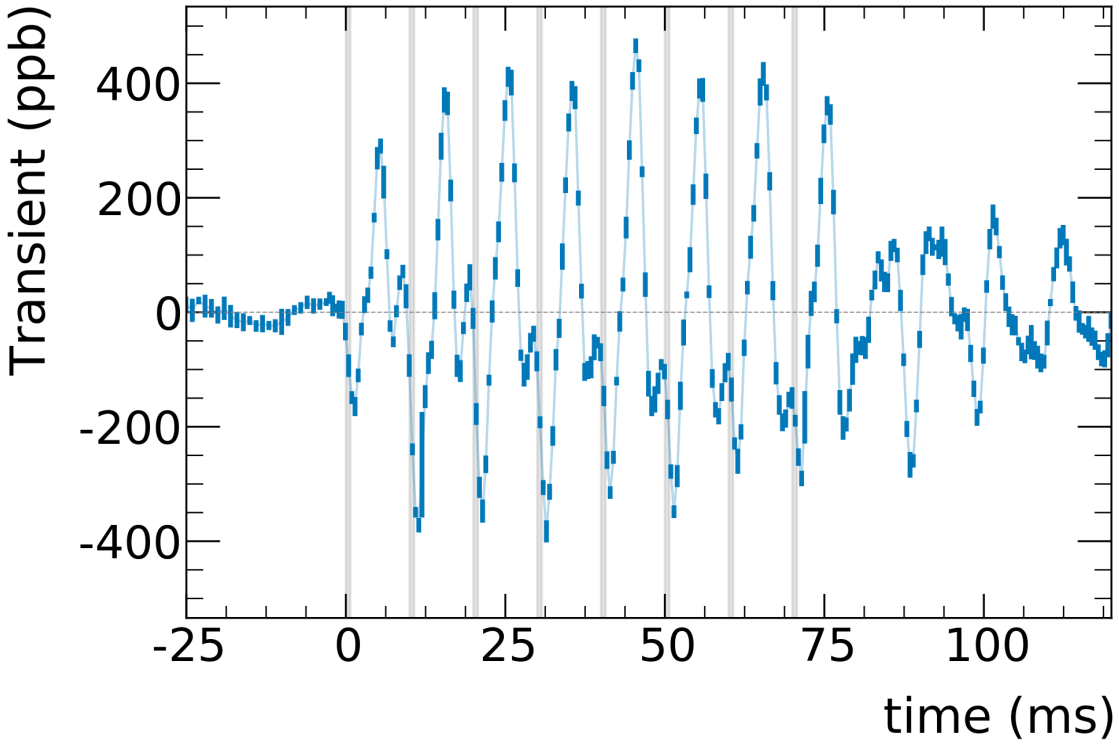

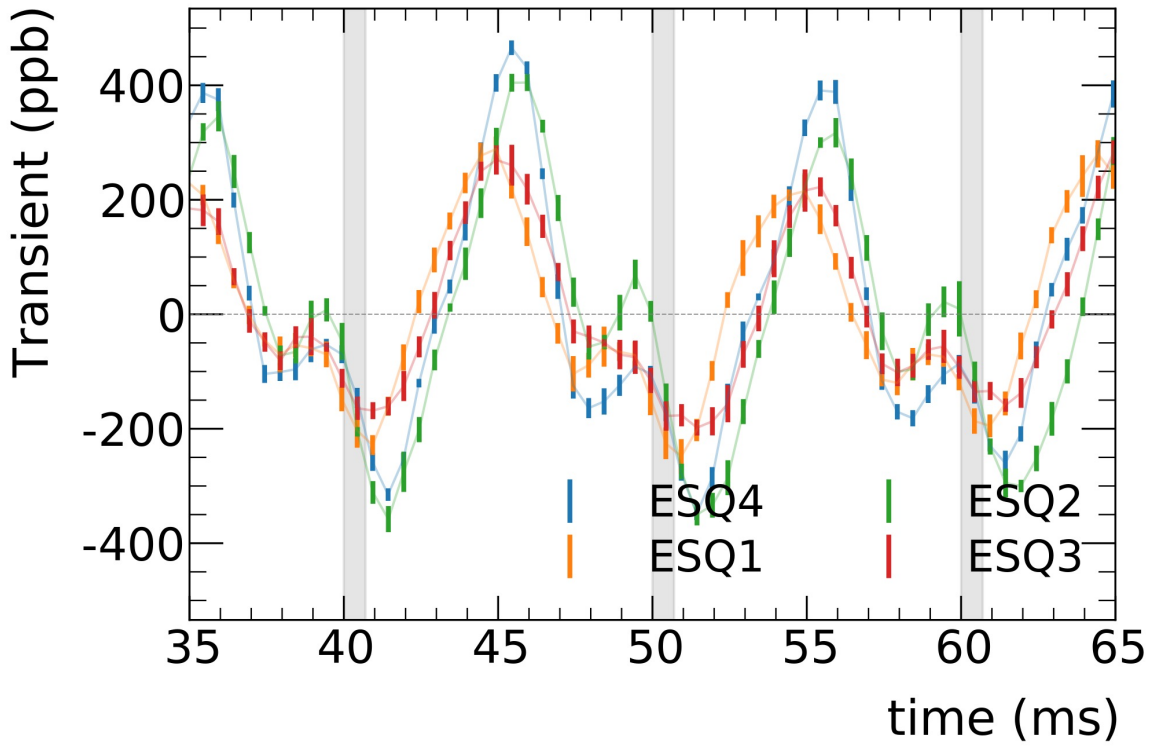

Transient from ESQ B_q

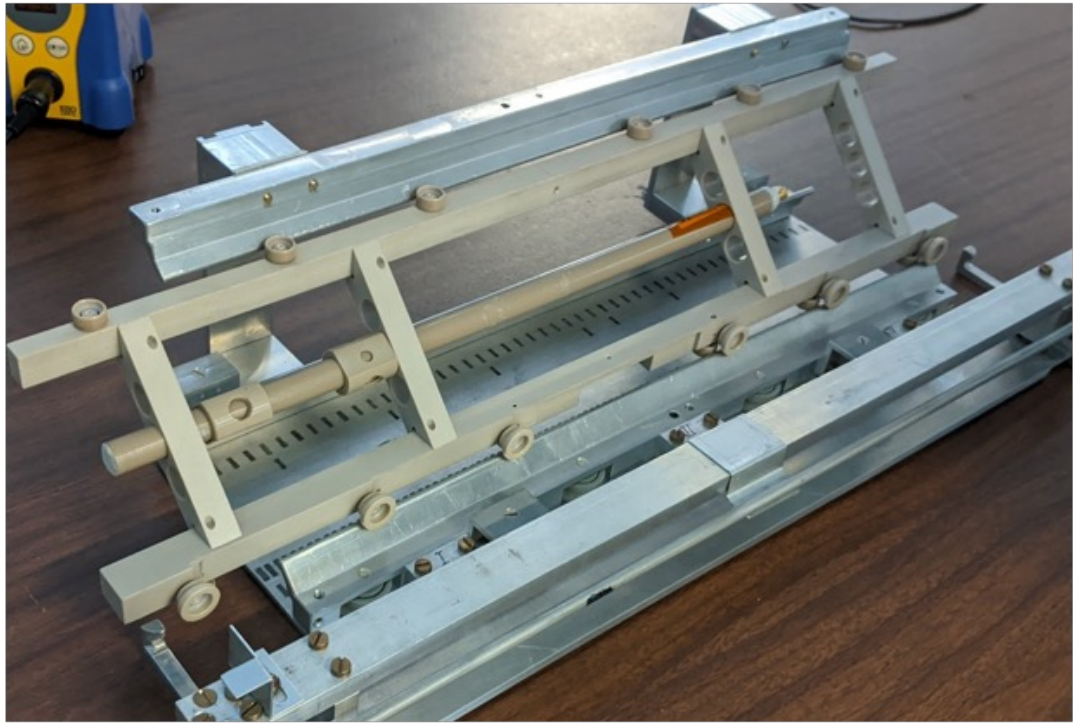

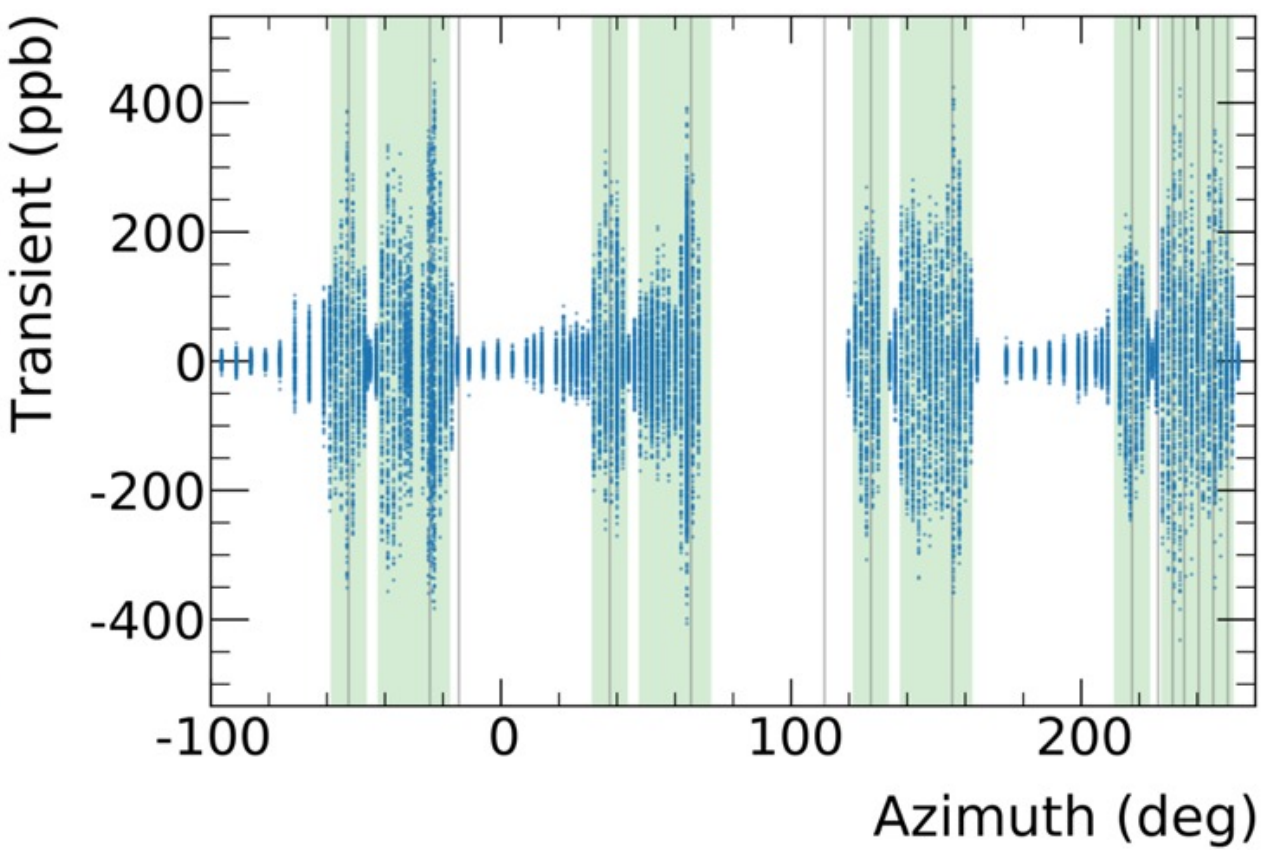

ESQ Transient mapping

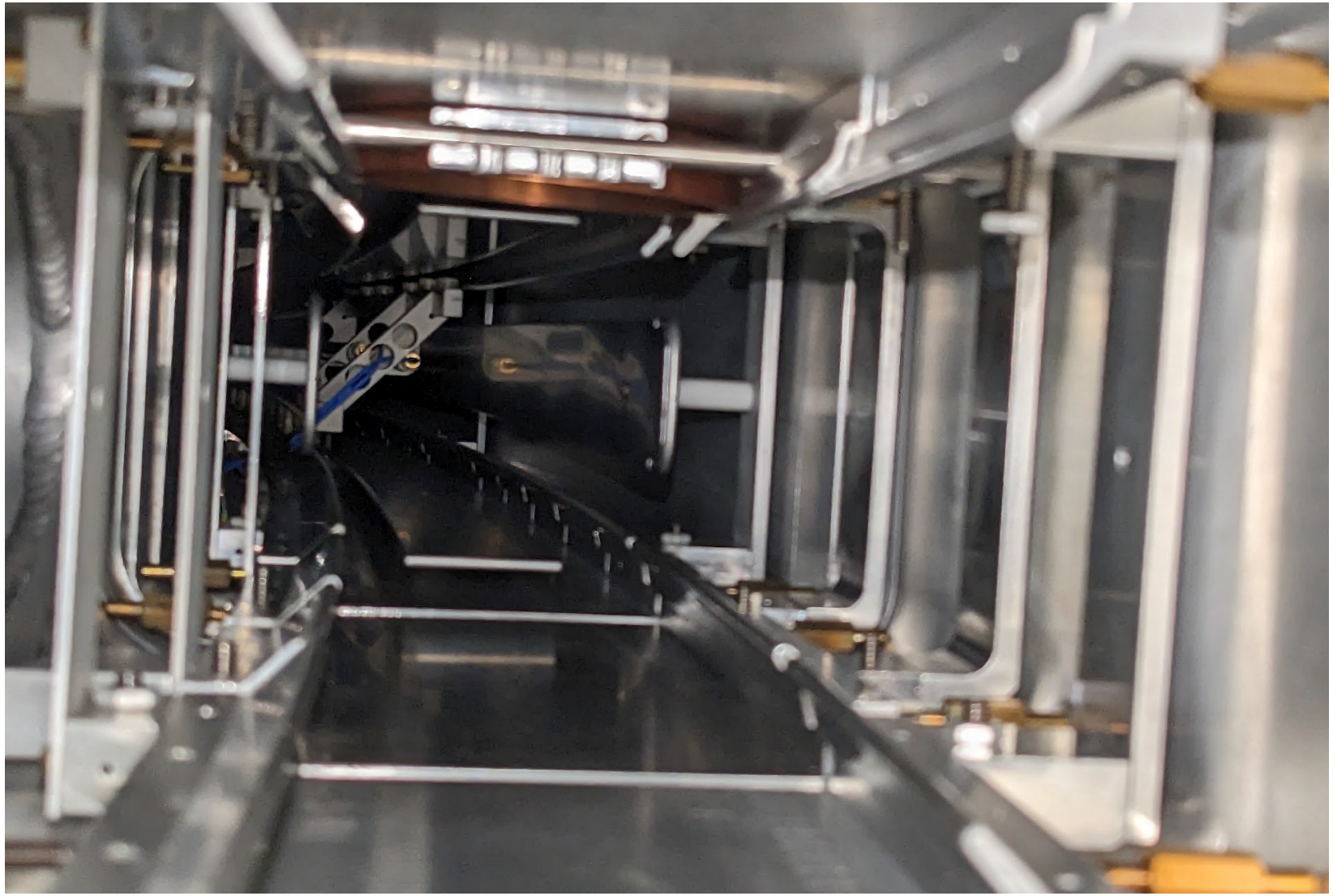

Magnetic Field

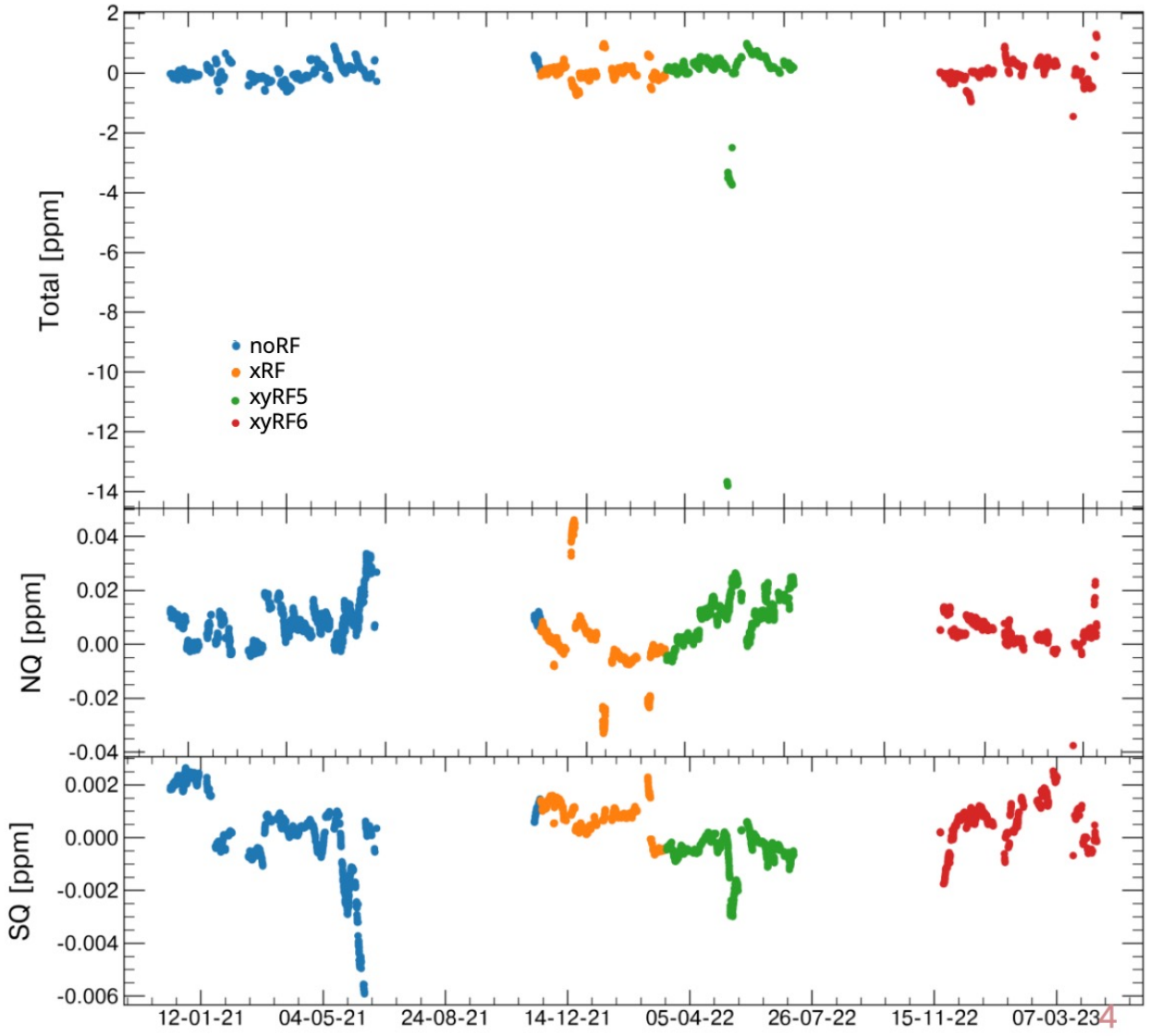

Trolley Calibration

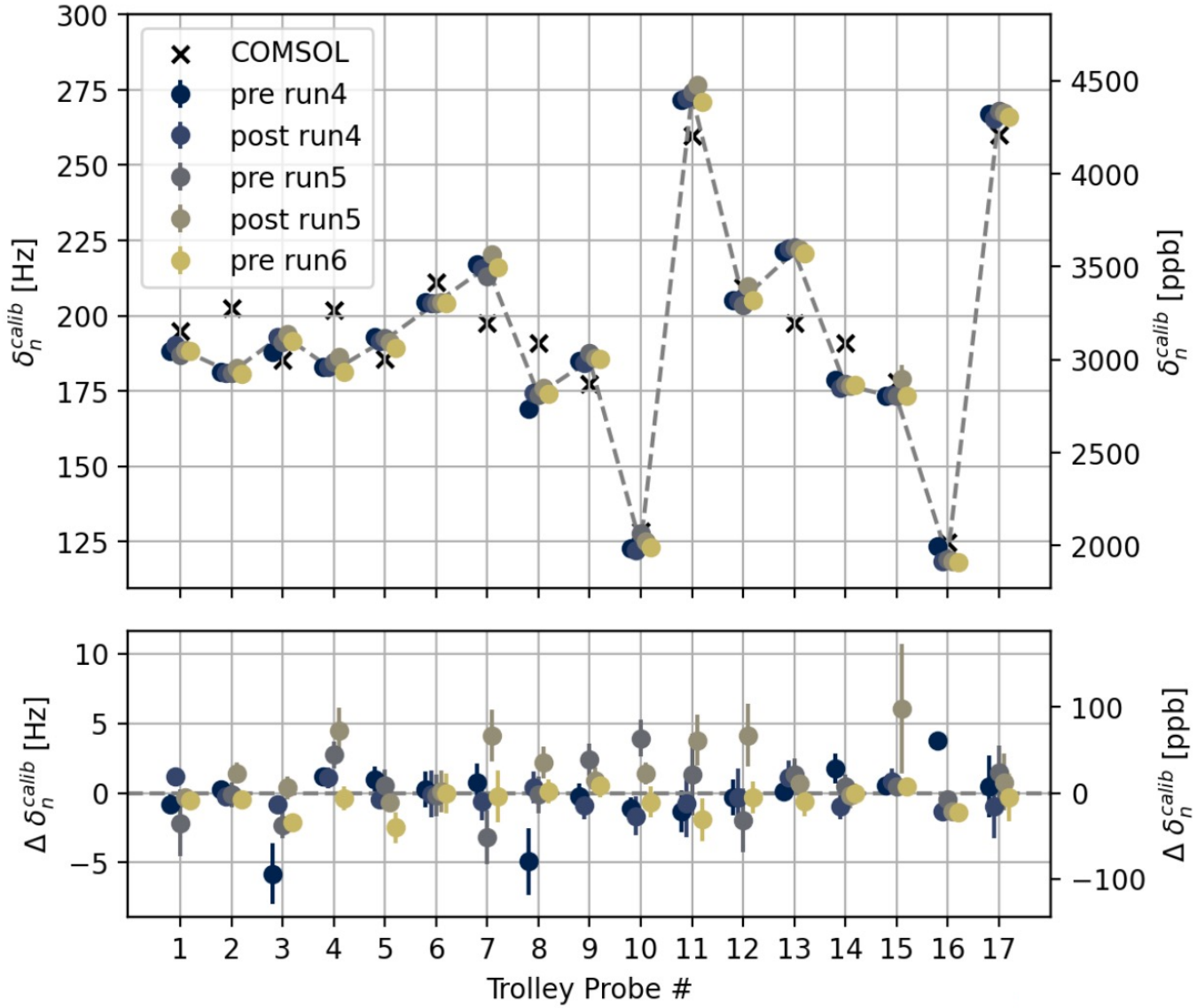

ω_a

Measuring the Spin Precession ω_a

Due to parity violation, "self-analyzing", the number of **high energy e⁺** oscillates as the **μ⁺ spin** rotates

Count **e⁺ above threshold** (or weight)

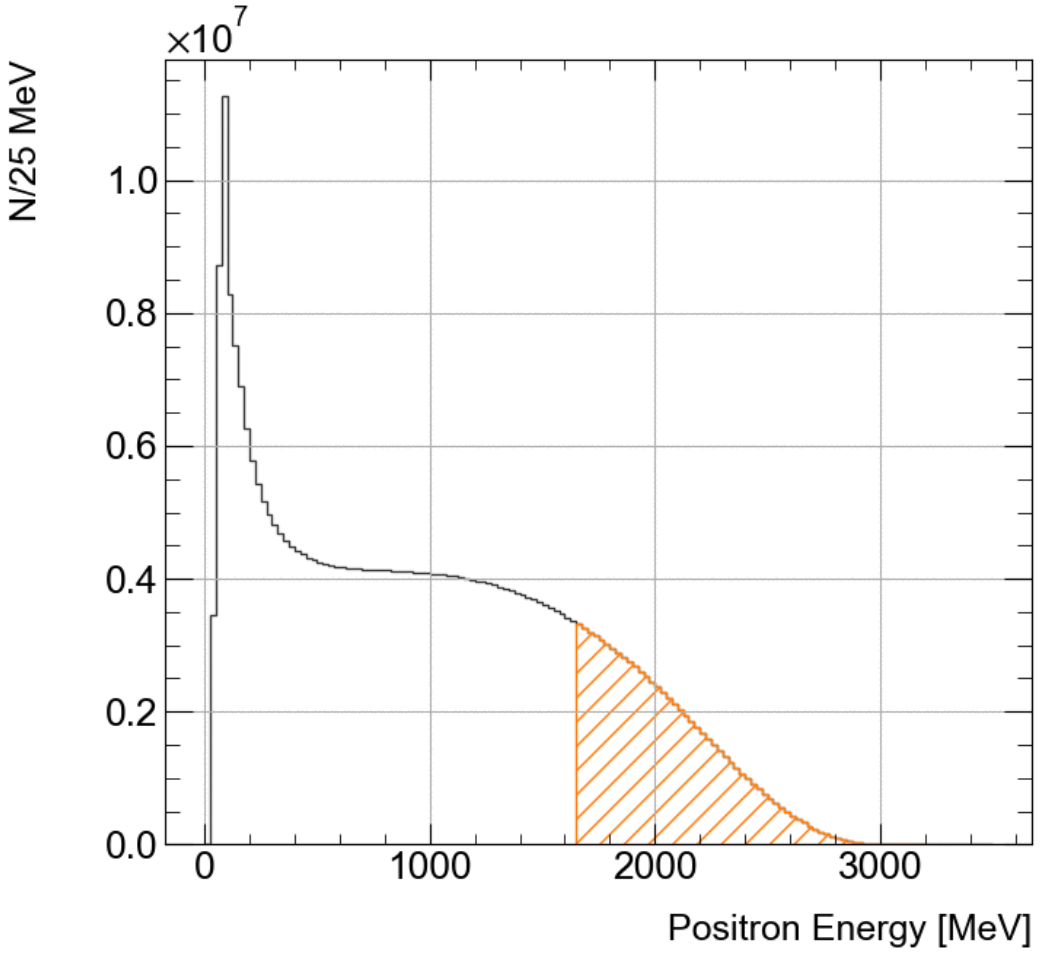

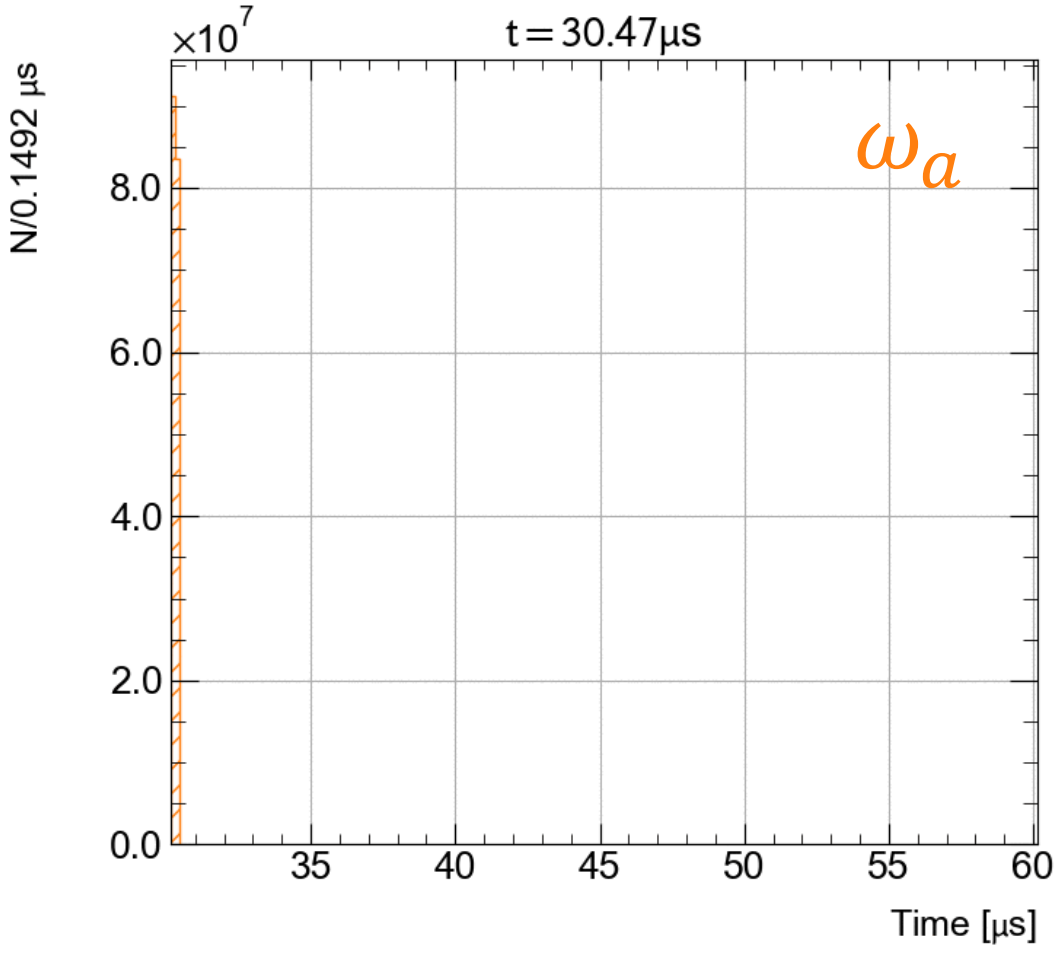

Gain-Like Detector Effects

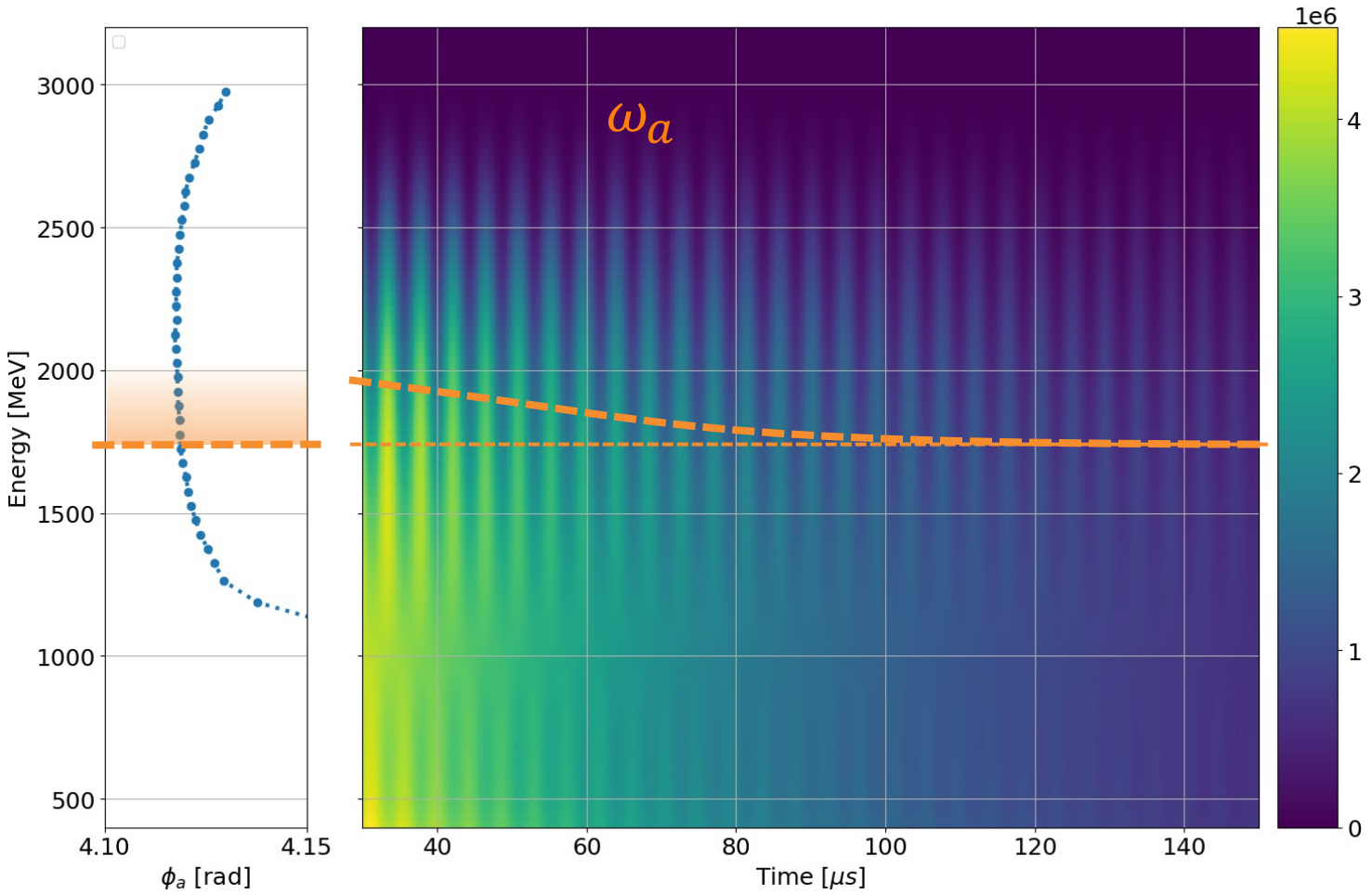

Effective **threshold changes** over time

Laser system to correct the gain on 10^{-4} –level

Gain-Like Detector Effects

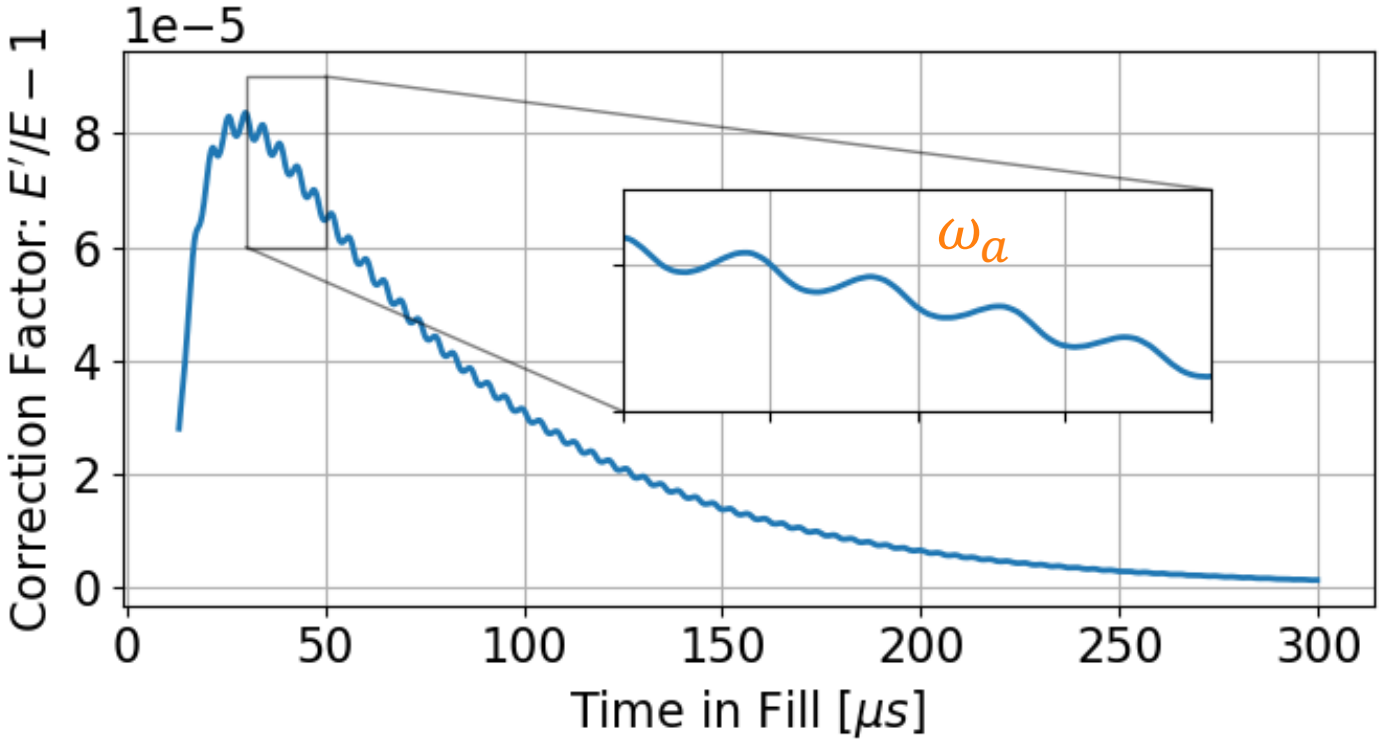

*noRF dataset

New! Sensitive also below 10^{-4} if

- Rate & Energy dependent
- Time constant $\sim 1/\omega_a$
- Correction shows ω_a-behavior but **out of phase**
- Time-dependent phase-change
- Fitted ω_a sensitive to such effects

Residual Slow Term

- known in Run-1: “early-to-late effects” 10-22 ppb uncertainty
- better understood in Run-2/3: split into reconstruction & detector part with

  “Possible sources […] changes in gain, acceptance, or reconstruction over the duration of a fill.” 5-14 ppb uncertainty

Residual Slow Term

- known in Run-1: “early-to-late effects” 10-22 ppb uncertainty
- better understood in Run-2/3: split into reconstruction & detector part with
  “Possible sources […] changes in gain, acceptance, or reconstruction over the duration of a fill.” ~~5-14 ppb uncertainty~~
  New! **36 pbb** uncertainty
- **Run-4/5/6: New! Identified physical explanation**
  - Detector effect due to preceding positron hits (rate dependent): 20-40 ppb effect, ~25ppb uncertainty

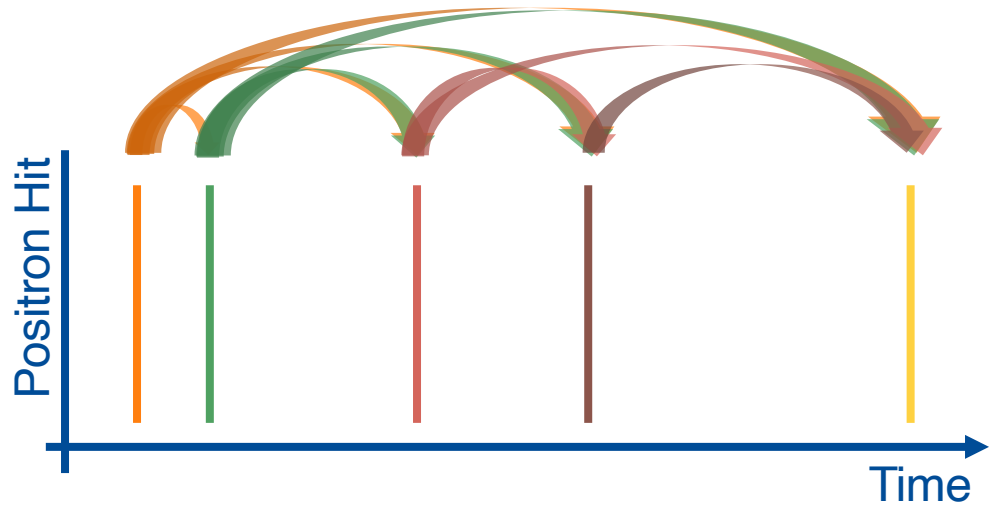

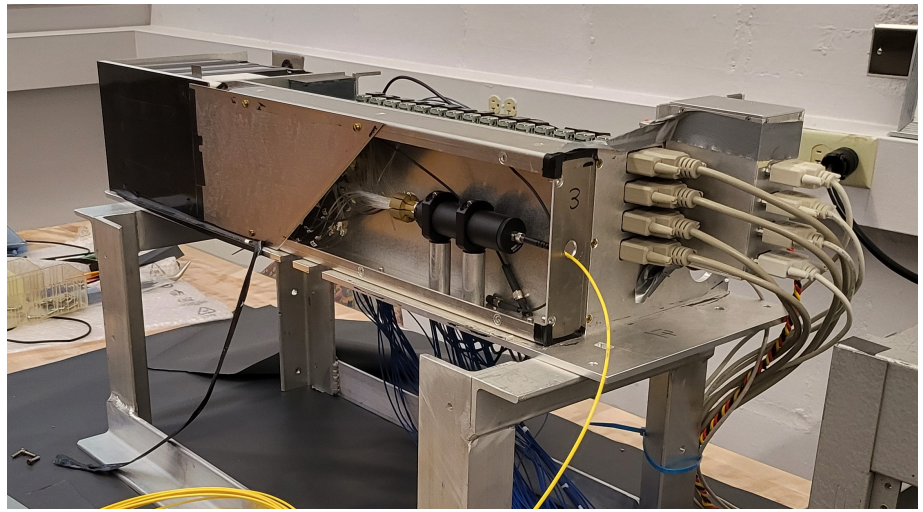

Calorimeter in lab for dedicated measurements

* electronics board dependent

Symptoms of Such An Effect I Toy MC Example

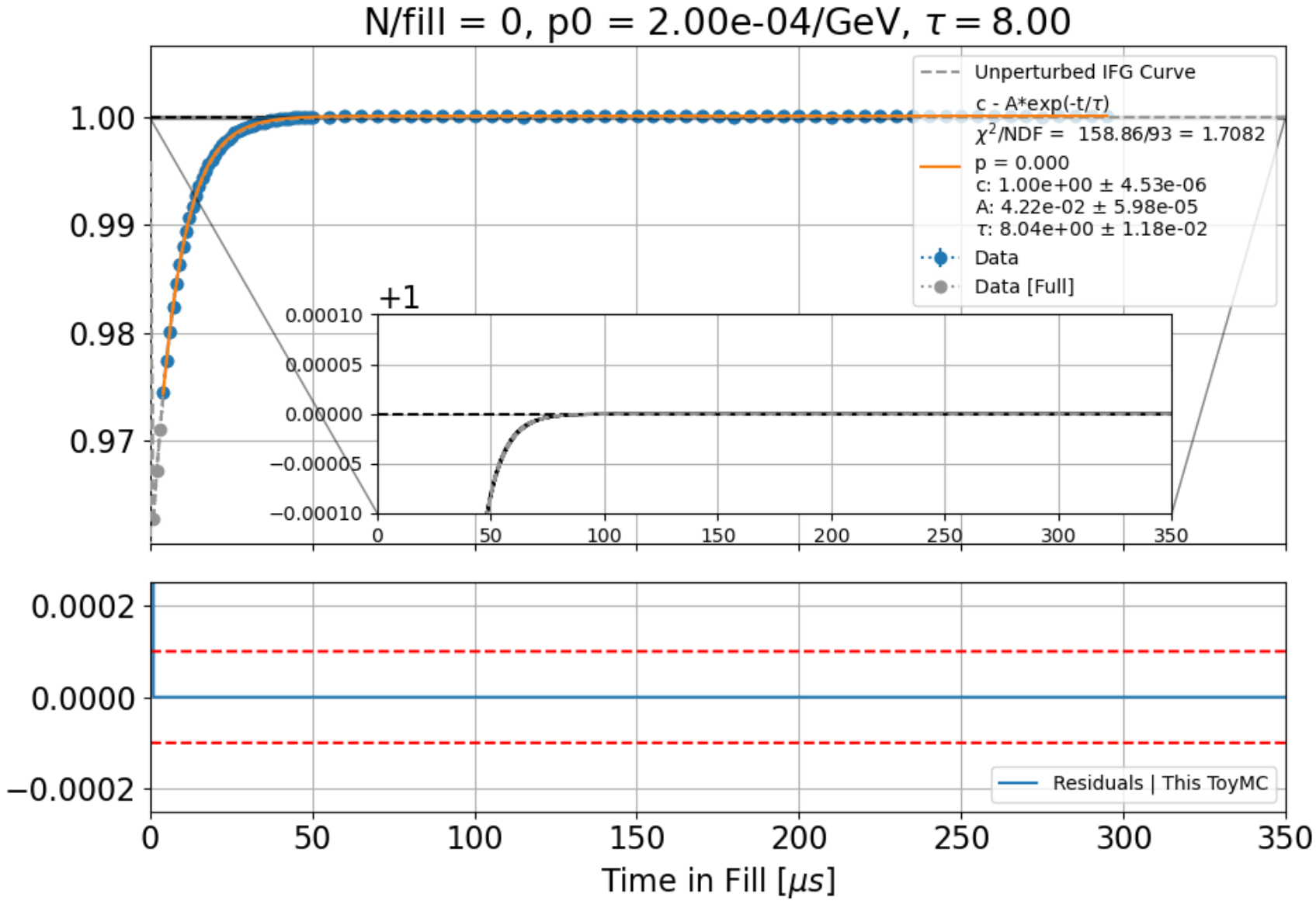

Symptoms of Such An Effect I Toy MC Example

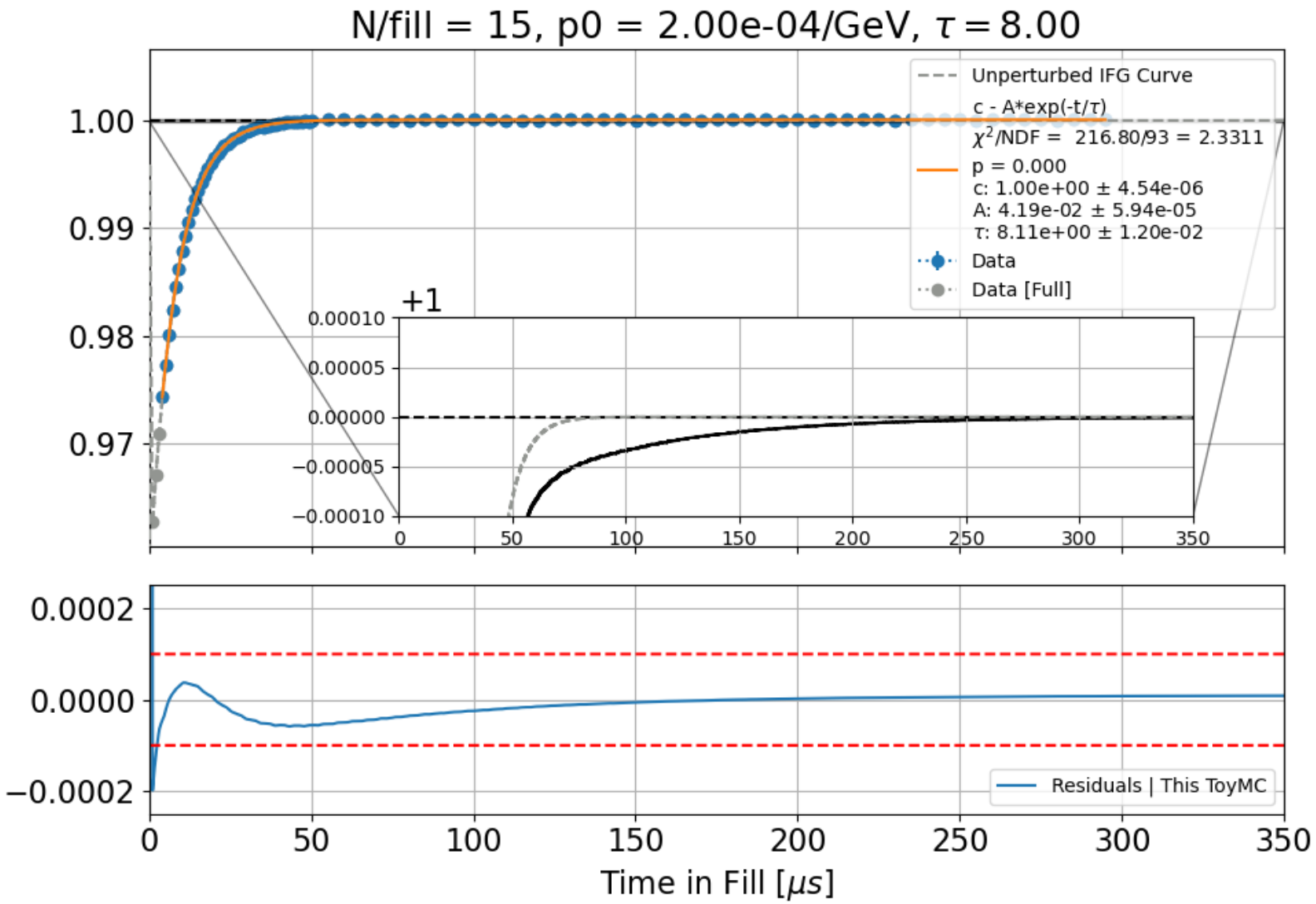

Symptoms of Such An Effect I Toy MC Example

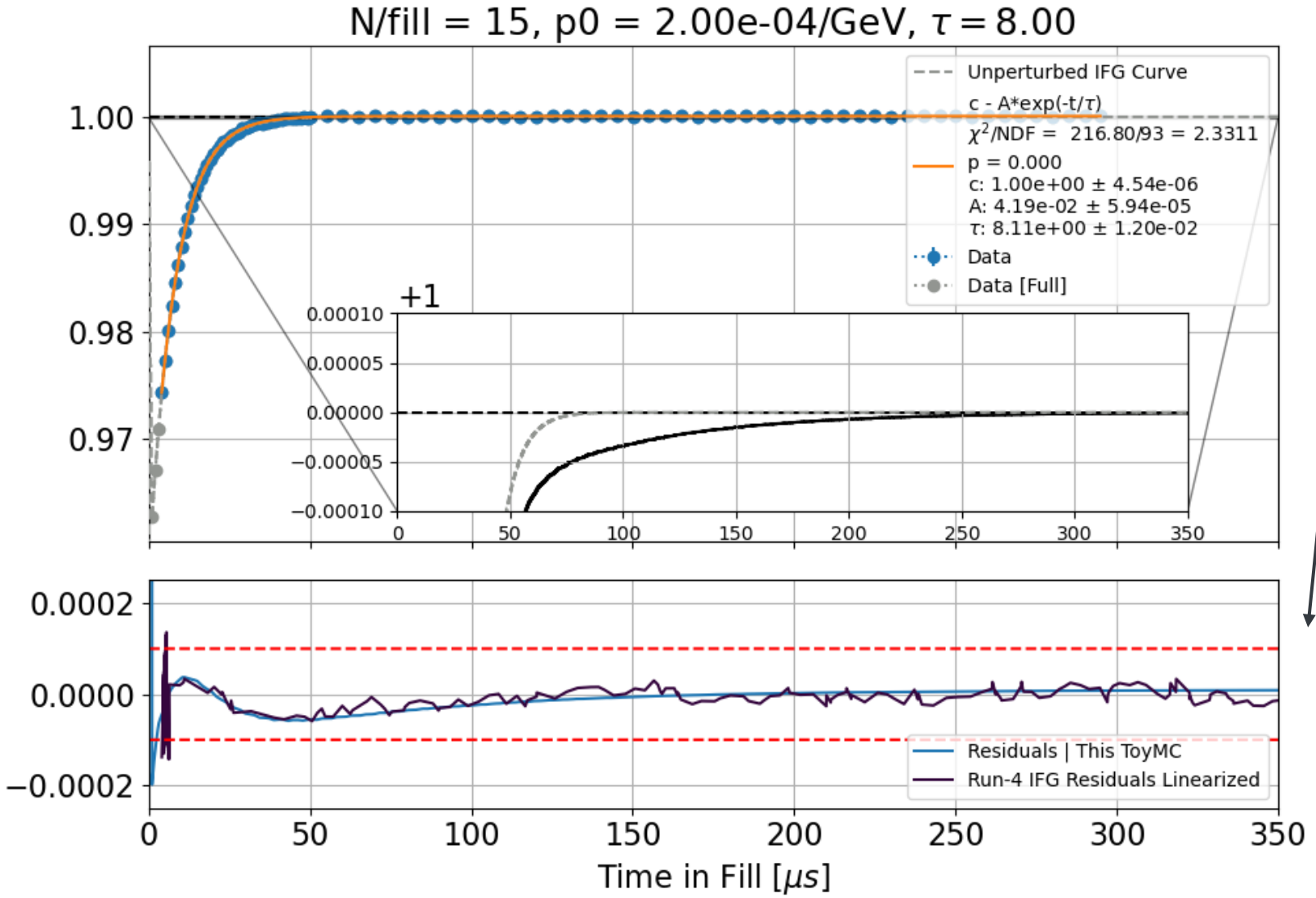

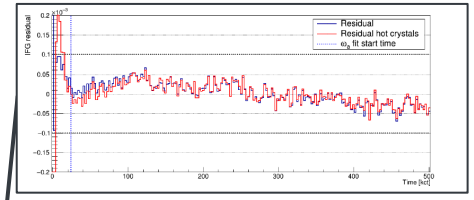

The shape induced by the ITDP effect matches the real IFG residuals

Damaged Resistors

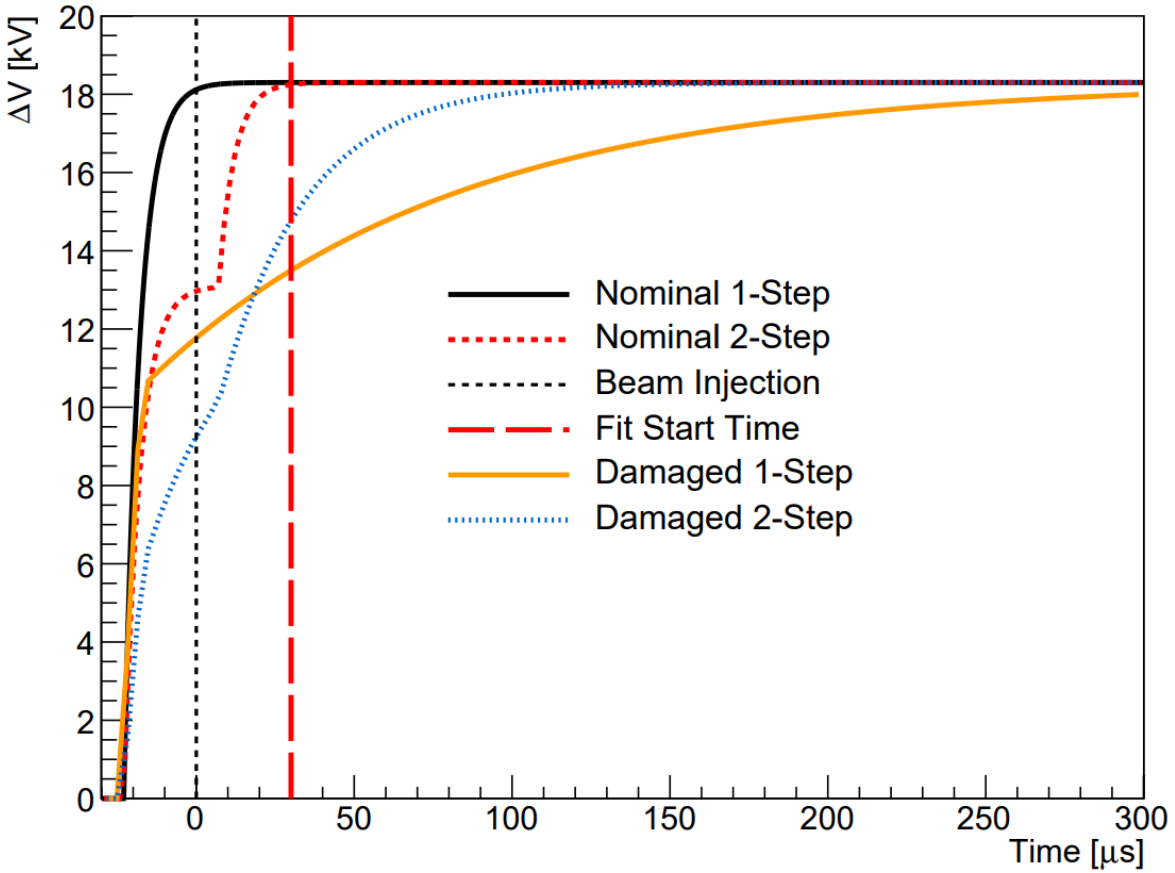

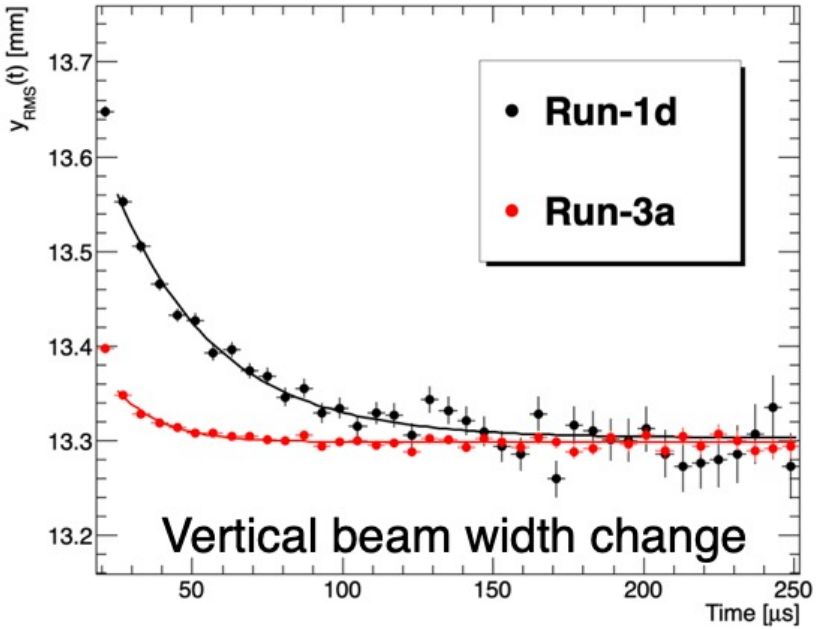

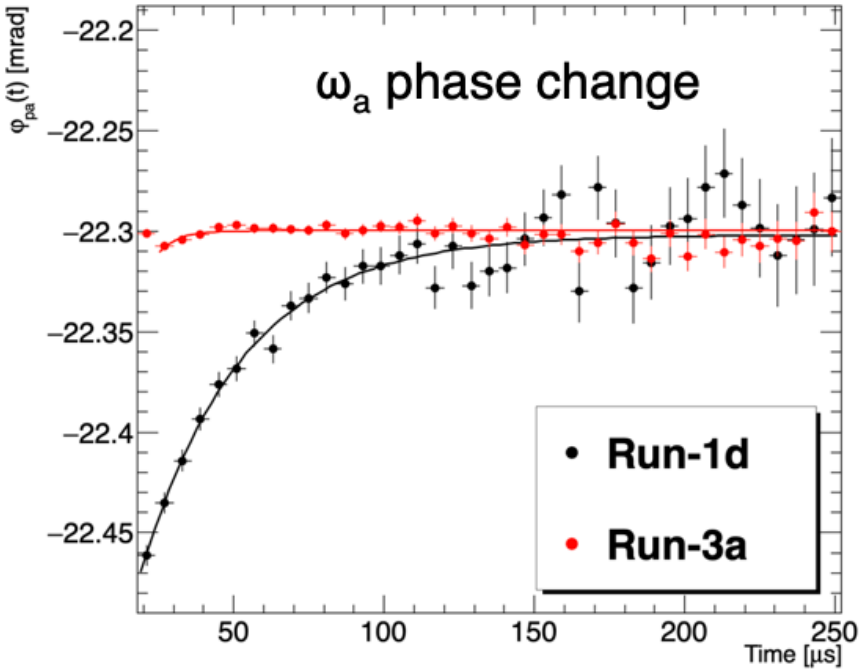

Measuring the Spin Precession

Simplest fit model captures **exponential decay** & **g-2 oscillation**

Must account for **beam oscillations**, **muons losses**, and **detector effects**

5 groups, 8 method using between
7 and 50 parameters

Example:

Beam dynamics modeling, such as CBO

- if not accounted for: ~800 ppb effect without the additional RF
- if not accounted for: ~80 ppb effect with the additional RF

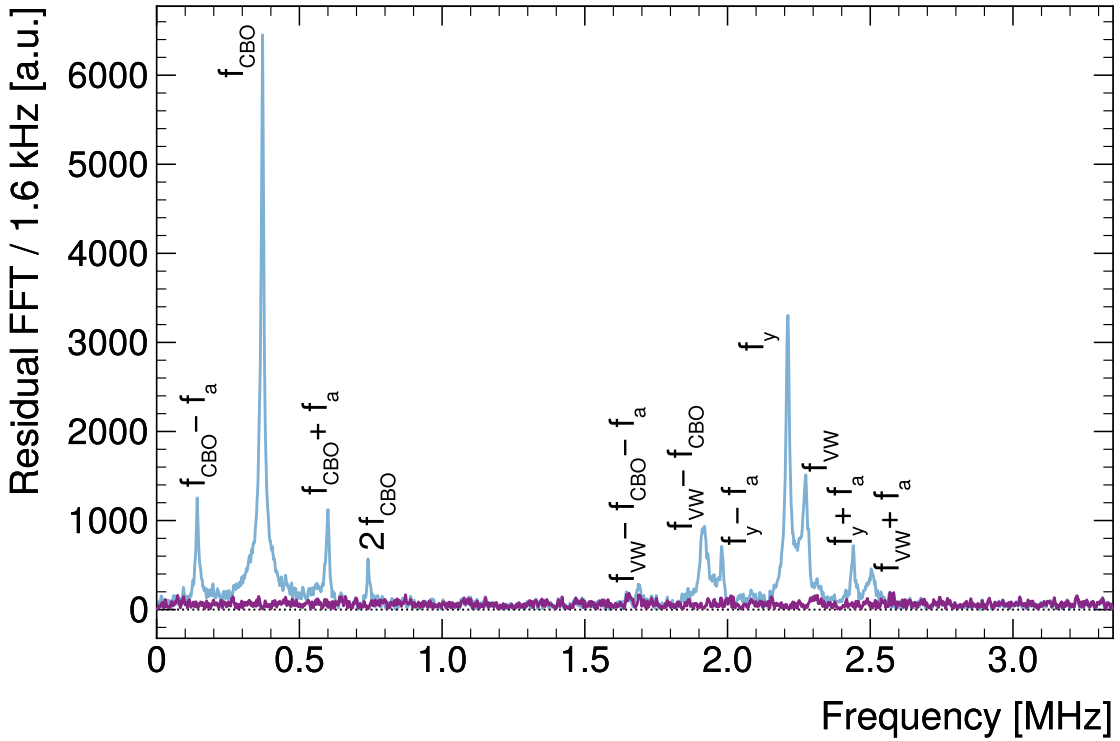

The **large** Run-4/5/6 dataset, split into noRF, xRF, xyRF, allowed to demonstrate **consistency** between largely different conditions.

Start Time Scan

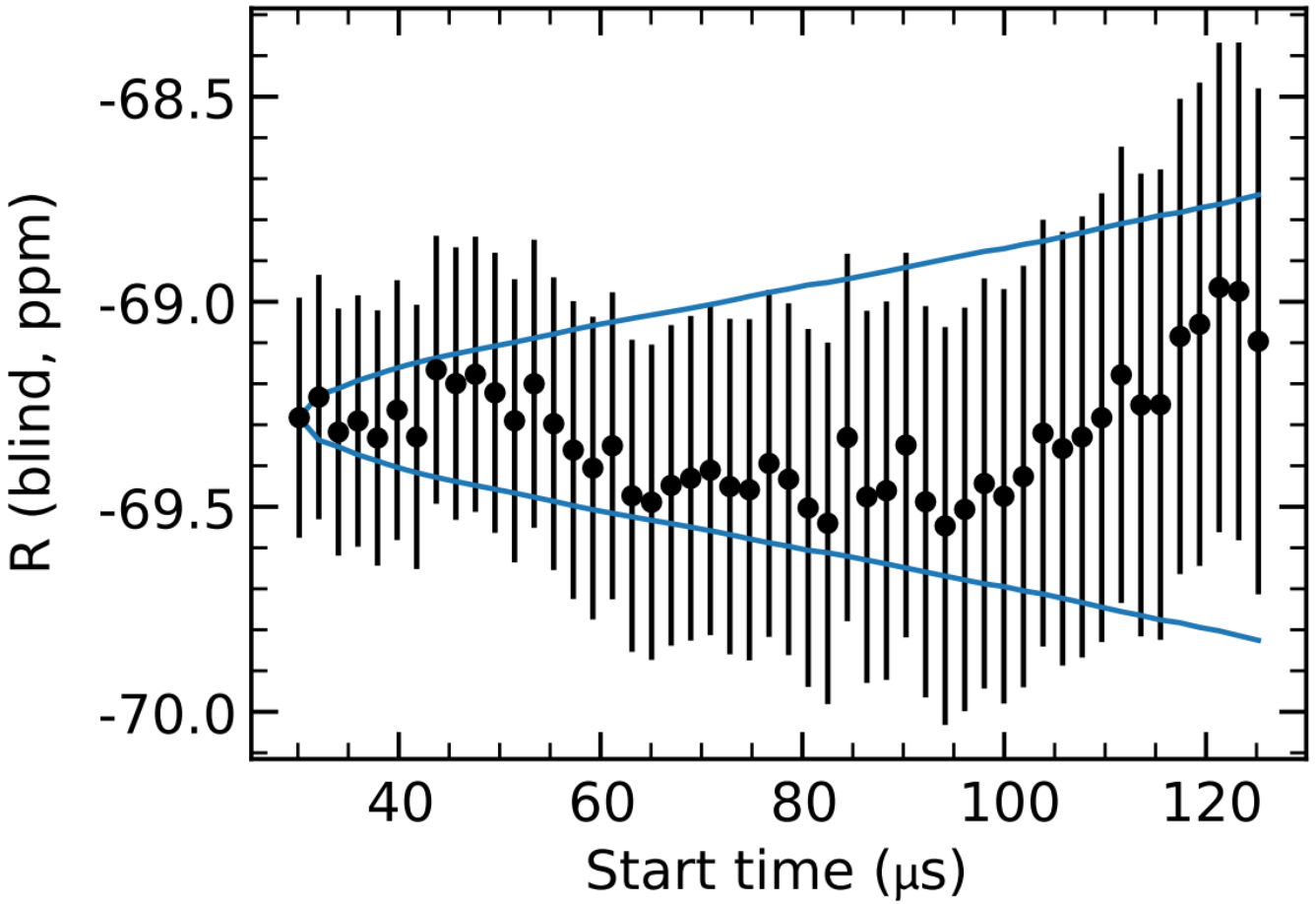

Numbers

Statistics

$\frac{\omega_a}{\tilde{\omega}'_p}$	Analyzed Positrons (10^9)	Fraction (%)	Stat. Uncertainty (ppb)
Run-1	15.4	5	434
Run-2/3	70.9	23	201
Run-4/5/6	222.2	72	114
Run-1-6	**308.5**	…	**98**

TDR goal: 100 ppb ✓

Uncertainties

$\frac{\omega_a}{\tilde{\omega}'_p}$	Stat. Uncertainty (ppb)	Syst. Uncertainty (ppb)	Total Uncertainty (ppb)
Run-1	434	159*	462
Run-2/3	201	78*	216
Run-4/5/6	114	76	137
Run-1-6	**98**	**78**	**125**
	TDR goal 100 ppb ✓	TDR goal: 100 ppb ✓	TDR goal: 140 ppb ✓

*corrected

Consistency Checks

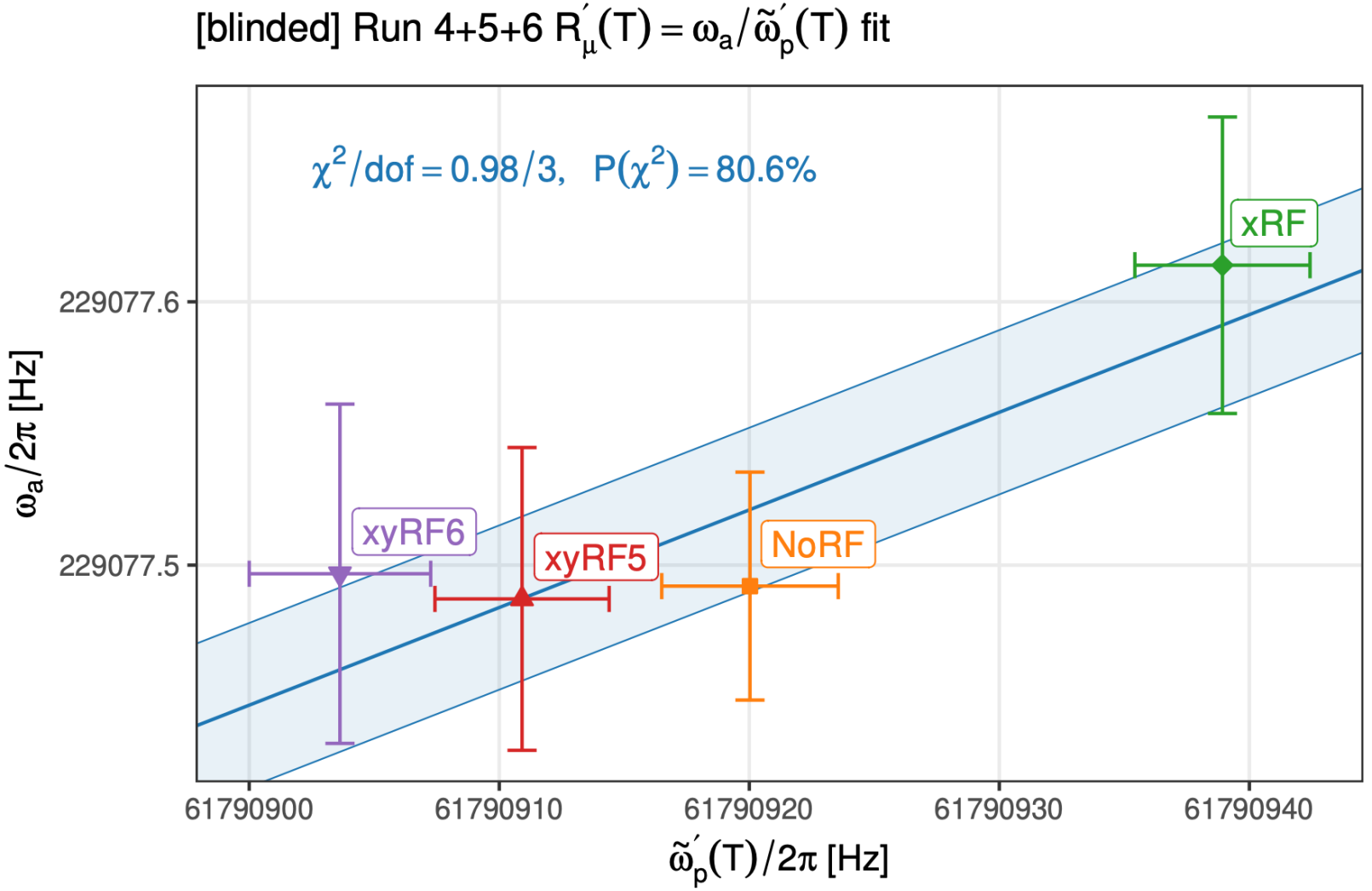

Run-4/5/6 Analysis Overview

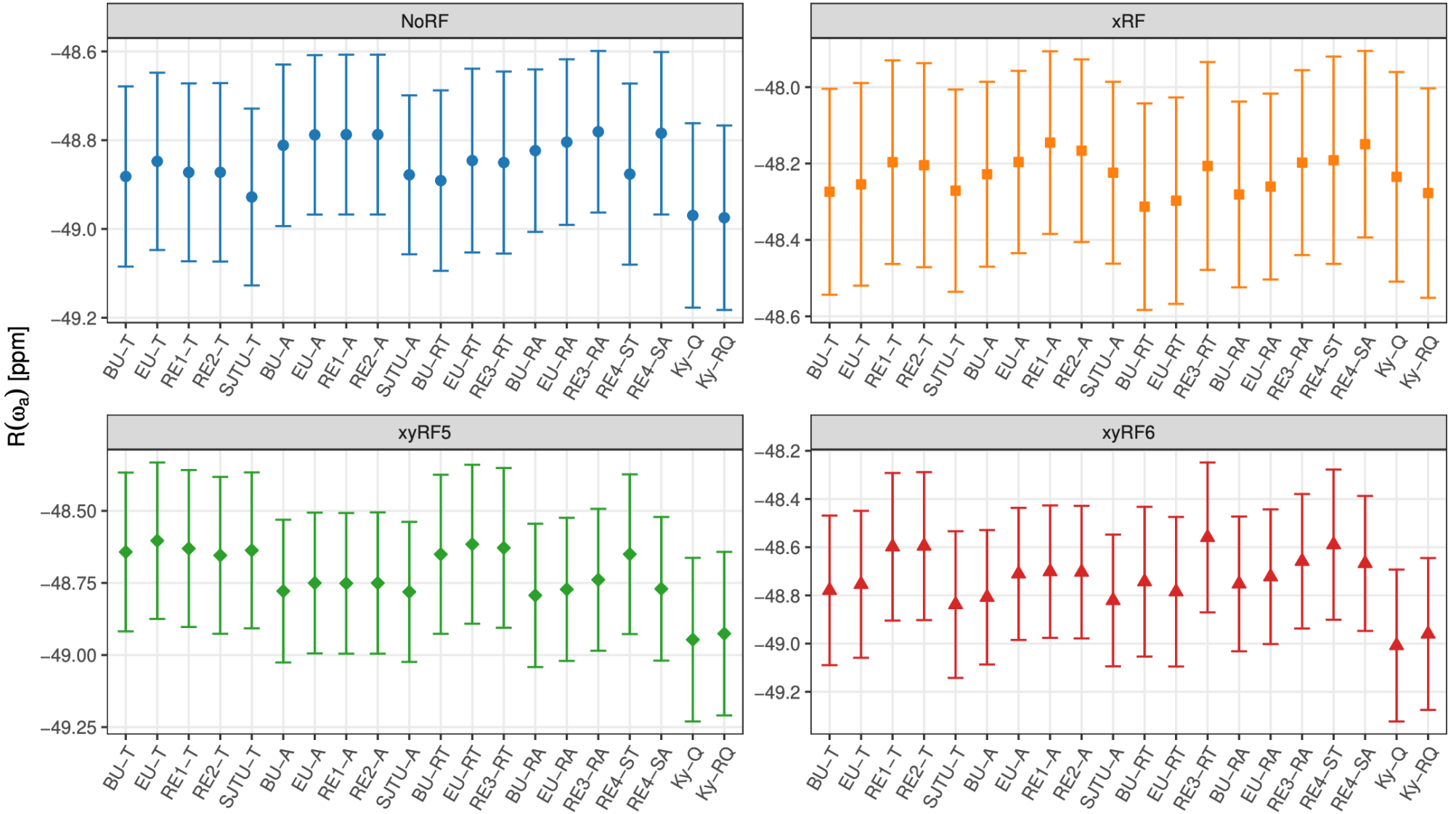

Systematics

New! Run-4/5/6

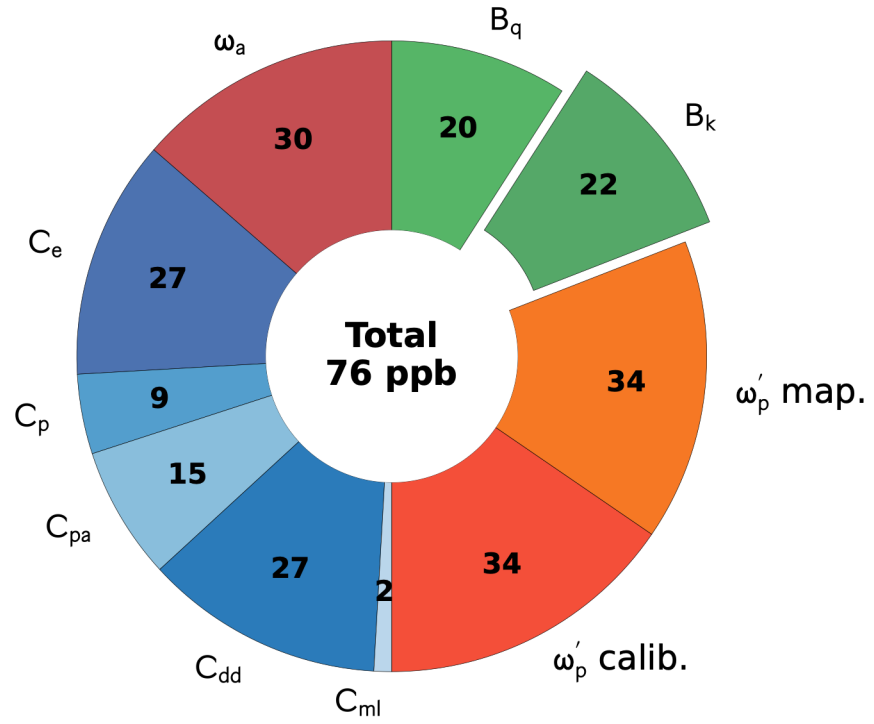

- Run-2/3 with Run-4/5/6 knowledge
- Identified physical source for residual slow term effects
- Dedicated MiniSciFi detector and further improved methods
- Improved understanding, leading to more conservative uncertainty (sign error correction in one component)
- More conservative uncertainty motivated by additional cross-calibration
- Reduction of uncertainties due to additional measurement
- Additional measurement lead to refined spatial model

Run-1, Run-2/3, Run-4/5/6 comparisons

	Run-1		Run-2/3		Run-4/5/6	
Quantity	Cor. (ppb)	Unc. (ppb)	Cor. (ppb)	Unc. (ppb)	Cor. (ppb)	Unc. (ppb)
ω_a^m (statistical)	···	434	···	201	···	114
ω_a^m (systematic)	+50	63	+47	35	···	30
C_e			451	32	347	27
C_p			170	10	175	9
C_{pa}			-27	13	-33	15
C_{dd}			17	22	26	27
C_{ml}			0	3	0	2
$f_{\text{calib}} \cdot \langle \omega_p'(\vec{r}) \times M(\vec{r}) \rangle$			···	46	···	48
B_k			-40	26	-37	22
B_q			-21	20	-21	20
Total systematic for $\mathcal{R}'_\mu$	···	158	···	78	···	77

	Run-1		Run-2/3	
Quantity	Cor. (ppb)	Add. Unc. (ppb)	Cor. (ppb)	Add. Unc. (ppb)
IDTP	+50	29	+47	24
C_{dd}	···	···	+32	17
B_k	···	···	-19	23
Total for $\mathcal{R}'_\mu$	+50	29	+98	33

corrections

Why a_μ and not a_e?

- Coupling of virtual loops goes as m^2 (dimensional analysis)
- Therefore, while a_μ is measured ~20x less precisely than the a_e, it has better sensitivity to heavy physics scales:

$$\left(\frac{m_\mu}{m_e}\right)^2 \simeq 43,000$$

- E.g. lowest-order hadronic contribution to a_e is
  $a^{had,LO} = (1.875 \pm 0.017) \times 10^{-12}$ (1.5 ppb of a_e)
- By comparison, the muon's hadronic contribution is ~60 ppm.

BSM Analysis

Muon EDM

Muon EDM

non-zero EDM (η) modifies the spin equation

$$\vec{\omega}_{a\eta} = a_\mu \frac{e}{m}\vec{B} + \eta\frac{e}{2m}\left[\frac{\vec{E}}{c} + \vec{\beta}\times\vec{B}\right]$$

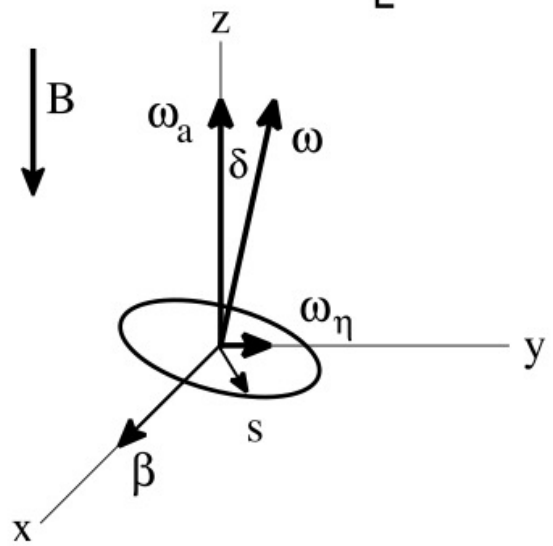

Search for an up/down asymmetry out of phase with ω_a

BNL: tracker-based analysis

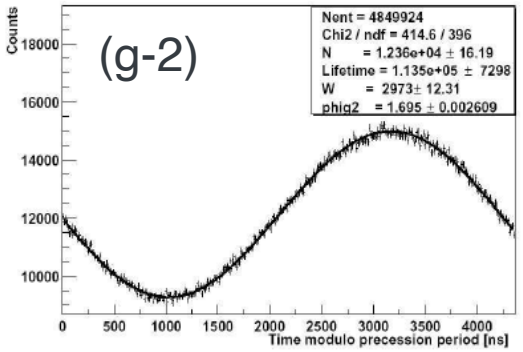

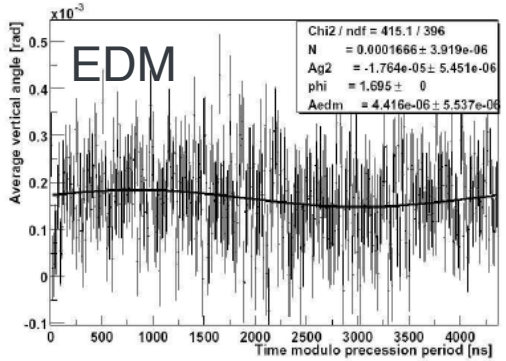

CPT and Lorentz Violations

Lorentz Violation –
existence of a preferred direction

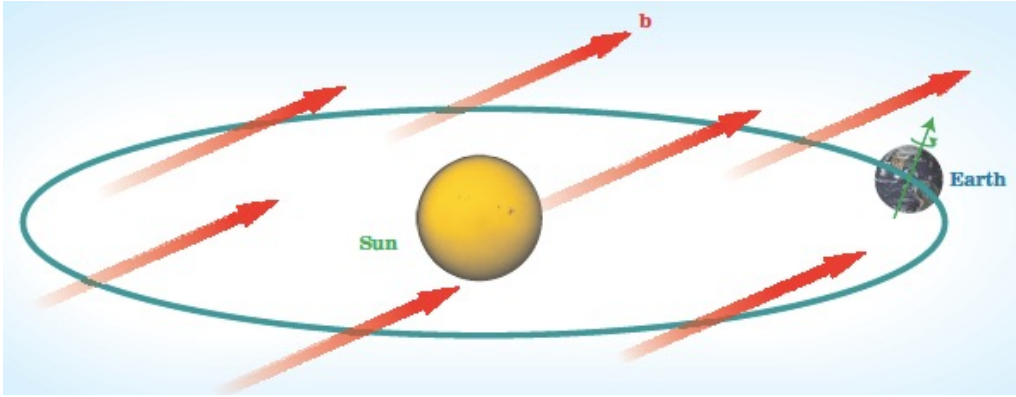

- Uniform background vector, *b*
- What could it come from?
  Spontaneous Symmetry Breaking,
  - **SM**: In EWSB, scalar field gets non-zero vacuum expectation value, filling vacuum with *Lorentz Symmetric quantities*
  - **SME**: Can have Lorentz SB, where vector field gets non-zero vev, filling vacuum with *4-dimensionally oriented quantities* → preferred direction in space → LV!
  - Possibilities: string theory, loop-quantum gravity, etc.

CPT Violation

- LV *allows* but does not *require* CPTV, because CPT Theorem no longer holds (but CPTV does require LV)

Dark Matter - Physics Signature

Muon $g-2$ has a competitive sensitivity to the **ultralight (thus bosonic and wave-like field) muonic DM**. It is the first direct DM search with muons in a storage ring.

- Scalar field (Yukawa coupling) $\phi = \phi_0 \cos(m_\phi t)$
  - It induces oscillating m_μ.

$$\mathcal{L} \supset -g\phi\bar{\mu}\mu - g'\phi^2\bar{\mu}\mu \quad \Rightarrow \quad m_\mu \to m_\mu + g\phi + g'\phi^2$$

  - It leads ω_a to oscillate: $\omega_a \to \omega_a(1 + A_\phi \cos m_\phi t)$

- Pseudoscalar axion-like field $a = a_0 \cos(m_a t)$
  - EDM coupling induces oscillating EDM (d_μ).

$$\mathcal{L} \supset -ig_{\mathrm{EDM}} a\bar{\mu}\sigma^{\lambda\nu}\gamma_5\mu F_{\lambda\nu} \Rightarrow d_\mu \to d_\mu + g_{\mathrm{EDM}} a$$

  - Gradient coupling induces oscillating spin along the axis of the muon's motion.

$$\mathcal{L} \supset g_{a\mu}\partial_\lambda a\bar{\mu}\gamma^\lambda\gamma_5\mu \Rightarrow \mathcal{H} \supset g_{a\mu}\nabla a \cdot \mathbf{S}$$

  - Both lead to oscillating $\delta\boldsymbol{\omega}_a$ components perpendicular to $\boldsymbol{\omega}_a$.

Spin precession

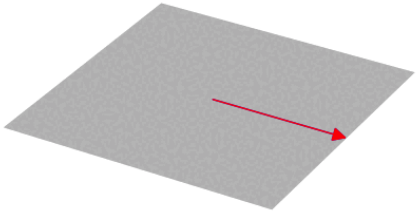

No DM

Gradient coupling (10% of ω_a)

Detectors

Temperature

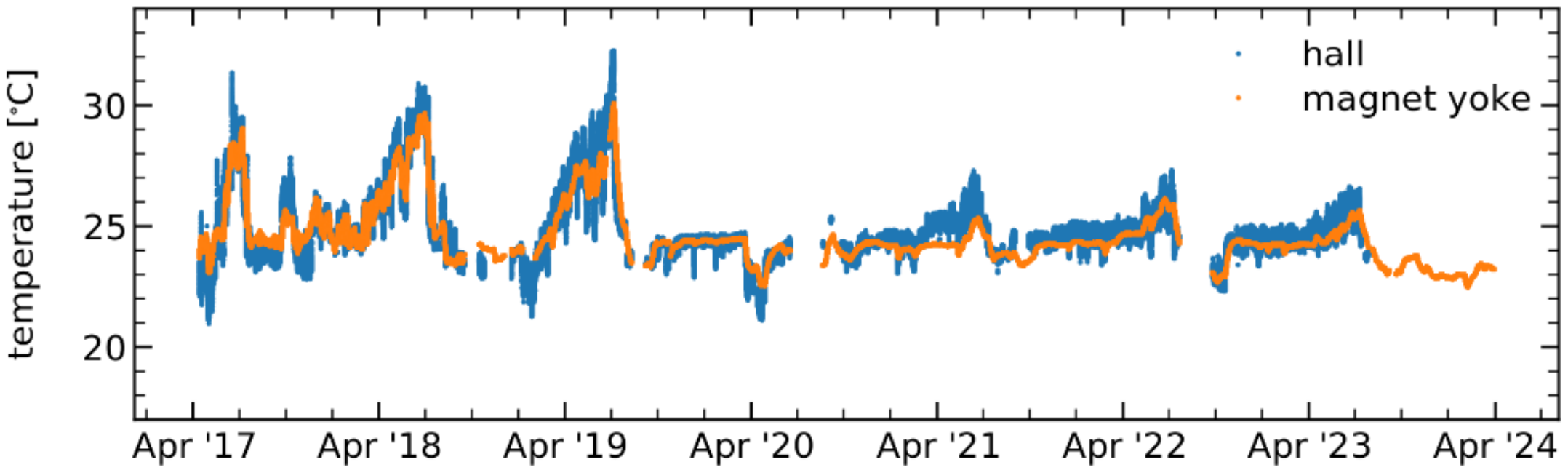

Kicker Upgrade

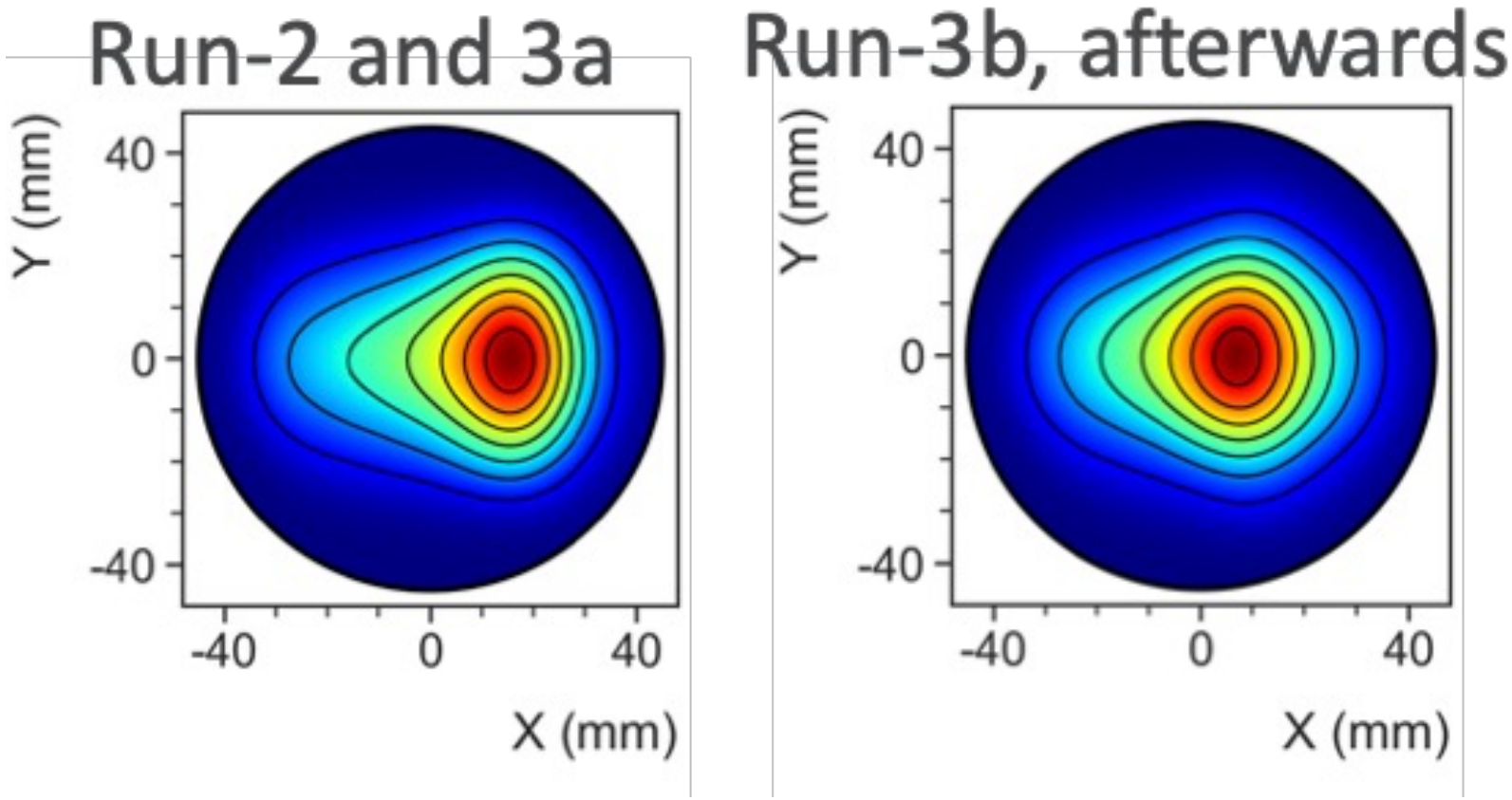

Calorimeters

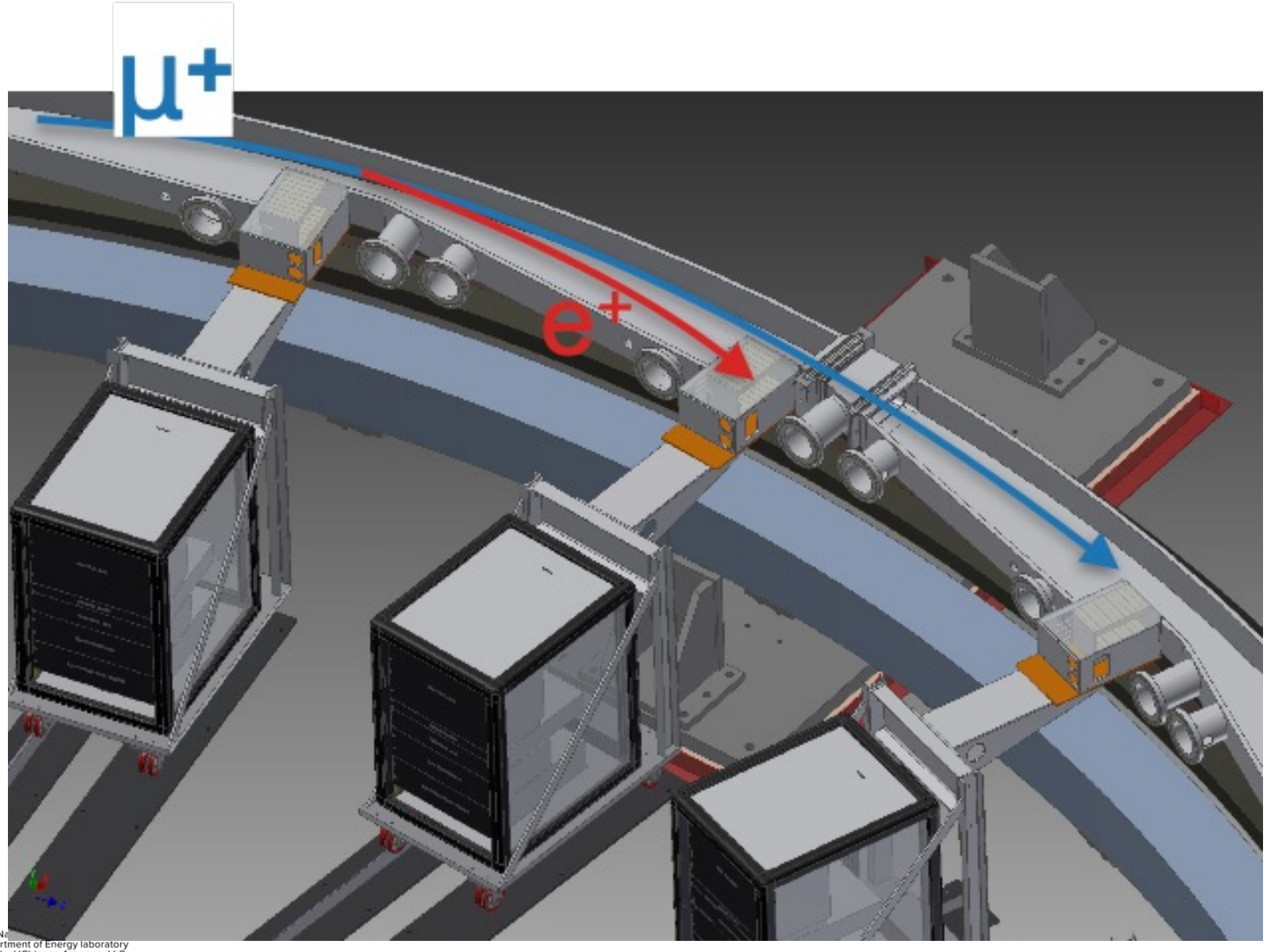

Other Experiment

CERN Experiments – what a difference!

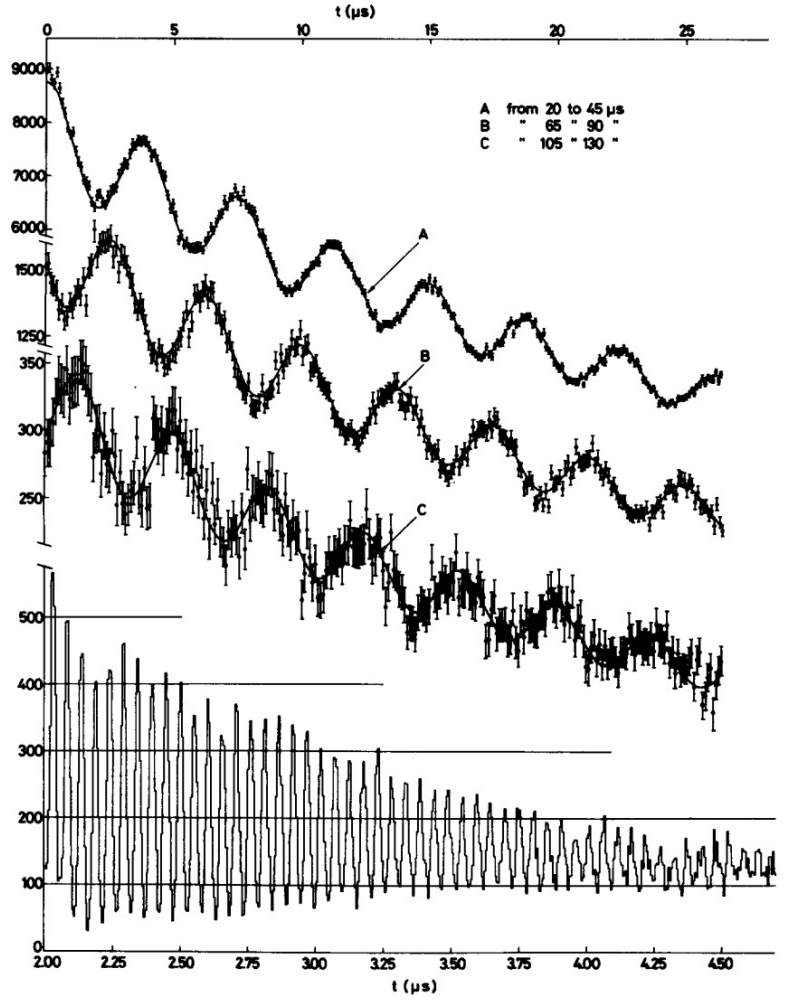

Fig. 2. Distribution of decay-electron events as a function of time. Lower curve shows rotation frequency of muon at early time. A, B, C: late time data, 20 – 130 μsec showing (g – 2)-precession. Data are fitted from 21 to 190 μsec.

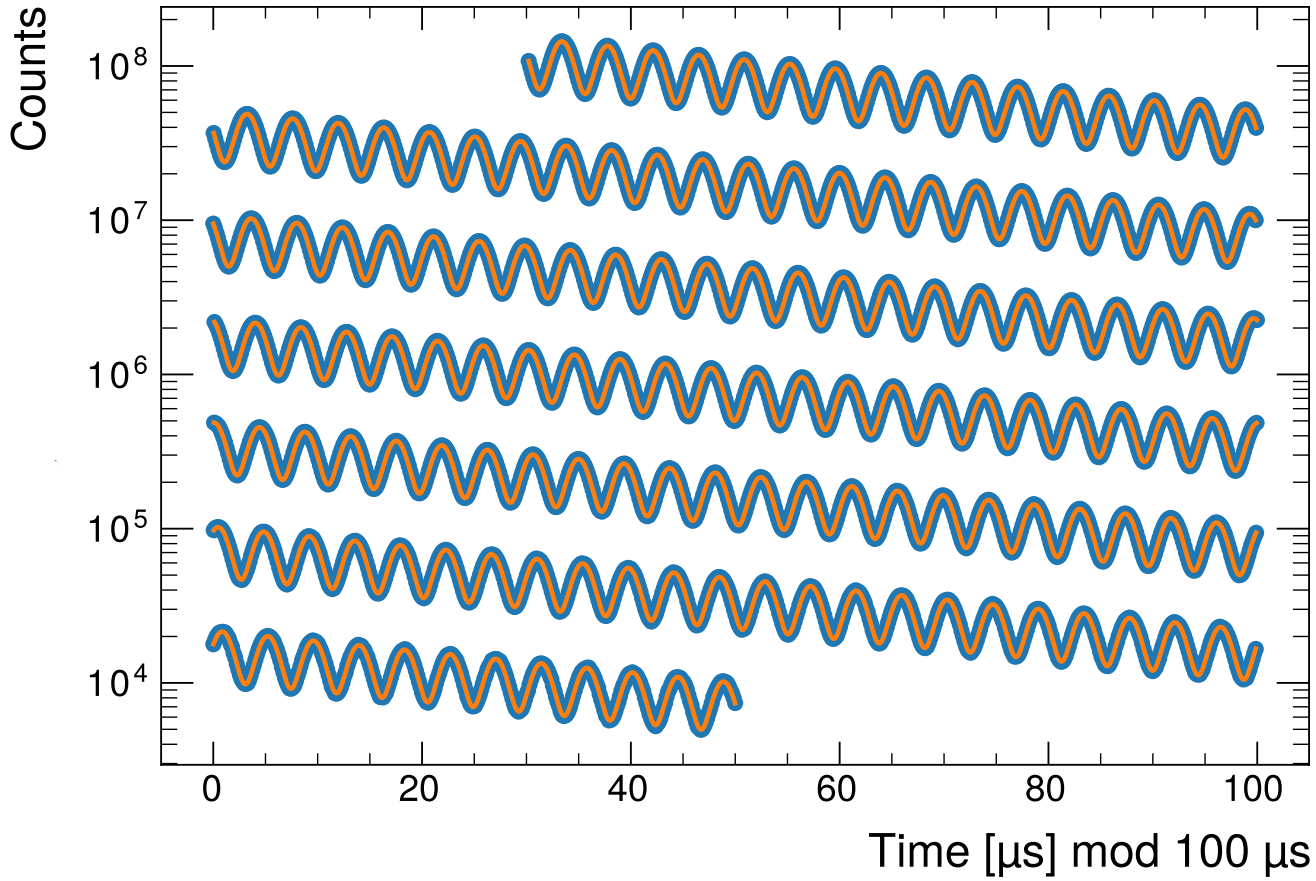

MUonE

MUonE uses a new, independent evaluation of a^{HLO}

$$a_\mu^{HLO} = \frac{\alpha}{\pi}\int_0^1 dx(1-x)\Delta\alpha_{had}[t(x)]$$

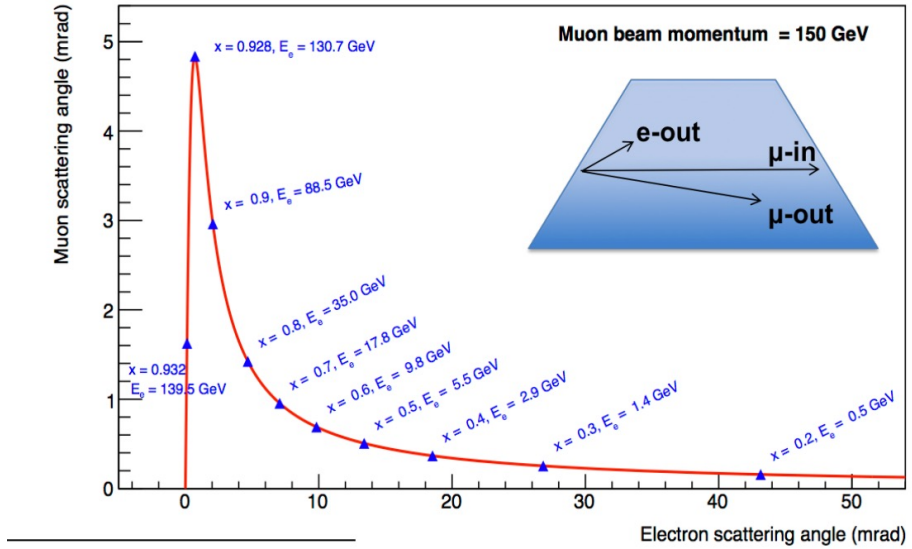

Δa_{had}: hadronic contribution to the running of α in the space-like region

$\Delta a_{had}(t)$: can be extracted from the shape of $\mu e \to \mu e$ differential cross section

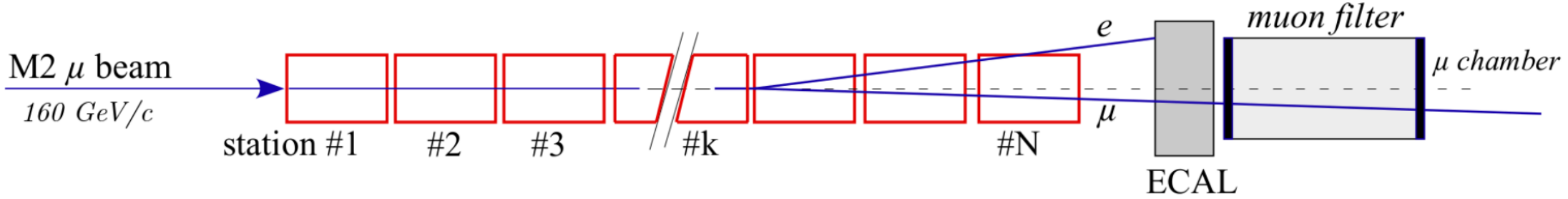

Figure 24: Schematic view of the MUonE experimental apparatus (not to scale).

J-PARC g-2/EDM

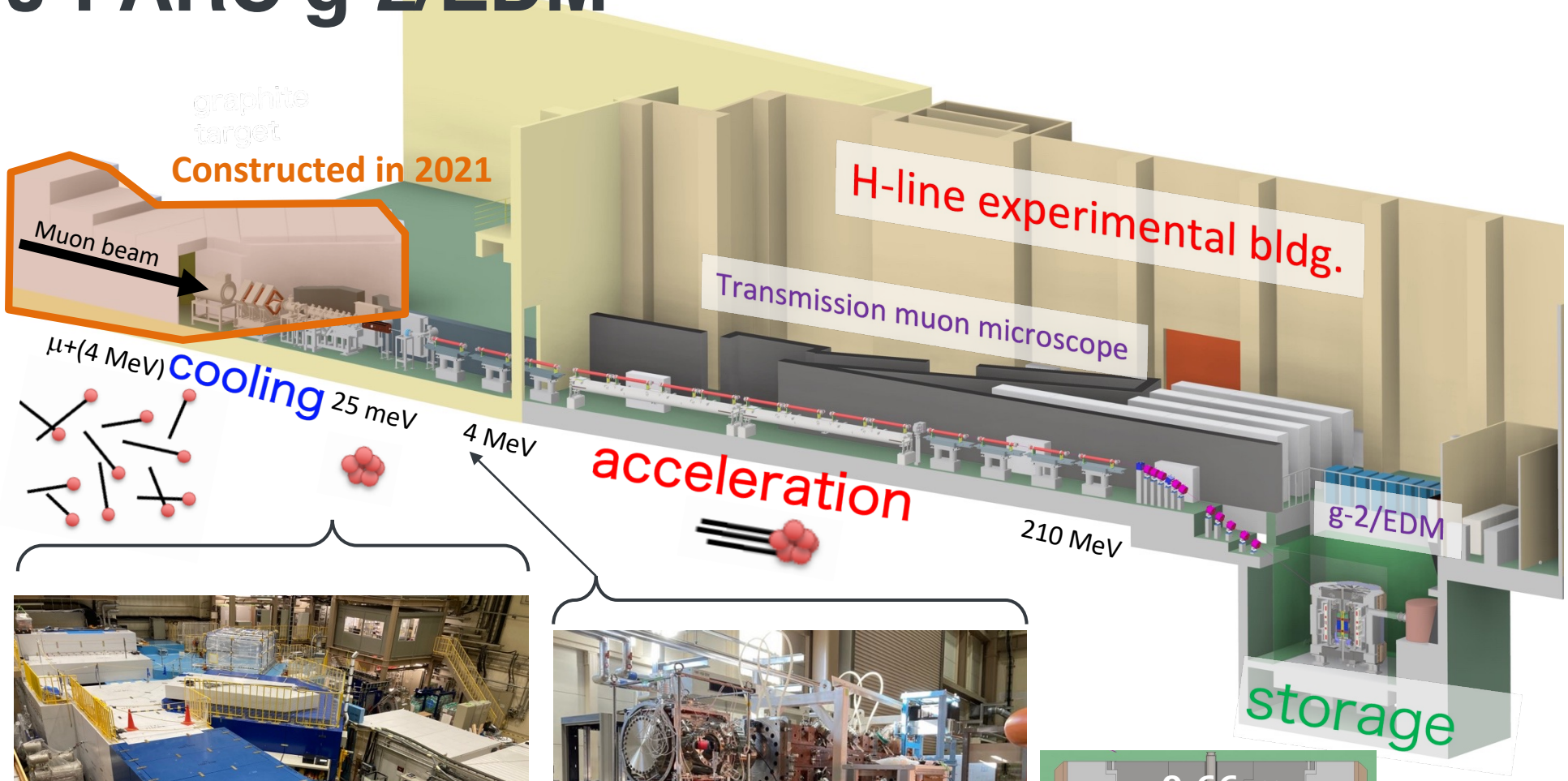

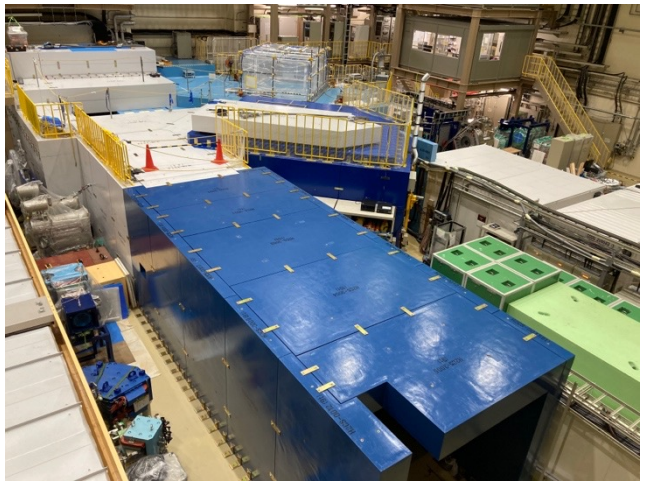

Shields, area control (2022)

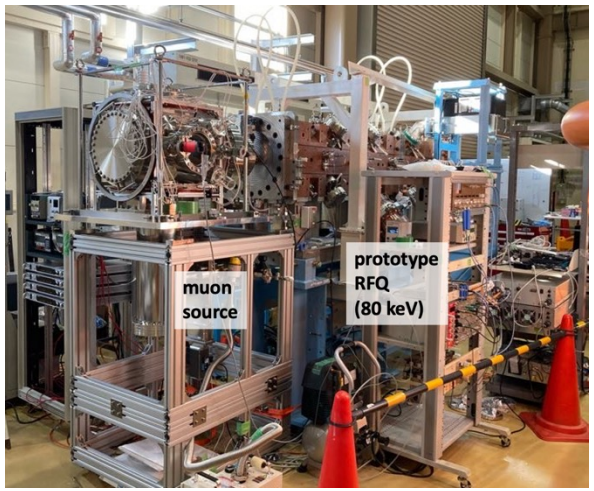

RF Acc. Test at S2 area (May 2023)